# TECTONIC EVOLUTION OF SYRIA INTERPRETED FROM INTEGRATED

# GEOPHYSICAL AND GEOLOGICAL ANALYSIS

A Dissertation

Presented to the Faculty of the Graduate School

of Cornell University

in Partial Fulfillment of the Requirements for the Degree of

Doctor of Philosophy

by

Graham Edward Brew

January 2001

# TECTONIC EVOLUTION OF SYRIA INTERPRETED FROM INTEGRATED GEOPHYSICAL AND GEOLOGICAL ANALYSIS

Graham E. Brew, Ph.D.

Cornell University 2001

Using a variety of geophysical and geological data, the Phanerozoic tectonic evolution of Syria has been interpreted. The study is inspired by the diverse styles of tectonic deformation within Syria generated by long-lived proximity to active plate boundaries. The work is also relevant to hydrocarbon exploration. The availablity of seismic reflection and refraction profiles, wells, and other resources made this research possible.

Three studies focused on specific areas of Syria are presented. The first is a seismic refraction interpretation along a north – south profile in eastern Syria. The results show that metamorphic basement depth (and hence Paleozoic thickness) in southeast Syria is greater, by >2 km, than that in the northeast.

The next study interprets the structure and tectonics in northeast Syria. During Late Paleozoic and Mesozoic time northeast Syria was an extension of the Palmyride trough. In the Maastrichtian, regional extension opened the Abd el Aziz and Sinjar graben that were structurally inverted in the Late Cenozoic to form the present topography.

The third study concerns the Ghab Basin in western Syria. This 3.4 km deep Plio-Quaternary pull-apart basin suggests that the Dead Sea Fault System has only been active in Syria since the end of the Miocene in accordance with a two-phase model of Red Sea opening.

The final study integrates the previous interpretations with new work to provide a tectonic evolutionary model that shows the Phanerozoic development of all Syria. This model is closely tied to stratigraphic data that improve the interpretation of many tectonic events, and put the results into a paleogeographical context. The model shows how specific deformation episodes within Syria have been penecontemporaneous with regional plate tectonic events. The Late Paleozoic / Mesozoic northeast trending Palmyride / Sinjar trough formed across central Syria in response to Permo-Triassic opening of the NeoTethys Ocean. Proximal subduction in the NeoTethys created the Late Cretaceous Euphrates Fault System and Abd el Aziz / Sinjar graben in eastern Syria. Late Cretaceous to Late Miocene collisions and shortening along the northern Arabian margin caused platform-wide structural inversion, uplift, and shortening. This compression continues today under the influence of Arabia / Eurasia convergence.

# BIOGRAPHICAL SKETCH

Graham Brew was born in 1974 in Staffordshire, England, not far from the sprawling metropolis of Birmingham where he spent most of his childhood. Through family vacations and school trips he developed a love for the outdoors that still endures. Moreover, during his secondary schooling dedicated and devoted teachers instilled in Graham a passion for science, especially physics and geography. Combining these interests he enrolled as a geophysics major at University College, London. There he had the great fortune to work with many astute geoscientists who further kindled his love for earth science. One of his professors, John Milsom, was also instrumental in securing Graham a challenging and enlightening internship in Santiago, Chile, during the austral winter of 1994.

Upon deciding to continue his education, Graham applied to study geophysics at Cornell University. His application was intercepted by Muawia Barazangi, who, with higher wisdom, saw a vision of a budding research scientist. Thus Graham swapped the bright lights of London for the more relaxed, rustic charms of Ithaca, New York. We can now argue that Muawia's vision was correct. More than five years, and a great deal of lost sleep later, Graham looks ready to receive his doctorate.

For the short-term Graham will continue to live in Ithaca and work as a post-doctoral associate with Muawia. His wife, Chris, who somehow pried Graham away from seismic lines and Adobe Illustrator long enough to marry him, continues her graduate study in biochemistry. Once their time in Ithaca draws to a close, Graham and Chris will follow their joint love of science, but as yet they are not quite sure where.

The scientist does not only study nature because it is useful;

he studies it because he delights in it, and he delights in it

because it is beautiful.

JULES HENRI POINCARÉ (1854 – 1912)

**Dedicated to my family**

# ACKNOWLEDGMENTS

# TABLE OF CONTENTS

# LIST OF FIGURES

**CHAPTER THREE**

**CHAPTER FOUR**

# LIST OF TABLES

**CHAPTER TWO**

# LIST OF PLATES

Plate 1: Tectonic map of Syria representing the current significant structural elements in the country. Surface geology is modified from Ponikarov (1966), modified using the volcanic aging results of Devyatkin et al. (1997), and Lebanese geology from Dubertret (1955), and is shown shaded with topographic imagery. Surface mapped tectonic elements modified from Ponikarov (1966) and Dubertret (1955), in addition to our own mapping, are shown in black. Tectonic elements that are only identified in the subsurface are shown in red. See legend for additional information and see Chapter 5 for complete discussion...............................................................Back Pocket

Plate 2: Syrian tectonic evolution model showing regional plate reconstructions (left), timelines of significant regional and local tectonic events (center), and Syrian tectonic evolution (right). Note that the plate reconstructions (after Stampfli, 2000) are simplified and are shown for orientation only. In each plate reconstruction frame, north is approximately upward, and present Arabia is highlighted, however each frame is not to scale relative to the others. For the Syrian tectonic frames, no palinspastic reconstruction is attempted; the tectonics are shown in the correct position for the time of emplacement. Modern-day geography fixed on central and eastern Syria is shown for reference. Facies distributions, water depths, and tectonic elements in Syrian frames are generalized. See Chapter 5 for full discussion...........................Back Pocket

# CHAPTER ONE

# Introduction

This dissertation concerns the tectonic evolution of Syria. Various geophysical and geological data have been interpreted in unison to document and analyze the Phanerozoic structural deformation of several areas within Syria. These interpretations are combined with previous work, and knowledge of regional plate tectonics, to form a complete Phanerozic tectonic model for all Syria.

The work presented here is the latest contribution of the 'Cornell Syria Project'. This academic / industrial collaboration has been active for over twelve years studying the northern Arabian Platform. Interest in Syria and the surrounding areas comes from several geologic and logistic motivations. The primary rationale is to study intracontinental areas that have experienced significant tectonism. Even a casual consideration of Syria shows that it is currently proximal to several active plate boundaries (Figure 1.1), and has been through much of geologic time, especially the Mesozoic and Cenozoic. Previous work of the Cornell Syria Project (e.g. Barazangi et al., 1993), and this dissertation, show how activity on these nearby plate boundaries has affected the deformation within Syria.

A further motivation is the very diverse styles and timing of tectonics within Syria. Tectonism within the country is concentrated in four major tectonic zones. These include a fold and thrust belt, a plate boundary transform fault, inverted basins and an extensive aborted rift. Inspection of the topography of Syria (Figure 1.2) immediately reveals the physiographic provinces that have prominent topographic expression.
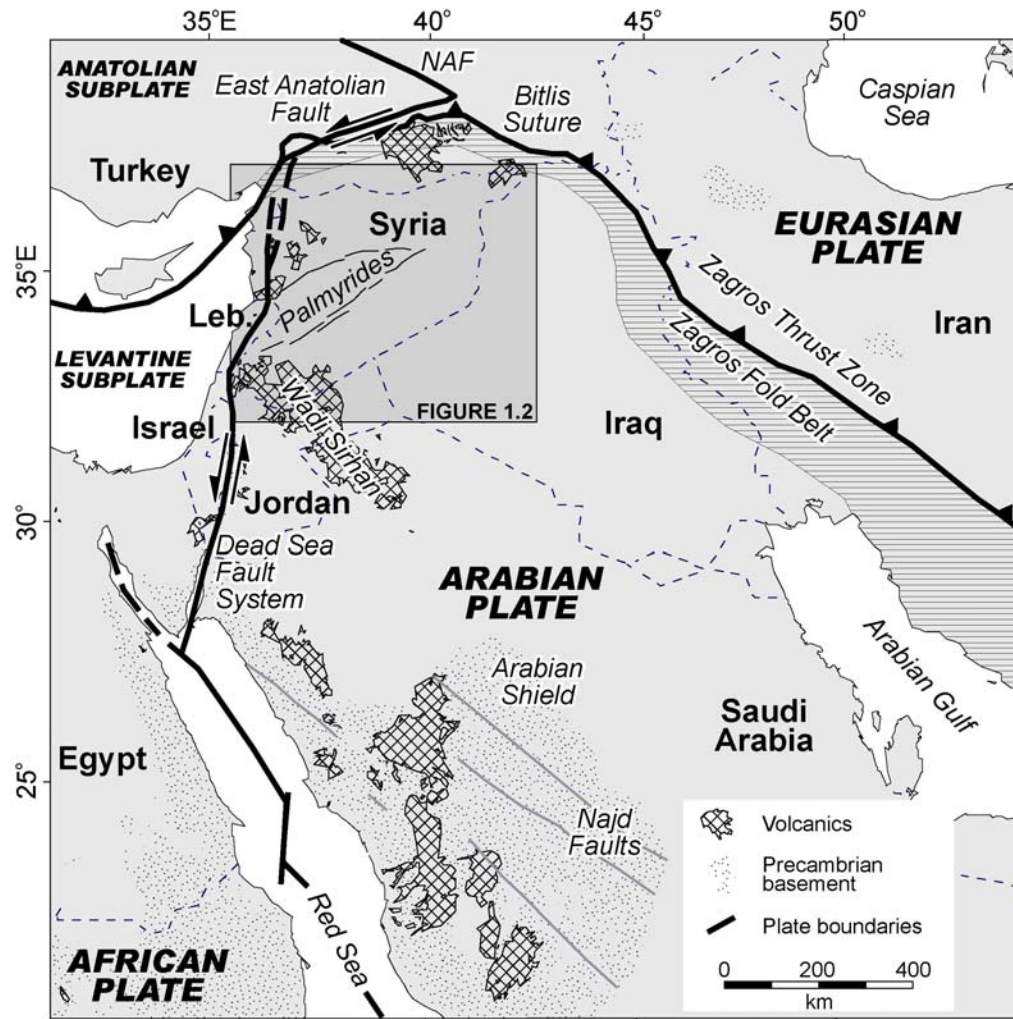
**Figure 1.1:** Map showing regional setting of Syria, almost surrounded by currently active plate boundaries.  NAF = North Anatolian Fault.

**Figure 1.2:** Map showing topographic contours and general tectonic zones in Syria. The areas investigated in Chapters 2, 3, and 4 of this dissertation are indicated. Chapter 5 concerns the tectonic evolution of all Syria.
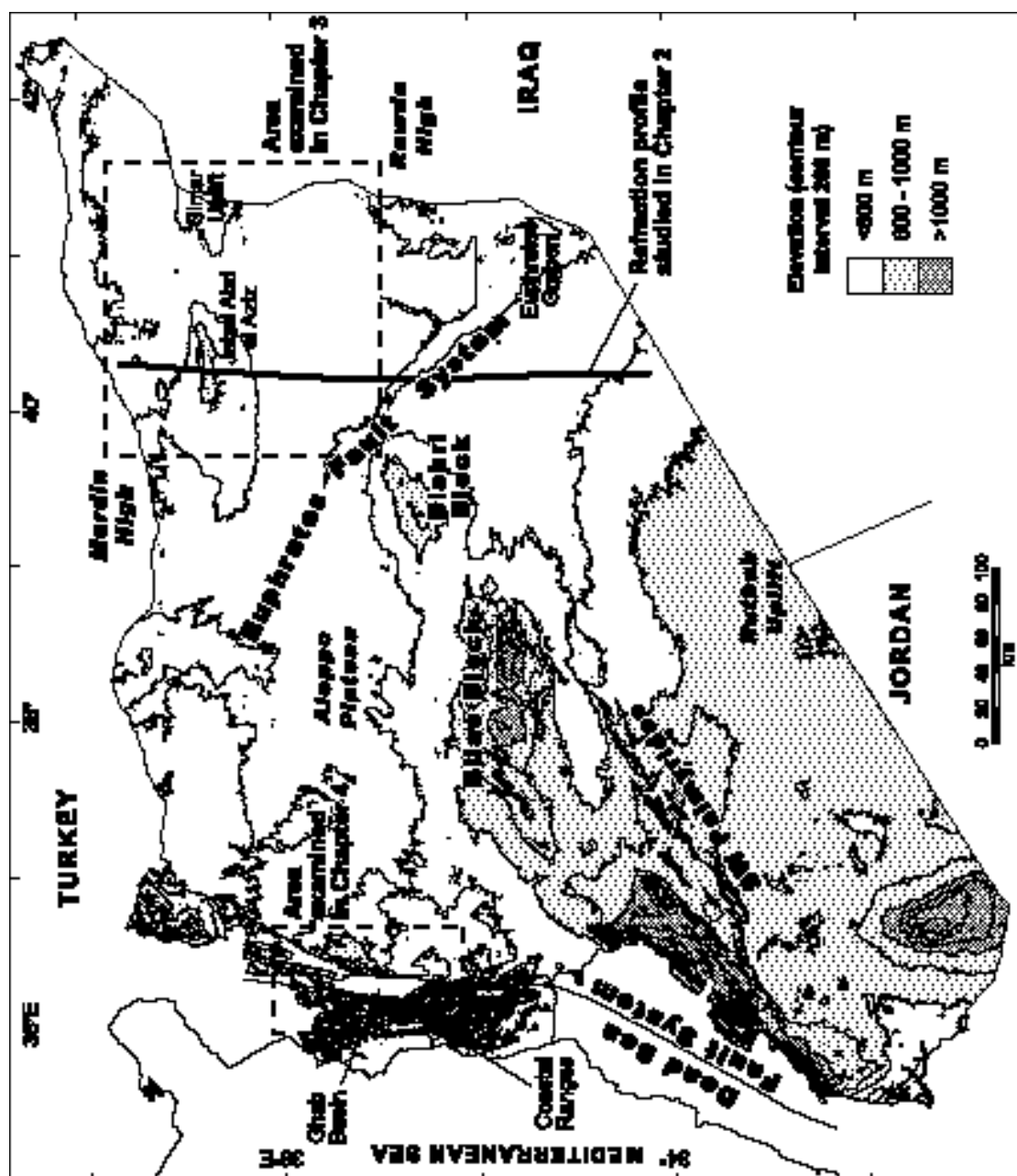
The final motivation for the study of Syria is the relevance this work has in the search for hydrocarbons. Although not comparable with the vast reserves of the Arabian Gulf states, the oil and gas reserves of Syria are nonetheless important to the local economy. The maturation of many of Syria's older fields leads impetuous for new discoveries. Many recent efforts have focused on exploration in Paleozoic strata, deeper than most previous discoveries. Our mapping of stratigraphic distributions and structures, as well as regional tectonic elements, can assist in this search.

It is our great fortune that we have access to a very extensive geophysical and geological database that can be used to examine the diverse and interesting tectonics of Syria. Through the generosity of the Syrian Petroleum Company (SPC), the Cornell Syria Project has access to many thousands of kilometers of seismic reflection profiles, data from hundreds of wells, and many other data sets. Detailed descriptions and maps of these data are given in later chapters.

This dissertation is presented as a series of self-contained chapters, each concerned with a certain facet of Syrian tectonic evolution. Chapter 2, 3, and 4 examine the tectonic style and history within three distinct areas of Syria (Figure 1.2). Chapter 5 is concerned with the tectonic evolution of all Syria. In the remainder of this chapter (Chapter 1) a very brief tectonic tour of Syria is undertaken. The direct contributions of this dissertation to the understanding of these tectonics is given with reference to later chapters.

Syria consists of four major tectonic zones separated by less deformed areas. Extending ~400 km northeast from the Lebanese border in the west into central Syria are the Palmyrides, the largest topographic feature, and the first tectonic zone of Syria. The

Palmyrides can be further divided, on the basis of topography and structure, into the Southwest Palmyrides (a fold and thrust belt), and the Bilas and Bishri blocks, Mesozoic sub-basins inverted during Cenozoic compression. The Palmyrides have been well studied previously by the Cornell Syria Project including Best et al. (1990; 1993), Chaimov et al. (1990; 1992; 1993), McBride et al. (1990), Al-Saad et al. (1991; 1992), Barazangi et al. (1993), Seber et al. (1993), and Alsdorf et al. (1995). They showed how the Palmyride area was an extensive Permo-Triassic rift, formed under regional extension associated with the opening of the NeoTethys Ocean and the eastern Mediterranean. While this dissertation does not directly add to their understanding, the Palmyrides are included in our discussion of regional tectonic evolution (Chapter 5). This includes structural maps for the Palmyrides, stratigraphic descriptions, isopachs, and seismic reflection examples showing the various styles of deformation.

The subdued topography of the second major tectonic zone, the Euphrates Fault System, belies its complex structure that harbors the greatest oil production in Syria. The Euphrates Fault System (Figure 1.2) extends across Syria from the Iraqi border in the southeast to the Turkish border in the northwest. The southeastern area, the 'Euphrates Graben' is the most intensely deformed part, and most reminiscent of a classic steep-sided graben. The Euphrates Fault System was rigorously studied by Cornell Syria Project researchers (Sawaf et al., 1993; Litak et al., 1997, 1998). They concluded that moderate latest Cretaceous rifting, distributed among many branching faults, was aborted near the end of the Cretaceous. Extensive Paleogene thermal sag above the rift was followed by very minor compression and structural reactivation in the Neogene. The structure, stratigraphy, and evolution of the Euphrates Fault System is detailed in Chapter 5 in the context of the regional tectonic evolution.

Chapter 2 of this dissertation is an investigation of the deep structure of the Euphrates Fault System and the areas north and south of the rift. This study is based on the interpretation of a seismic refraction profile (see profile location in Figure 1.2). The powerful explosions used in the seismic acquisition and high density of data collection make this a very high quality dataset, unique for Syria. Offsets were long enough to record refractions from sedimentary basement in many places on the profile. These are the best constraints on basement depth available, as metamorphic basement is not penetrated by drilling or imaging on reflection data. The refraction data were interpreted using a ray-tracing approach together with other elements of our database to decrease ambiguity. The results show much deeper basement, and hence a thicker Paleozoic sedimentary section, south of the Euphrates. The interpretation also shows that the faulting in the Euphrates is complex, deep-seated, and steeply dipping.

Two topographically prominent uplifts in northeast Syria, the Abd el Aziz and Sinjar structures, reveal the location of the third major tectonic zone that is considered in Chapter 3 (see Figure 1.2 for location). Almost wholly unstudied in previously published work, the proximity to the northern Arabian margin and topographic expression made this an intriguing target for research. Chapter 3 presents many examples of seismic reflection profiles and maps that show the evolution of this zone. For much of the Late Paleozoic and Mesozoic the area was the northeastern extension of the Palmyride trough. This broad downwarping accumulated many thousands of meters of predominantly clastic Paleozoic strata and Mesozoic carbonates. In the latest Cretaceous this area was affected by the extensional tectonics that created the Euphrates Fault System. East – west striking normal faults formed the Abd el Aziz and Sinjar grabens that amassed up to 1.6 km of syn-extensional marly limestone. Chapter 3 goes on to show how these latest Cretaceous normal faults were structurally inverted from Late Pliocene time onwards. Fault-propagation folding above the

structurally inverted latest Cretaceous normal faults has created the topography that is observed in northeastern Syria today.

The fourth and final major tectonic zone is the Dead Sea Fault System, an active transform plate boundary in western Syria. Chapter 4, the final study of a specific area in this dissertation, examines the Ghab Basin, a pull-apart structure on the Dead Sea Fault System. The Plio-Quaternary age of the Ghab Basin suggests that the Dead Sea Fault System did not propagate through Syria until after the Miocene. This observation fits with previous models of two-phase Red Sea opening and Dead Sea Fault movement. The Late Cretaceous to Recent uplift of the Syrian Coastal Ranges is also documented. This prominent topography directly west of the Dead Sea Fault in Syria is shown to be part of the Syrian Arc deformation, albeit strongly modified on its eastern limb by the Dead Sea Fault System and Ghab Basin formation.

The ultimate result of this dissertation is a new regional tectonic evolutionary model for Syria, presented in Chapter 5. This brings together many of the observations made in Chapters 2, 3, and 4, together with results from previous research and new interpretations. For the first time, data from all Syria are considered in totality. Adding significantly to this is the incorporation of many stratigraphic observations that refine the timing of many of the tectonic events that are discussed, and set the model into a regional paleogeographic framework. Additional products include a series of subsurface structural maps for the whole country and a new lithostratigraphic chart.

The plates presented in the back pocket of this dissertation are discussed in Chapter 5. Plate 1 is a new tectonic map for Syria. It shows a summary of our mapped tectonic elements, together with Syria geology (Ponikarov, 1966), topography, seismicity and other

relevant data.  Annotations on the map make it a single primary reference for any researcher concerned with the structure and tectonics of Syria.  This mapping clearly shows how the vast majority of tectonic deformation within Syria is focused in the four major tectonic zones as outlined above.  Plate 2 is our regional tectonic evolutionary model.  It shows two different views of the northern Arabian Platform at twelve time points throughout the Phanerozoic.  The first view is of regional plate tectonic reconstruction (modified from Stampfli et al., 2000), and the second is a schematic map of tectonic deformation in Syria. The timelines on Plate 2 show the timing of global, regional, and local tectonic events.  In summary, Plate 2 contains the essence of all Cornell Syria Project work concerned with timing and styles of tectonic evolution.  This chart shows the contemporaneous evolution of many structures within Syria, and the relationships between this evolution and regional plate tectonic events.  To date, this is the single most complete tectonic summary, based on the most extensive data, ever proposed for Syria.

# REFERENCES

Al-Saad, D., T. Sawaf, A. Gebran, M. Barazangi, J. Best and T. Chaimov 1992. *Crustal structure of central Syria: The intracontinental Palmyride mountain belt*. Tectonophysics, **207,** 345-358.

Al-Saad, D., T. Sawaf, A. Gebran, M. Barazangi, J. Best and T. Chaimov 1991. *Northern Arabian platform transect across the Palmyride mountain belt, Syrian Arab Republic*. Global Geoscience Transect 1, The Inter-Union Commission on the Lithosphere and the American Geophysical Union, Washington, D. C.

Alsdorf, D., M. Barazangi, R. Litak, D. Seber, T. Sawaf and D. Al-Saad 1995. *The intraplate Euphrates depression-Palmyrides mountain belt junction and relationship to Arabian plate boundary tectonics*. Annali Di Geofisica, **38,** 385-397.

Barazangi, M., D. Seber, T. Chaimov, J. Best, R. Litak, D. Al-Saad and T. Sawaf 1993. *Tectonic evolution of the northern Arabian plate in western Syria.* In E. Boschi, E. Mantovani and A. Morelli (Eds.), Recent Evolution and Seismicity of the Mediterranean Region, Kluwer Academic Publishers, 117-140.

Best, J.A., M. Barazangi, D. Al-Saad, T. Sawaf and A. Gebran 1990. *Bouguer gravity trends and crustal structure of the Palmyride Mountain belt and surrounding northern Arabian platform in Syria*. Geology, **18,** 1235-1239.

Best, J.A., M. Barazangi, D. Al-Saad, T. Sawaf and A. Gebran 1993. *Continental margin evolution of the northern Arabian platform in Syria*. American Association of Petroleum Geologists Bulletin, **77,** 173-193.

Chaimov, T., M. Barazangi, D. Al-Saad and T. Sawaf 1993. *Seismic fabric and 3-D upper crustal structure of the southwestern intracontinental Palmyride fold belt, Syria*. American Association of Petroleum Geologists Bulletin, **77,** 2032-2047.

Chaimov, T., M. Barazangi, D. Al-Saad, T. Sawaf and A. Gebran 1990. *Crustal shortening in the Palmyride fold belt, Syria, and implications for movement along the Dead Sea fault system*. Tectonics, **9,** 1369-1386.

Chaimov, T., M. Barazangi, D. Al-Saad, T. Sawaf and A. Gebran 1992. *Mesozoic and Cenozoic deformation inferred from seismic stratigraphy in the southwestern intracontinental Palmyride fold-thrust belt, Syria*. Geological Society of America Bulletin, **104,** 704-715.

Litak, R.K., M. Barazangi, W. Beauchamp, D. Seber, G. Brew, T. Sawaf and W. Al-Youssef 1997. *Mesozoic-Cenozoic evolution of the intraplate Euphrates fault system, Syria: implications for regional tectonics*. Journal of the Geological Society, **154,** 653-666.

Litak, R.K., M. Barazangi, G. Brew, T. Sawaf, A. Al-Imam and W. Al-Youssef 1998. *Structure and Evolution of the Petroliferous Euphrates Graben System, Southeast Syria*. American Association of Petroleum Geologists Bulletin, **82,** 1173-1190.

McBride, J.H., M. Barazangi, J. Best, D. Al-Saad, T. Sawaf, M. Al-Otri and A. Gebran 1990. *Seismic reflection structure of intracratonic Palmyride fold-thrust belt and surrounding Arabian platform, Syria*. American Association of Petroleum Geologists Bulletin, **74,** 238-259.

Ponikarov, V.P. 1966. *The Geology of Syria. Explanatory Notes on the Geological Map of Syria, Scale 1:200 000*. Ministry of Industry, Damascus, Syrian Arab Republic.

Sawaf, T., D. Al-Saad, A. Gebran, M. Barazangi, J.A. Best and T. Chaimov 1993. *Structure and stratigraphy of eastern Syria across the Euphrates depression.* Tectonophysics, **220,** 267-281.

Seber, D., M. Barazangi, T. Chaimov, D. Al-Saad, T. Sawaf and M. Khaddour 1993. *Upper crustal velocity structure and basement morphology beneath the intracontinental Palmyride fold-thrust belt and north Arabian platform in Syria.* Geophysical Journal International, **113,** 752-766.

Stampfli, G.M., J. Mosar, P. Favre, A. Pillevuit and J.-C. Vannay 2000. *Permo-Triassic evolution of the western Tethyan realm: The NeoTethys / east Mediterranean basin connection.* In W. Cavazza, A.H.F. Robertson and P. Ziegler (Eds.), Peritethyan rift/wrench basins and margins, PeriTethys Memoir #6, in press, Museum National d'Historie Naturelle, Paris.

# CHAPTER TWO

# Basement Depth and Sedimentary Velocity Structure in the Northern Arabian Platform, Eastern Syria[*]

## ABSTRACT

Basement depth in the Arabian plate beneath eastern Syria is found to be much deeper than previously supposed. Deep-seated faulting in the Euphrates fault system is also documented. Data from a detailed, 300 km long, reversed refraction profile, with offsets up to 54 km, are analyzed and interpreted, yielding a velocity model for the upper ~ 9 km of continental crust. The interpretation integrates the refraction data with seismic reflection profiles, well logs and potential field data, such that the results are consistent with all available information. A model of sedimentary thicknesses and seismic velocities throughout the region is established. Basement depth on the north side of the Euphrates is interpreted to be around 6 km, whilst south of the Euphrates basement depth is at least 8.5 km. Consequently, the potentially hydrocarbon-rich pre-Mesozoic section is shown, in places, to be at least 7 km thick. The dramatic difference in basement depth on adjacent sides of the Euphrates graben system may suggest that the Euphrates system is a suture / shear zone, possibly inherited from Late Proterozoic accretion of the Arabian plate. Gravity modeling across the southeast Euphrates system tends to support this hypothesis. Incorporation of previous results allows us to establish the first-order trends in basement depth throughout Syria.

---

**INTRODUCTION AND GEOLOGIC BACKGROUND**

We present an interpretation of seismic refraction data collected along a north-south profile in eastern Syria. The refraction data are interpreted in conjunction with well logs, seismic reflection data, gravity and magnetic data. Hence, previously unknown metamorphic basement depth, and pre-Mesozoic sedimentary thickness, in eastern Syria are established. Along with indications of basement and deep sedimentary structure, this can help to determine the intracontinental tectonic processes that have shaped the region.

The tectonic setting of Syria within the Arabian plate (Figure 2.1) shows that the country is almost surrounded by active plate boundaries. The western boundary is marked by the left-lateral Dead Sea fault system which extends from the Gulf of Aqaba in the south to the Cyprus subduction zone - Bitlis suture - Dead Sea transform triple junction in the north. The Dead Sea fault marks the boundary between the Arabian plate to the east and the Levantine (east Mediterranean) subplate to the west. To the north of Syria lies the Bitlis suture which represents the collision zone of the Arabian and Eurasian plates. Continuing movement along this boundary is accommodated by thrusting along the Bitlis suture as well as movement on the East Anatolian left-lateral fault, as the Anatolian subplate escapes collision. To the east and southeast of Syria the Neogene-Quaternary Zagros fold belt marks the collision zone of the Arabian plate with Iran (e.g. Sengor and Kidd 1979; Sengor and Yilmaz 1981).

It is generally believed that the movement along the surrounding plate boundaries controls the intraplate deformation observed in Syria (e.g. Barazangi et al. 1993). The two major structural features of the country are the Palmyride fold and thrust belt of
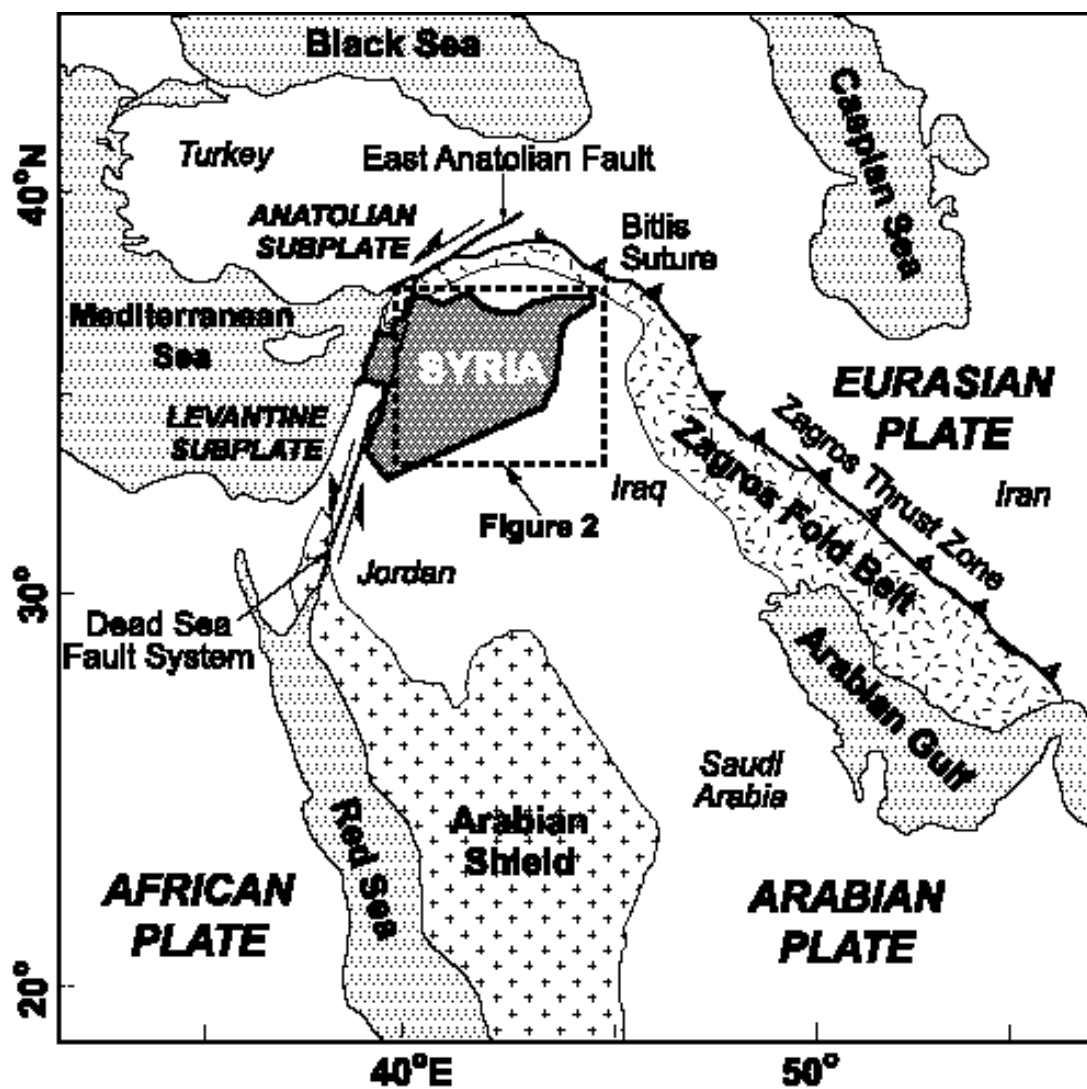
**Figure 2.1:** Regional tectonic setting of the northern Arabian platform.
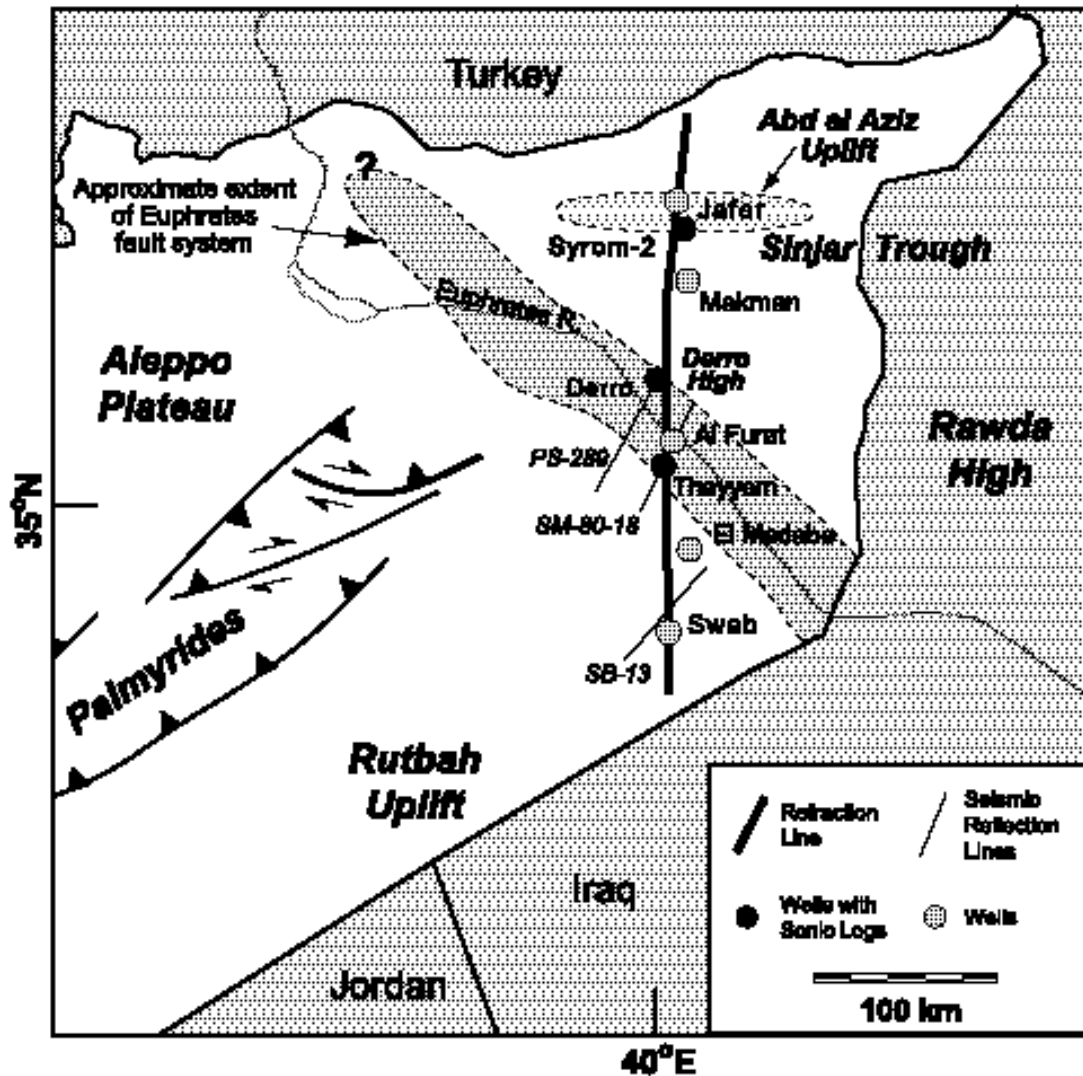
**Figure 2.2:** Map of eastern and central Syria showing location of selected data sources. Shaded area represents approximate location of Euphrates fault system. The extent of the faulting to the north and into Turkey is largely unconstrained. Only a small portion of the total number of seismic reflection lines used in this study are shown. Substantial additional well data farther from the refraction line were also available.

central Syria, and the Euphrates fault system in the east (Figure 2.2). It has been suggested (e.g. Best et al. 1990) that these structures could be formed by reactivation along zones of weakness in the Arabian plate - weaknesses that have perhaps persisted since the Proterozoic (e.g. Barazangi et al. 1993; Litak et al. 1997). However, whilst an appreciable amount of research has been conducted in the Palmyrides (e.g. Chaimov et al. 1990; McBride et al. 1990; Al-Saad et al. 1992; Barazangi et al. 1992), relatively little work has focused on eastern Syria. In particular, the Euphrates system has received limited attention in comparison to its geologic and economic importance (e.g. Beydoun 1991; de Ruiter et al. 1994). Recent work (Sawaf et al. 1993; Alsdorf et al. 1995; Litak et al. 1997, 1998) has increased understanding of the Euphrates system, but detailed assessment of basement structure and depth in this region has, until now, been unavailable. Hence, our results are a valuable contribution to the knowledge and understanding of the regional structure and tectonics of eastern Syria.

The area of eastern Syria focused upon in this study can be roughly divided into four structural zones of intraplate deformation, within which the deformation appears to be controlled by movement on the nearby plate boundaries. From north to south these are the Abd el Aziz structural zone, the Derro high, the Euphrates fault system and the Rutbah uplift (Figure 2. 2).

The Abd el Aziz uplift is an anticlinorium controlled mainly by a major south-dipping reverse fault (e.g. Ponikarov 1967; Lovelock 1984). It is thought that the Abd el Aziz was a sedimentary basin in the Mesozoic which inverted in the Neogene (Sawaf et al. 1993), and may have been the northwestern edge of the larger Sinjar trough which existed at that time (Lovelock 1984).

South of Abd el Aziz, and to the north of the Euphrates, is a series of structural highs, controlled by deeply penetrating faults. Most prominent of these is the Derro high which is interpreted to be bounded by north-dipping reverse faults that separate this area from the Abd el Aziz (Sawaf et al. 1993). Basaltic outcrops along some of the larger faults around the Derro high could offer further evidence for the deep-seated nature of faulting in this area.

Although largely unexpressed by surface features, the Euphrates fault system represents an aborted rift system, striking roughly NW-SE and extending completely across Syria. The faulting is thought to represent a Late Cretaceous transtensional graben system with minor reactivation in Neogene times (Lovelock 1984). The system can be roughly divided into three parts along its length (Litak et al. 1997): a northwestern segment exhibiting shallow grabens and significant inversion; a central segment where the Euphrates system bounds the Palmyrides and strike-slip movement is apparent; and the southeastern part which is characterized by deep graben features and only very minor inversion (Figure 2.2). Although Lovelock (1984) suggested that most movement in the system took place on a few major faults, recent work clearly indicates that the deformation is widely distributed (de Ruiter et al. 1994; Litak et al. 1997, 1998). Faulting, for the most part, is nearly vertical in most places, resulting in limited (< 6 km) extension across the system (Litak et al. 1998).

The southernmost section of the refraction profile crosses the eastern edge of the Rutbah uplift, an extensive upwarp which affects large parts of western Iraq, northern Jordan and southern Syria. Doming and extensive erosion of the area is known to have taken place during the Mesozoic and Tertiary (e.g. Lovelock 1984). Very little deformation is found in the strata of the Rutbah Uplift, except along the northeastern edge where it trends into the Euphrates depression.

**Basement Rocks in Syria**

The lack of current constraints on basement depth in Syria is a consequence of an almost complete absence of basement outcrops, and only one well, in the far northwest of the country, has penetrated the Precambrian (Ponikarov 1967). The few basement exposures that exist are in northwest Syria, Jordan, southern Israel and in southern Turkey, all at extensive distances from the study area, and in different geologic regimes (Ponikarov 1967; Sawaf et al. 1993). Leonov et al. (1989) constructed a depth to basement map within Syria based on well data and seismic reflection data, thus establishing the broad trends which are still generally accepted. However, the small scale and lack of direct evidence used in the study of Leonov et al. (1989) limit its applicability and new results presented here disagree somewhat with this earlier assessment. Best et al. (1993) mapped basement for the whole of Syria by using a prominent Mid-Cambrian reflection event as a proxy for basement rocks. However the results presented here show there can be substantial differences between the depth of the Middle Cambrian and basement rocks. Seber et al. (1993), using seismic refraction data, established basement depths in central Syria to be around 6 km beneath the Aleppo Plateau, 9-11 km beneath the Palmyrides and at least 8 km in the south of the country. Additionally, Seber et al. (1993) found seismic velocities of basement rocks to be around 6 km/s, in agreement with the findings of refraction surveys in Jordan which interpreted basement velocities of 5.8 - 6.5 km/s (Ginzburg et al. 1979; El-Isa et al. 1987). However, in the absence of previous investigations in eastern Syria, the results presented here offer a unique assessment of basement depth in this region, and hence offer new insight on the deformational history of the northern Arabian platform.

**DATA ANALYSIS**

**Data Acquisition**

The model of basement depth and deep sedimentary structure that we develop relies on the analysis of several data sources, particularly a 300 km long seismic refraction profile. The refraction data were collected as part of a larger seismic profiling effort spanning all of Syria, conducted by a Soviet/Syrian joint project in 1972-3. Nine refraction lines were shot, totaling 2592 km, providing unique data for the study of deep sedimentary structure.

The original analysis of the seismic refraction data (Ouglanov et al. 1974) relied on interpretation techniques that established velocities using simplistic formulae that are now known to be problematic. Additionally, the original interpretation attached stratigraphic significance to some of the velocity contrasts observed in the refraction interpretation. Data from wells drilled since this initial interpretation show these stratigraphic inferences to be incorrect. However, as this old interpretation was never written in final form, and was never published, further results of the 1974 analysis of the data are not discussed here. With the benefit of technological advances in the interpretation of these type of data, and aided by extensive supplementary data sources, we present a new interpretation of the original data showing basement depth to be much greater than originally interpreted.
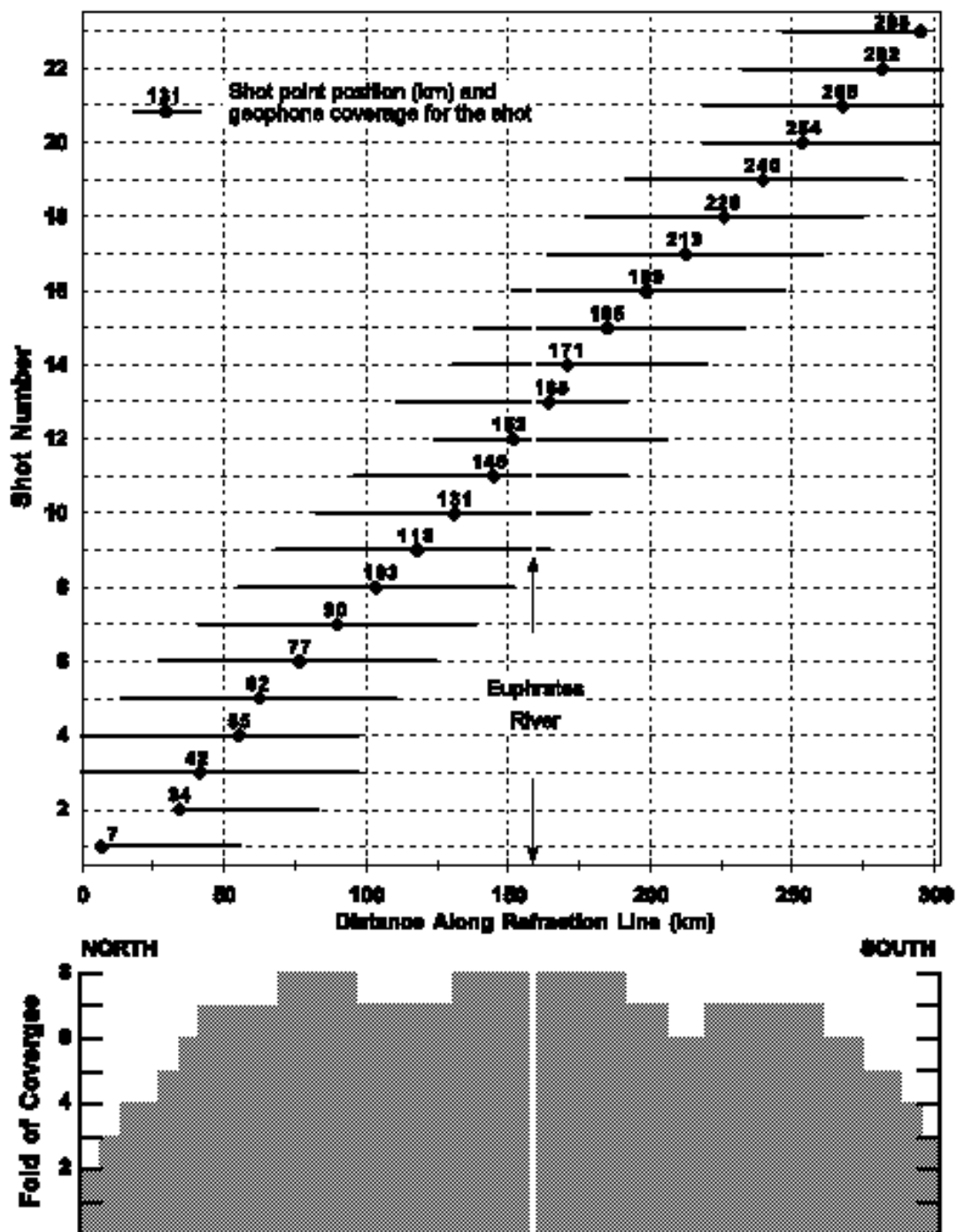
**Figure 2.3**: Configuration of shots and geophone spreads used in the refraction interpretation. Cumulative fold of coverage also shown.

Figure 2.2 shows the location of the refraction profile, the seismic reflection lines and the well logs used in this interpretation. The refraction line is 302 km long and oriented north-south. A total of 44 shot points were employed along the profile having a spacing of approximately 7 km. Shot sizes varied between 50 and 1250 kg dependent on geophone offset; data were recorded along forward and reverse geophone spreads for each shot, and geophone spacing was 150 meters. For most shots both a high and low gain analog recordings were made. The geophone spreads were of two types: every second shot point had 'short' spreads of 28 km maximum offset and the remaining, 'long', spreads had nominal maximum offsets of 48 km, with the longest spread being 54 km.

Since deep sedimentary structure was the primary focus of this investigation, it was decided that the shorter spreads (28 km offsets) contained little data that could not be obtained independently from the longer spreads. Thus, data from 23 shots, each with forward and reverse geophone spreads, are used in our interpretation. This yields a fold of coverage at least 700% in most places (Figure 2.3), unusually high for a survey of this type.

In analyzing these data the original photographic analog recordings from the survey were used to digitize first and, wherever possible, subsequent arrivals. Recognition of first arrivals was generally unambiguous owing to large shot sizes and relatively quiet recording conditions (Figure 2.4). Identification of subsequent arrivals, however, was generally precluded by the large amplitudes of the traces and short recording times. A total of approximately 17,000 arrivals were digitized.

**Figure 2.4:** Typical example of original refraction data. Part of reverse spread from shot 17. Note the good quality of first arrivals (highlighted with line added by authors) which were digitized to accomplish a ray-traced interpretation.

SHOT 17
213 km
Shot Size: 90 kg
Shot Depth: 45 m
High Gain Record
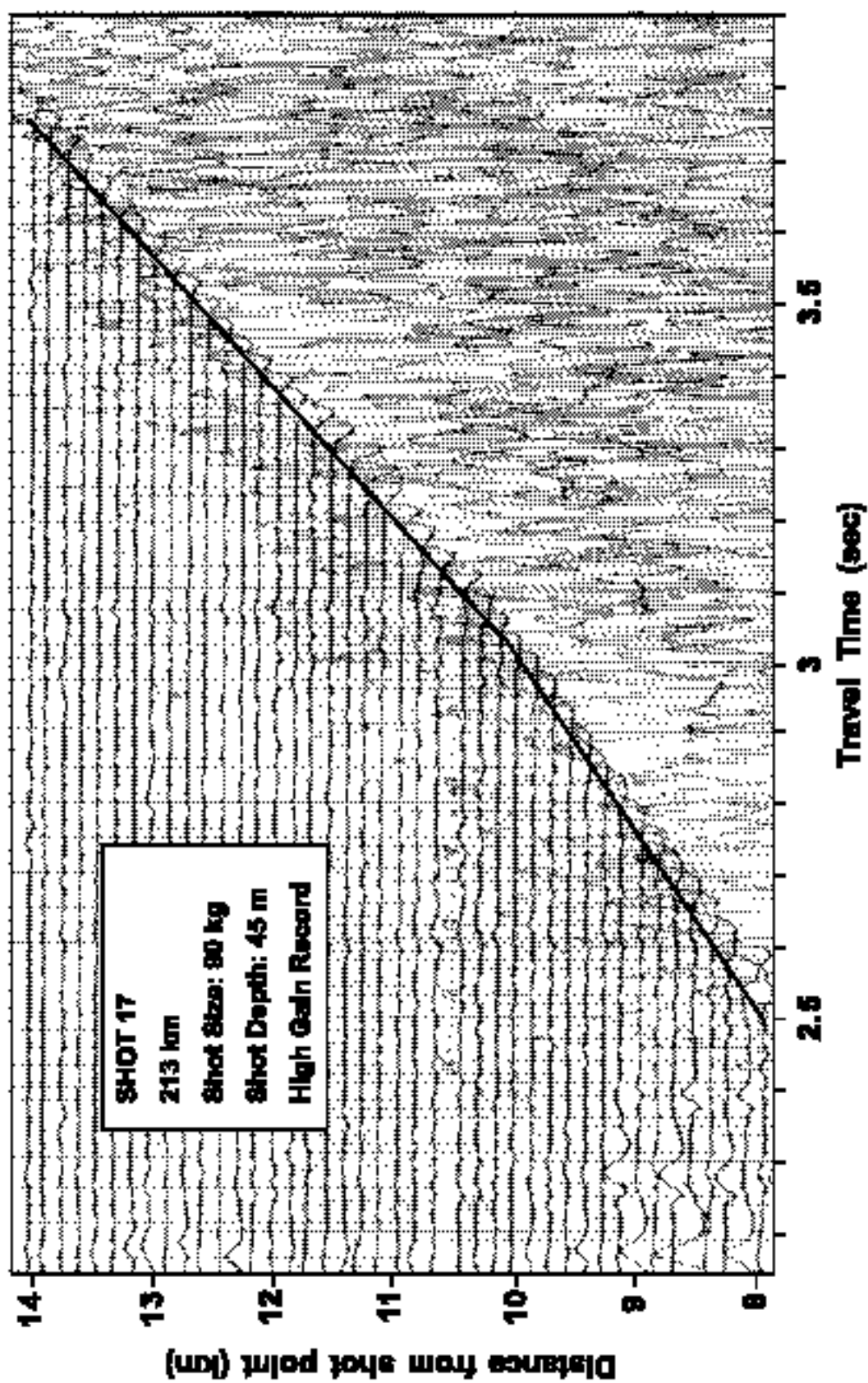
**Data Interpretation**

The refraction data were interpreted using a geometric ray-tracing approach utilizing the software of Luetgert (1992). Preliminary interpretation involved simple refraction modeling; the positions and velocities of various user-defined layers in the software were subtly altered until travel times of calculated rays-paths through the computer model matched those of the digitized arrival times. This preliminary-type interpretation produced a 7 layer model with seismic velocity increasing in each deeper layer. Although naturally in agreement with the refraction data, the velocity interfaces in this model were found to be in disagreement with some velocity boundaries observed in sonic logs and travel times from seismic reflection data. The disagreement was largely a consequence of the limitations in the refraction method, in particular the inability to resolve low-velocity layers that are clearly demonstrated by the sonic logs (Figure 2.5).

However, the ambiguity of low-velocity layers can be eliminated if velocity information is available from an independent source, or if reflection travel times are known in addition to refraction times (e.g. Kaila et al. 1981). Therefore, an interpretation strategy was adopted in which the refraction, reflection and well data were used simultaneously in the refinement of the velocity model, thus establishing a model consistent with all available data. This began with the construction of an initial velocity model constrained at shallow depths (< 4 km) by seismic reflection and well data, with sonic logs from parts of 3 wells (Figure 2.2) allowing estimates of seismic velocities. The deeper section of the initial model was less constrained and relied on extrapolation from the shallow section and limited reflection data. The ground surface of the model was extracted from digital topographic data, sub-sampled to approximately 1 km horizontal resolution. The initial model was refined through ray-

**Figure 2.5:** Sonic log and synthetic seismogram from Derro well (see Figure 2.2 for location). Velocities from final velocity model shown by heavy gray line on same scale. Sonic logs from this and several other wells were used to constrain the velocity model. Note the low-velocity Upper Paleozoic strata which are undetectable by refraction data alone. Seismic line PS-289 at the tie with the Derro well is shown for comparison to the synthetic seismogram.

| Selected Horizons from Well Log | Depth below ground level (meters) | Sonic Velocity and Velocity Model (km / s) | Synthetic Seismogram with AGC | Seismic Line PS-289 at tie with well | TWT Time (sec) |
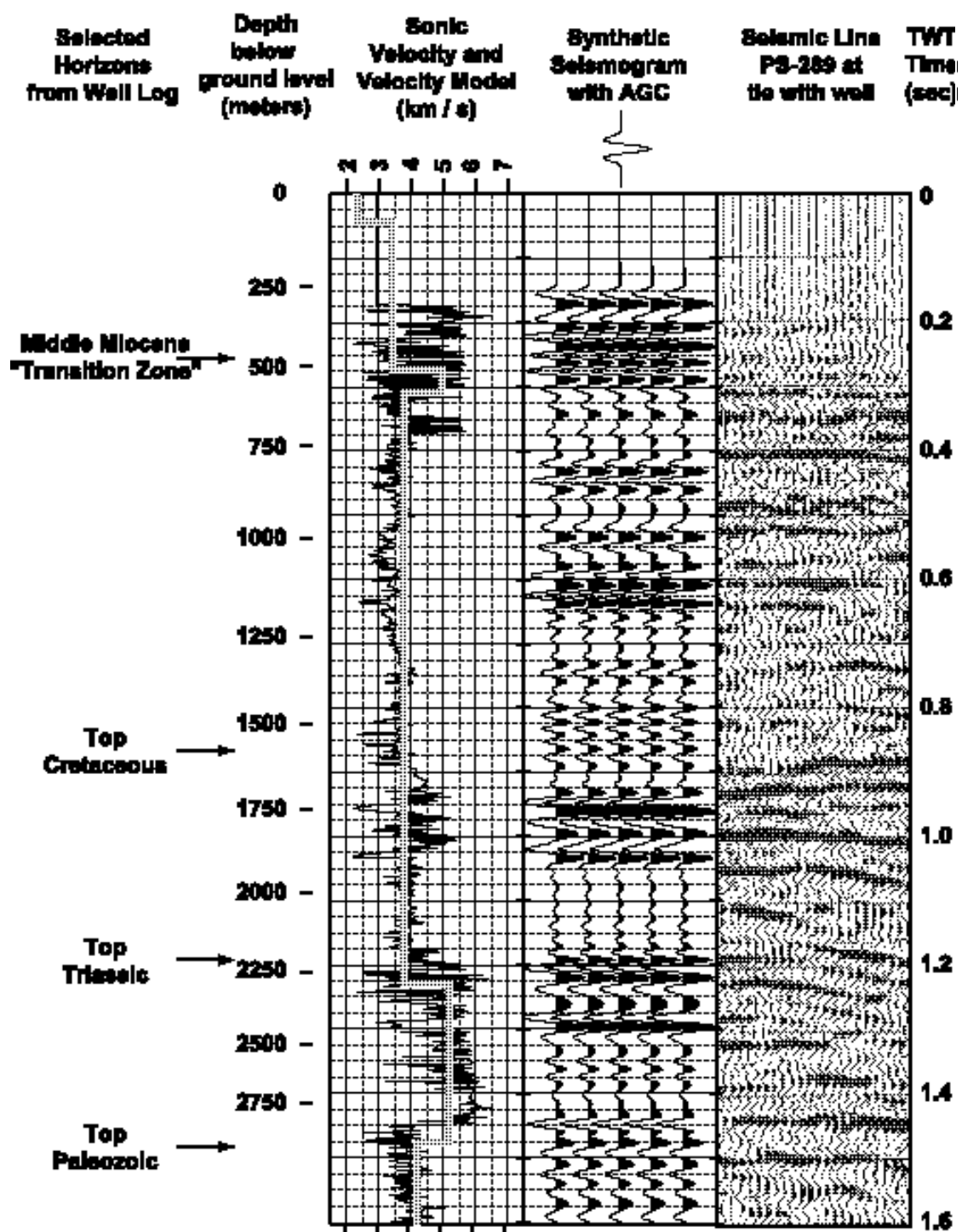
tracing to improve agreement with the various data, in particular the refraction arrival times. The modeling effort, described further below, culminated in what is hereafter referred to as the 'final velocity model' - a model consistent with all the available data.

Due to the high fold of coverage of the refraction data, and the various other constraining data, many iterations were necessary to produce a velocity model in agreement with all the data. The refraction interpretation was done by taking each individual shot in turn, and changing the velocity model to produce the best between the observed and the calculated arrivals for that shot. However, due to the higher than 100% fold of coverage, modifications made to the model by examining the fit for one shot obviously changed the fit between the observed and calculated arrivals for other adjacent shots. Thus, after each change to the velocity model, the fit between the calculated and observed arrivals from every shot had to be checked. The final velocity model was determined by obtained the best overall fit of the arrivals for all the shots. Although this was extremely time-consuming, the process yielded an essentially unique velocity model that is in agreement with all the refraction arrivals.

It was clear from the integrated modeling that some of the velocity interfaces detected by the refraction data coincided with age horizons and associated velocity changes in sonic log data. Figure 2.5 shows the sonic log and synthetic seismogram from the Derro well, along with velocities from the final velocity model. This shows how the velocities in the final model fit those found in the sonic log, whilst at the same time the depths of the velocity interfaces match the depths of certain age horizons found in the well. Where such correlations were observed the velocity model was modified to fit both the well data and the refraction data as accurately as possible.

**Figure 2.6:** Examples of correlations between seismic reflection data and two-way incidence reflection times deduced from the velocity model (see Figure 2.2 for location of seismic reflection lines). Interfaces not corresponding to velocity changes are shown as dotted lines on the velocity graph. Uncertain velocity interface positions shown as long dashed lines.

a) 8N B0-1B
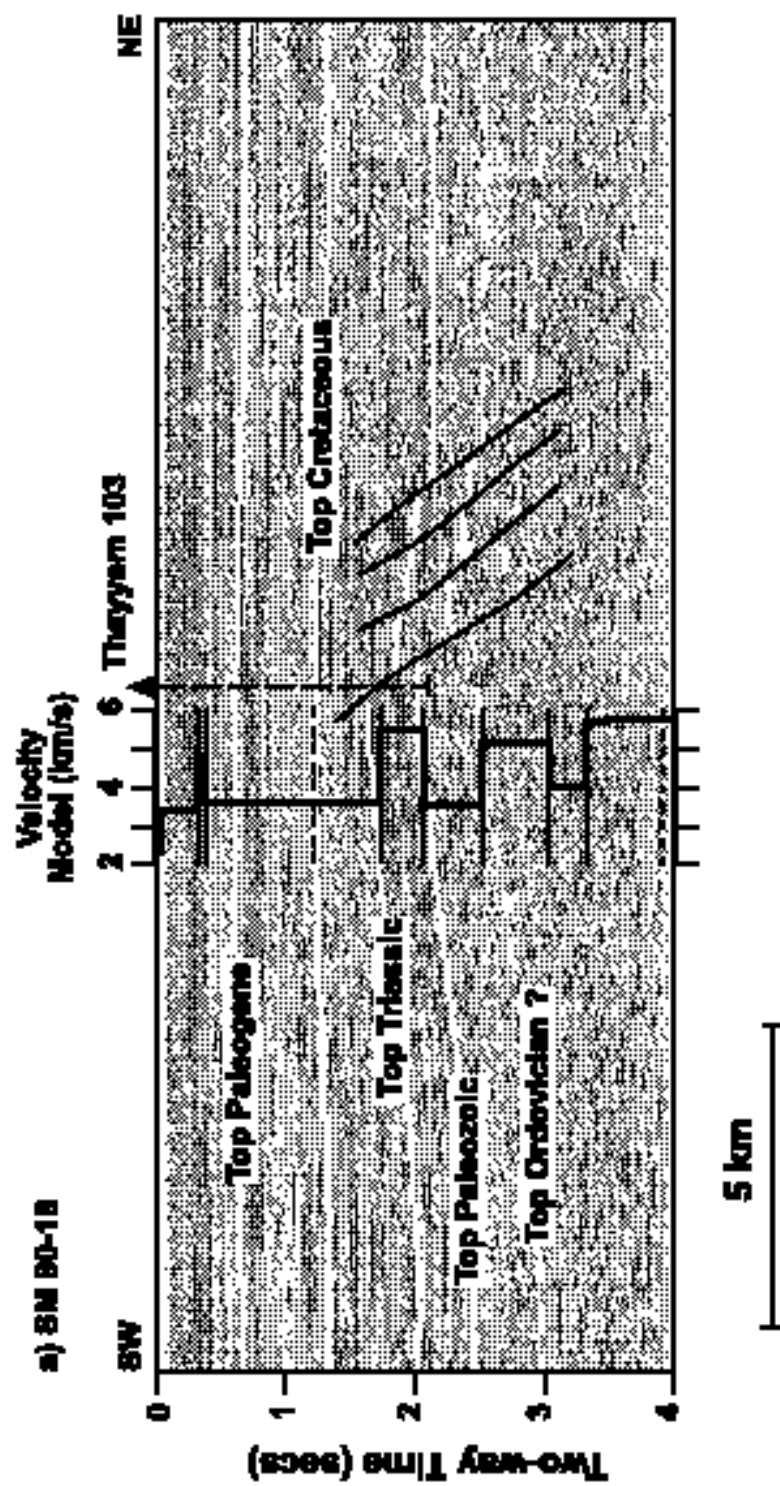
Figure 2.6 (continued):
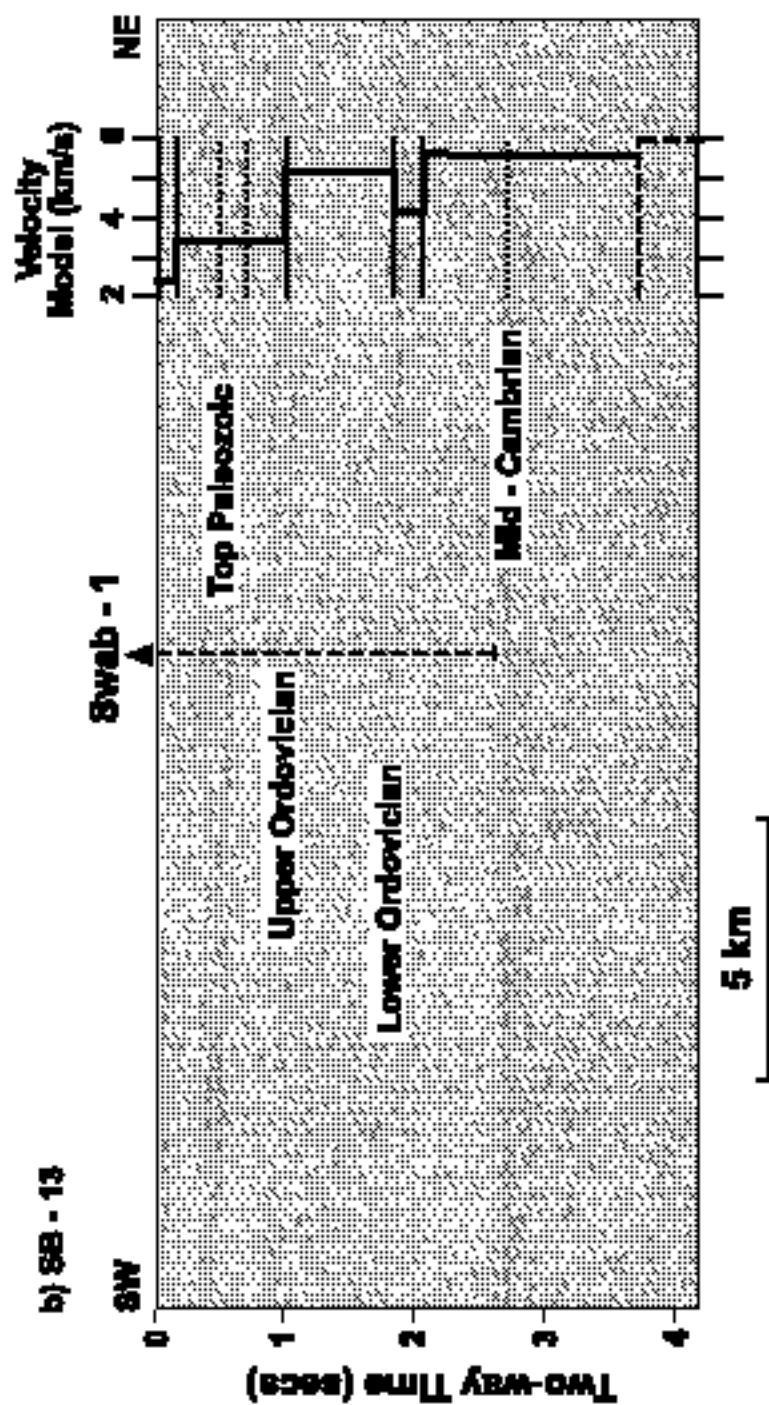
Knowing the age of certain velocity interfaces, reflection data were utilized in conjunction with the refraction data. Two-way reflection times derived from the final velocity model and those from seismic reflection data were compared to support the refraction interpretation and add further detail which could not be resolved by the refraction method alone. For example, faults interpreted from seismic reflection data were used to refine the detail of the final velocity model (e.g. Figure 2.6a). Figure 2.6 shows examples of how two-way times in the final velocity model compare to those from seismic reflection data. Although not all prominent reflections are associated with refractions (e.g. mid-Cambrian reflector, Figure 2.6b) most of the reflectors are correlated to refracting horizons, indicating a similar physical nature for refracting and reflecting horizons.

Aeromagnetic data (Filatov and Krasnov, 1959) show few anomalies of interest from the study region, with generally long wavelength, low amplitude variations indicating sources at significant depths. Assuming the source of the anomalies to be basement rocks then the magnetic data agree with the observations of large basement depths established in the velocity model, with shallower sources in the north. Isolated patches of short wavelength, high amplitude magnetic anomalies correspond with known basaltic outcrops. Additionally, gravity observations along the profile (BEICIP 1975) were compared to the gravity signature of the velocity model, with each velocity layer assigned an appropriate density. In this case also, the calculated and observed observations show overall agreement. More analysis of gravity data is presented in the next section.

**The Final Velocity Model**

The final velocity model that satisfactorily fits all available data is presented in Figure 2.7a. The velocities in some of the layers change laterally, but layers have uniform velocities in a

vertical direction. Well data along the profile, superimposed on the velocity interfaces and their presumed stratigraphic significance, demonstrate the close semblance between the model and well data (Figure 2.7b).

However, despite direct evidence for the majority of the model, a few uncertainties remain. For example, no direct evidence exists for parts of some low velocity layers, hence the exact position of these horizons is, in places, uncertain. It is also not possible to obtain exact measures of the velocities of the low-velocity zones in these cases and so parts of the layers have been given velocities that are interpolations between well-determined values. Additionally, the depth to basement in the far south of the model is only thought to be a minimum constraint. No refractions were observed in this part of the refraction profile at velocities considered typical of those for metamorphic basement rocks, either because basement velocities are appreciably slower in this region, or because the geophone spreads employed were too short to sample refractions from the apparently deeper basement in this region. The latter explanation is considered more probable, therefore the depth to basement shown is a minimum (Figure 2.7). Another uncertainty concerns the interface signified as top of Khanasser (Lower Ordovician) in the north of the model. The interface interpreted based on the refraction data does not correspond exactly with observations from the Jafer well (Figure 2.7b). Therefore, the refractor in this region is labeled 'Infra-Khanasser'.

**Figure 2.7:** Cross section showing the final velocity model. Model interfaces not corresponding to velocity changes are shown as dotted lines. Uncertain interfaces positions shown as long dashed lines. (a) shows seismic velocity model and interface positions. Locations of shots used in Figure 2.8 also shown. (b) demonstrates the correlation between the velocity interfaces and age boundaries sampled in wells along the refraction profile.

a)

Figure 2.7 (continued):
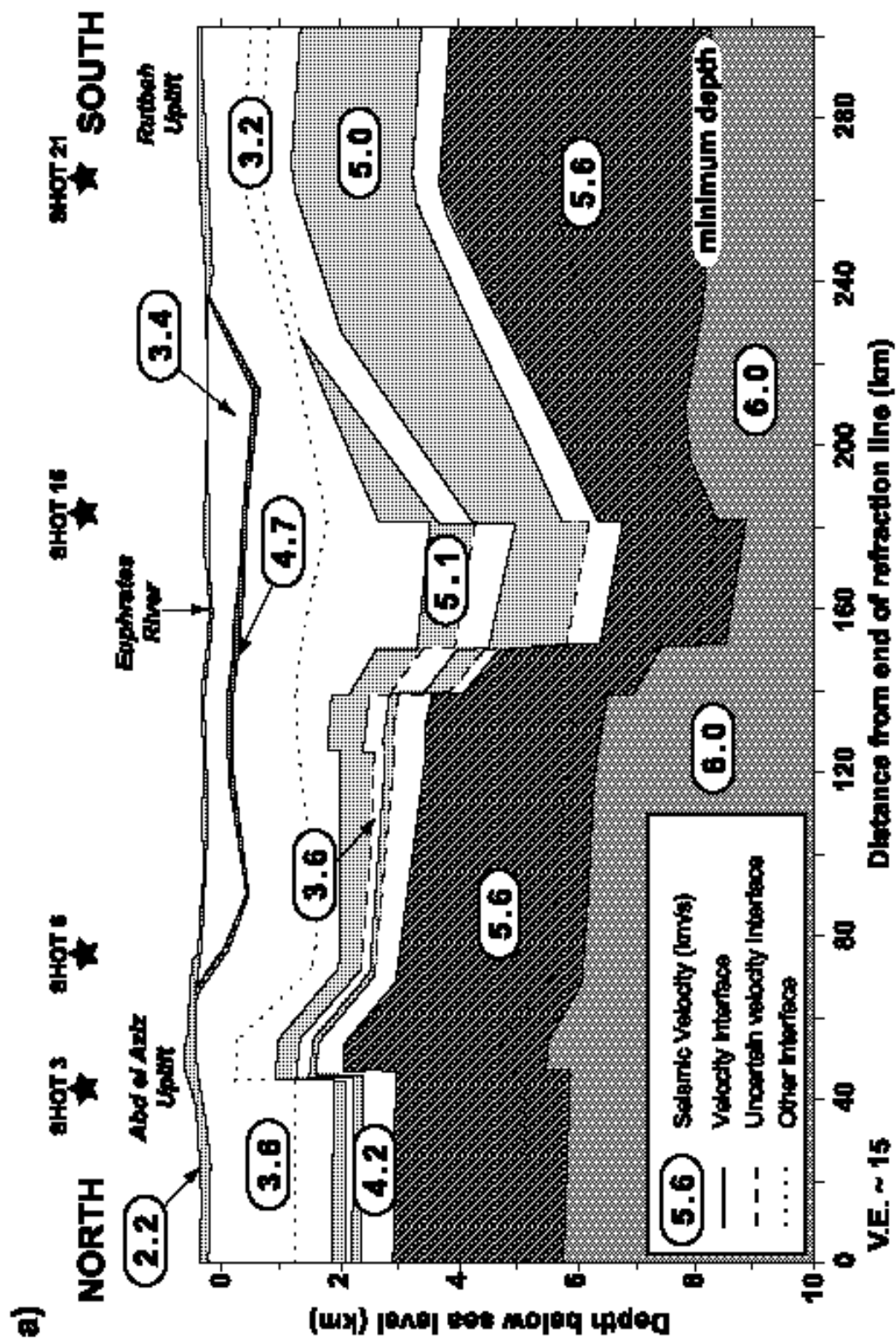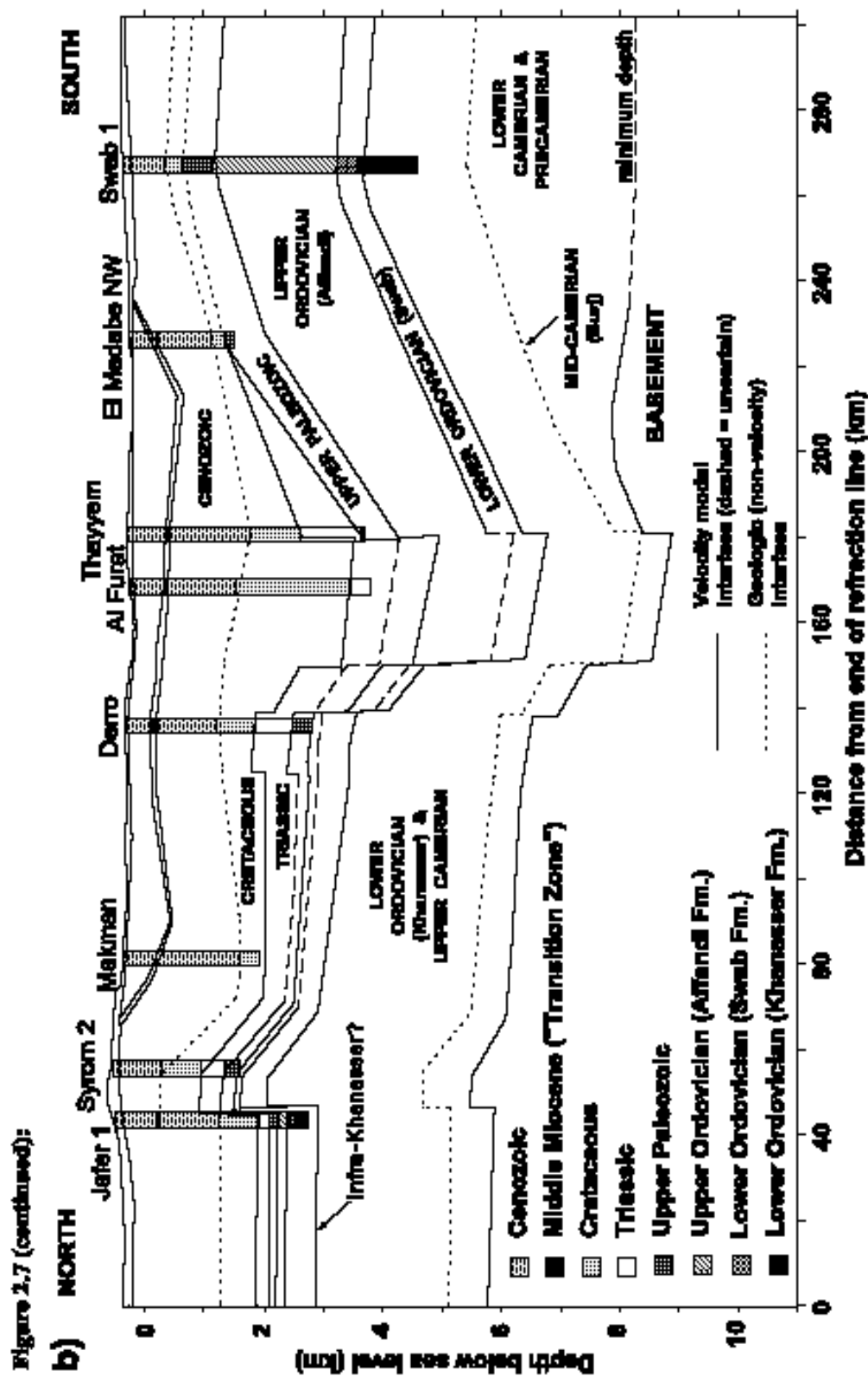
Despite these shortcomings, the majority of the final velocity model is based on direct evidence from at least one and, in many cases, several sources. In general, the modeled refraction times show excellent agreement with the observed arrivals from the refraction data. Four examples of this, from various points in the transect, are shown in Figure 2.8. Each of the other shots, not shown here, demonstrate similar agreement between the velocity model and the observed arrival times. Given reasonable inaccuracies in the fit between observed and calculated refraction arrivals, such as those indicated in Figure 2.8, the errors in the bulk of the model can be shown to be relatively small, with approximately $\pm$ 200 m error in depth to most interfaces and less than $\pm$ 0.1 km/s in velocities.

## DISCUSSION

A model of seismic velocity down to basement in eastern Syria has been constructed from the interpretation of refraction data and additional coincident data sources (Figure 2.7). The model shows basement-involved tectonics beneath the Euphrates graben system and the Abd el Aziz uplift. The faulting is steeply dipping (even though the model is oblique to the dominant strike of the area), a result supported by the extensive seismic reflection analysis of Litak et al. (1998). In the area where the refraction transect crosses the Euphrates, Litak et al. (1998) reported that the graben morphology in the upper sedimentary section is similar to the 'classic' model of a normally-faulted rift system, more so than elsewhere along the Euphrates. Our model shows this style of faulting persists to basement depth.

The model indicates that whilst increasing formation age generally causes increasing seismic velocity, velocity is also controlled by depth of burial and, more significantly,

**Figure 2.8:** Examples of ray-tracings from the final velocity model chosen to represent the full range of structures interpreted along the transect. Numbers represent seismic velocities in km/s. Note the effect of the near-surface high-velocity layer in (c). Modeled refractions from basement in (d) do not necessarily fit observed arrivals, but are shown to illustrate that basement depth for this part of the model is a minimum.
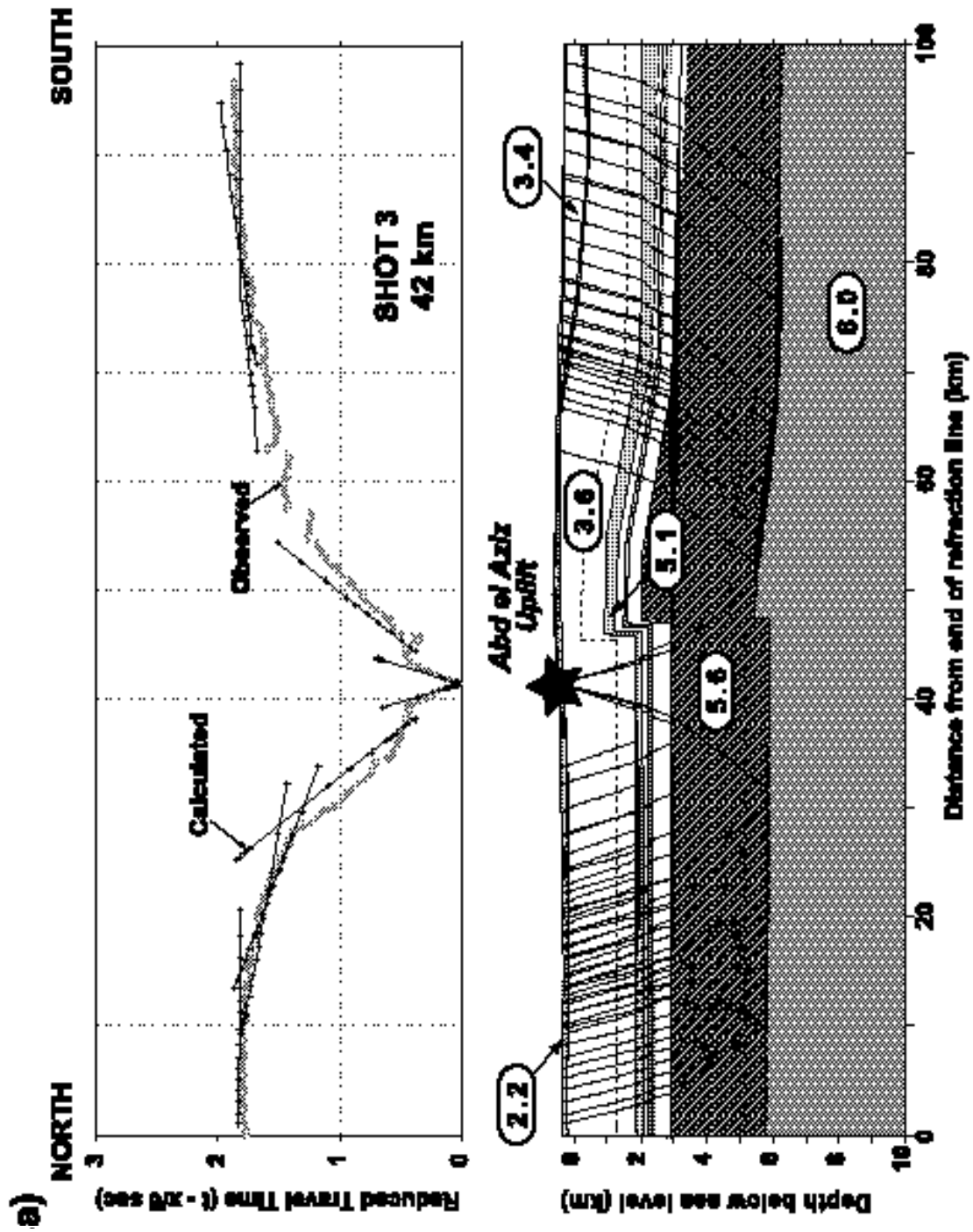
Figure 2.8 (continued):

Figure 2.6 (continued):

42



Figure 2.8 (continued):

d) NORTH ... SOUTH
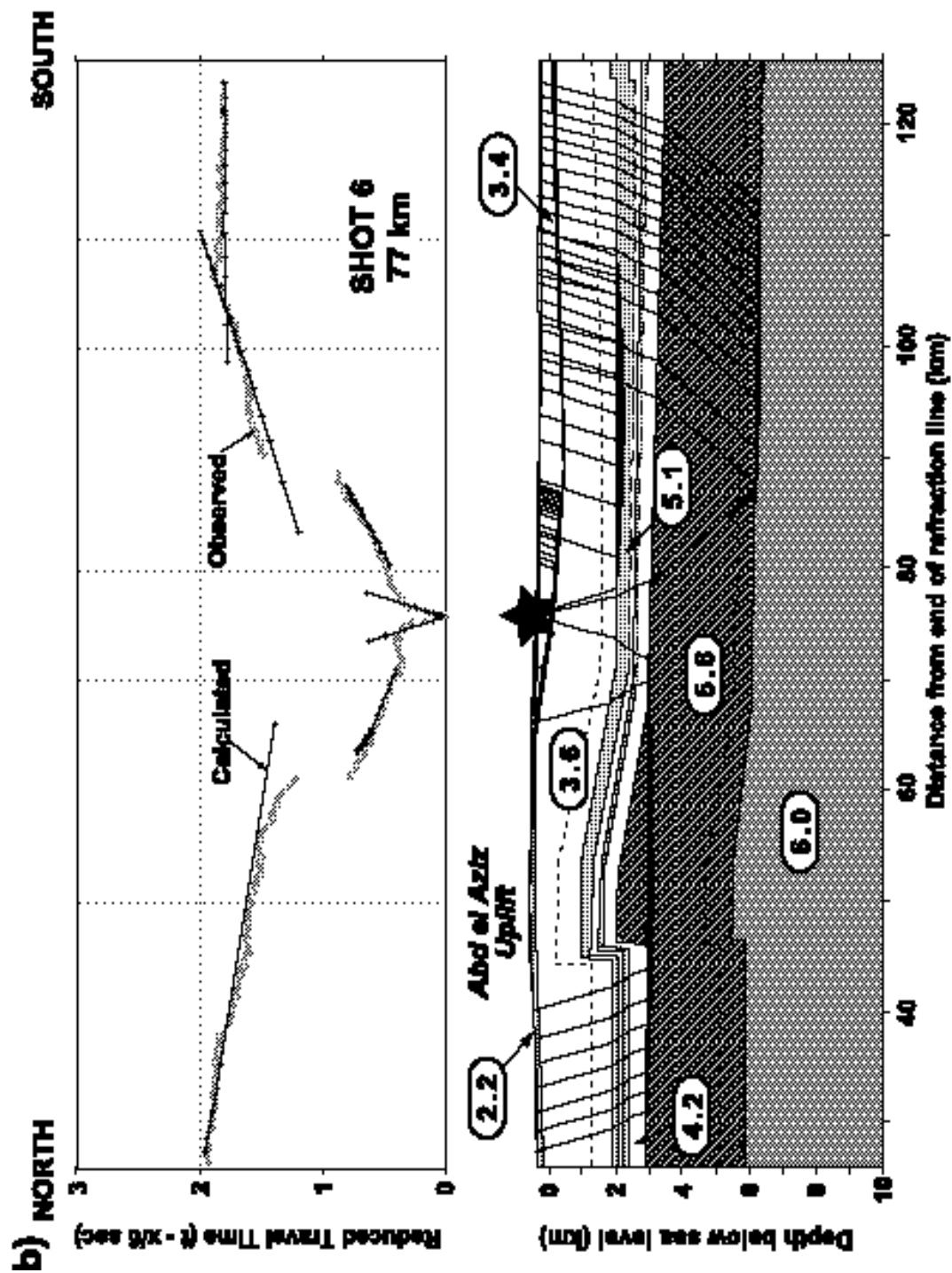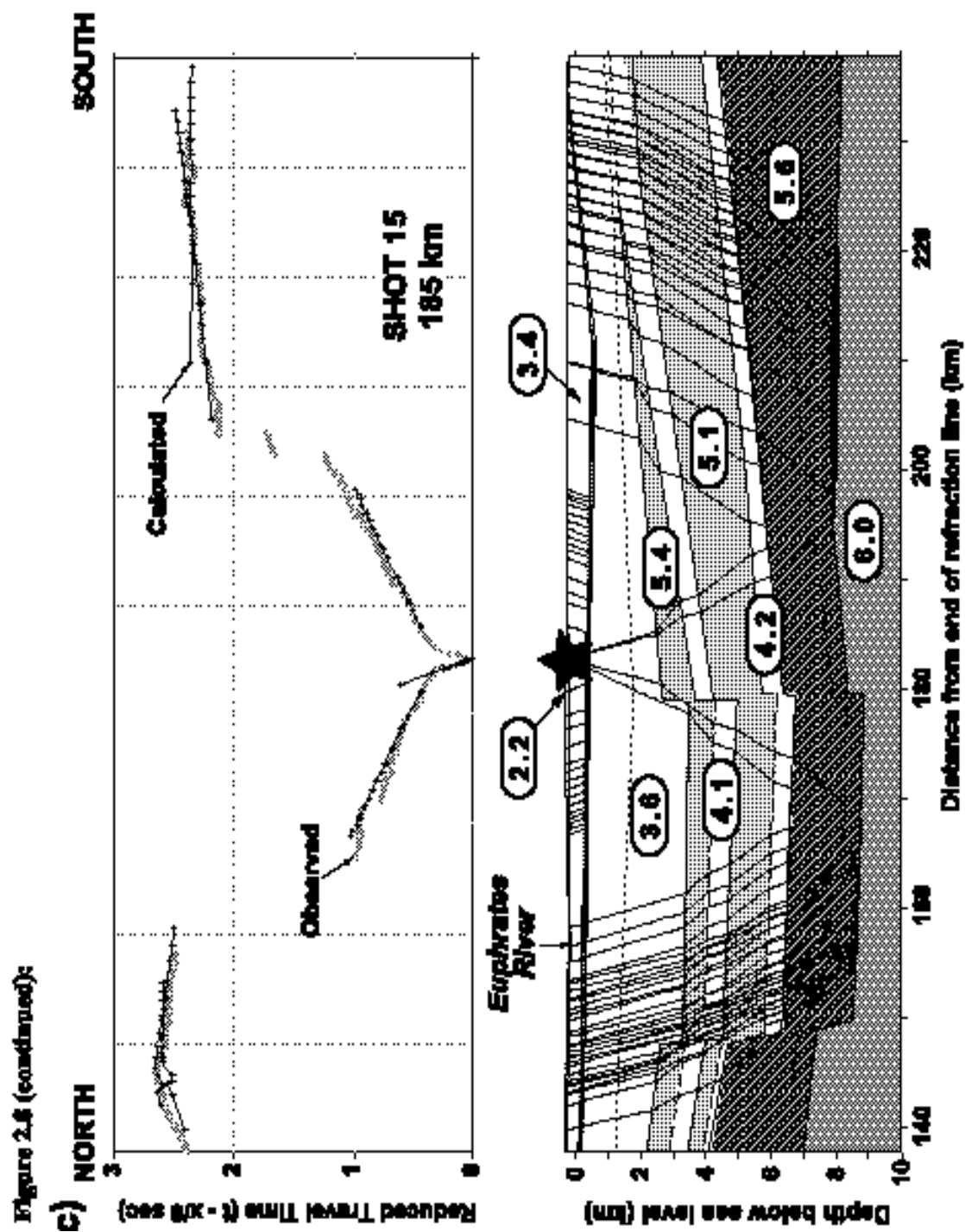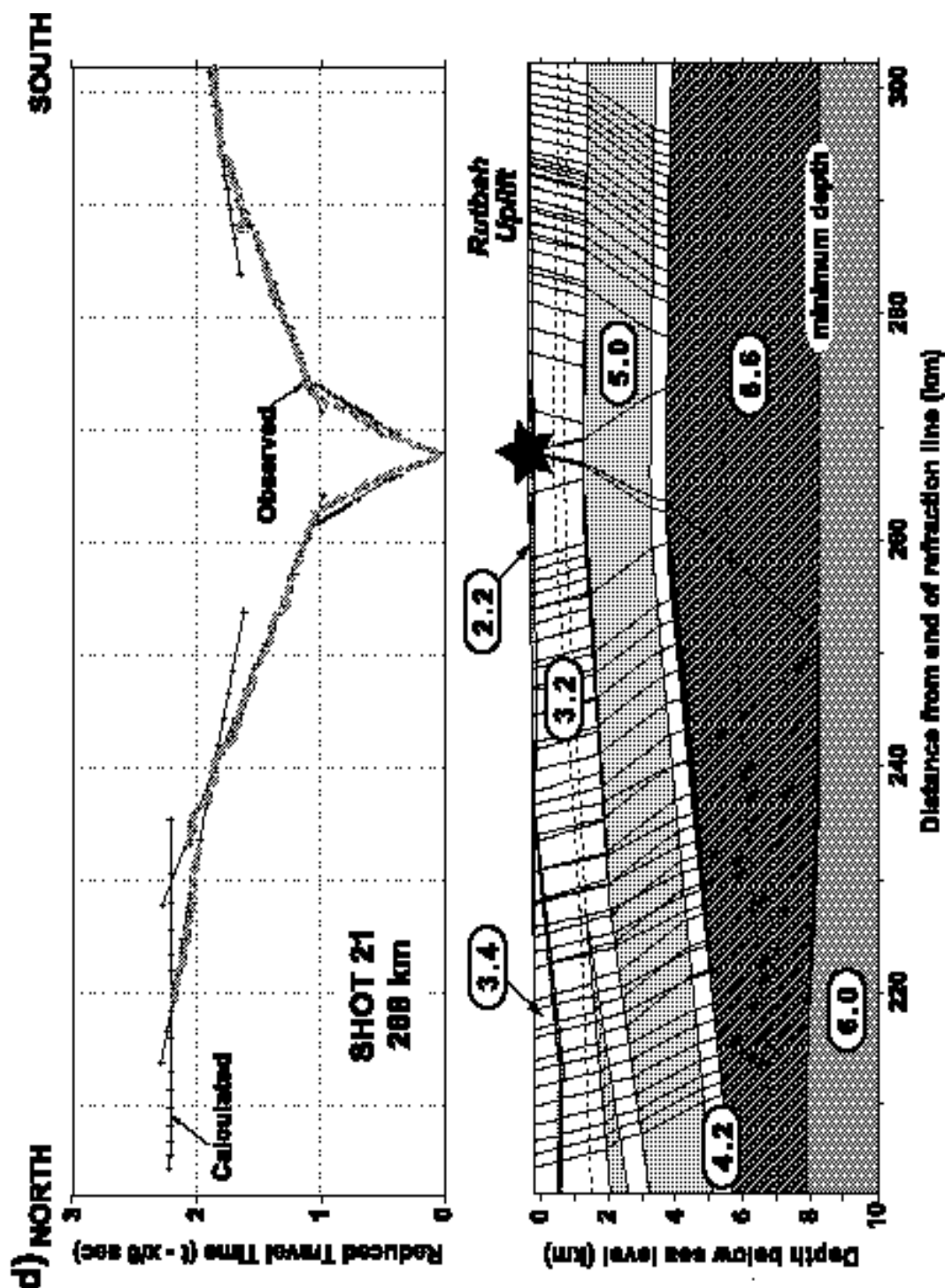
by lithology. These, and other ideas, are explored below as each of the velocity layers, from shallowest to deepest, are discussed in relation to their stratigraphic significance and relevance to regional tectonics.

## Cenozoic and Mesozoic

The uppermost velocity layer (2.2 km/s), is interpreted as being a superficial covering of weathered and poorly consolidated material underlain by more competent rocks of various ages (3.2 - 3.6 km/s). Somewhat deeper is a relatively high velocity (4.7 km/s) layer extending across the middle portion of the model (Figure 2.7a). This stratum hindered refraction interpretation by acting as a 'screening layer' (as described by Rosenbaum 1965; Poley and Nooteboom 1966), preventing some seismic energy from reaching deeper interfaces. However, enough energy was returned from deeper horizons to permit meaningful analysis (e.g. Figure 2.8c). The position of the 4.7 km/s layer was correlated with well data (Figures 2.5 and 2.7b) to a Middle Miocene sequence of anhydrites, gypsum and limestone, known locally as the 'Transition Zone' (Sawaf et al. 1993). Slight doming of this horizon, as well as the underlying top of Cretaceous interface, that was not detected as a refractor but which is mapped on the basis of well logs and reflection data, may be due to minor inversion on the north side of the Euphrates graben. This inversion is probably the result of the continued Cenozoic collision between the Arabian and Eurasian plates along the Bitlis suture and Zagros collision zone (Litak et al. 1998).

Below the Cretaceous, the Triassic layer (5.1 - 5.4 km/s), of predominantly dolomites and anhydrites, produces good refractions of characteristically high seismic velocity. The Triassic strata pinch out in the south whilst thinning slightly away from the graben toward the north (Figure 2.7b).

**Paleozoic**

The Upper Paleozoic formations - Permian, Carboniferous, Silurian (Devonian is entirely absent) - are grouped together on the basis of their similar seismic velocities (3.2 - 3.6 km/s) (Figure 2.7a). These mainly shale and sandy shale formations (Table 1), show slight thinning towards the north. The thinning is a result of extensive erosion that took place whilst northern Syria formed an intermittent broad subaerial uplift from Late Silurian to Permian time (Sawaf et al. 1993). The uppermost Ordovician, the Affendi formation (5.0 - 5.1 km/s), is clearly of higher velocity than the overlying rocks, presumably due to its predominately sandstone lithology. The Affendi formation shows thinning by around 2 km from south to north, again possibly due to uplift in northern Syria.

Below the Affendi formation is a 4.0 - 4.2 km/s layer corresponding to the shaley Swab formation of Early Ordovician age deposited during the Llandeilian regression (Husseini 1990). Beneath the Swab is the lowest Ordovician formation, the Khanasser, a predominately quartzitic sandstone unit with correspondingly high seismic velocity of 5.5 - 5.6 km/s. The Khanasser formation, combined with the Upper Cambrian sediments, show a thickening of around 1.7 km from south to north. This observation corresponds with the map of Husseini (1989) that shows isopachs of these units following the edge of the Arabian plate, with thickening of the Upper

**Table 2.1:** Stratigraphy of the Paleozoic in Syria (modified from Best *et al.* 1993).

| SYSTEM | | FORMATION | LITHOLOGY |
|---|---|---|---|
| Permian | | Amanous | Shale / sandstone |
| Carboniferous | | Markada | Sandy shales |
| Devonian | | - | (not present) |
| Silurian | Upper | - | (not present) |
| | Lower | Tanf | Shale |
| Ordovician | Upper | Affendi | Sandstone with minor shale |
| | Lower | Swab | Mainly shale |
| | | Khanasser | Quartzitic sandstone |
| Cambrian | | Sosink | Quartzitic sandstone |
| | | Burj | Limestone |
| | | Zabuk | Sandstone |
| Pre-Cambrian | | Saramuj | ? |

Cambrian/Lower Ordovician sediments away from the center of the Arabian platform towards the Tethys Ocean to the northeast.

Global sea-level rise in the Early to Mid-Cambrian caused the deposition of an extensive carbonate layer, the Mid-Cambrian Burj limestone, throughout Syria. Due to the high impedance contrast with the surrounding clastic rocks, this horizon forms a prominent reflection event which is correlated across much of the country (e.g. Figure 2.6b). However, perhaps because of the limited thickness of this unit (< 200 meters), no definitive refraction arrivals are observed from the Burj formation. Thus reflection times from seismic data have been combined with the velocity model to give an approximate position of the Burj limestone within the model (Figure 2.7b).

Thinning of the strata between the Burj limestone and basement rocks by more than 2 km from the south to the north is observed (Figure 2.7b). This extensive thickness of Lower Cambrian / Precambrian clastics to the south of the Euphrates could be a consequence of pre-Mid-Cambrian rifting and subsidence. It is thought that during the Early Cambrian (600 - 540 Ma) the Arabian plate underwent NW-SE crustal extension (e.g. Husseini 1988, 1989; Cater and Tunbridge 1992). This rifting is evidenced in the extensive evaporite basins of Pakistan, Oman and the Arabian Gulf region, and rifting farther to the northwest is possible.

Seber et al. (1993), using similar refraction data, also established a thickened pre-Mid-Cambrian section in south-central Syria, as did the gravity interpretation of Best et al. (1990) which showed the likelihood of thickened Lower Paleozoic / Precambrian sediments to the south of the Palmyrides. These observations could show that the Early Cambrian rifting was extensive across southern Syria whilst the north of the country remained structurally high.

An alternative, better supported, explanation for the thickened pre-Mid-Cambrian section in the south, could be that the Euphrates trend formed a suture / shear zone caused by the Proterozoic accretion of the Arabian plate. This idea is expanded upon in the Precambrian discussion below.

Overall, the thickness of the pre-Mesozoic sedimentary section demonstrated here is significantly greater, by more than 3 km in places, than any previous estimates. These observations have important economic implications since extensive Paleozoic clastic reservoir rocks and source rocks are known to exist in eastern Syria and elsewhere in the Middle East (e.g. Husseini 1990). As emphasized in the regional summary of Beydoun (1991), Paleozoic plays are likely to be a significant factor in future Middle East hydrocarbon production.

**Precambrian**

Although no wells penetrate basement rocks in Syria and basement has not been unambiguously identified on seismic reflection sections, previous refraction studies (Ginzburg et al. 1979; El-Isa et al. 1987; Seber et al. 1993) have established basement velocities to be around 6 km/s. Therefore, we assume the velocity layer of 6 km/s in the velocity model represents basement (Figure 2.7a). Across the Rutbah uplift in the far south of the profile, basement depth is at least 8.5 km. Along the southern margin of the Euphrates fault system we have definitive refraction arrivals that put the basement at 8 km below surface. North of this region, the basement deepens through faulting into the deepest part of the Euphrates graben system, where basement depth is around 9 km. To the north of the Euphrates basement depth is around 6 km.

Although previous investigations are consistent with these general trends in basement depth (Lovelock 1984; Leonov et al. 1989; Best et al. 1993), our interpretation generally puts basement somewhat deeper than the earlier suggestions. This is particularly true in the Rutbah uplift where the estimates of both Lovelock (1984) and Leonov et al. (1989) suggest basement depth at least 3 km shallower than the new results.

The obvious difference in basement depth on either side of the Euphrates graben system could be evidence of a terrane boundary along the Euphrates trend. The Arabian shield (Figure 2.1) accreted from discrete crustal blocks during the Late Proterozoic (e.g. Fleck et al. 1980; Pallister et al. 1987; Stoesser and Camp 1985; Vail 1985) and it is thought that similar processes might have formed the northern Arabian platform. Zones of weakness inherited from the accretion might control regional tectonics in the platform (e.g. Barazangi et al. 1993; Best et al. 1993, Litak et al. 1997), but thick sedimentary cover across the region makes such ideas difficult to prove. The stark difference in basement depth across the Euphrates could be an indication of two different crustal blocks accreting somewhat to the southwest of what is now the Euphrates graben system. This accretion could have been in the form of a suture zone, a shear zone, or some combination of the two - current data do not allow the definition of the precise mechanism. The possible accretion event in Syria would have to be Proterozoic, or very early Phanerozoic, in age since seismic reflections from the Mid-Cambrian Burj limestone (e.g. Figure 2.6b) are continuous across most of Syria (e.g. Best et al. 1993).

This accretionary hypothesis, previously implied by Best et al. (1993) and Sawaf et al. (1993), is also consistent with gravity investigations. Bouguer gravity observations (BEICIP 1975) show a clear difference across the Euphrates with generally high gravity values to the northeast, and lower values to the southwest of the graben system (Figure 2.9a). We model

a profile across these observations, constraining the upper structure of the model in accordance with seismic reflection interpretation, and changing the deep crustal structure to obtain the best fit with the gravity values. Densities are constrained in the upper section by well logs from the El Madabe and Thayyem wells (Figure 2.2).

Figure 2.9b shows a geological model that accounts for the gross trends in the gravity observations. The difference in gravity values on either side of the Euphrates is modeled by invoking differences in the density of basement and lower crustal rocks, and by differences in basement depth (as derived from our refraction modeling). Even though maximum basement depth to the southwest is largely unconstrained, modeling the large scale gravity anomaly with variations in basement depth alone is not plausible, and a crustal density contrast is required. In this model (Figure 2.9b) the difference in crustal density and basement depth on opposite sides of the Euphrates supports the suture / shear zone hypothesis. Previous gravity models (e.g. Best, Wilburt and Watkins 1973; Gibb and Thomas 1976) show that, in a wide variety of settings, crustal density contrasts are a common feature of suture zones. The Euphrates graben is in isostatic equilibrium, compensated by an elevated Moho. It is interesting to note that the gravity observations also tend to refute the Early Cambrian / Late Proterozoic rifting hypothesis discussed in the previous section. The gravity data

**Figure 2.9:** (a) Map showing Bouguer gravity anomalies in southeastern Syria across the Euphrates graben system. Bouguer reduction density = 2.53 kg m-3. Contour interval 2 mGal. (b) Gravity model to explain gross trends in gravity anomalies. Gravity high to NE of Euphrates modeled using shallower basement and a reduction in crustal / upper mantle density contrast. (c) Refinement of the model in which gravity high 'A' in (a) is modeled with dipping high-density body in crust.
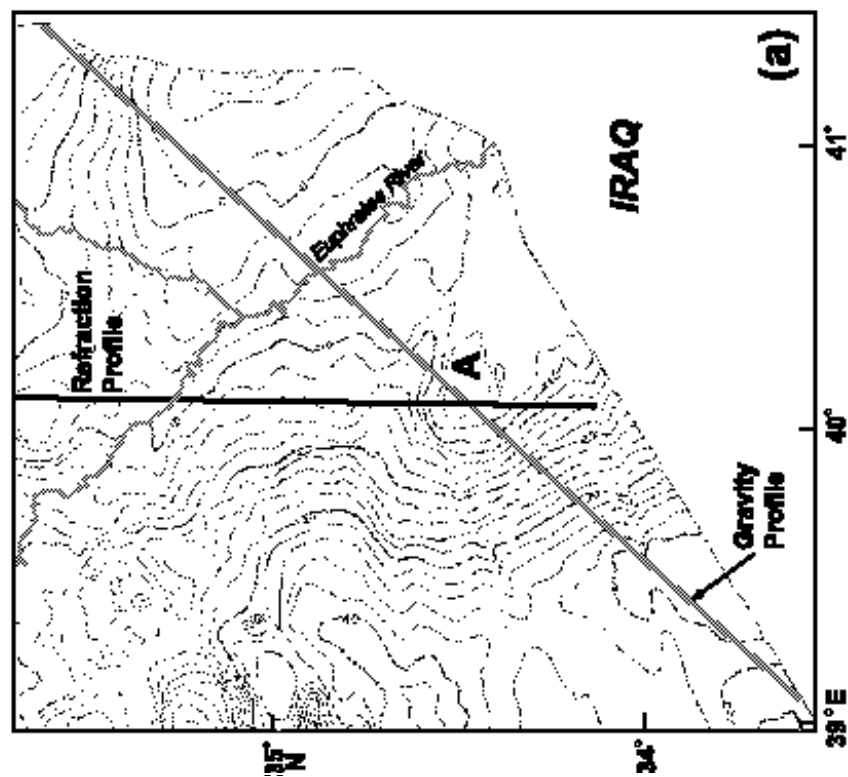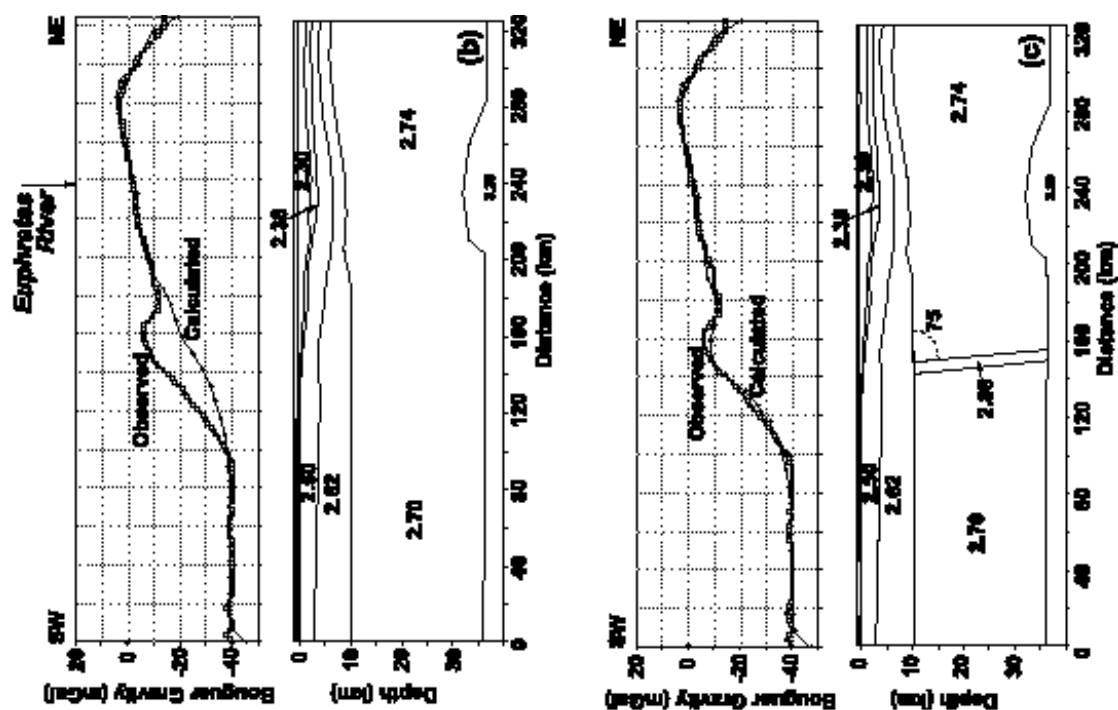
observations do not support a thinning of the crust to the south, which one would expect in a rifted area.

Further gravity modeling (Figure 2.9c) attempts to explain the local gravity high on the southwest margin of the Euphrates (labeled 'A' in Figure 2.9a), which extends a considerable distance into Iraq to the southeast (not shown). Although a basement high is thought to exist in this area (based on seismic reflections from the Mid-Cambrian Burj reflector), no reasonable uplift of the basement could account for this significant gravity anomaly. The high could be explained by a dipping, high-density mafic body extending to Moho depth (Figure 2.9c). The location of this gravity high also appears to correspond with a magnetic anomaly from a deep source, perhaps further evidence for a mafic or ultramafic body at depth within the crust. The dip of the body shown in Figure 2.9c is fairly arbitrary, and many variations of this shape could be made to fit the observations. A similar high-density body was modeled by Hutchinson, Grow and Klitgord (1983) as part of their gravity interpretation of the Piedmont gravity gradient along a possible Appalachian suture zone.

Obviously, the gravity models presented here are highly non-unique (e.g. Hutchinson et al. 1983). Constant ambiguity exists between density and structure, for example, basement depth verses crustal density contrast. However, our gravity modeling appears to show that the hypothetical suture / shear zone across the Euphrates shares many features in common with other sutures documented elsewhere. Such a zone along the trend of the Euphrates graben could offer a unified explanation for various tectonic and geophysical observations in the area. The accretionary hypothesis lends considerable support to the ideas of Best et al. (1990, 1993) which were expanded upon by Litak et al. (1997). These authors implied a regional NW-SE trend of weak zones beneath the northern Arabian platform, inherited from Proterozoic / Earliest Phanerozoic tectonics, amongst which is the Euphrates trend.

Incorporation of our results with those from other workers leads to a regional picture of basement depth and trends across much of Syria. Figure 2.10 shows our results, along with basement depths derived using similar data by Seber et al. (1993), and selected deep well data. We see a clear trend of deeper basement to the south of the Palmyrides and to the southwest of the Euphrates, and shallower basement to the north. The deepest basement is located actually beneath the Euphrates and Palmyride structures. The locations of possible suture / shear zones (modified from Best et al. 1993) are also shown. Whilst the suture / shear zones along the Euphrates and Palmyride trends have now been documented with gravity and refraction data, the zone to the northeast remains untested and is largely hypothetical.

## CONCLUSIONS

Basement depth and the location of several deep sedimentary interfaces are mapped from the interpretation of seismic refraction data incorporated with seismic reflection data, well logs and potential field data. Thus, basement depth beneath eastern Syria is found to be greater, by between 1 and 3 km, than previously supposed. Across the Rutbah uplift the basement is at least 8.5 km deep, in the Euphrates depression it is around 9 km, and to the north of the Euphrates basement is between 5.5 and 6.5 km in depth (Figure 2.7). Hence, extensive thicknesses of pre-Mesozoic rocks are documented. Deeply penetrating faults are identified in the Euphrates graben system demonstrating the thick-skinned tectonic style of this region. Incorporation of results
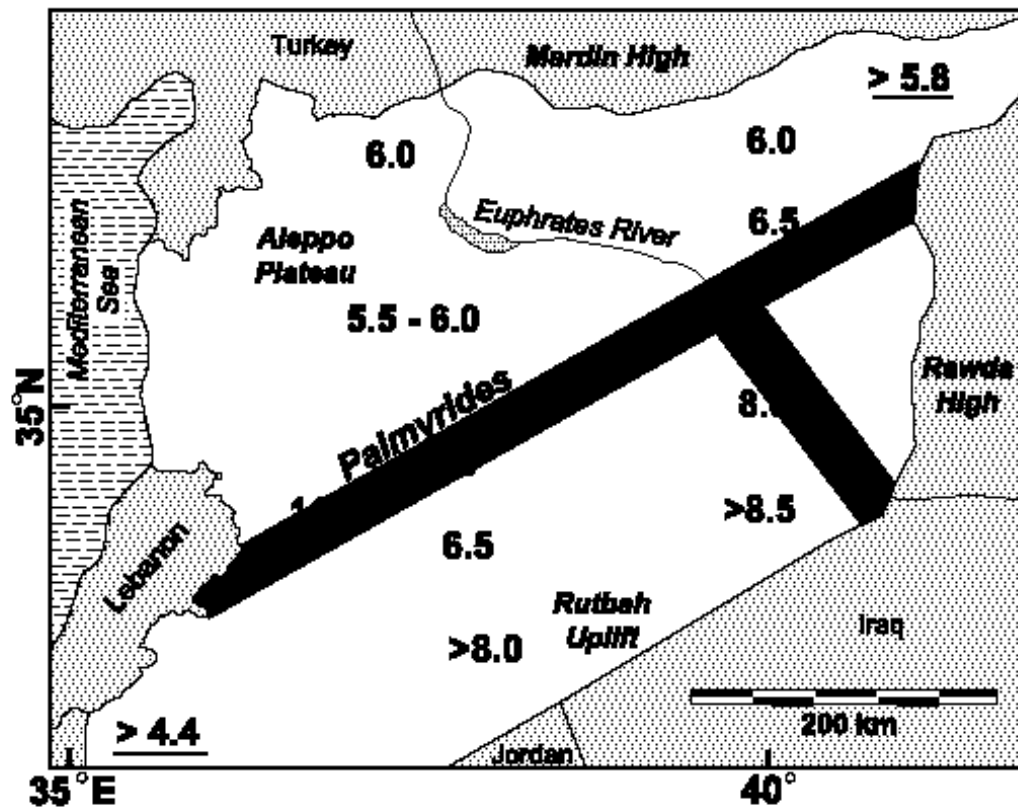
**Figure 2.10:** Map showing basement depths in Syria in kilometers below surface. Results from this study and previous refraction interpretation of Seber et al. (1993). Underlined data points are from selected deep well data. Shading represents locations of possible suture / shear zones.

from previous research allows gross trends in basement depth across Syria to be presented (Figure 2.10).

Clearly different basement depths on the northern and southern sides of the Euphrates graben could be evidence for the Late Proterozoic accretion of the northern Arabian platform with the Euphrates fault system as a suture / shear zone. This idea is supported by gravity observations that suggest higher density crust to the northeast of the Euphrates trend - a common feature of other suture zones. This leads support to the speculation of a system of weak zones beneath the northern Arabian platform, inherited from Late Proterozoic / Early Cambrian accretion, which continue to control regional tectonics.

# REFERENCES

Al-Saad, D., T. Sawaf, A. Gebran, M. Barazangi, J. Best and T. Chaimov, 1992. *Crustal structure of central Syria: the intracontinental Palmyride Mountain belt*. Tectonophysics, **207**, 345-358.

Alsdorf, D., M. Barazangi, R. Litak, D. Seber, T. Sawaf, and D. Al-Saad, 1995. *The intraplate Euphrates depression-Palmyrides mountain belt junction and relationship to Arabian plate boundary tectonics*. Annali Di Geofisica, **38**, 385-397.

Barazangi, M., D. Seber, D. Al-Saad, and T. Sawaf, 1992. *Structure of the intracontinental Palmyride mountain belt in Syria and its relationship to nearby Arabian plate boundaries*. Bulletin of Earth Sciences, Cukurova University, Adana, Turkey, **20**, 111-118.

Barazangi, M., D. Seber, T. Chaimov, J. Best, R. Litak, D. Al-Saad and T. Sawaf 1993. *Tectonic Evolution of the Northern Arabian Plate in Western Syria*. In E. Boschi, E. Mantovani and A. Morelli (Eds.), Recent Evolution and Seismicity of the Mediterranean Region, Kluwer Academic Publishers, Netherlands, 117-140.

BEICIP, 1975. *Gravity maps of Syria: Damascus (Syria)*. Bureau d'études industrielles et de coopération de l'institut francais du pétrole, Hauts de Seine, 96 pp.

Best, J. A., M. Barazangi, D. Al-Saad, T. Sawaf, and A. Gebran, 1990. *Bouguer gravity trends and crustal structure of the Palmyride Mountain belt and surrounding northern Arabian platform in Syria*. Geology, **18**, 1235-1239.

Best, J. A., M. Barazangi, D. Al-Saad, T. Sawaf, and A. Gebran, 1993. *Continental margin evolution of the northern Arabian platform in Syria*. American Association Petroleum Geologists Bulletin, **77**, 173-193.

Beydoun, Z. R., 1991. *Arabian plate hydrocarbon geology and potential – a plate tectonic approach*. In Studies in Geology, **77**, Tulsa, Oklahoma, USA: American Association of Petroleum Geologists.

Cater, J. M. L. and I. P. Tunbridge, 1992. *Paleozoic tectonic history of SE Turkey*. Journal of Petroleum Geology, **15**, 35-50.

Chaimov, T., M. Barazangi, D. Al-Saad, T. Sawaf, and A. Gebran, 1990. *Crustal shortening in the Palmyride fold belt, Syria, and implications for movement along the Dead Sea fault system*. Tectonics, **9**, 1369-1386.

de Ruiter, R. S. C., P. E. R. Lovelock, and N. Nabulsi, 1994. *The Euphrates graben, Eastern Syria: A new petroleum province in the northern Middle East*. In Geo 94, Middle East Petroleum Geosciences, edited by Moujahed Al-Husseini, 357-368. Manama, Bahrain: Gulf PetroLink.

El-Isa, Z., J. Mechie, C. Prodehl, J. Makris, and R. Rihm, 1987. *A crustal structure study of Jordan derived from seismic refraction data.* Tectonophysics, **138**, 235-253.

Filatov, V. and A. Krasnov, 1959. *On aeromagnetic surveys carried out over the Syrian territory, the United Arab Republic during 1958-1959*. Technoexport report, Damascus, 33 pp.

Fleck, R. J., W. R. Greenwood, D. G. Hadley, R. E. Anderson, and D. L. Schmidt, 1980. *Rubidium-Strontium geochronology and plate-tectonic evolution of the southern part of the Arabian shield*. United States Geological Survey Professional Paper, **1131**, 38 pp.

Gibb, R. A. and M. D. Thomas, 1976. *Gravity signature of fossil plate boundaries in the Canadian shield*. Nature, **262**, 199-200.

Ginzburg, A., J. Markris, K. Fuchs, C. Prodehl, W. Kaminski, and U. Amitai, 1979. *A seismic study of the crust and upper mantle of the Jordan-Dead Sea rift and their transition toward the Mediterranean Sea*. Journal of Geophysical Research., **84**, 1569-1582.

Hutchinson, D. R., J. A. Grow, and K. D. Klitgord, 1983. *Crustal structure beneath the southern Appalachians: nonuniqueness of gravity modeling*. Geology, **11**, 611-615.

Husseini, M., 1988. *The Arabian Infracambrian extensional system*. Tectonophysics, **148**, 93-103.

Husseini, M. I., 1989. *Tectonic and deposition model of late Precambrian-Cambrian Arabian and adjoining plates*. American Association of Petroleum Geolologists Bulletin, **73**, 1117-1131.

Husseini, M. I., 1990. *The Cambro-Ordovician Arabian and adjoining plates: A glacio-eustatic model*. Journal of Petroleum Geology, **13**, 276-288.

Kaila, K. L., H. C. Tewari, and V. G. Krishna, 1981. *An indirect method for determining the thickness of a low-velocity layer underlying a high velocity layer*. Geophysics, **46**, 1003-1008.

Leonov, Y. G., S. P. Sigachev, M. Otri, A. Yusef, T. Zaza, and T. Sawaf, 1989. *New data on the Paleozoic complex of the platform cover of Syria*. Geotectonics, **23**, 538-542.

Litak, R. K., M. Barazangi, W. Beauchamp, D. Seber, G. Brew, T. Sawaf, and W. Al-Youssef, 1997. *Mesozoic-Cenozoic Evolution of the Euphrates Fault System, Syria: Implications for Regional Kinematics*. Journal of the Geological Society, London, **154**, 653-666.

Litak, R. K., M. Barazangi, G. Brew, T., Sawaf, A. Al-Imam, and W. Al-Youssef, 1998. *Structure and Evolution of the Petroliferous Euphrates Graben System, Southeast Syria*. American Association of Petroleum Geologists Bulletin, **82**, 1173-1190.

Lovelock, P. E. R., 1984. *A review of the tectonics of the northern Middle East region*. Geological Magazine, **121**, 577-587.

Luetgert, J. H., 1992. *Interactive two-dimensional seismic ray-tracing for the Macintosh™*. United States Geological Survey Open File Report **92-356**.

McBride, J. H., M. Barazangi,, J. Best, D. Al-Saad., T. Sawaf, M. Al-Otri and A. Gebran, 1990. *Seismic reflection structure of intracratonic Palmyride fold-thrust belt and surrounding Arabian platform, Syria.* American Association of Petroleum Geologists Bulletin, **74**, 238-259.

Ouglanov, V., M. Tatlybayev, and V. Nutrobkin, 1974. *Report on seismic profiling in the Syrian Arab Republic.* General Petroleum Company Report, Aleppo, Syria, 73 pp.

Pallister, J. S., J. S. Stacey, L.B. Fischer, and W. R. Premo, 1987. *Arabian shield ophiolites and late Proterozoic microplate accretion.* Geology, **15**, 320-323.

Poley, J. Ph. and J. J. Nooteboom, 1966. *Seismic refraction and screening by thin high-velocity layers (A scale model study).* Geophysical Prospecting, **14**, 184-203.

Ponikarov, V. P., 1967. *The geology of Syria: explanatory notes on the geological map of Syria, scale 1:500,000 part I: stratigraphy, igneous rocks and tectonic*s. Damascus, Syrian Arab Republic, Ministry of Industry.

Rosenbaum, J. H., 1965, *Refraction arrivals through thin high-velocity layers.* Geophysics, **30**, 204-212.

Sawaf, T., D. Al-Saad, A. Gebran, M. Barazangi, J. A. Best, and T. Chaimov, 1993. *Structure and stratigraphy of eastern Syria across the Euphrates depression.* Tectonophysics, **220**, 267-281.

Seber, D., M. Barazangi, T. Chaimov, D. Al-Saad, T. Sawaf, and M. Khaddour, 1993. *Upper crustal velocity structure and basement morphology beneath the intracontinental Palmyride fold-thrust belt and north Arabian platform in Syria.* Geophysical Journal International, **113**, 752-766.

Sengor, A. M. C. and W. S. F., Kidd, 1979. *Post-collisional tectonics of the Turkish-Iranian plateau and a comparison with Tibet.* Tectonophysics, **55**, 361-376.

Sengor, A. M. C. and Y. Yilmaz, 1981. *Tethyan evolution of Turkey: A Plate tectonic approach.* Tectonophysics, **75**, 181-241.

Stoesser, D. B. and V. E. Camp, 1985. *Pan-African microplate accretion of the Arabian shield.* Geological Society of America Bulletin, **96**, 817-826.

Vail, J. R., 1985. Pan-African (late Precambrian) tectonic terrains and the reconstruction of the Arabian-Nubian Shield. Geology, **13**, 839-842.

# CHAPTER THREE

# Tectonic Evolution of Northeast Syria: Regional Implications and Hydrocarbon Prospects[†]

## ABSTRACT

We present the Phanerozoic tectonic evolution of northeast Syria and incorporate the results into regional deformation models of the northern Arabian platform and nearby Arabian plate boundaries. Based on analysis of extensive seismic reflection profiles and well data, we interpret that the Sinjar - Abd el Aziz area in northeast Syria was subsiding under extension at various rates from the Carboniferous until the end of the Mesozoic, most markedly during the latest Cretaceous. The predominant basin through most of the Late Paleozoic and Mesozoic was SW-NE trending; this formed the northeast extension of the major Palmyride basin to the southwest. During the Late Cretaceous, extension in eastern Syria initiated along SE-NW and then E-W trends - possibly as a result of changing subduction geometries and plate motions in the NeoTethys to the northeast. The E-W striking faulting resulted in syntectonic deposition of up to ~1600 m of Late Campanian - Maastrichtian marly limestone in the Sinjar - Abd el Aziz area. The area was subjected to horizontal shortening throughout the Cenozoic, primarily during Plio-Pleistocene time, resulting in structural inversion along some of the faults. Although crustal shortening through the Syrian Sinjar and Abd el Aziz structures is relatively minor (~1%), this has been critical to hydrocarbon trap formation in Mesozoic and Cenozoic strata through the formation of fault-propagation folds. We present regional models that show the interrelated tectonic history of northeast Syria, the Palmyrides,

---

[†] Originally published as "Tectonic evolution of northeast Syria: Regional implications and hydrocarbon prospects", by G. Brew, R. Litak, M. Barazangi and T. Sawaf, GeoArabia, 4, 389-318, 1999.

and the Euphrates fault system are all inseparably linked to the polyphase opening and closing of the nearby NeoTethys Ocean.

## INTRODUCTION

Syria, and the surrounding northern Arabian platform, offer an exemplary environment in which to study intraplate tectonic deformation. It has been established that tectonic deformation within Syria (e.g. Barazangi et al., 1993) has been controlled by repeated collisions, openings, and movements on the plate boundaries that almost completely surrounded the country (Figure 3.1, inset). Previous workers have studied certain elements of northern Arabian tectonics in great detail, including the Palmyride fold and thrust belt in central Syria (e.g. Chaimov et al., 1990; Best et al., 1993), and the Euphrates graben in eastern Syria (Litak et al., 1997; 1998). Until recently northeast Syria remained relatively unstudied. Interpretation of the geologic history of that area can help to further develop tectonic models of the region. Northeast Syria is the site of significant oil accumulations, and the focus of continuing exploration activity.

The most comprehensive account of northeast Syria was by Metwalli et al. (1974) who examined the stratigraphic and depositional development of that area together with northwestern Iraq. The geology of northeast Syria was also discussed in a minor way by Ponikarov (1966); Ala and Moss (1979); Lovelock (1984); Leonov et al. (1986); Sawaf et al. (1993) and Laws and Wilson (1997), without exclusive focus on that area. An important contribution by Kent and Hickman (1997) was based upon petroleum exploration of the Abd el Aziz anticlinorium (Figure 3.1). Their work was a very

**Figure 3.1:** A topographic image of northeast Syria. Reds represent high topography, blues are lows – color scale is non-linear; maximum elevation is ~1460 m on the top of the Sinjar Uplift and minimum is ~150 m near the Euphrates river in the south of the image. Note the Palmyride fold and thrust belt that extends significantly to the southwest, and the Euphrates River valley, that lies roughly above the Euphrates fault system. Arrow highlights surface expression of faulting discussed in text. Inset figure shows location of Syria and the surrounding northern Arabian platform in plate tectonic context. Dashed box shows location of main figure. NAF = North Anatolian Fault; EAF = East Anatolian Fault.
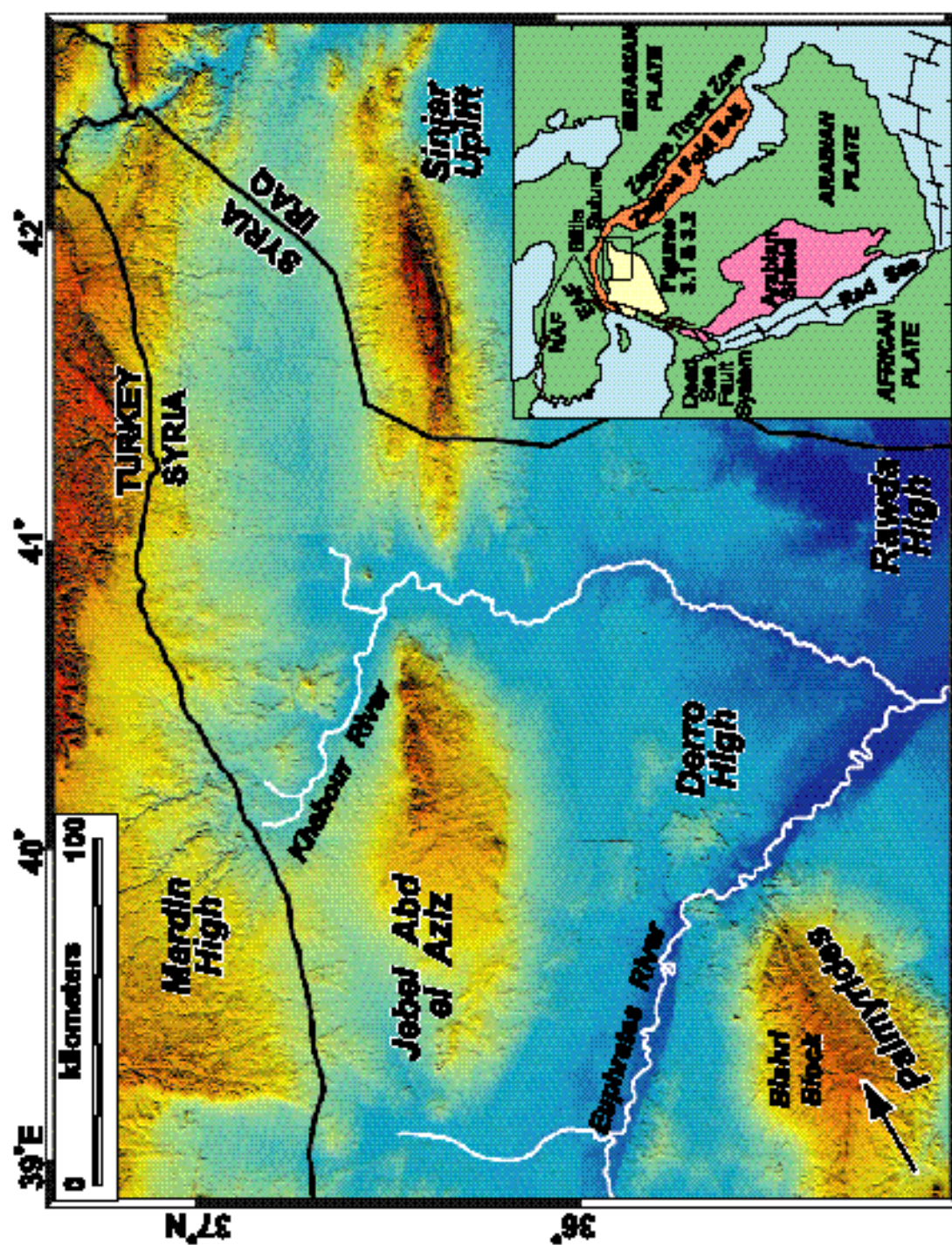
thorough account of the evolution of that structure since the Late Mesozoic, and was the first detailed subsurface investigation within northeast Syria to be published.

We present a spatially and temporally more expansive study, based on more extensive data, than any previously published work on this area. Our findings are set into a regional tectonic context by incorporating results from this, and similar studies of Syria, into a model of northern Arabian plate deformation since the Late Paleozoic. We find that previous suggestions of an aulacogen in central Syria (e.g. Best et al., 1993) can explain the Late Paleozoic and Early Mesozoic evolution of these features, but more enigmatic causes are involved in the Late Cretaceous rifting in eastern Syria. The entire area has been subjected to compression in the Neogene. The implications of these findings for hydrocarbon exploration are considered.

## DATA AND METHODOLOGY

The data used in this study were primarily around 3300 km of 2-D seismic reflection profiles and information from over 60 wells (Figure 3.2). These data were provided by the Syrian Petroleum Company (SPC) and are part of a much larger database held at Cornell University as part of ongoing joint collaborative research between SPC and Cornell. Limited data from Iraq were obtained from the literature including Al-Naqib (1960) and Al-Jumaily and Domaci (1976). Seismic data were mainly migrated 4.0 seconds TWT hardcopy records, collected using Vibroseis sources during the 1970's, 80's and early 90's. Formation top data were available for all wells, with wire-line logs available for around a quarter of the holes. The available sonic logs (Figure 3.2) were digitized to produce synthetic seismograms that were tied to the seismic data. Seismic refraction data (Brew et al., 1997) provided some information on the deeper

**Figure 3.2:** Database map showing locations of selected data sources used in this study. Hydrocarbon status of wells is indicated based on various sources referred to in the text. Abandoned and suspended wells not distinguished. Dashed box (approx. 175 km x 175 km) marks primary study area. The Tichreen 2 well marked in green is location of backstripping analysis (Figure 3.7).
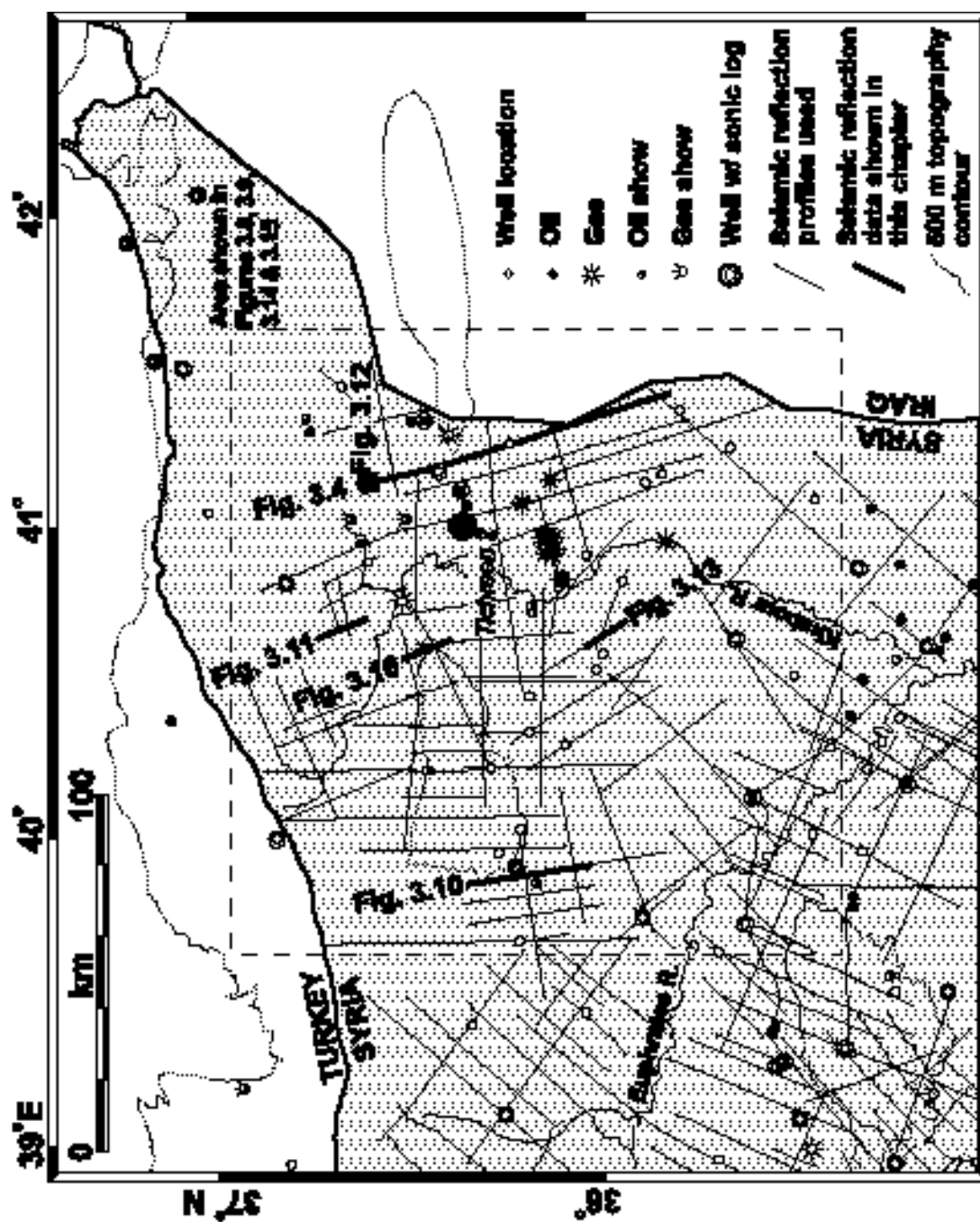
sedimentary and basement structure. In addition, 1:200,000 scale geologic maps and reports (Ponikarov, 1966), gravity field data (BEICIP, 1975), high resolution topography (e.g. Figure 3.1) and Landsat TM imagery (see Kent and Hickman, 1997) were available for the whole study area.

We interpreted the seismic reflection profiles and tied them to coincident or nearby wells for stratigraphic identification. Where possible, synthetic seismograms were used for the ties, alternatively time-depth charts constructed from sonic logs facilitated the ties. Several reflectors, chosen for their prominence, continuity, and geological significance, were mapped over the study area (shown as bold interfaces in Figure 3.3). At each stage in the interpretation all the available information was integrated to ensure the interpretation agreed with all the data sources.

## TIMING AND STYLES OF DEFORMATION

Northeast Syria and northwest Iraq are dominated by two topographic and structural highs (Figure 3.1). These are the Sinjar uplift (length ~150 km, max. elevation 1463 m) and Jebel Abd el Aziz (length ~100 km, max. elevation 920 m), separated by the Khabour river. We refer to this combined region as the 'Sinjar - Abd el Aziz area'. These highs are the result of Pliocene - Recent structural reactivation of normal faults forming fault-propagation folds and some associated break-through faults. This reactivation has structurally inverted many older structures. The original normal faults were roughly east - west striking and were active almost exclusively in the latest Cretaceous (latest Campanian - Maastrichtian), extending from the west through Jebel Abd el Aziz and eastwards well into Iraq (Figure 3.1). Prior to this episode of normal

| System / Series | | Formation | ID # on Figs. 3.5 & 3.6 | Lithology | Notes / Tectonic Events |
|---|---|---|---|---|---|
| Quaternary | | Bakhtiary | 1 | conglomerate w/ sandstone | |
| Tertiary | Pliocene | Upper Fars | 2 | sandstone w/ shale | Shortening in Euphrates and Sinjar / Abd el Aziz |
| Tertiary | Miocene | Lower Fars A | 3 | anhydrite, gypsum, sh. | |
| Tertiary | Miocene | Transition Zone | 4 | anhydrite, gypsum, sh. | Episodic uplift and shortening in Palmyrides |
| Tertiary | Miocene | Jeribe | 5 | dolomitic lmst., anhyd. | |
| Tertiary | Miocene | Dibbane | 6 | limestone and marly ls. | |
| Tertiary | Oligocene | Chilou | 7 | limestone and marly ls. | Extension in Sinjar / Abd el Aziz |
| Tertiary | Eocene | Jaddala | 8 | marly ls. & limestone | Horizon mapped in Figure 3.15 |
| Tertiary | Paleocene | Kermav | 9 | marl & marly shale | |
| Cretaceous | Upper - Maastrichtian | Shiranish | 10 | marl & argil. limestone | Post-extension unconformity |
| Cretaceous | Upper - Campanian | Soukhne/Massive | 11 / 12 | marl over cherty lmst. | Pre-extension unconformity |
| Cretaceous | Upper - Santonian | Soukhne/Massive | 11 / 12 | marl over cherty lmst. | |
| Cretaceous | Upper - Coniacian | Derro | 13 | red congl. sandstone | Rifting in Euphrates fault system |
| Cretaceous | Upper - Turonian | Judea / Hayan | 14 / 15 | dolomitic ls w/ anhydrite | |
| Cretaceous | Upper - Cenomanian | Judea / Hayan | 14 / 15 | dolomitic ls w/ anhydrite | Horizon mapped in Figure 3.14 |
| Cretaceous | Lower | Rutba / Ghoune | 16 | sst. over some basalt | Early Cretaceous unconformity |
| Jurassic | | Hamamoun | 17 | limestone | |
| Triassic | Upper | Sarjelu | 18 | dolomite w/ shale | Subsidence / rifting in Palmyride / Sinjar trough |
| Triassic | Upper | Allan/Muss | 19 | dolomite w/ shale | |
| Triassic | Upper | Adaya | 20 | shale, anh. & dolomite | |
| Triassic | Upper | Butma | 21 | dolomite w/ shale | |
| Triassic | Middle | K. Anhydrite | 22 | anhydrite | Reactivation of some faults |
| Triassic | Middle | K. Dolomite | 23 | dolomite w/ some ls. | |
| Triassic | Lower | Amanous Shale | 24 | shale | Permo-Triassic unconformity |
| Permian | | Amanous | 25 | sandstone | Episodic rifting in Palmyride / Sinjar |
| Carboniferous | | Markada | 26 | sst w/ some dolomite | |
| Devonian | | | ABSENT | | |
| Silurian | | Tanf | 27 | shale w/ interbed. silst. | |
| Ordovician | | Affendi | 28 | sandstone w/ shale | |
| Ordovician | | Swab | 29 | shale w/ minor sst. | |
| Ordovician | | Khanasser | 30 | sandstone | |
| Cambrian | | Saairk | NOT PENETRATED | quartzitic sandstone? | |
| Cambrian | | Burj | NOT PENETRATED | dolomitic limestone? | |
| Cambrian | | Zabuk | NOT PENETRATED | quartzitic sandstone? | |

**Figure 3.3:** Generalized stratigraphic column of northeast Syria. Turkish and Iraqi formations use different nomenclature and are not listed - see Beydoun (1991). Note alternative nomenclature for Early Mesozoic formations. Unconformities marked as wavy lines with the most significant interfaces highlighted in bold.

faulting, the area was host to a northeast trending basin, associated with the Palmyride rift and subsequent subsidence, that extended across Syria since Carboniferous time.

Figure 3.4 clearly shows the greatly-thickened, syn-extensional uppermost Cretaceous section and underlying Mesozoic basin beneath the Sinjar structure. The figure.also illustrates the reactivation of the normal faulting in a reverse sense, and the consequent structural inversion, that has formed the present topography. Although similarly deformed since the latest Cretaceous, Jebel Abd el Aziz had a significantly different earlier history compared to the Sinjar structure. Whilst the Sinjar uplift is underlain by a Late Paleozoic and Early Mesozoic sedimentary basin (Figures 3.4 and 3.5), there is no such obvious thickening beneath the Abd el Aziz area (Figure 3.6). The Abd el Aziz experienced somewhat less deposition during the latest Cretaceous extensional episode (compare Figures 3.5 and 3.6).

A subsidence reconstruction of the westernmost Sinjar area based on well data (Tichreen 2, location on Figure 3.2) is shown in Figure 3.7. Present-day formation thicknesses are projected back in time by estimating compaction rates, densities and porosity values for the sediments following the method of Sclater and Christie (1980). Formation thicknesses for the Paleozoic section are projected from nearby wells. There is uncertainty of erosion rates at the unconformities, thus this curve represents the minimum subsidence amount. We see three episodes of significant sedimentation; in the Carboniferous, in the Permian, followed by continued subsidence in the Early Mesozoic, and in the latest Cretaceous. Sawaf et al. (1999) and Stampfli et al. (1999) had similar findings.

**Figure 3.4:** Depth converted seismic interpretation along seismic profile DH-46. See Figure 3.2 for location. As with all seismic profiling, fault interpretation at depth is somewhat speculative due to degradation of signal with increasing depth. Also, the data do not allow an accurate differentiation of Paleozoic formations along this line. Total depths (TD) in this, and all subsequent figures, are in meters below kelly bushing, and the distances that the wells were projected onto the seismic lines are indicated.
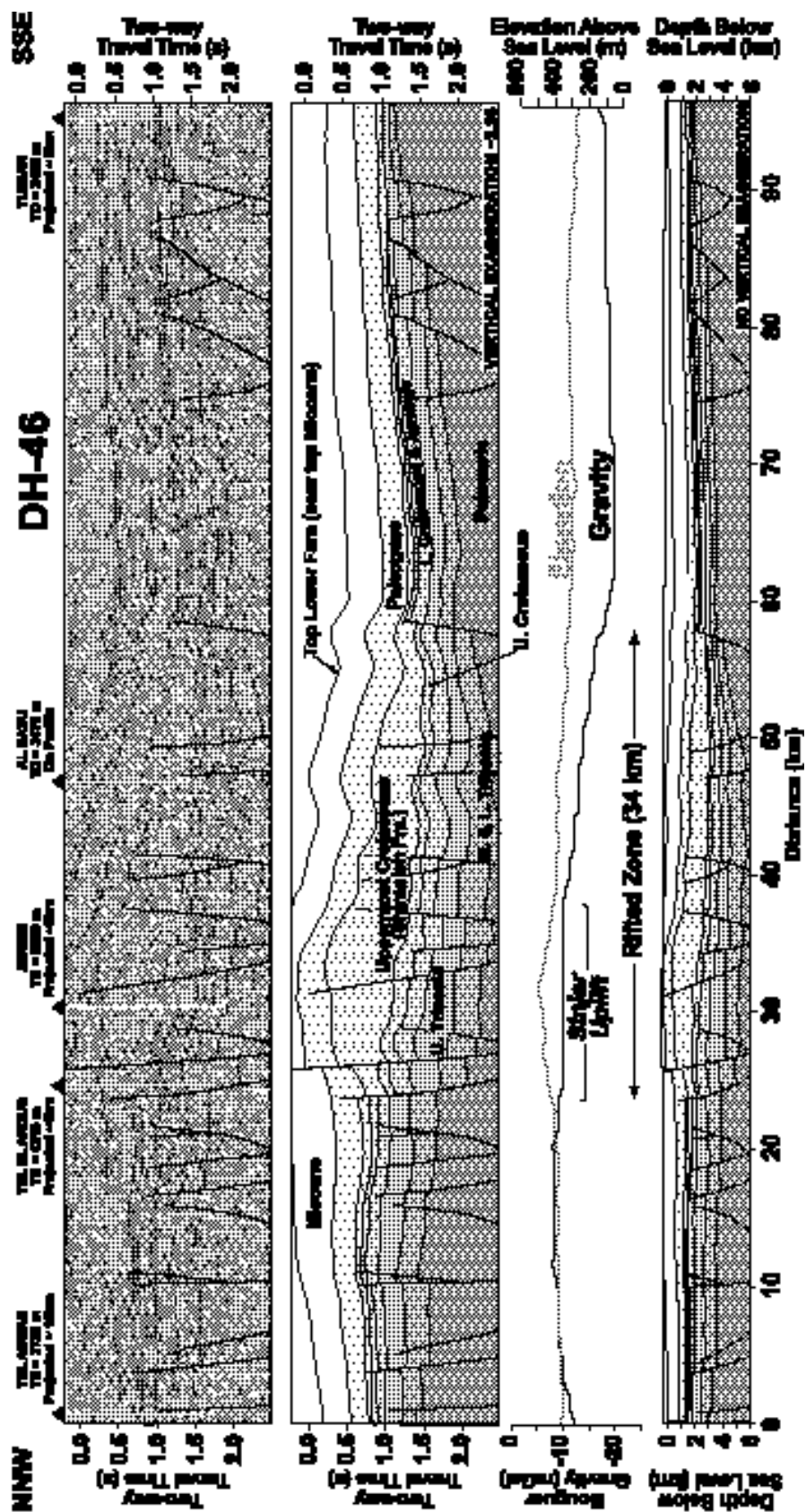
**Figure 3.5:** Well correlation section across the western portion of the Sinjar structure in Syria. See inset for location. Major stratigraphic boundaries, unconformities and formation numbers are shown with reference to Figure 3.3.
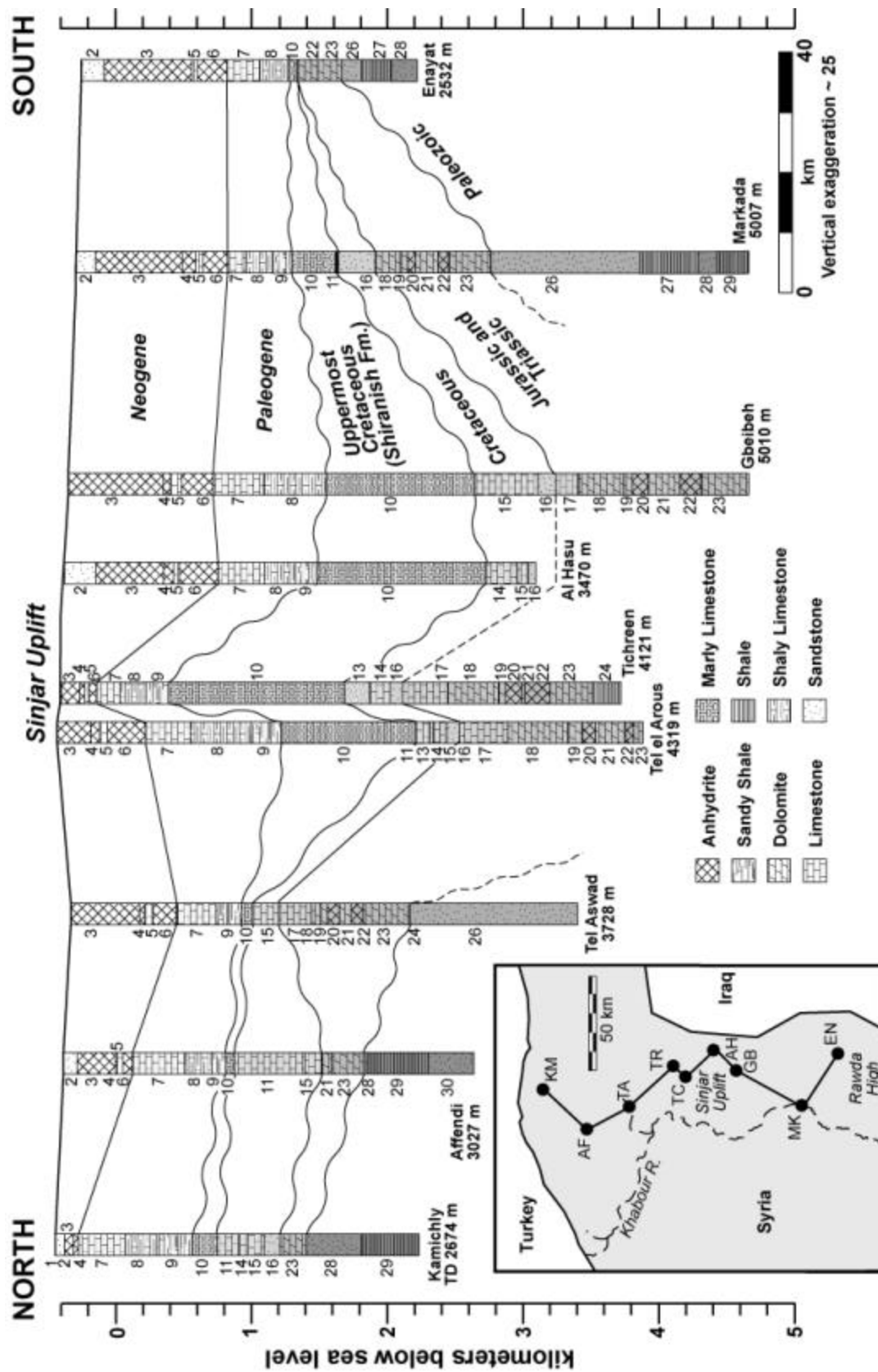
**Figure 3.6:** Well correlation section across the Abd el Aziz structure in northeast Syria. See inset for location. Major stratigraphic boundaries, unconformities and formation numbers are shown with reference to Figure 3.3. Lithology key is the same as in Figure 3.5.
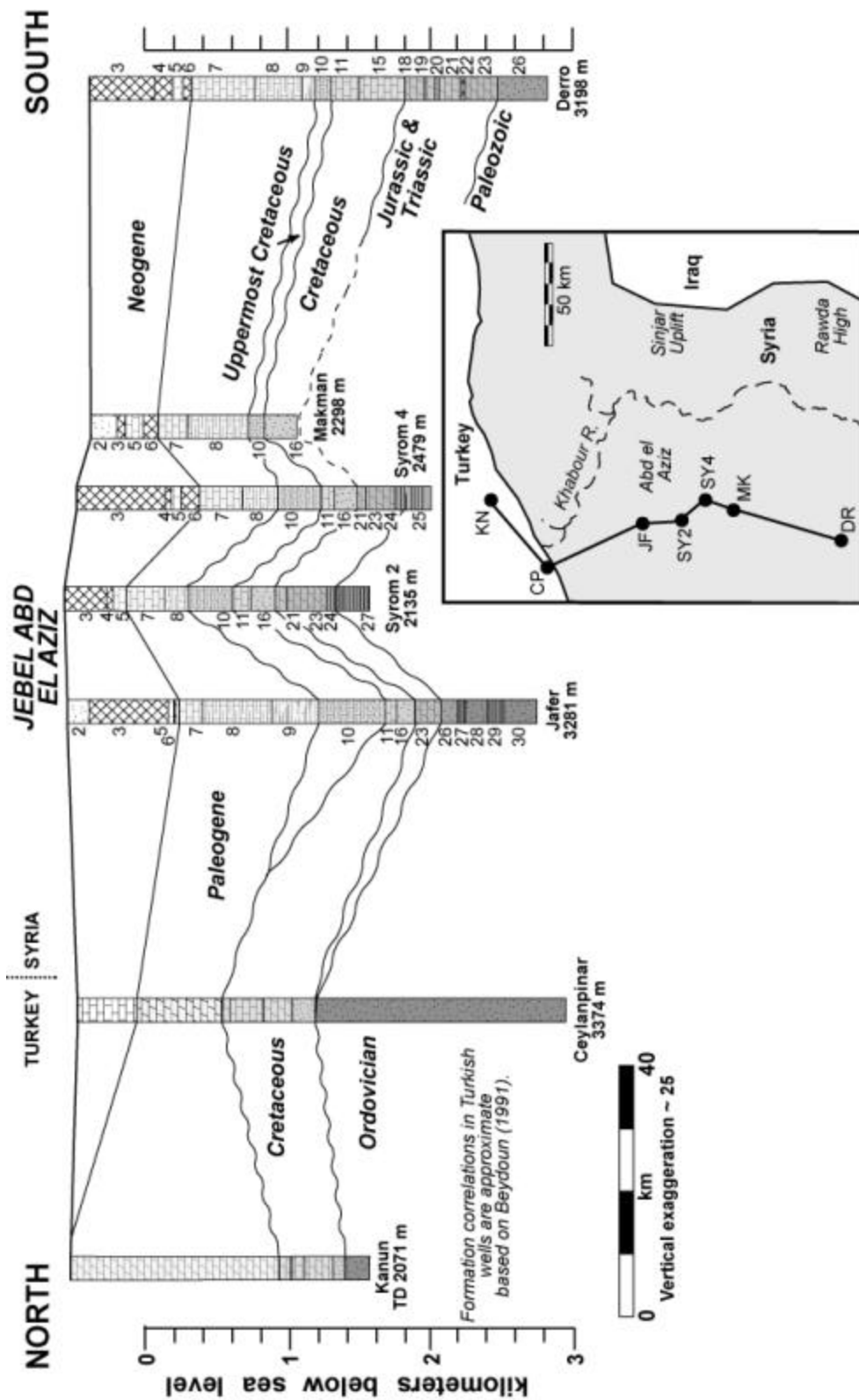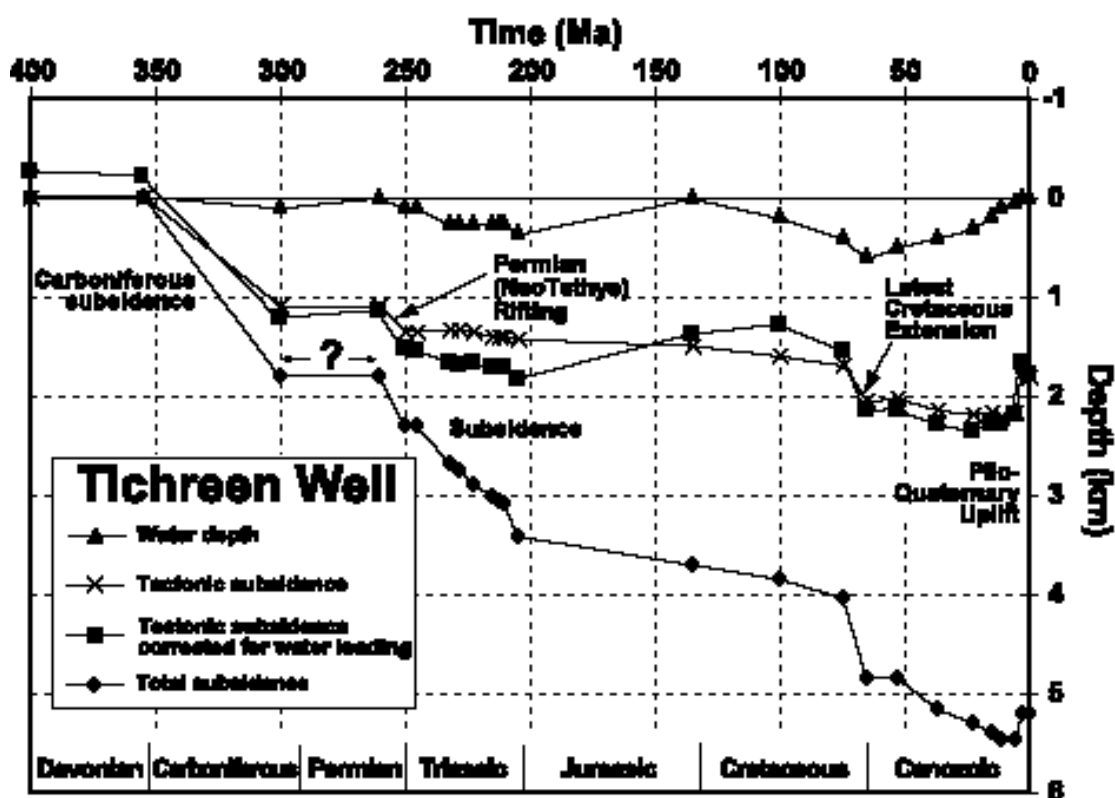
**Figure 3.7:** Subsidence curves constructed from analysis of current formation thicknesses in the Tichreen 2 well in the Sinjar area (see Figure 3.2 for location). Total subsidence, corrected for compaction, is shown. Also shown are curves corrected for sediment loading effects, and water loading. The assumed paleobathymetry is poorly constrained.

Based upon our integrated interpretations, Figure 3.8 presents an overall schematic model of the tectonic evolution of northeast Syria.  This model clearly illustrates the three basic stages of the evolution, namely Late Paleozoic / Early Mesozoic trough formation, latest Cretaceous east - west trending normal faulting, and Plio-Pleistocene structural inversion.  The evidence behind the model presented in Figure 3.8, and certain complexities not illustrated by this schematic model, are now chronologically discussed.

**Paleozoic**

Since no well penetrates the metamorphic basement in Syria, depth to basement estimates of around 6 km come from a detailed refraction data analysis (Brew et al., 1997).  Cambrian sediments are also not penetrated within the study area, but Ordovician clastics are found over the entire region (Figure 3.9) and form a sequence many kilometers thick (Sawaf et al., 1993).  Lower Silurian shales were deposited throughout the region by repeated regressions and transgressions (Beydoun, 1991).  However, Upper Silurian and Devonian formations are entirely absent.  The top of the Silurian unconformity, where observed, shows little structure, perhaps suggesting a regional Silurian / Devonian uplift.

Carboniferous time, coincident with eustatic transgression, appears to have marked the beginnings of a northeast - southwest trending trough running through Syria roughly along the axis of the present-day Palmyride fold and thrust belt, with continuation to the northeast (e.g. Best et al., 1993).  Figure 3.10 shows some fault-related stratigraphic thickening of Carboniferous strata on the northwestern margin of the clastic basin, and some subtle onlap of the Carboniferous towards the north.   Abrupt

**Figure 3.8:** Schematic block diagrams showing the geologic evolution of northeast Syria since the Late Paleozoic.  See Figure 3.2 for location.

82



End
Cretaceous

End
Paleogene

Plio-
Pleistocene

NORTH

End
Paleozoic

End
Early
Cretaceous

Late
Campanian
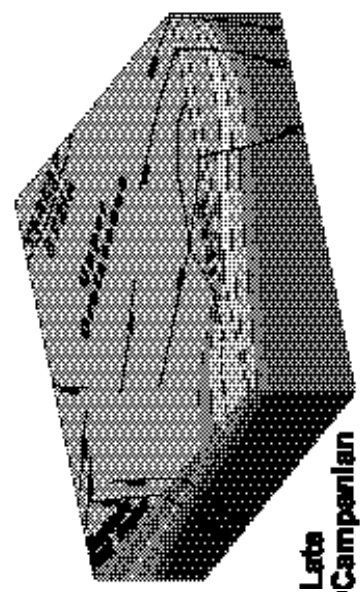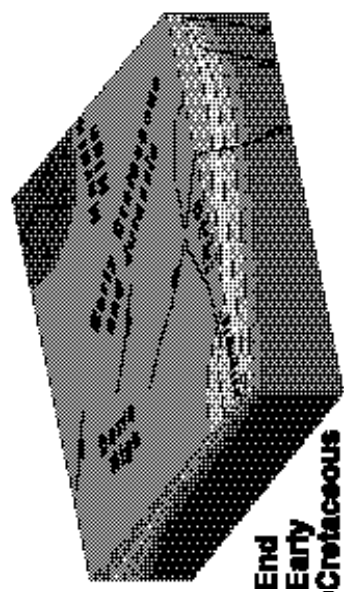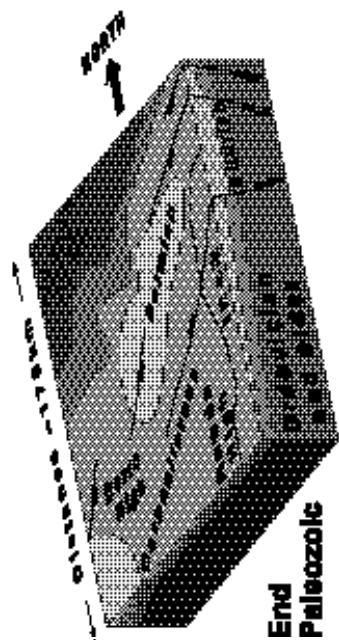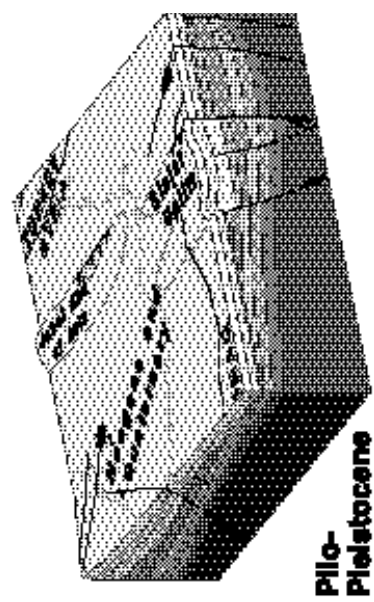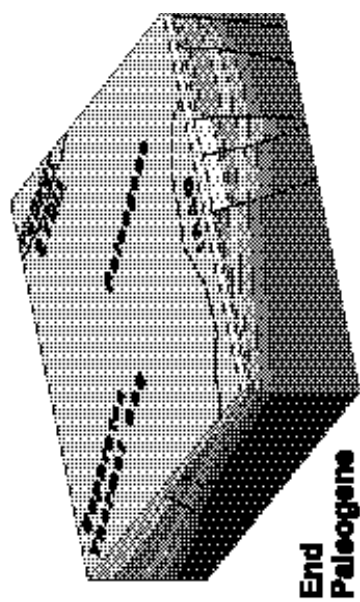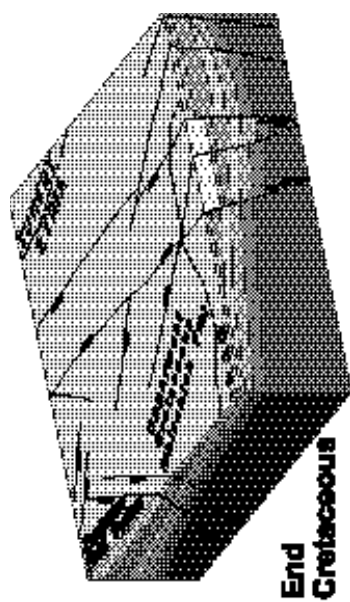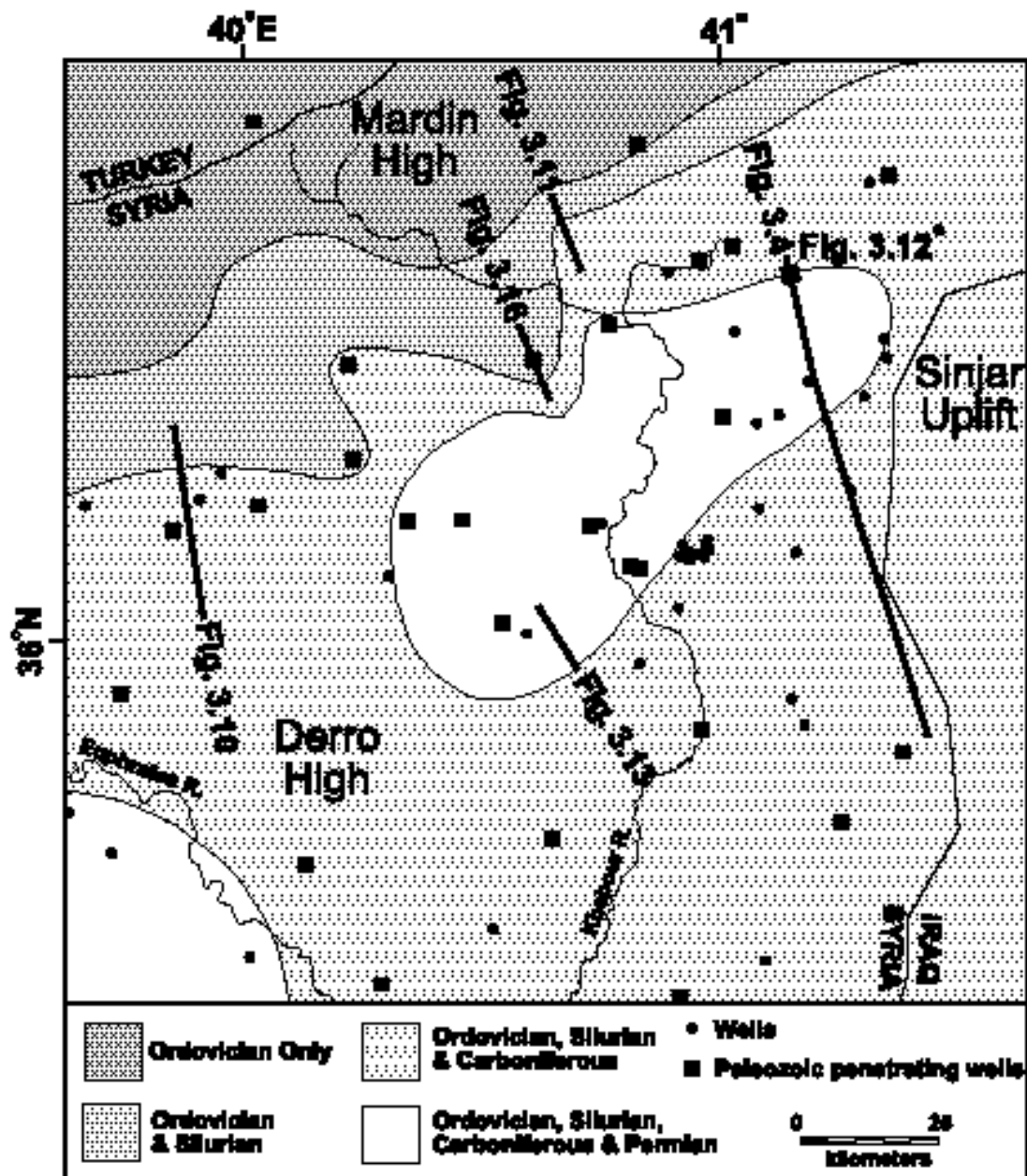
**Figure 3.9:** Map showing generalized distribution of Ordovician and younger Paleozoic formations in the study area based on well and seismic data. See Figure 3.2 for location.

**Figure 3.10:** Migrated seismic section AB-06.  See Figure 3.2 for location.  Major faults are shown.  Note the distinct thickening of the Carboniferous unit towards the south-southeast.
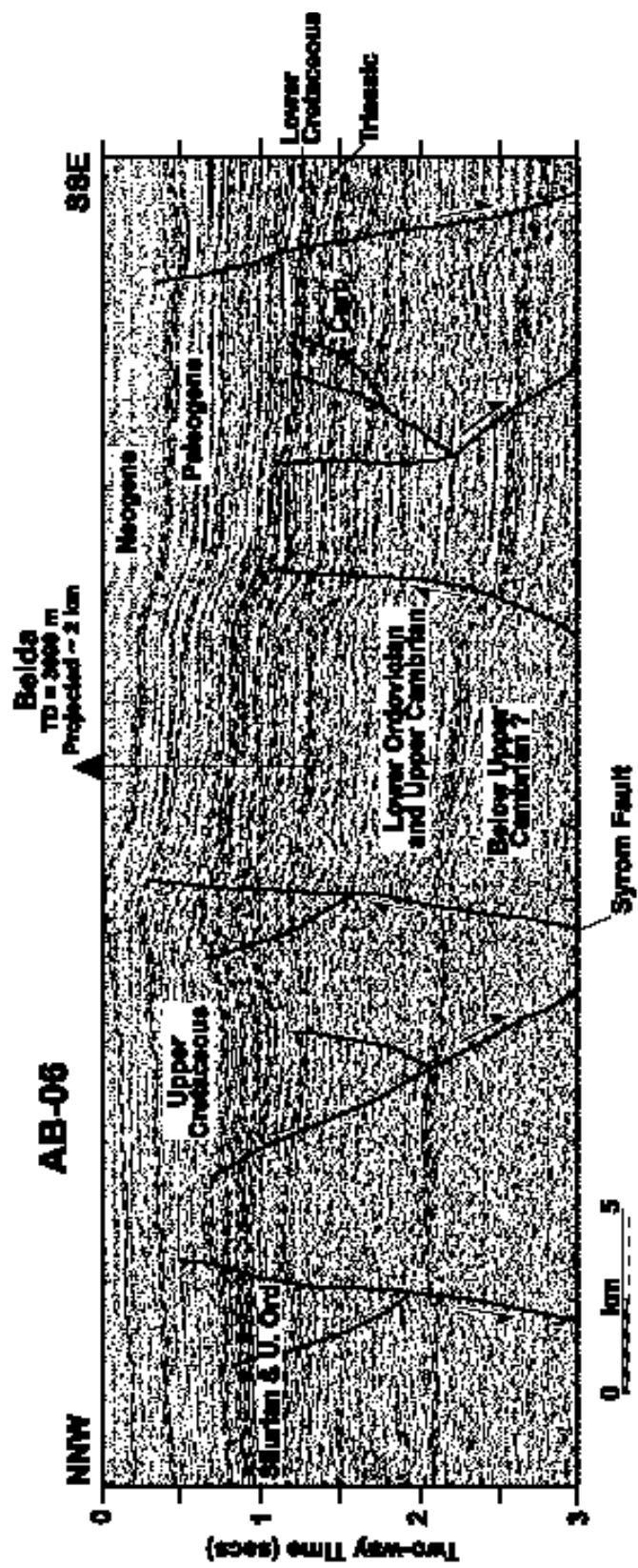
thickness changes of Carboniferous strata in adjacent wells elsewhere in the Sinjar area point to some fault-related thickening. Subsidence analysis (Figure 3.7) based on well sections also indicates a Carboniferous event, and isopachs show that much of the thickening appears to be a consequence of broad subsidence, rather than being purely fault controlled.

The lack of Late Carboniferous and Early Permian age deposits in the region suggests emergence at that time, although this could be due to Early Triassic erosion. Subsidence analysis (Figure 3.7) and isopachs suggest rifting and subsidence in the Late Permian that propagated along the line of the Carboniferous subsidence event. At the Permo-Triassic boundary the region underwent broad uplift and was again exposed and eroded. Thus only the deepest parts of the Palmyride / Sinjar rift preserved the Late Permian Amanous sandstone formation, as it was eroded out or not deposited to the north and south. Carboniferous and Lower Silurian formations were also eroded out to the north on the Mardin high during this episode (Figures 3.8 and 3.11). This led to a Paleozoic subcrop distribution where the oldest formations the most extensive, and younger ones are progressively limited by widespread Permo-Triassic erosion (Figure 3.9). Whilst we report only limited Paleozoic faulting in this area, evidence for such activity is somewhat obscured by poorer quality seismic data and more recent tectonic events. Even so, isopach data suggest that most of the Paleozoic stratigraphic thickening in the Sinjar area was subsidence related.

The Derro high (Figures 3.1 and 3.9) was an uplift between the Palmyride / Sinjar basins during much of their formation. Well data indicate that either the Derro high was an uplift during Permo - Carboniferous time, or was subjected to later uplift and

**Figure 3.11:** Portion of seismic line SA-12. See Figure 3.2 for location. The seismic interpretation is tied to the nearby Affendi and South Al Bid wells.
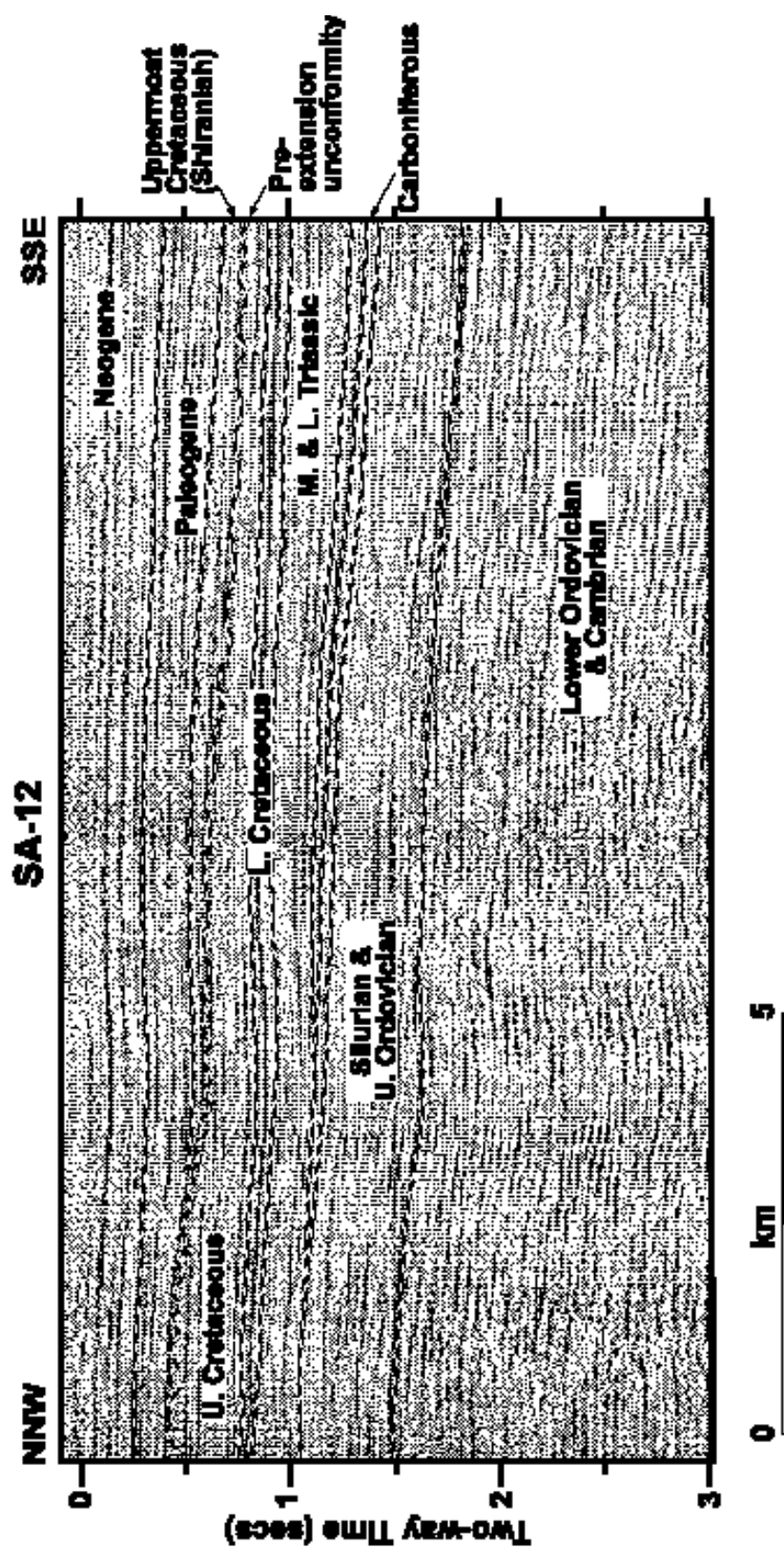
extensive Permo-Triassic erosion; seismic data does not permit the resolution of this issue.

**Mesozoic**

The very limited subcrops of the Lower Triassic Amanous shale (Muloussa A) formation encountered in the southwest of the study area are indicative of continued Permo-Triassic emergence and only gradual transgression from the Palmyride area towards the northeast. The situation changed substantially in the Middle Triassic when deposition was again widespread. The Middle Triassic Kurrachine Dolomite (Muloussa B) formation (Figure 3.3) is preserved in subcrop everywhere in the study area, except in the Turkish borderlands where it was lost to later erosion.

During the Early Mesozoic, the Palmyride / Sinjar basins accumulated great thicknesses of Triassic shallow marine carbonates. The thickening in the Sinjar basin at this time was predominately accommodated through broad downwarping, as illustrated by onlapping relationship of Triassic strata onto Paleozoic formations (e.g. Figure 3.11). This pattern persisted throughout the Mesozoic until Coniacian times (Figure 3.7). Some evidence for Early Mesozoic fault related thickening is shown in Figures 3.12 and 3.13. These figures show northeast - southwest striking faults that accommodated some movement in the Triassic, and in some cases have been active until at least Neogene time (Figure 3.13). Further examples of this orientation of faults are found (Figure 3.14). Note that Figure 3.13 also shows possible thickening of the Permian and Carboniferous strata across some of these northeast - southwest trending faults, indicating that these faults may also have been active in the Late Paleozoic rifting event.
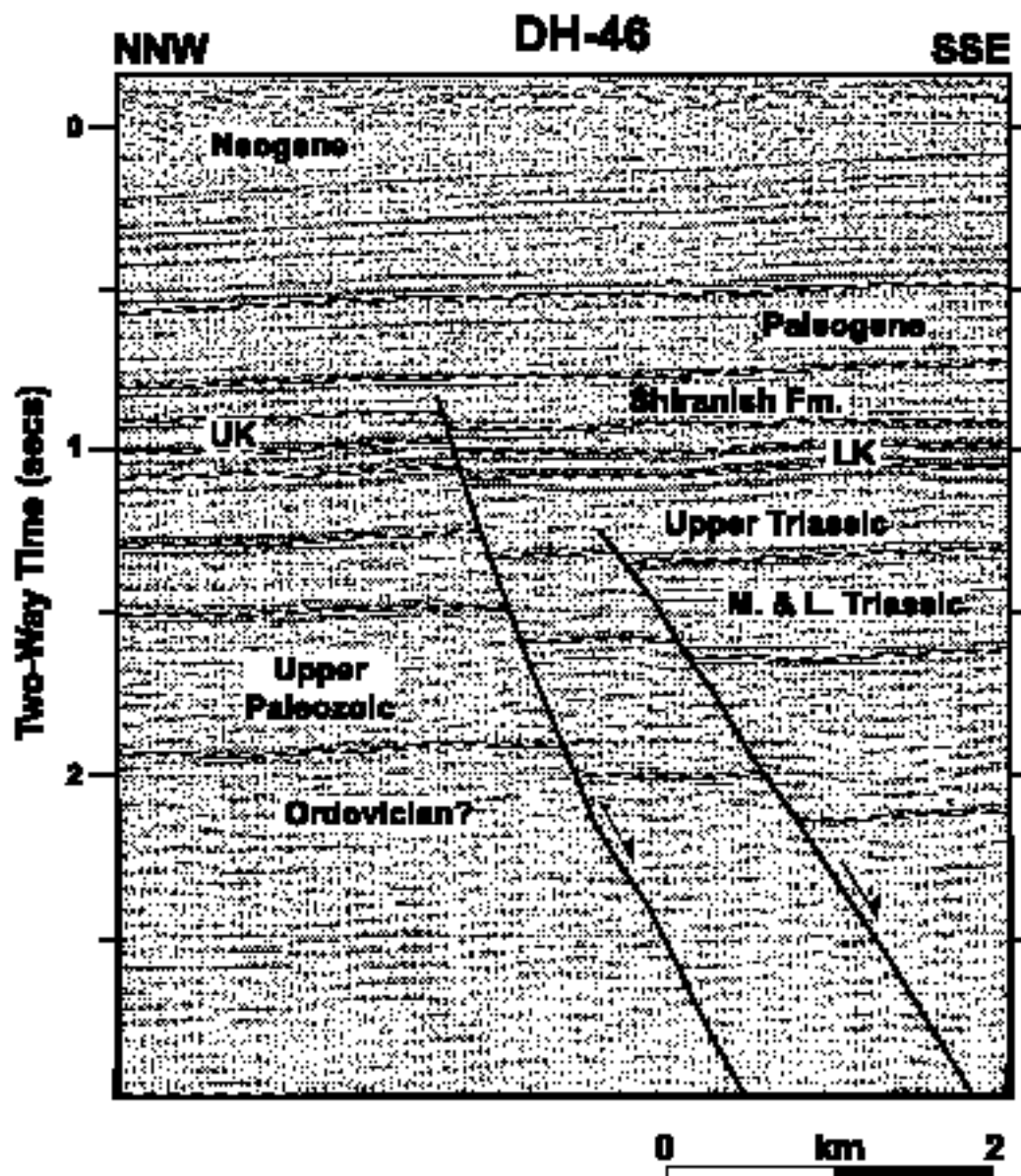
**Figure 3.12:** Enlarged portion of migrated seismic line DH-46 (Figure 3.4) showing an example of Early Mesozoic and Paleozoic fault controlled thickening in the study area. See Figure 3.2 for location.

**Figure 3.13:** Composite of migrated seismic lines TSY-88-201 and TSY-90-201X with interpretation that is tied to nearby wells.  See Figure 3.2 for location.

TSY-201
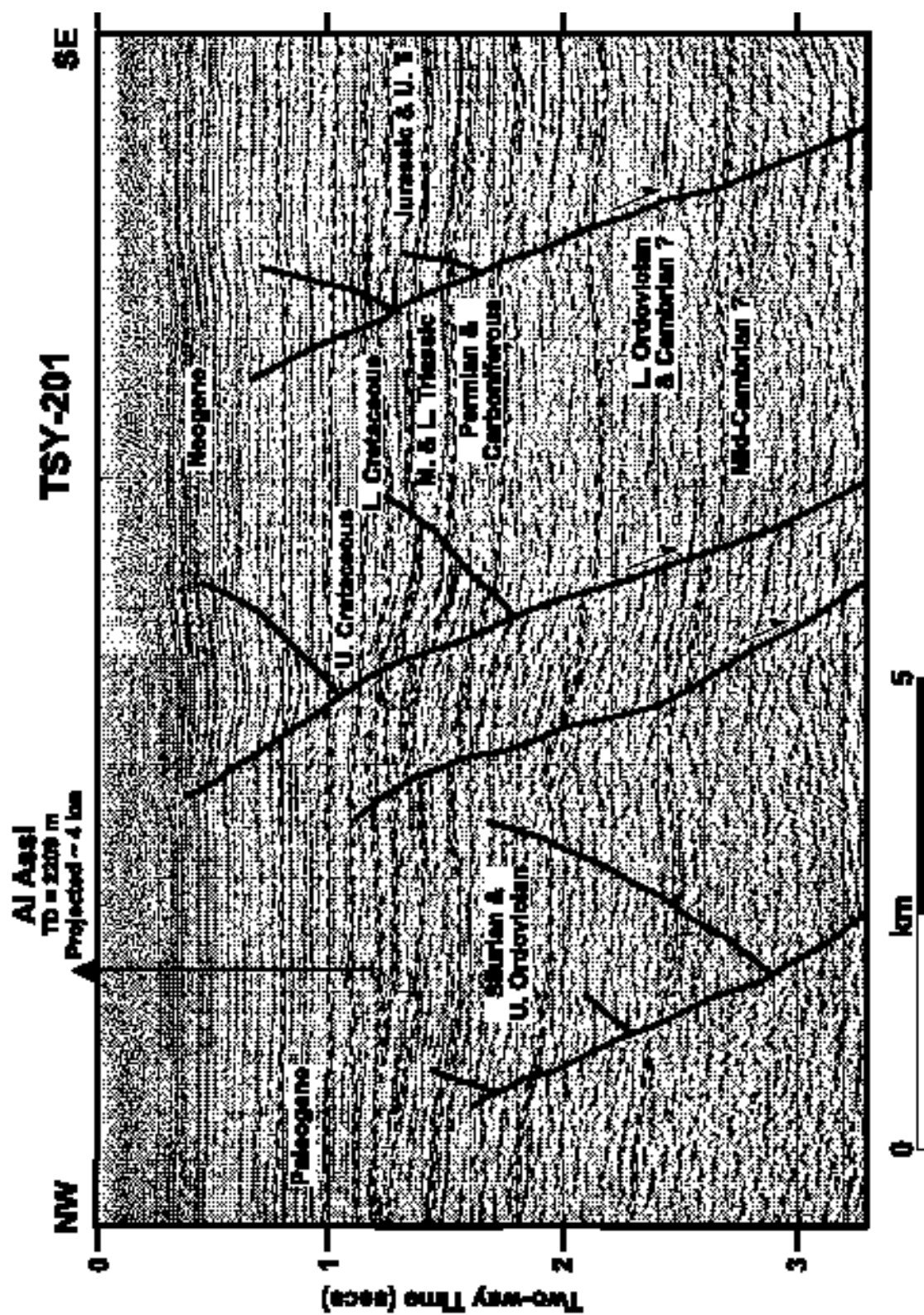
**Figure 3.14:** Smoothed structure map near top of the Lower Cretaceous Rutbah formation (see Figure 3.3 for stratigraphy and Figure 3.2 for location). Major faults are shown with sense of movement indicators. The most significant faults are shown as bolder lines. Note that the history of movement on many of these faults is complex, and the symbols are only a generalized account of the movement. Some faults of indeterminate displacement are not symbolized. Note the three structural trends: Northeast - southwest predominately along the Palmyride / Sinjar trend; northwest-southeast along the Euphrates fault system; and east - west in the Sinjar - Abd el Aziz area.
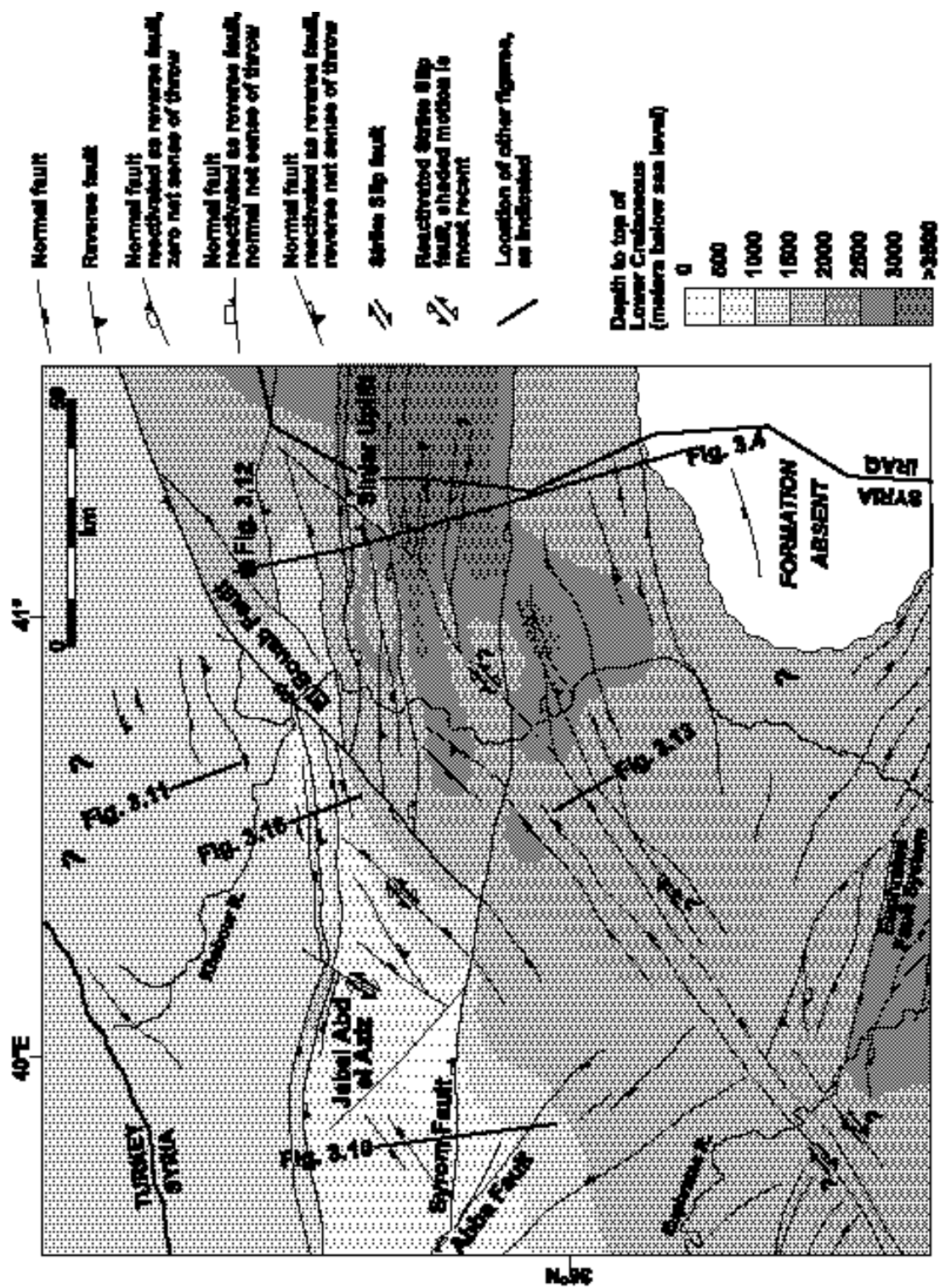
The broad downwarping and deposition continued into the Jurassic and ended with a major uplift event during the Late Jurassic that continued into the Early Cretaceous. With widespread erosion of much of the Jurassic and Triassic section at this time, Jurassic sediments are only preserved in the deepest parts of the Sinjar and Palmyride areas. Sawaf et al. (1993) described the Neocomian age deltaic sandstone and conglomerates of the reservoir-quality Rutba formation (Figure 3.3) that were deposited in eastern Syria during this regression. Transgression during Aptian - Albian time allowed deposition to resume in the Sinjar basin, with perhaps even less fault-related stratigraphic thickening than the Early Mesozoic (e.g. Figure 3.13).

Beginning in Coniacian times, there was a major change from northwest - southeast extension to a southwest - northeast extensional regime. This is manifest in the opening of the Euphrates fault system with associated faulting striking northwestwards to the west of the Abd el Aziz area (Figure 3.14) (Kent and Hickman, 1997; Litak et al., 1997). From well data it is clear that thickening of the mid-Senonian Soukhne formation took place to the southwest across the Abba fault (Figure 3.14) - part of the Euphrates faulting event.

The northeast - southwest striking faults mentioned previously (Figure 3.13) are seen to be older than the Euphrates faulting and, as mentioned, may have their origin in the Paleozoic rifting and trough formation in central Syria. These older faults partially control the Maastrichtian sedimentation in the Euphrates fault system (Alsdorf et al., 1995). Also, the strike direction of faults in the Euphrates system reorient at this point (Figure 3.14), and no northwest - southeast trending Euphrates-type faults that cross the older northeast - southwest faults are found (Figure 3.14).

The Late Campanian was a time of further change when a new set of roughly east-west striking faults developed in the Sinjar - Abd el Aziz area (Figure 3.14). It is most likely that these were transtensional structures, and antithetic faults on some of these major latest Cretaceous faults attest to this (Figures 3.4, 3.10, and 3.13). The amount of strike-slip was likely relatively small, although very difficult to quantify given the current data. The overwhelming development at this stage was normal movement on the east - west faults focusing the deposition of the Shiranish formation (Figure 3.4). Similar structures extend eastwards into Iraq (e.g. Hart and Hay, 1974), eventually curving more northwest - southeast before merging with the more prominent Zagros trend. The timing of the faulting is consistent throughout the trend with thickening constrained to Late Campanian - Maastrichtian time. No fault-related thickening found either immediately above or below this interval. The Shiranish formation was a high fluid content body that would easily have flowed to fill the space created by the normal faulting (Hart and Hay, 1974). Paleocurrent studies by Kent and Hickman (1997) on sand bodies within the Shiranish show that currents were mainly from the north and northeast, that is, from the Mardin high.

To the west, the Abd el Aziz faulting appears to have been bounded by the previously mentioned Abba fault (Figure 3.14). Well data indicate that Shiranish thickness is approximately 200 meters greater on the Abd el Aziz (northeast) side of this fault, thus the Abba fault shows signs of motion both down to southwest and subsequently down to the northeast.

During the latest Cretaceous extensional phase, the earlier northeast - southwest striking faults most likely underwent transtension and acted as transfer faults between the east - west striking faults (Figure 3.8). Chaimov et al. (1993) documented a similar set of faults active during the Mesozoic in the southwest Palmyrides. Figures 3.12 and 3.13 show some

thickening of the Shiranish formation across these faults. Given the more recent stages of movement on these structures, the amount of strike-slip that they underwent is difficult to quantify, although the minor deformation caused by these faults as a whole would suggest it was limited.

The latest Cretaceous normal faulting that we document here appears to have been a thick-skinned phenomenon. No detachment is apparent on any of the seismic lines examined from the area. Although the quality of the seismic data degrades with time, and most sections are only 4 seconds TWT, many of the faults appear to be slightly listric with depth. We speculate that these faults are detaching at some deeper level in the crust.

The limited spatial and temporal extent of the latest Cretaceous faulting suggest that perhaps the whole crust was not involved in this event. Thus we do not consider this structure to be a 'rift' in the true sense, and avoid the use of that term here (e.g. Sengor, 1995). This observation is supported by the lack of extensive pre-rifting erosion, and the absence of a Cenozoic thermal sag basin above the Sinjar area (Figure 3.15), such as the sag clearly evident above the Euphrates graben (Litak et al., 1998).

Estimates of extension, through line-length balancing, have been made assuming that all of the extension took place within a 34 km zone (Figure 3.4), and that the strike-slip activity had negligible effect. Only the latest Cretaceous extensional event was considered. The balancing yields an extensional estimate of around 3.5 % (1.2 km); the value is probably greater for the Iraqi portion of the Sinjar structure. Crustal-scale models based on the thickness of the syn-rift sedimentation and the assumption of

**Figure 3.15:** Smoothed structure map near top of Cretaceous (see Figure 3.2 for location). Cretaceous rock outcrop marked with wavy line. Symbols same as Figure 3.14. Note that the top of Cretaceous surface closely follows the topography (Figure 3.1) indicating the lack of any significant Cenozoic sag basin above the Sinjar region.
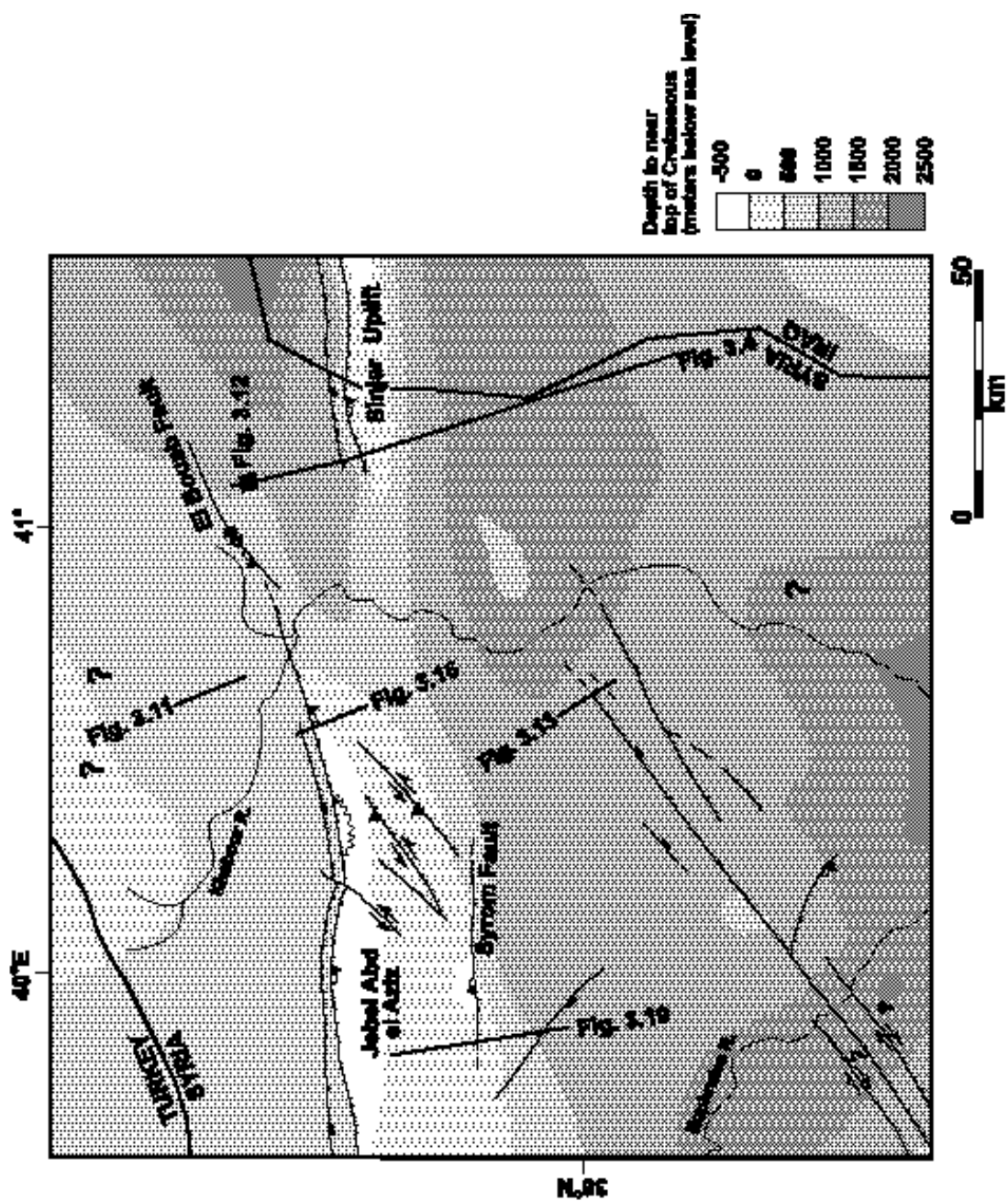
isostatic equilibrium yield a much greater value of stretching. This discrepancy could be because the extension was of such limited spatial and temporal extent that isostasy was not maintained, and perhaps the whole crust was not involved in the latest Cretaceous extensional event.

**Cenozoic**

Although there are hints of minor pulses of contractional tectonics during the Eocene and Miocene (Kent and Hickman, 1997), most horizontal shortening of the Sinjar - Abd el Aziz area did not take place until the Late Pliocene. This timing has been established using stratigraphic relationships by workers in the field (Ponikarov, 1966; Kent and Hickman, 1997), and is supported by the examples we have presented. Figure 3.4 shows uniform stratigraphic thickness throughout the Miocene section, with no signs of onlap. Some of the poorly reflective Pliocene section also records no tectonism, suggesting that the shortening event began here probably no earlier than about 3 Ma. This would make the timing of the uplift and folding approximately synchronous with the deposition of the Bakhtiary conglomerate formation. Reactivation and shortening took place largely in the form of fault-propagation folds (e.g. Suppe and Medwedeff, 1984) above the latest Cretaceous normal faults (Figure 3.4). In some cases the reactivation has extended these faults into the Cenozoic section, and even to the surface (Ponikarov, 1966) (Figures 3.4 and 3.16). The pattern of shortening and reactivation can be demonstrated by the mapping of the pre-compressional top of Cretaceous horizon (Figure 3.15) and is prominently reflected in the current topography (Figure 3.1). Figure 3.4 demonstrates how the larger, bounding faults of the Sinjar deformation are those which experienced most reverse movement.

**Figure 3.16:** Seismic reflection profile UN-350. See Figure 3.2 for location. Major faults are shown with stratigraphic picks tied to Maghlouja and other nearby wells.
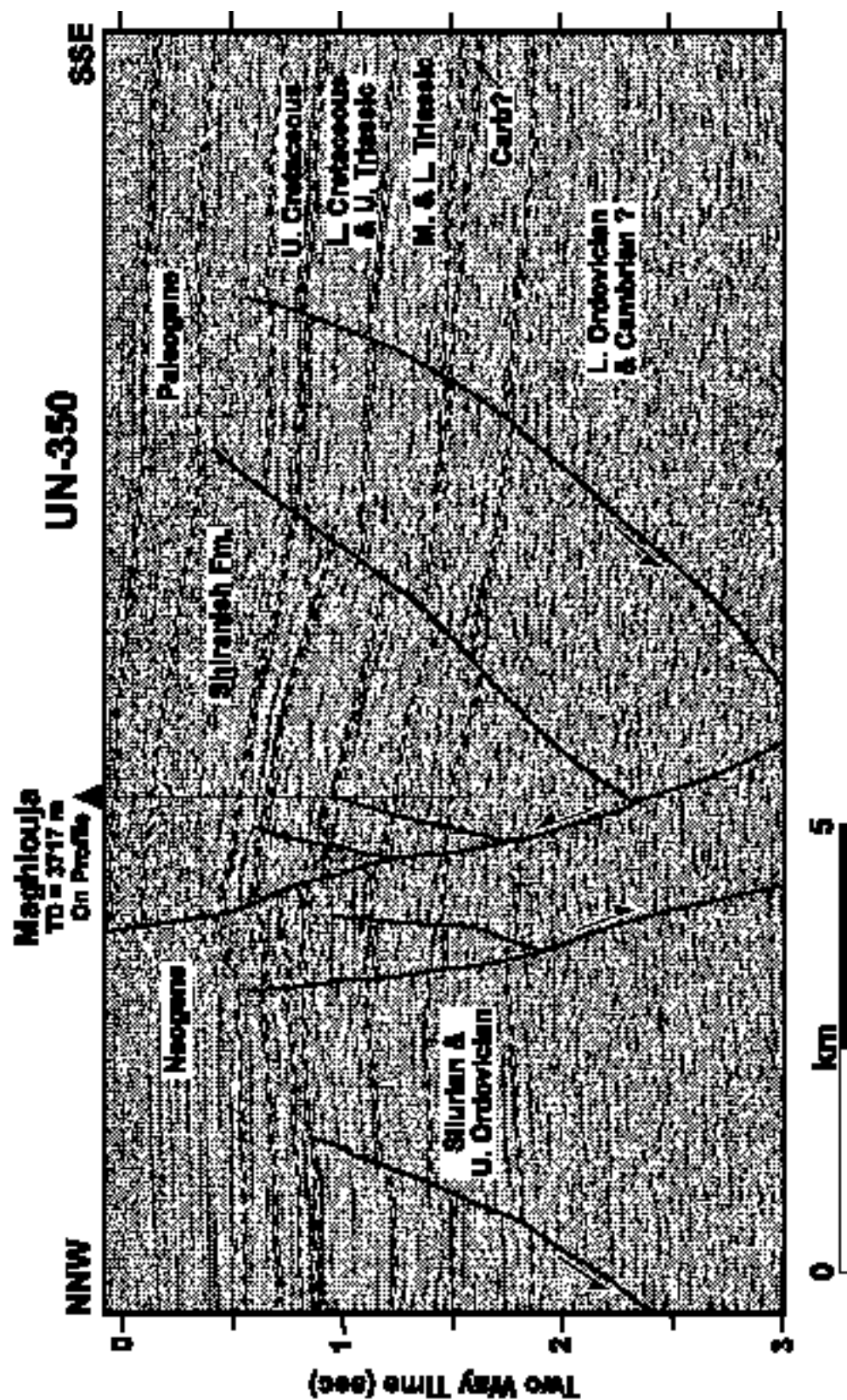
There is no outcrop evidence for any Cenozoic strike-slip having occurred on these east - west faults during the reactivation, although such movement is possible.

The easterly trends of structure and topography observed in Syria continue into Iraq. The Iraqi portions of these structures are poorly studied, but the geological and geophysical interpretations of Abdelhady et al. (1983), Naoum et al. (1981) and Hart and Hay (1974), as well as Landsat TM imagery interpretations show that a similar pattern of deformation extends significantly to the east (Figures 1 and 14). Line length balancing through the Syrian Sinjar structure (Figure 3.4) produces overall horizontal shortening estimates of around 1 % (~350 m). Similar work across the Jebel Abd el Aziz (Kent and Hickman, 1997) puts shortening there at less than 1 %. However, it is clear from topographic images (Figure 3.1) and Landsat TM data that the amount of horizontal shortening in the Iraqi portion of the Sinjar structure is significantly higher than this.

Cenozoic reactivation and inversion of an older northeast - southwest normal fault (the El Bouab fault) appears to be controlling the southeastern edge of the Abd el Aziz uplift (Figures 3.1, 3.14 and 3.15). Ponikarov (1966) reported ~5 km of left-lateral displacement of Upper Miocene rocks, together with a minor amount of reverse movement on a exposure of this fault, and a repeated section is observed in the nearby El-Bouab well. Ponikarov (1966) also mapped similar structures with smaller amounts of offset in the Jebel Abd el Aziz (Figure 3.14) where they have offset the east-west fault traces. Seismic reflection profiles (Figure 3.13), topography (see arrow on Figure 3.1) and earthquake catalogs (Chaimov et al., 1990; Litak et al., 1997) indicate that the northeast - southwest striking faults mapped from the Palmyride fold and thrust belt towards the northeast have been active recently. However, as discussed by Litak et al. (1997) the sense of motion on these faults is ambiguous. It is possible that they are currently right-lateral and form continuations of

dextral faults mapped in the Palmyride fold and thrust belt (e.g. Searle, 1994). Alternatively they could be left-lateral, similar to the El Bouab fault and others in Jebel Abd el Aziz.

## DISCUSSION

### Paleozoic

We now place our findings from northeast Syria into the context of regional tectonics (Figure 3.17a - f). After relatively stable conditions for most of the Early Paleozoic during which Arabia resided on the southern margin of the Tethys ocean, we observe a regional unconformity during the Late Silurian and Devonian. This event is observed contemporaneously in many localities around northern Gondwana and could be interpreted as a consequence of uplift on the flanks of PaleoTethyan rifts, rather than an orogenic event (personal communication, G. Stampfli, 1998).

Evidence from many sources points to the initiation of subsidence along the Palmyride / Sinjar trend beginning in the Carboniferous and rifting activity in the Late Permian (e.g. Robertson et al., 1991; Stampfli et al., 1991; Best et al., 1993; Ricou, 1995). The Carboniferous subsidence event is attributed to a reorganization of lithospheric stresses resulting from the docking of the Hun superterrane (Stampfli et al., 1999), or possibly as a result of continued extensional tectonics generated by the opening of the PaleoTethys (Sengor et al., 1988). The more important Late Permian rifting was a result of the formation of the NeoTethys as the Cimmerian superterrane broke away from Gondwana towards the northeast through oceanic accretion, and spreading began

**Figure 3.17:** Summary maps of the geologic evolution of the northern Arabian platform showing preserved sediment thickness and schematic tectonic events. The isopachs are based on our data plus Al-Naqib (1960); Rigo de Righi and Cortesini (1964); Al-Jumaily and Domaci (1976); Al-Laboun (1988); Abd-Jaber et al. (1989); Sage and Letouzey (1990); May (1991) and Litak et al. (1997). Paleo-plate boundaries are based on Robertson and Dixon (1984), Dercourt et al. (1986), Guiraud (1998) and Stampfli et al. (1999). Each frame illustrates the end of the stated time interval.

a) Late Paleozoic (Carboniferous and Permian). The almost ubiquitous cover of Triassic formations indicates that the sediment thicknesses shown here have not been subjected to post-Early Triassic erosion, although significant Permo-Triassic erosion took place. Opening of the NeoTethys ocean along the northeast margin of the Arabian plate was concurrent with rifting along the Palmyride / Sinjar trend.

b) Early Mesozoic (Triassic and Jurassic). The greatest preserved Mesozoic section is along the Levantine margin and in the deepest parts of the Palmyride / Sinjar basins that were thermally subsiding with some fault reactivation at this time.

c) Cretaceous (Late Campanian - Maastrichtian excluded). Cretaceous rocks outcrop in many parts of the Palmyride fold and thrust belt. Subduction in the NeoTethys caused new extensional events in eastern Syria.

d) Late Campanian and Maastrichtian. Cretaceous rocks outcrop in many parts of the Palmyride fold and thrust belt. Extension in northeast Syria took place.

e) Paleocene. Paleogene or older rocks outcrop in most areas west and south of the Euphrates river. After abrupt cessation of extension throughout the northern Arabian platform at the end of Cretaceous, the Paleogene was largely quiescent.

f) Neogene and Quaternary. Neogene or older rocks outcrop throughout almost the entire study area. Note the thinning over the uplifted areas in the northeast formed largely since the Pliocene as a result of collision along the northern margin.

**a)** Carboniferous & Permian

**b)** Triassic & Jurassic

Figure 3.17 (continued):



c) Early Cretaceous - Late Campanian

d) Late Campanian & Maastrichtian

Figure 3.17 (continued):



Neogene & Quaternary

Paleogene
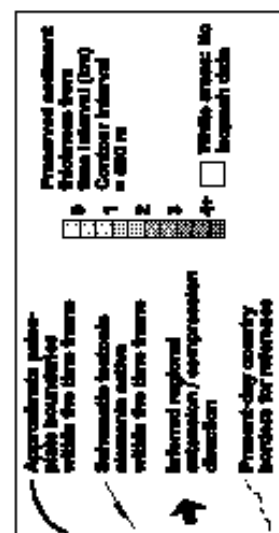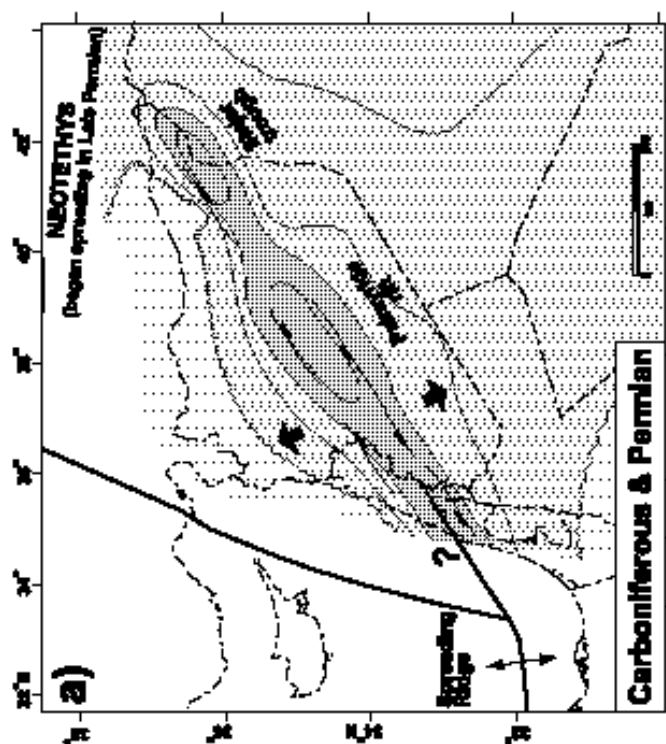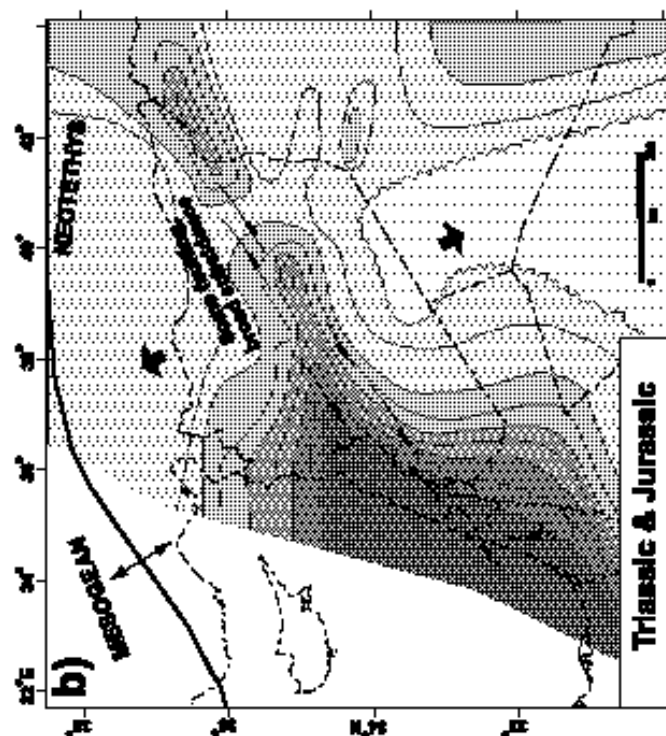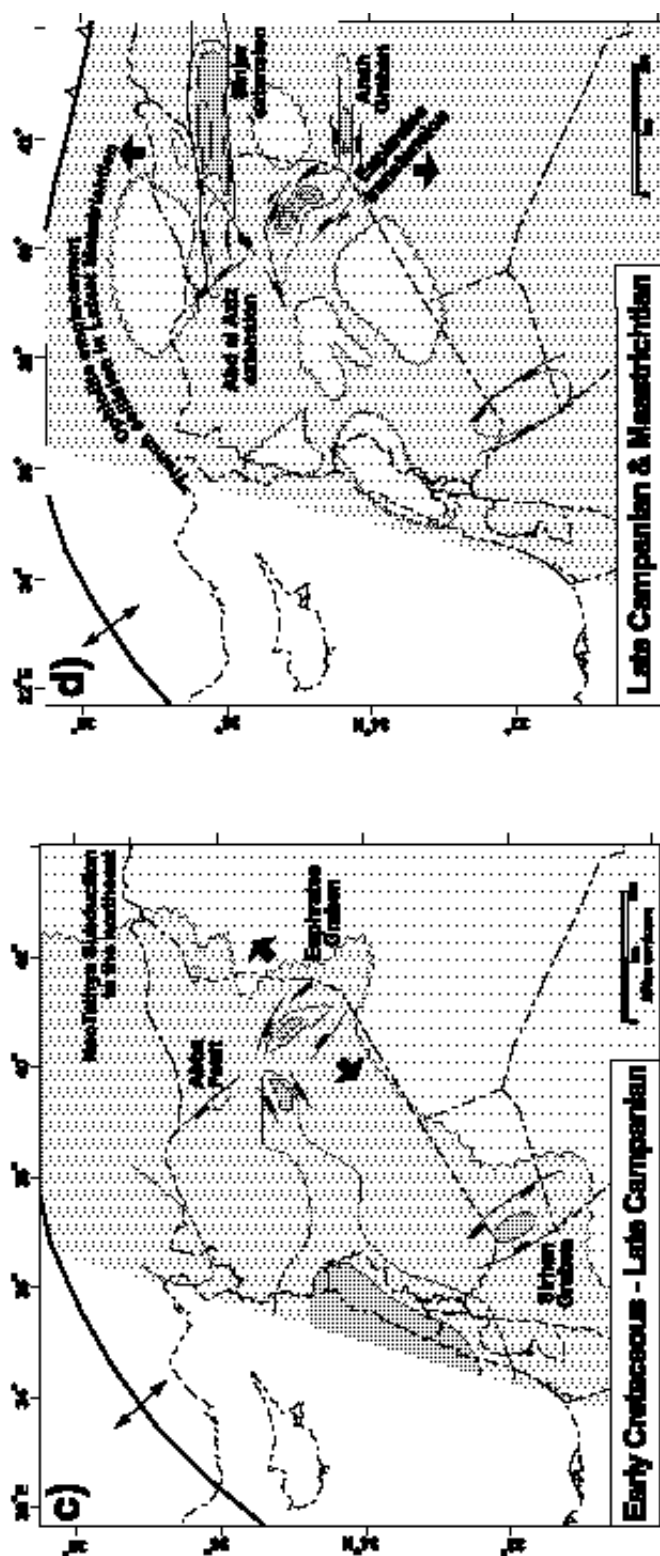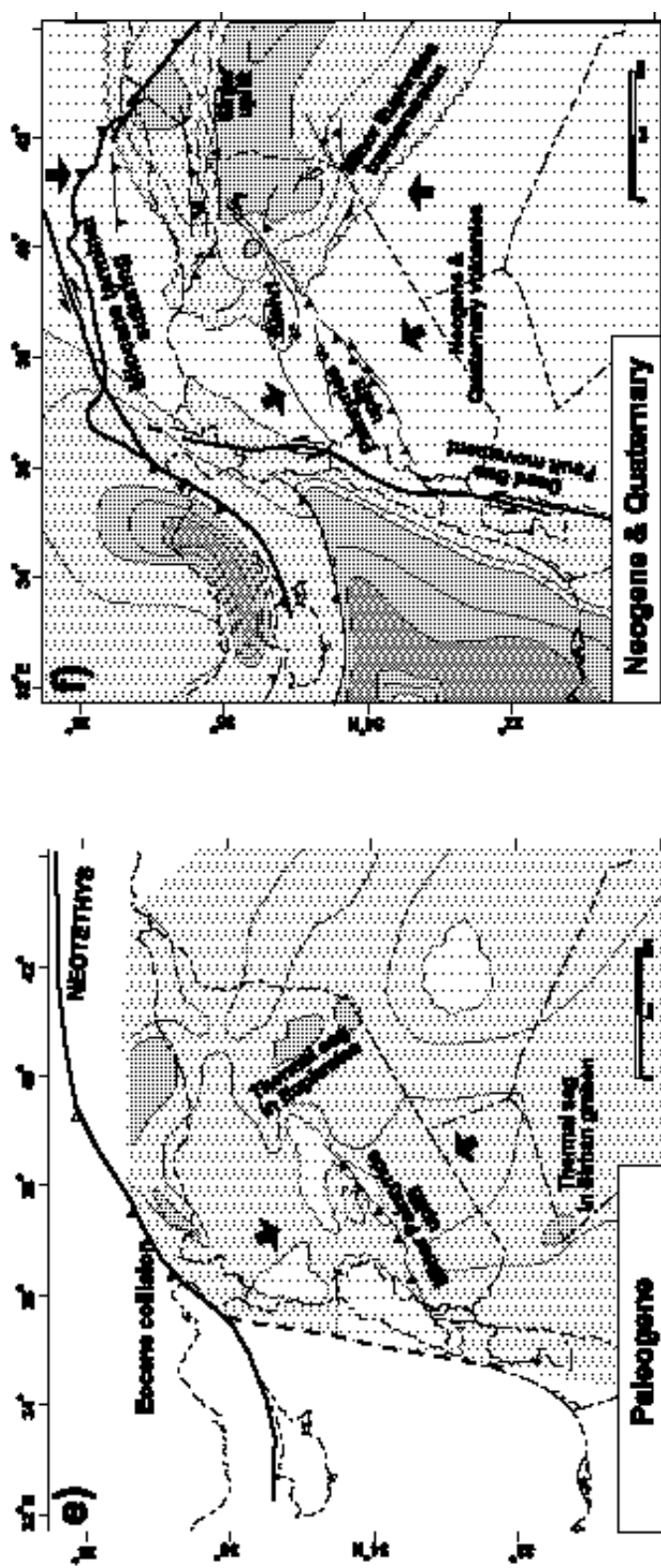
in what is now the eastern Mediterranean (Garfunkel, 1998). We support the hypothesis that the Palmyride / Sinjar structure could be an aulacogen (e.g. Ponikarov, 1966; Best et al., 1993), and note that in most respects it fits the definition of an aulacogen as used by Sengor (1995). Sengor (1995) described an aulacogen as the failed arm of a rift-rift-rift triple junction with mainly clastic syn-rift fill covered by carbonate post-rift sediments, repeatedly reactivated with some strike-slip parallel to the rift axis, and possibly formed along a much older zone of weakness. Furthermore, the amount of faulting and deformation in the Palmyride / Sinjar structure diminishes towards the northeast, again similar to the along-strike variation that would be expected in an aulacogen (Figure 3.17a). The plate reconstructions of Ricou (1995) and Stampfli et al. (1999) would allow for rifting in the Palmyrides, as would certain paleogeographic scenarios considered by Robertson et al. (1996).

Further evidence for Late Permian and Early Mesozoic rifting in the vicinity of the Palmyride / Sinjar rift is found in Israel farther to the southwest (Guiraud and Bosworth, 1997) where syn-sedimentary thickening and volcanics are described. This activity continued into the Mesozoic related to the formation of the Levantine passive margin there. Limited well data from Lebanon inhibit interpretations from that area although Beydoun (1981) speculated on the occurrence of an Lebanese aulacogen in Late Paleozoic / Mesozoic time.

The Late Paleozoic rifting and subsidence activity observed along the Palmyride / Sinjar trend could have been concentrated there along a zone of crustal weakness relic from the Late Proterozoic (Pan-African) accretion of the Arabian platform (e.g. Stoesser and Camp, 1985). It has previously been suggested that the Palmyrides might lie above such a suture or shear zone (e.g. Best et al., 1990) that could form a mobile zone between the relatively

stable crustal blocks of the platform, for instance the Aleppo plateau in the north and the Rutbah uplift in the south.

The exception to the pattern of NE-SW rifting in Syria is the Derro high of central Syria (Figure 3.1). As discussed, this area was a structural high in the Early Triassic and possibly the Carboniferous, and represents the 'Beida Arch' of Kent and Hickman (1997) that connects the adjacent Rawda and Mardin highs (Figure 3.1). The work of Brew et al. (1997) suggests that the Derro high is a basement uplift, partially bounded by faults, a conclusion supported by the present seismic reflection interpretations and previous work (Sawaf et al., 1993). Thus the uplifting of the Derro high is not part of the structural shortening of the Palmyride fold and thrust belt that began in the Late Cretaceous (e.g. Chaimov et al., 1993). We speculate, admittedly with limited evidence, that this structure could be the interior corner of a old continental block that participated in the accretion of the Arabian platform in the Proterozoic. Such an accretionary pattern, in which suture zones would underlie the Palmyride fold and thrust belt and the Euphrates graben, but not the Sinjar, was suggested by Litak et al. (1997) as a modification of the original suggestion of Best et al. (1993). As a result of such an arrangement, rifting in the present Sinjar region would be less pronounced than in the Palmyrides. This could further explain the relatively limited occurrences of Late Paleozoic faulting in northeast Syria.

**Mesozoic**

Widespread erosion around the Permo-Triassic boundary left Permian deposits preserved in only the deepest parts of the Palmyride / Sinjar rift (Figure 3.9). This pattern could be interpreted as a result of post-rift thermal uplift, as well as a consequence of globally low sea levels. It is debated whether rifting on the northern margin of Gondwana continued into the

Triassic (Robertson et al., 1991), or if rifting terminated in the Permian and thermal subsidence dominated Triassic tectonics (Stampfli et al., 1991). Although the current data do not allow a complete answer to this, much of the Mesozoic sedimentation in the Palmyride / Sinjar basin is more concordant with thermal subsidence above the rift.

During the Triassic, Syria changed from being an east-facing margin, to a westward-facing one (Best et al., 1993) as the Mesogean ocean formed in the west. This is illustrated in the isopach for that time (Figure 3.17b) that shows the further development of the Palmyride / Sinjar basins along the axis of the earlier Paleozoic rift. Clearly the Palmyride basin is connected to the developing margin along the Levantine where most sediment accumulation was occurring. In this respect the Palmyride basin was similar to the Benue trough in Nigeria that formed an embayment on the margin of the opening Atlantic (e.g. Sengor, 1995). Isopachs also show distinct thickening northeast of the Sinjar area in northeast Syria (Figure 3.17b). The Sinjar region was linked to the major Middle Eastern basin in the northeast that was developing along the northern passive margin of Gondwana (Lovelock, 1984). Thus sedimentation there was controlled by this as well as the rifting and subsidence of the Palmyride / Sinjar trend. Some evidence points towards renewed rifting in the Late Triassic (Delaune-Mayere, 1984). This is seen as a slight acceleration in both the subsidence curve shown here (Figure 3.7) and in Sawaf et al. (1999). Undoubtedly, the opening of the NeoTethys was a prolonged and complex event distributed widely in time and space. This complexity is manifest in the geologic history of northeast Syria and the rest of the Arabian platform.

The Late Jurassic / Early Cretaceous was the time of a significant regional unconformity throughout the northern Arabian platform. Laws and Wilson (1997) suggested that this regional uplift could be associated with plume activity, as it occurred synchronously with

widespread volcanic activity having possible plume-type geochemical signatures. The somewhat accelerated deposition found in the Sinjar area, the Palmyrides (Best, 1991; Chaimov et al., 1992) and the eastern Mediterranean at this time could also be a result of this regional volcanic / tectonic activity. Some researchers have also documented that accelerated spreading in the eastern Mediterranean perhaps contributing to the Late Jurassic / Early Cretaceous faulting (Robertson and Dixon, 1984).

During Cretaceous time, a major plate boundary reorganization took place (Figure 3.17c). Sea-floor spreading was dying out and subduction was underway on the northern margin of the NeoTethys ocean as its consumption commenced. Through the dating of volcanics and other work, Dercourt et al. (1986) found evidence for a new northeast-dipping, northwest - southeast striking, intra-oceanic subduction zone in the NeoTethys near the margin of Arabia around the Turonian / Coniacian boundary. In the Euphrates graben major rifting seems to have commenced in the Coniacian (Lovelock, 1984; Litak et al., 1997).

We suggest that the extension in Syria at this time was a consequence of stresses originating from slab pull along this subduction zone, as first proposed by Lovelock (1984). Zeyen et al. (1997) calculated that slab pull effects could extend a crust that was already under the influence of a mantle plume for instance, such as that proposed by Laws and Wilson (1997). Additionally, it has been suggested that the crust beneath the axis of the Euphrates fault system was a weak zone inherited from Proterozoic accretion of the Arabian platform (Litak et al., 1997), as discussed above. Thus the northwest - southeast striking subduction zone, together with plume activity and a possible pre-existing weak zone, caused extension in the Euphrates fault system. Stampfli et al. (1999) suggested a similar slab pull mechanism could have created the Syrt (Sirte) basin in Libya.

An alternative mechanism for the extension in the Euphrates and Sinjar - Abd el Aziz areas was proposed by Alsdorf et al. (1995). Using the principles of Sengör (1976), they suggested that the initial latest Cretaceous continental collision along the northern margin of the Arabian plate caused tensional forces orthogonal to the collision, thus creating the Euphrates fault system and Sinjar - Abd el Aziz faulting. However, the earlier initiation of faulting in the Euphrates graben (Litak et al., 1998), the increasing tectonism away from the collision (Litak et al., 1997), and the relatively large distance of the Euphrates from the collision, tend to invalidate this suggestion. For the Sinjar - Abd el Aziz area, the strongly oblique angle and distance from the initial collision, suggests this mechanism is also unlikely to have been the cause of faulting there. Rather, we propose that the initial collision caused the abrupt cessation of extension in the Euphrates and Sinjar - Abd el Aziz areas as detailed below.

Beginning in the Late Campanian - Maastrichtian further change took place and pronounced east-west oriented graben formation in the Sinjar - Abd el Aziz area began (Figures 3.8 and 3.17d). This was also the time of most active formation of the east - west trending Anah and Sinjar graben in Iraq (Ibrahim, 1979). We suggest that the formation of east - west trends at this time was a consequence of lithospheric tension created by reorienting subduction off the north and northeast margins of the Arabian peninsula (Dercourt et al., 1986), although the precise orientation and location of this subduction is difficult to ascertain. Additionally, the relative southerly advance of ophilolitic nappes that were to obduct onto the northern margin could have contributed to normal faulting through loading effects (Yilmaz, 1993). These factors could cause roughly north - south stress that resulted in extension, or more likely transtension, within the Sinjar - Abd el Aziz area. Perhaps the strain was accommodated there because it represented a structurally weak zone of thick sedimentation on the northern

edge of the Sinjar basin, although the precise reasons for east - west striking fault formation here remains somewhat enigmatic.

The Euphrates fault system at this time was experiencing transtension under the influence of the more obliquely oriented, north - south directed, extension direction (Figure 3.17d). In agreement with this, Litak et al. (1997) reported that strike-slip features are more common amongst the northwest - southeast striking faults of the Euphrates deformation, than amongst the west-northwest - east-southeast striking structures.

Extension in all areas stopped abruptly very near the end of the Maastrichtian. This is evidenced by the unconformities in the Euphrates graben and Abd el Aziz areas and the absence of faulting in the Tertiary section (e.g. Figure 3.4). Late Maastrichtian folding and basin inversion are widely reported in the southwestern Palmyride fold and thrust belt (e.g. Chaimov et al., 1992; Guiraud and Bosworth, 1997) signaling that the stresses that stopped the rifting in the east of Syria, caused uplift in the west. Latest Maastrichtian time also saw some relatively minor shortening in the foothills of Turkey farther to the north (Cater and Gillcrist, 1994). This transition from an extensional to a contractional regime was perhaps due to collision of the Arabian platform with the intra-oceanic subduction trench in the north and east, as suggested by Lovelock (1984). This event was related to widespread Maastrichtian obduction of supra-subduction ophiolites along the northern and northeastern margin of Arabia (Robertson et al., 1991). This was not the Eurasian - Arabia collision, however, and the NeoTethys ocean, with associated subduction, persisted to the north and east.

**Cenozoic**

The Paleogene was largely a time of quiescence in the northern Arabian platform with widespread thermal subsidence following rifting in the Euphrates and Sirhan grabens (Figure 3.17e) and deposition of significant open marine sediments elsewhere. Chaimov et al. (1992) documented minor uplift in the southwest Palmyride fold and thrust belt in Middle Eocene time, and minor shortening is also reported in the Mardin area in southern Turkey for that time (Cater and Gillcrist, 1994). The Late Eocene was important in the development of the Syrian Arc (Guiraud and Bosworth, 1997) and detailed field work by Kent and Hickman (1997) reveals that the Abd el Aziz was perhaps a very subtle structural high during latest Eocene. The mid-late Eocene has been documented as a period of collision in the northwestern corner of Arabia (e.g. Hempton, 1987; Ricou, 1995) with what Dercourt et al. (1986) call the Kirsehir block, thus explaining these observations (Figure 3.17e).

Around mid-Miocene time (~15 Ma) (Hempton, 1987; Yilmaz, 1993) terminal suturing occurred between Arabia and Eurasia along the Bitlis and Zagros sutures, bringing with it widespread horizontal shortening throughout the region. This collision caused accelerated basin inversion of the Palmyride fold and thrust belt (Chaimov et al., 1992), minor shortening in the northwest portion of the Euphrates fault system (Litak et al., 1997), and shortening in the Turkish foothills (Cater and Gillcrist, 1994) and the Zagros (Ala, 1982).

Kent and Hickman (1997) report signs that the Abd el Aziz may have been a subtle high during the Late Miocene. However, major uplift of the Sinjar - Abd el Aziz only occurred in the mid / late Pliocene - Recent. Interestingly, Pliocene time saw renewed northward movement of Arabia with respect to Eurasia under the influence of renewed spreading in the Red Sea accommodated by escape along the then newly active North and East Anatolian

faults (Hempton, 1987). This interpretation is supported by Féraud et al. (1985) who dated dikes and volcanic alignments in Syria, and related them to crustal stress directions. They found that there was a reorientation at around 5 Ma from northwest - southeast maximum compressive stress, to a more north - south direction. This could explain why north - south shortening in the Sinjar - Abd el Aziz area occurred distinctly after northwest - southeast shortening in the Palmyrides.

The southeast of the Euphrates fault system has also experienced Pliocene transpression (Litak et al., 1997) that geomorphological evidence suggest might be still active today (Ponikarov, 1966). The Euphrates fault system shows much less shortening than the Sinjar - Abd el Aziz area due to the latter's proximity to the northern margin, and its nearly perpendicular orientation to the maximum horizontal compression, in contrast to the Euphrates fault system's oblique angle (Figure 3.17f).

Currently the Palmyride region is deforming by transpression (Chaimov et al., 1990; Searle, 1994), under the influence of stresses from the northwest (Figure 3.17f). Our analysis suggests that the northeast trending faults mapped from the Bishri block towards the Abd el Aziz (Figures 3.1, 3.14 and 3.17f) could be acting to translate right lateral shear away from the Palmyride region. This would imply counterclockwise rotation of the Bishri block. Alternatively, these could be sinistral faults active under the north - south compression, implying that the Bishri block is undergoing clockwise rotation (Best, 1991). Focal mechanisms and surface evidence are not yet sufficient to resolve this issue.

**HYDROCARBON POTENTIAL**

Historically, northeast Syria was the most hydrocarbon-productive region in the country, although the Euphrates graben (Figure 3.2) is now volumetrically more prolific (e.g. Litak et al., 1998). Estimated recoverables from Syria are about 2.5 Bbbl of oil and 8.5 TCF of gas (Oil & Gas Journal, December 1998). The northeast fields still form an appreciable part of the country's 550,000 barrels a day of oil production with, for instance, the Tichreen field (see location on Figure 3.2) producing about 10 % of this (GeoArabia, E & P Features, September 1997).

The relatively minor Late Mesozoic extension and Late Cenozoic horizontal shortening described in this paper were critical to the plays in northeast Syria, southeast Turkey, and northwest Iraq (e.g. Harput et al., 1992). Hydrocarbons are trapped in fault blocks and fault-propagation folds above reactivated normal faults. These relationships are evident from a cursory comparison between field locations (Figure 3.2) and Figures 3.1 and 3.4. Most source rocks in northeast Syria are thought to be of Cretaceous and Triassic age (Metwalli et al., 1974; Ala and Moss, 1979). Reservoirs are predominately found in Mesozoic and Cenozoic fractured carbonates that were charged during the Late Mesozoic and Late Cenozoic; many fields have multiple objectives in the Miocene, Cretaceous and Triassic (Ala and Moss, 1979). Sealing is accomplished by shales and evaporites that are distributed throughout the Mesozoic and Cenozoic sections. The older reservoirs tend to harbor lighter oils or gas. As an example of current production in northeast Syria, the Tichreen field produces from four horizons: the Chilou (Oligocene), Jaddala (Middle Eocene), Shiranish (Maastrichtian) and Kurrachine (Middle Triassic). All of these formations are carbonates with generally low porosity and fracture permeability. Oils of ~18 API gravity are produced from the upper formations, and gas from the Triassic (Alsharhan and Nairn, 1997).

In Syria, producing Cenozoic reservoirs in fault-propagation formed anticlinal traps have been charged since the initiation of Late Cenozoic fault reactivation (Ala and Moss, 1979). However, farther north in Turkey, a greater amount of shortening has led to fault propagation breaching many of the reservoirs (Cater and Gillcrist, 1994). This illustrates the critical relationship between the extent of structural inversion and the formation of viable hydrocarbon traps. The reservoirs in northeast Syria are reminiscent of those in the Zagros where Ala (1982) reported various levels of fractured carbonate reservoirs, with traps formed mainly in anticlines. Migration of the oil into these traps has occurred since the folding events that, as in northeast Syria, are a Late Cenozoic phenomenon.

As production has declined in these relatively younger fields more attention has focused on possible Paleozoic plays, as elsewhere within Arabia (Al-Husseini, 1992). Graptolitic Silurian shale source rocks of the Tanf formation (Figure 3.3), have been documented in the Euphrates graben and through most of the Middle East. Additionally, the Lower Ordovician Swab formation seems to form a viable source (Alsharhan and Nairn, 1997). In northeast Syria the Tanf shales exist over much of the area (Figure 3.9) before being eroded out towards Turkey; the Swab is ubiquitous. The top of the Tanf is found between ~1400 mbmsl (meters below mean sea level) and ~2300 mbmsl across much of the study area, but deepens to ~4000 mbmsl in the vicinity of the Khabour river in the south of the study area. The top of the Swab formation is generally found ~500 m or more deeper than the top of the Tanf formation, except on the Mardin high where the Silurian and Upper Ordovician have been lost to erosion (Figure 3.9). The work of Serryea (1990) suggests that the Silurian and Ordovician age sources in northeast Syria are generally mature. In southeast Turkey, where Silurian oil and gas discoveries have been made, the Silurian Dadas formation is the best

source with TOC of 2 - 5 % and favorable maturity (Harput et al., 1992), similar to results from the Tanf formation in north Syria.

In Syria reservoir rocks in the Paleozoic could include Permo-Carboniferous and Ordovician sandstones that are present over most of the region (Figure 3.9). The depth to top of the Paleozoic section varies significantly throughout the study area from around sea level on the Derro High to more than 3700 mbmsl in the Sinjar trough. Well data from northeast Syria show Upper Ordovician age Affendi sandstones to have 15-25 % porosity and permeabilities of up to 500 md. The Maghlouja well on the Abd el Aziz structure (Figures 3.2 and 3.16) found Paleozoic oil and gas in uneconomic qualities (Kent and Hickman, 1997). This well had shows of gas in the Silurian section, and limited shows of relatively light oil (39 API gravity) in the Upper Ordovician Affendi formation (K. Norman, personal communication, 1998). Perhaps this oil was sourced in the Silurian and migrated after fault inversion juxtaposed that unit with the Ordovician in the Neogene (Figure 3.16)? This potentially recent migration could be the cause of low charge. For other potential Paleozoic reservoirs, transgressive and regressive cycles that prevailed through much of the Paleozoic could have left viable stratigraphic traps in place, whilst fault control is possible along the axis of the Euphrates faulting west of Abd el Aziz. Timing of migration could be the deciding factor for Paleozoic production in this area. Current exploration in eastern Syria (GeoArabia, E & P Features, September 1997) will reveal more about Paleozoic hydrocarbon potential.

## CONCLUSIONS

The Sinjar area of northeast Syria was part of the larger southwest - northeast trending Palmyride / Sinjar basins from Late Paleozoic to Late Cretaceous time. Although rifting took

place in the Palmyrides / Sinjar in the Late Paleozoic, during the Mesozoic most of the stratigraphic thickening was subsidence related.  Following plate tectonic reorganization in Cretaceous time, rifting commenced along northwest - southeast trends in the Euphrates fault system beginning in the Coniacian.  In later Cretaceous time, extension began across east - west striking faults in the Sinjar - Abd el Aziz area causing substantial thicknesses of syn-extensional Late Campanian - Maastrichtian marly limestone to be deposited there.

A latest Cretaceous collisional event along the northern Arabian plate margin terminated the extension in the Sinjar - Abd el Aziz area.  Eocene - Miocene suturing of Arabia to Eurasia had little effect on the structures of northeast Syria, despite being the cause of significant uplift in the adjacent Palmyride fold and thrust belt.  Rather, the stress reorganization and northward Arabian plate movement experienced since Pliocene time has caused reactivation of the normal faults in a reverse sense in northeast Syria.  Fault-propagation folding and structural inversion have resulted in the topography that persists in the area today.  This late stage structural reactivation is critical to Cenozoic and Mesozoic anticlinal hydrocarbon trapping in the area.  Paleozoic horizons remain to be fully explored.

## REFERENCES

Abdelhady, Y.E., A. Tealeb and F.A. Ghaib 1983. *Tectonic Trends Inferred from Gravity Field Analysis in the Sinjar Area, Northwest Iraq*. International Basement Tectonics Association, **4**, 237-244.

Abu-Jaber, N.S., M.M. Kimberley and V.V. Cavaroc 1989. *Mesozoic-Palaeogene Basin Development within the Eastern Mediterranean Borderland*. Journal of Petroleum Geology, **12**, 419-436.

Al-Husseini, M.I. 1992. *Potential Petroleum Resources of the Paleozoic Rocks of Saudi Arabia*. Proceedings of the World Petroleum Congress, Buenos Aires, Argentina, 1991, **13**, 3-13.

Al-Jumaily, R. and L. Domaci 1976. *Geological and Tectonic Position of Jebel Sasan-Jebel Ishkaft Area, NW of Tel Afar, Iraq*. Journal of the Geological Society of Iraq, **9**, 101-115.

Al-Laboun, A. 1988. *The Distribution of Carboniferous-Permian Siliclastic Rocks in the Greater Arabian Basin*. Geological Society of America Bulletin, **100**, 362-373.

Al-Naqib, K.M. 1960. *Geology of the Southern Area of Kirkuk Liwa, Iraq*. Second Arab Petroleum Congress, Beirut, Lebanon, The Secretariat General of the League of Arab States, 1-49.

Ala, M.A. 1982. *Chronology of Trap Formation and Migration of Hydrocarbons in the Zagros Sector of Southwest Iran*. American Association of Petroleum Geologists Bulletin, **66**, 1535-1541.

Ala, M.A. and B.J. Moss 1979. *Comparative Petroleum Geology of Southeast Turkey and Northeast Syria*. Journal of Petroleum Geology, **1**,. 3-27.

Alsdorf, D., M. Barazangi, R. Litak, D. Seber, T. Sawaf and D. Al-Saad 1995. *The Intraplate Euphrates Depression - Palmyrides Mountain Belt Junction and Relationship to Arabian Plate Boundary Tectonics*. Annali Di Geofisica, **38**, 385-397.

Alsharhan, A.S. and A.E.M. Nairn 1997. *Sedimentary Basins and Petroleum Geology of the Middle East*. Elsevier, Amsterdam, 843 p.

Barazangi, M., D. Seber, T. Chaimov, J. Best, R. Litak, D. Al-Saad and T. Sawaf 1993. *Tectonic Evolution of the Northern Arabian Plate in Western Syria.* In E. Boschi, E. Mantovani and A. Morelli (Eds.), Recent Evolution and Seismicity of the Mediterranean Region, Kluwer Academic Publishers, Netherlands, 117-140.

BEICIP 1975. *Gravity Maps of Syria: Damascus (Syria)*. Bureau d'etudes industrielles et de cooperation de l'institut francais du petrole, Hauts de Seine, 96 p.

Best, J.A., 1991. *Crustal Evolution of the Northern Arabian Platform Beneath the Syrian Arab Republic*. Ph.D. Thesis, Cornell University, Ithaca, New York, 152 p.

Best, J.A., M. Barazangi, D. Al-Saad, T. Sawaf and A. Gebran 1990. *Bouguer Gravity Trends and Crustal Structure of the Palmyride Mountain Belt and Surrounding Northern Arabian Platform in Syria*. Geology, **18**, 1235-1239.

Best, J.A., M. Barazangi, D. Al-Saad, T. Sawaf and A. Gebran 1993. *Continental Margin Evolution of the Northern Arabian Platform in Syria*. American Association of Petroleum Geologists Bulletin, **77**, 173-193.

Beydoun, Z. 1981. *Some Open Questions Relating to the Petroleum Prospects of Lebanon*. Journal of Petroleum Geology, **3**, 303-314.

Beydoun, Z.R. 1991. *Arabian Plate Hydrocarbon Geology and Potential – a Plate Tectonic Approach*. Studies in Geology, **33**, American Association of Petroleum Geologists, Tulsa, Oklahoma, USA, 77 p.

Brew, G.E., R.K. Litak, D. Seber, M. Barazangi, A. Al-Imam and T. Sawaf 1997. *Basement Depth and Sedimentary Velocity Structure in the Northern Arabian Platform, Eastern Syria*. Geophysical Journal International, **128**, 617-631.

Cater, J.M.L. and J.R. Gillcrist 1994. *Karstic Reservoirs of the Mid-Cretaceous Mardin Group, SE Turkey: Tectonic and Eustatic Controls on their Genesis, Distribution and Preservation*. Journal of Petroleum Geology, **17**, 253-278.

Chaimov, T., M. Barazangi, D. Al-Saad and T. Sawaf 1993. *Seismic Fabric and 3-D Upper Crustal Structure of the Southwestern Intracontinental Palmyride Fold Belt, Syria*. American Association of Petroleum Geologists Bulletin, **77**, 2032-2047.

Chaimov, T., M. Barazangi, D. Al-Saad, T. Sawaf and A. Gebran 1990. *Crustal Shortening in the Palmyride Fold Belt, Syria, and Implications for Movement Along the Dead Sea Fault System*. Tectonics, **9**, 1369-1386.

Chaimov, T., M. Barazangi, D. Al-Saad, T. Sawaf and A. Gebran 1992. *Mesozoic and Cenozoic Deformation Inferred from Seismic Stratigraphy in the Southwestern Intracontinental Palmyride Fold-Thrust Belt, Syria*. Geological Society of America Bulletin, **104**, 704-715.

Delaune-Mayere, M. 1984. *Evolution of a Mesozoic Passive Continental Margin: Baër-Bassit (NW Syria).* In J.E. Dixon and A.H.F. Robertson (Eds.), The Geologic Evolution of the Eastern Mediterranean, Blackwell Scientific Publications, Edinburgh, Scotland, 151-159.

Dercourt, J., L.P. Zonenshain, L.-E. Ricou, V.G. Kazmin, X. LePichon, A.L. Knipper, C. Grandjacquet, I.M. Sbortshikov, J. Geyssant, C. Lepvrier, D.H. Pechersky, J. Boulin, J.-C. Sibuet, L.A. Savostin, O. Sorokhtin, M. Westphal, M.L. Bazhenov, J.P. Lauer and B. Biju-Duval 1986. *Geological Evolution of the Tethys Belt from the Atlantic to the Pamirs Since the Lias*. Tectonophysics, **123**, 241-315.

Feraud, G., G. Giannerini and R. Campredon 1985. *Dyke Swarms as Paleostress Indicators in Areas Adjacent to Continental Collision Zones: Examples from the European and Northwest Arabian Plates*. Mafic Dyke Swarms, Erindale College, University of Toronto, Ontario, Canada, International Lithosphere Program, 273-278.

Garfunkel, Z. 1998. *Constrains on the Origin and History of the Eastern Mediterranean Basin*. Tectonophysics, **298**, 5-35.

Guiraud, R. 1998. *Mesozoic Rifting and Basin Inversion Along the Northern African Tethyan Margin: An Overview*. In D.S. Macgregor, R.T.J. Moody and D.D. Clark-Lowes (Eds.), Petroleum Geology of North Africa, Geological Society of London, Special Publication **132**, 217-229.

Guiraud, R. and W. Bosworth 1997. *Senonian Basin Inversion and Rejuvenation of Rifting in Africa and Arabia: Synthesis and Implications to Plate-Scale Tectonics*. Tectonophysics, **282**, 39-82.

Harput, O.B., F. Goodarzi and O. Erturk 1992. *Thermal Maturation and Source Rock Potential of Sedimentary Succession in Southeast Anatolia, Turkey*. Energy Sources,. **14**, 317-329.

Hart, E. and J.T.C. Hay 1974. *Structure of the Ain Zalah Field, Northern Iraq*. American Association of Petroleum Geologists Bulletin, **58**, 973-981.

Hempton, M. 1987. *Constraints on Arabian Plate Motion and Extensional History of the Red Sea*. Tectonics, **6**, 687-705.

Ibrahim, M.W. 1979. *Shifting Depositional Axes of Iraq: An Outline of Geosynclinal History*. Journal of Petroleum Geology, **2**, 181-197.

Kent, W.N. and R.G. Hickman 1997. *Structural Development of Jebel Abd Al Aziz, Northeast Syria*. GeoArabia, **2**, 307-330.

Laws, E.D. and M. Wilson 1997. *Tectonics and Magmatism Associated with the Mesozoic Passive Continental Margin Development in the Middle East*. Journal of the Geological Society, **154**, 459-464.

Leonov, Y.G., K. Makarem and T. Zaza 1986. *Olistostrome Origin for Rocks in the Core of the Abd El Aziz Anticline, Syria*. Geotectonics, **20**, 142-146.

Litak, R.K., M. Barazangi, W. Beauchamp, D. Seber, G. Brew, T. Sawaf and W. Al-Youssef 1997. *Mesozoic-Cenozoic Evolution of the Intraplate Euphrates Fault System, Syria: Implications for Regional Tectonics*. Journal of the Geological Society, **154**, 653-666.

Litak, R.K., M. Barazangi, G. Brew, T. Sawaf, A. Al-Imam and W. Al-Youssef 1998. *Structure and Evolution of the Petroliferous Euphrates Graben System, Southeast Syria*. American Association of Petroleum Geologists Bulletin, **82**, 1173-1190.

Lovelock, P.E.R. 1984. *A Review of the Tectonics of the Northern Middle East Region*. Geological Magazine, **121**, 577-587.

May, P.R. 1991. *The Eastern Mediterranean Mesozoic Basin: Evolution and Oil Habitat*. American Association of Petroleum Geologists Bulletin, **75**, 1215-1232.

Metwalli, M., G. Philip and M. Moussly 1974. *Petroleum-Bearing Formations in Northeastern Syria and Northern Iraq*. American Association of Petroleum Geologists Bulletin, **58**, 1781-1796.

Naoum, A.A., M.S. Atiya and M.R. Al-Ubaidi 1981. *Mesoscopic Structures Associated with Sinjar Anticline*. Journal of the Geological Society of Iraq, **14**, 71-80.

Ponikarov, V.P. 1966. *The Geology of Syria. Explanatory Notes on the Geological Map of Syria, Scale 1:200 000*. Ministry of Industry, Damascus, Syrian Arab Republic.

Ricou, L.E. 1995. *The Plate Tectonic History of the Past Tethys Ocean.* In A.E.M. Nairn, L.-E. Ricou, B. Vrielynck and J. Dercourt (Eds.), The Ocean Basins and Margins: The Tethys Ocean, Plenum Press, New York, 3-70.

Rigo de Righi, M. and A. Cortesini 1964. *Gravity Tectonics in Foothills Structure Belt of Southeast Turkey*. American Association of Petroleum Geologists Bulletin, **48**, 1911-1937.

Robertson, A.H.F., P.D. Clift, P.J. Degnan and G. Jones 1991. *Palaeogeographic and Palaeotectonic Evolution of the Eastern Mediterranean Neotethys*. Palaeogeography, Palaeoclimatology, Palaeoecology, **87**, 289-343.

Robertson, A.H.F. and J.E. Dixon 1984. *Aspects of the Geological Evolution of the Eastern Mediterranean.* In J.E. Dixon and A.H.F. Robertson (Eds.), The Geologic Evolution of the Eastern Mediterranean, Blackwell Scientific Publications, Edinburgh, Scotland, 1-74.

Robertson, A.H.F., J.E. Dixon, S. Brown, A. Collins, A. Morris, E. Pickett, I. Sharp and T. Ustaomer 1996. *Alternative Tectonic Models for the Late Paleozoic-Early Tertiary Development of the Tethys in the Eastern Mediterranean Region.* In A. Morris and D.H. Tarling (Eds.), Paleomagnetism and Tectonics of the Mediterranean Region, Geological Society of London Special Publication **105**, 239-263.

Sage, L. and J. Letouzey 1990. *Convergence of the African and Eurasian plate in the Eastern Mediterranean.* In J. Letouzey (Ed.), Petroleum and Tectonics in Mobile Belts; proceedings of the IFP exploration and production research conference, Editions Technip, Paris, 49-68.

Sawaf, T., D. Al-Saad, A. Gebran, M. Barazangi, J.A. Best and T. Chaimov 1993. *Structure and Stratigraphy of Eastern Syria Across the Euphrates Depression.* Tectonophysics, **220**, 267-281.

Sawaf, T., G.E. Brew, R.K. Litak and M. Barazangi 2000. *Geologic Evolution of the Intraplate Palmyride Basin and Euphrates Fault System, Syria (in press).* In W. Cavazza, A. Robertson and P. Ziegler (Eds.), Peritethyan Rift / Wrench Basins and Margins, PeriTethys Memoir #6, Museum National d'Historie Naturelle, Paris.

Sclater, J.G. and P.A.F. Christie 1980. *Continental Stretching: An Explanation of the Post-Mid-Cretaceous Subsidence of the Central North Sea Basin.* Journal of Geophysical Research, **85**, 3711-3739.

Searle, M.P. 1994. *Structure of the Intraplate Eastern Palmyride Fold Belt, Syria.* Geological Society of America Bulletin, **106**, 1332-1350.

Sengör, A. 1976. *Collision of Irregular Continental Margins: Implications for Foreland Deformation of Alpine-Type Orogens*. Geology, **4**, 779-782.

Sengor, A.M.C. 1995. *Sedimentation and Tectonics of Fossil Rifts.* In C.J. Busby and R.V. Ingersoll (Eds.), Tectonics of Sedimentary Basins, Blackwell Science, Cambridge, 53-117.

Sengor, A.M.C., D. Altmer, A. Cin, T. Ustaomer and K.J. Hsü 1988. *Origin and Assembly of the Tethyside Orogenic Collage at the Expense of Gondwana Land.* In M.G. Audley-Charles and A. Hallam (Eds.), Gondwana and Tethys, Geological Society London Special Publication, 119-181.

Serryea, O.A. 1990. *Geochemistry of Organic Matter and Oil as an Effective Tool for Hydrocarbon Exploration in Syria*. Oil and Arab Cooperation, **16**, 31-74.

Stampfli, G., J. Marcoux and A. Baud 1991. *Tethyan Margins in Space and Time.* Palaeogeography, Palaeoclimatology, Palaeoecology, **87**, 373-410.

Stampfli, G.M., J. Mosar, P. Favre, A. Pillevuit and J.-C. Vannay 2000. *Permo-Triassic Evolution of the Western Tethyan Realm: The NeoTethys / East Mediterranean Basin Connection (in press).* In W. Cavazza, A.H.F. Robertson and P. Ziegler (Eds.), Peritethyan Rift / Wrench Basins and Margins, PeriTethys Memoir #6, Museum National d'Historie Naturelle, Paris.

Stoesser, D.B. and V.E. Camp 1985. *Pan-African Microplate Accretion of the Arabian Shield*. Geological Society of America Bulletin, **96**, 817-826.

Suppe, J. and D.A. Medwedeff 1984. *Fault-Propagation Folding*. Geological Society of America Abstract Program, **16**, 670.

Yilmaz, Y. 1993. *New Evidence and Model on the Evolution of the Southeast Anatolian Orogen*. Geological Society of America Bulletin, **105**, 251-271.

Zeyen, H., F. Volker, V. Wehrle, K. Fuchs, S.V. Sobolev and R. Altherr 1997. *Styles of Continental Rifting: Crust-Mantle Detachment and Mantle Plumes*. Tectonophysics, **278**, 329-352.

# CHAPTER FOUR

# Structure and tectonic development of the Dead Sea Fault System and Ghab Basin in Syria

## ABSTRACT

We examine the structure and evolution of the Ghab Basin that formed on the active, yet poorly understood, northern Dead Sea transform fault system. Interpretations of seismic reflection and well data, gravity modeling, and surface geology yield a subsurface image of the basin. The basin formed in Plio-Quaternary time at a complex step-over zone on the fault. Subsidence occurred along cross-basin and transform-parallel faults in two asymmetric depocenters. The larger depocenter in the south end of the basin is asymmetric towards the east, the margin along which most active transform displacement is occurring. Our analysis is enhanced by comparison to deformation and deposition observed in other strike-slip basins and physical models.

The topographically and structurally high Syrian Coastal Ranges, located directly west of the Ghab Basin, are a consequence of Late Cretaceous and Cenozoic regional compression, heavily modified by the Plio-Quaternary Dead Sea Fault System and Ghab Basin formation. They are part of the broader scheme of Syrian Arc deformation. Plio-Quaternary uplift of the Coastal Ranges has been preferentially focused west of the Dead Sea Fault, possibly through reverse movement detached along the fault. A Plio-Quaternary age for the development of the Dead Sea Fault System in northwest Syria is consistent with previously proposed models of two-phase Dead Sea Fault System movement and Red Sea spreading.

## INTRODUCTION

Continental transform faults, such as the San Andreas Fault in California, the Alpine Fault in New Zealand, the North Anatolian Fault in Turkey, and the Dead Sea Fault System (DSFS), involve complex structural and sedimentary regimes. This complexity relates to the history of displacement along these fundamental components of the global plate tectonic framework. Our work concerns the development of structures and history of deposition along the northern DSFS that is relatively little studied compared to the southern DSFS (i.e., south of the Lebanese restraining bend, Figure 4.1). The evolution of the DSFS remains one of the most contentious issues of Middle Eastern tectonics.

This work begins with a very brief review of the DSFS. After a description of available data, we present our interpretation of the structure of the Ghab Basin that lies along the northern DSFS (Figures 4.1 and 4.2). This interpretation is largely based on high quality seismic reflection profiles from the basin that are published here for the first time. Our analysis, integrated with interpretations of Bouguer gravity anomalies and surface geology, shows the deep, asymmetric, double-depocenter structure of the Plio-Quaternary Ghab Basin. We compare this to other strike-slip basins and models of strike-slip basin formation to provide further insight into the tectonic controls on basin formation and evolution of the basin through time. The gross scale topographic signature of the adjacent Syrian Coastal Ranges is then considered. This prominent topography (Figure 4.2) is shown to be part of the regional Late Cretaceous and Cenozoic Syrian Arc uplift, albeit strong modified by the Plio-Quaternary propagation of the DSFS and development of the Ghab Basin. Our new regional model, founded on the previous work of Hempton (1987) and Chaimov et al. (1990), illustrates how the

**Figure 4.1:** Regional shaded relief image of the Eastern Mediterranean illuminated from the northwest. The Dead Sea Fault System (DSFS) extends from the Gulf of Aqaba to Turkey, as highlighted between the two large arrows on this figure. Numerous flat-bottomed step-over basins along the fault, and significant asymmetric topography on either side of the fault, are clear in this image. The proposed location of the Roum fault (e.g. Butler et al., 1997) is also shown. Locations of traverses shown in Figure 4.9 are indicated. The dashed box marks the extents of Figures 4.2, 4.3 and 4.11. Inset illustrates the regional plate tectonic setting (EAF = East Anatolian Fault).
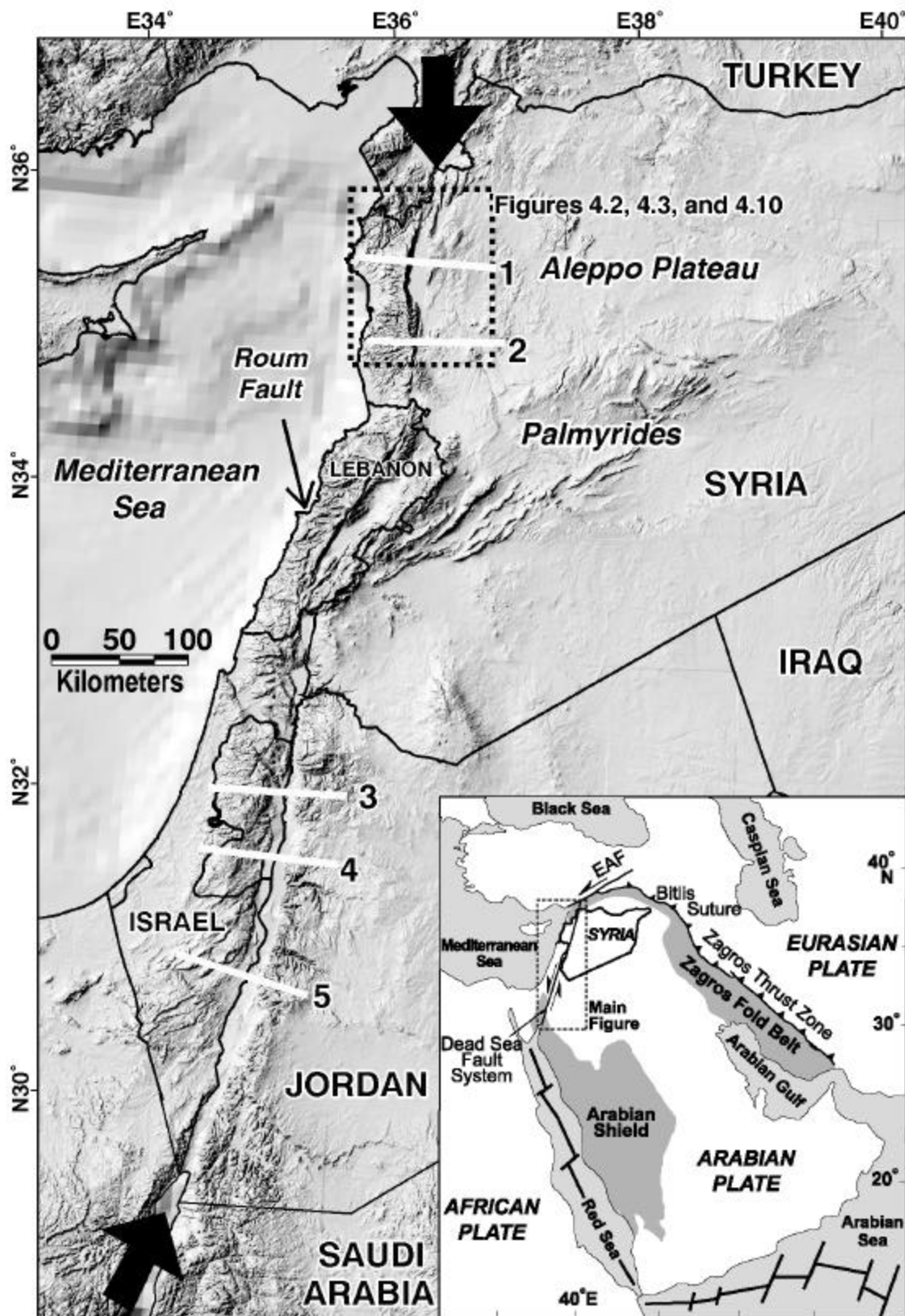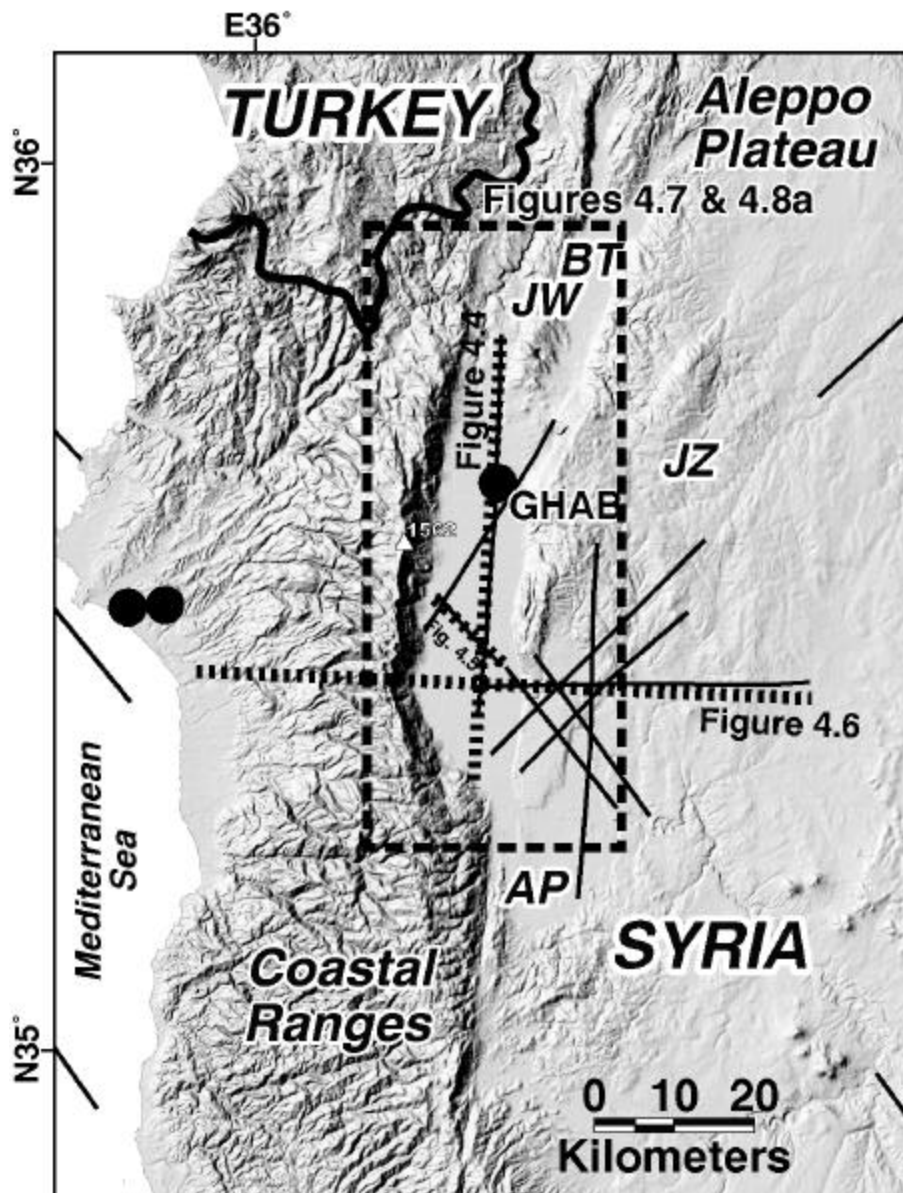
**Figure 4.2:** Shaded relief image of the area immediately surrounding the Ghab Basin illuminated from the northwest, location shown in Figure 4.1. The very low relief Ghab Basin is at an elevation of ~170 m, and the marked peak of the Coastal Ranges is 1562 m. Locations of other figures are shown. Seismic reflection profile locations are shown as thin black lines and well locations are illustrated with solid circles. (AP = Asharneh Plain, JW = Jebel Wastani, JZ = Jebel Az-Zawieh, BT = Balou Trough.)

evolution of the Ghab Basin integrates with theories of Late Cretaceous Cenozoic plate motions in the eastern Mediterranean indicating that the DSFS only propagated through northwest Syria after the Miocene.

**The Dead Sea Fault System**

The DSFS is a transform fault linking Red Sea / Gulf of Aqaba seafloor-spreading to NeoTethyan collision in Turkey. Most researchers agree that in total ~107 km of sinistral motion has taken place on the 'southern' portion of the fault, south of the Lebanese restraining bend (Figure 4.1) (e.g. Dubertret, 1932). In concert with the episodic rifting in the Red Sea area (Hempton, 1987), many authors have suggested that the lateral motion on the DSFS occurred during two different episodes (e.g. Quennell, 1959; Freund et al., 1970; Beydoun, 1999). In this scenario there was ~65 km of movement during the Early - Middle Miocene, with the remaining ~42 km of from earliest Pliocene until present.

More controversial is the amount of translation experienced by the 'northern' DSFS in Lebanon and farther north in northwest Syria. The controversy arises from limited mapping of the trace of the DSFS, and a lack of piecing points by pre-Pliocene features, making total offset mapping in Lebanon and Syria extremely difficult (Chaimov et al., 1990). Displacement of ophiolite cut by the DSFS in Turkey is open to very broad interpretations, but was used by (Freund et al., 1970) to suggest ~70 km of total sinistral movement on the northern DSFS.

Chaimov et al. (1990), expanding on the ideas of Quennell (1959), suggested that only the second episode of motion on the DSFS (~40 - 45 km since the start of the Pliocene) has affected the northern DSFS. In this scenario shortening in the southwest Palmyride fold and

thrust belt (Figure 4.1) accommodated ~20 km of sinistral movement, leaving ~20 - 25 km of movement to be transferred to the DSFS north of the Palmyrides. Supporting evidence for the post-Miocene development of the northern DSFS includes offsets of Pliocene basalt (Quennell, 1984), Quaternary fans, and Mesozoic ophiolite (Freund et al., 1970), although this last interpretation is discounted by many (e.g. Quennell, 1984). The Roum Fault in Lebanon (Figure 4.1) or similar structures, may have translated the ~65 km of pre-Pliocene displacement offshore, hence explaining the absence of a northern DSFS in Miocene time.

Another scenario suggests that the northern DSFS has been inactive since the Miocene (Butler et al., 1997). Given the geomorphic evidence for Pliocene – Recent tectonic activity on the fault, however, together with seismicity (Ambraseys and Jackson, 1998) and GPS measurements (McClusky et al., 2000), this inactive northern fault hypothesis seems improbable.

The recent tectonics of the Ghab Basin (Figure 4.2) further attest to the current activity along the northern DSFS. Ponikarov (1966) considered the Ghab Basin to be a Pliocene - Recent feature, and recognized that the basin developed on a left-step in the DSFS (Figure 4.3). These findings were echoed in geomorphic studies by Hricko (1988), Domas (1994), and Devyatkin et al. (1997). Paleostress analysis on faults around the Ghab Basin by Mater and Mascle (1993) further suggest an active step-over geometry. Herein we do not present direct evidence regarding the history of movement on the northern DSFS, however, we suggest that the Ghab Basin formed through left-lateral strike-slip since earliest Pliocene. This is supports the scenario of
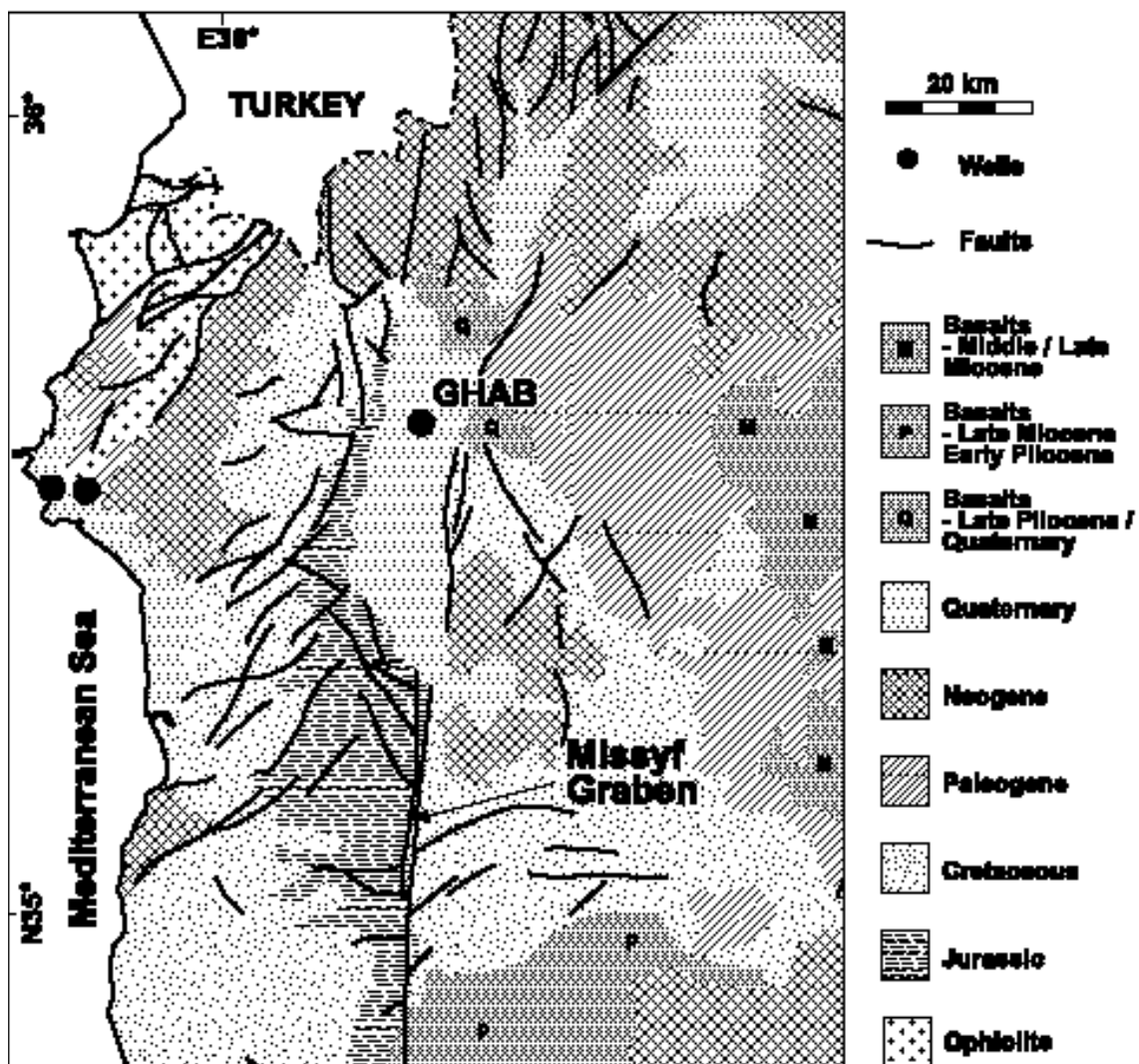
**Figure 4.3:** Generalized geologic and fault map of the study area; location shown in Figure 4.1. Sense of fault movement was not reported by the original author (Ponikarov, 1966).

northern DSFS development in which ~20 - 25 km of sinistral displacement has occurred on the northern DSFS since the earliest Pliocene (Chaimov et al., 1990).

**Data and Interpretation Methodology**

Among the data used for our subsurface analysis of the Ghab Basin are ~260 km of 2-D migrated seismic reflection profiles (Figure 4.2), acquired during 1994 using a Vibroseis source to six seconds two-way time. These data were processed and migrated using standard seismic processing flows. Interpretation utilized the Landmark SeisWorks software package. The sections shown here are in time, rather than depth. Within the basin seismic p-wave velocities are $2.0 \pm 0.2$ km/s as derived from sonic logs and seismic stacking velocities (Dzhabur, 1985). Hence the two-way time scales in Figures 4.4, 4.5, and 4.6 are a close approximation for depth in kilometers for the basin fill. The data are largely not interpretable past four seconds two-way time.

The one deep well within the basin (Ghab, Figure 4.2) was used, together with seismic signatures, to provide stratigraphic control on the seismic interpretations. There is very limited penetration of the basin fill by drilling (Figure 4.4), so while there is good stratigraphic control of older horizons within and around the basin, age control for the basin fill remains speculative. Regardless, the main objectives of this interpretation – the mapping of the structure of the basin – are met using the seismic data (Figure 4.7).

Geologic maps (Figure 4.3) and gravity interpretations provide additional information especially where seismic data are lacking. We modeled the Bouguer gravity data from a grid of eight profiles, two of which are presented here (Figures 4.4 and 4.5). The gravity modeling software permitted  changing densities and body lengths in the strike

**Figure 4.4.** Transect along the Ghab Basin (see Figure 4.2 for location) showing a seismic reflection profile, density model and associated gravity anomalies. Dashed box on density model illustrates extent of seismic reflection data coverage. Intersections with other seismic reflection profiles are shown as small arrows; different line patterns are used to distinguish different reflectors. Densities shown on model are $g/cm^3$, see text for discussion. Quaternary age deposits form the surface layers along the entire length of the transect. Most of the faults shown have components of both normal and strike-slip fault movement. Deeper structure cannot be constrained with current data (see text).
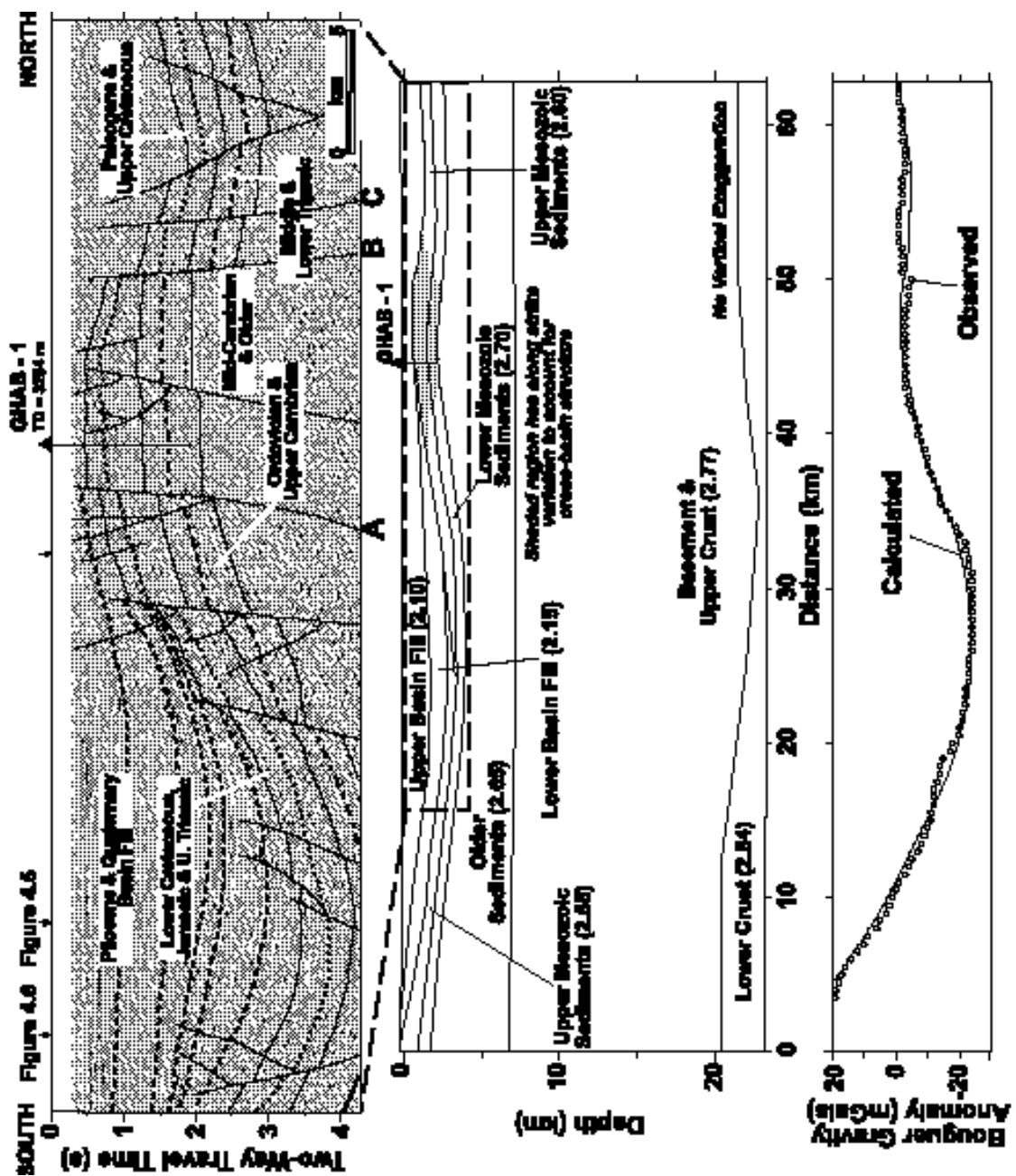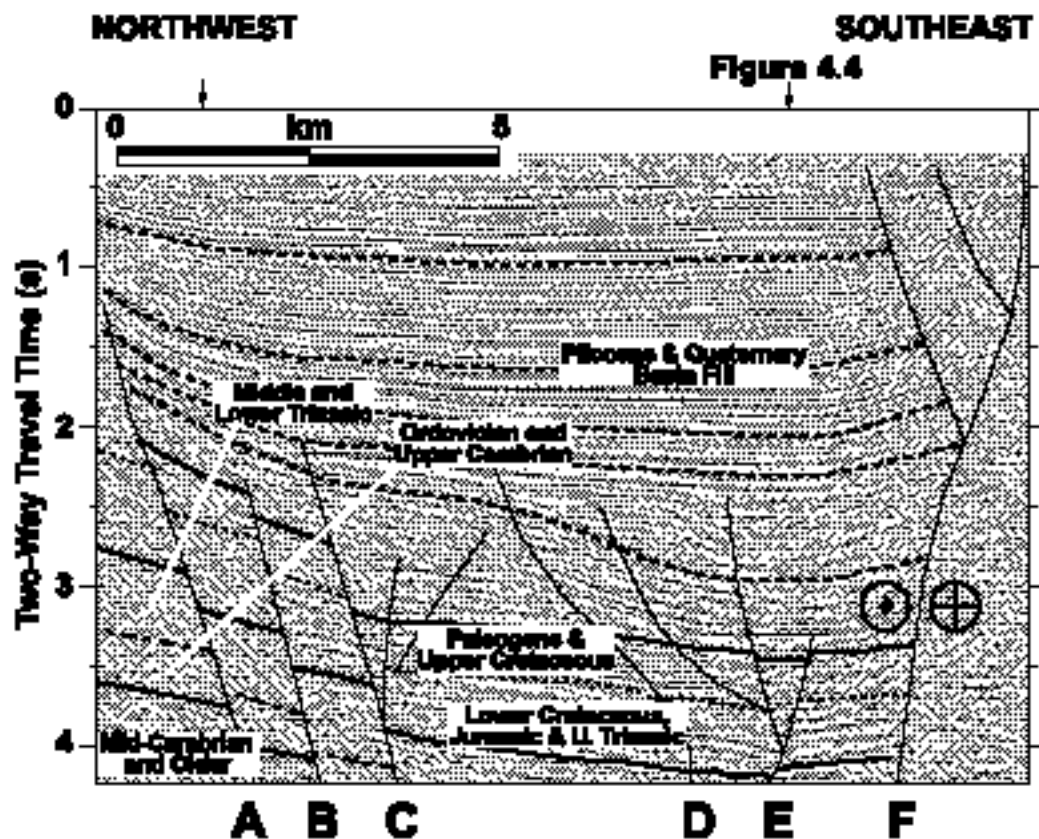
Figure 4.6

**Figure 4.5:** Interpreted migrated seismic profile across the Ghab Basin. See Figure 4.2 for location. Intersections with other seismic reflection profiles are shown as small arrows; different line patterns are used to distinguish different reflectors. Quaternary age deposits are the surfical strata along the whole line. Most of the faults shown have components of both normal and strike-slip fault movement. The fault marked F is the main strand of the DSFS and the major eastern bounding fault of the Ghab Basin, see text for discussion.

**Figure 4.6:** Transect across the Ghab Basin (see Figure 4.2 for location) showing a seismic reflection profile, density model and corresponding gravity anomalies along transect. Dashed box on density model illustrates extent of seismic reflection data coverage. Intersections with other seismic reflection profiles are shown as small arrows; different line patterns are used to distinguish different reflectors. Densities shown on model are $g/cm^3$, see text for discussion. The faults marked A are the along strike continuation of the main strand of the DSFS (as shown in Figure 4.3). The faults marked B and C have surface expression, as documented by Ponikarov (1966). Most of the faults shown have components of both normal and strike-slip fault movement. Note the required thinning of the crust toward the Mediterranean Basin, as commonly observed long the Levantine margin (e.g. ten Brink et al., 1990), although exact lower crustal structure is indeterminate. Step shown in the Moho is not resolvable in the gravity data.

Figure 4.4

**Figure 4.7:** Perspective view from the northwest of the Ghab Basin, looking to the southeast. See Figure 4.2 for location. The top layer represents the topography surrounding the Ghab Basin. For this, and the middle layer, darker shades representing higher levels and illumination is from the northeast. Middle layer is a representation of the base of Ghab Basin sedimentary fill; the slightly angular appearance is a consequence of the gridding process. Lowermost layer shows Bouguer gravity contours (BEICIP, 1975). Contour interval is 2 mGal, bolder lines every 10 mGal. Note the large depocenter in the south of the Basin.

Trace of
Dead Sea Fault

Seismic reflection
coverage

Coastal Ranges

GHAB
WELL

Baiou
Trough

Jebel
El -Wastani

Main depocenter
maximum
depth ~3400 m

Secondary
depocenter

40

-10

20

-10

0
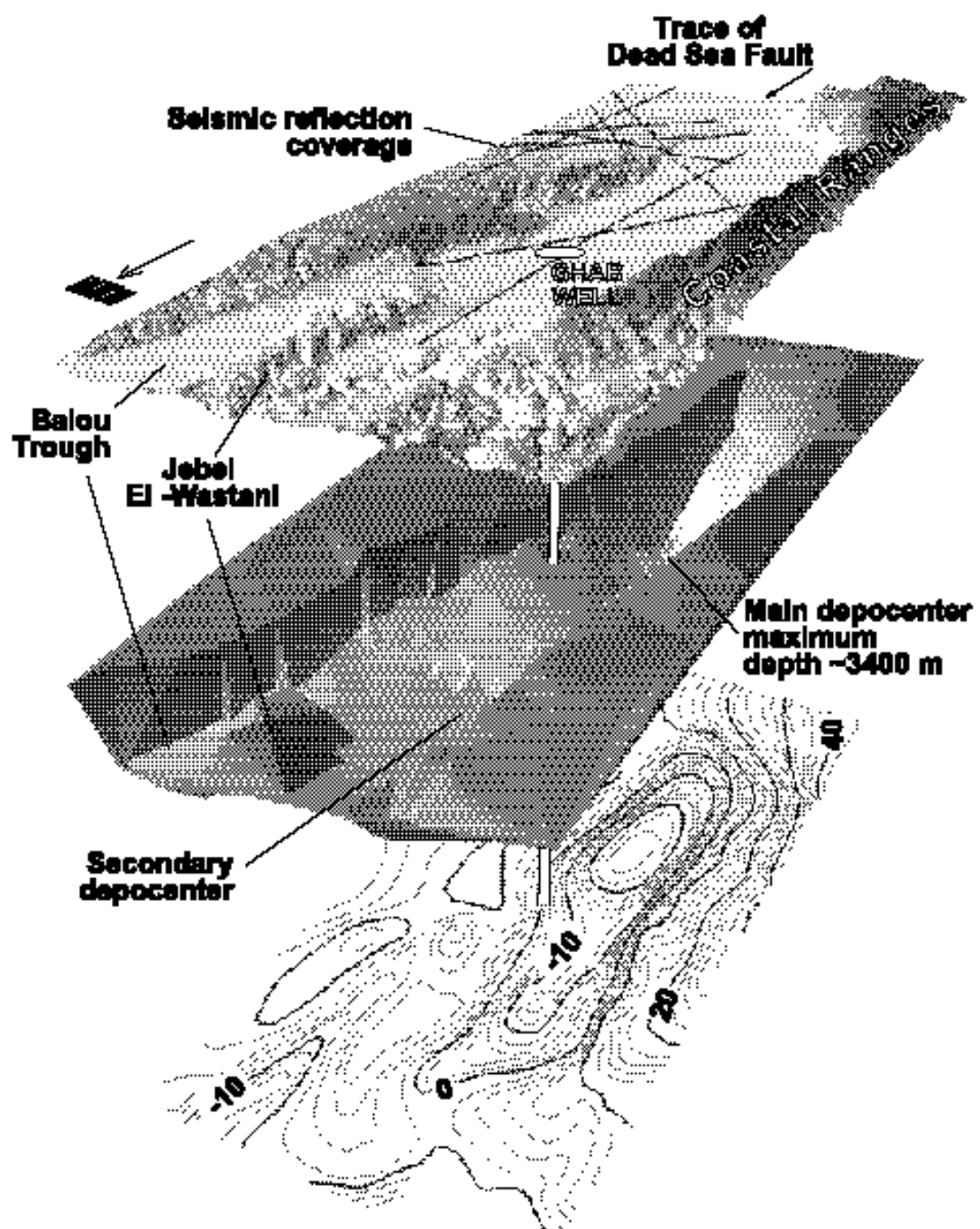
direction; hence, the models are sensitive to lateral variations beyond what is usually considered two-dimensional modeling. Along-strike variations, at distances farther than ~5 km from the profile, caused no appreciable impact on the modeled anomaly. Consequently, with the exception of the profile along the axis of the basin (Figure 4.4), the modeling presented here is sufficiently accurate with no along-strike variations. Likewise, faults were not directly incorporated into the density models because of its insignificant effect relative to continuous surfaces. The final models give a reasonable fit (< 3 mGal difference) between calculated and observed anomalies.

During the gravity modeling, density information came from field samples (Hricko, 1988), borehole density logs (this study and Lupa, 1999), and seismic refraction data (Seber et al., 1993). Depth limits came from seismic refraction and reflection data, and well data, as presented in this study (for locations see Figure 4.2). Where density logs from wells were not directly available, sonic log velocities borehole sonic logs (this study and Dzhabur, 1985) were converted to densities using well-established velocity-density curves. Rigorous comparisons between densities obtained directly from density logs, those estimated from sonic logs, and those from direct field samples show differences of less than $\pm 0.1$ g/cm$^3$ (for further details, see Lupa, 1999). Furthermore, the resulting densities were found to be reasonable according to our knowledge of lithologies derived from drilling information. Given these external controls on densities and depths, this gravity modeling is better-determined and less ambiguous than typical gravity studies.

**GHAB BASIN**

**Geomorphology**

The surface expression of the Ghab Basin is an extensive, flat plain with almost no topographic relief thus betraying its recent lacustrine history. The plain is ~60 km long and ~15 km wide (Figure 4.2). In the south, between two strands of the DSFS, is the Missyf Graben (Figure 4.3). The eastern fault strand can be traced northward at the surface along the eastern margin of the Ghab Basin before bifurcating to the north-northeast (Figure 4.3). No definitive termination of this eastern fault is observed along the basin margin.

The Syrian Coastal Ranges - that Ponikarov (1966) referred to as Jebel An-Nusseriyeh - rise dramatically by ~1300 m in just four kilometers of distance (Figure 4.2), exposing Jurassic, and even uppermost Triassic, strata (Figure 4.3) directly west of the basin (Mouty, 1997). This steep flank suggests geologically recent uplift along the western margin of the Ghab Basin (the origin of the Coastal Ranges is discussed below). In contrast to the eastern margin, this edge of the basin is poorly defined, obscured by significant mass-wasting and large blocks detached from the Coastal Ranges (Domas, 1994). Faults would be expected along the western margin given a typical fault step-over arrangement for the Ghab Basin. However, no surface expression has been detected along these margins, except in the far north (Figure 4.3), probably owing to burial by mass-wasting.

At the northern end of the Ghab Basin, the surface plain bifurcates and the Balou Trough extends to the north-northeast; Jebel El-Wastani - up to 800 m high - divides this from the northern Ghab (Figure 4.2). Surface observations indicate the Ghab Basin fill is Neogene -

Quaternary lacustrine and alluvial deposits, finer grained in the basin center (Domas, 1994; Devyatkin et al., 1997).

**Subsurface Analysis**

*Stratigraphy*

In our seismic interpretations (Figures 4.4, 4.5, and 4.6), tied to the Ghab well, the deepest mapped reflector is a relatively thin bed of Mid-Cambrian age limestone (Best et al., 1993). The unconformity at the top of Paleozoic (generally Upper Ordovician strata) presents a clear reflector where the mainly carbonate Mesozoic section overlies a largely clastic Paleozoic section. Middle Triassic age anhydrite and dolomite form a sequence of strong reflectors, as does Early Cretaceous sandstone. The uppermost mapped reflector, (other than arbitrarily traced horizons within the basin fill shown by dashed lines in Figures 4.4, 4.5, and 4.6), is at the base of basin fill that is Middle Eocene age, or in the south of the basin, Upper Cretaceous (Devyatkin et al., 1997).

The Ghab well penetrates Middle Eocene limestone immediately beneath Pliocene strata. A clear unconformity at this point is expressed by abrupt facies change (clay to limestone), paleontologic evidence, and an absence of volcanic detritus that is found throughout the younger strata. We interpret this unconformity (at a depth of 350 m in the Ghab well, but dropping sharply to the south and north, Figure 4.4) as the base of basin fill. This puts initial Ghab Basin formation, at least at the latitude of the Ghab well, in Pliocene time. Furthermore, we interpret a very thin layer of volcanic rocks encountered at a depth of 200 m within the basin fill in the Ghab well is part of a nearby 1-2 Ma sequence.

Since most of the Ghab Basin fill has not been drilled, directly dating the overall onset of extension and basin formation is not possible. However, when the seismic data are tied to the well data, there is no evidence of basin strata older than earliest Pliocene. Shallow borings (< 500 m) in the main depocenter have also failed to penetrate rocks older than Pliocene, and find Mesozoic strata immediately below Pliocene (Devyatkin et al., 1997). Furthermore, outcrop studies have shown marine Pliocene strata at the northern end of the current Ghab Basin, but continental strata of the same age near the south end of the basin (Ponikarov, 1966). Thus the full extent of the Ghab Basin topographic depression was not fully established until at least after the earliest Pliocene. In summary, the balance of evidence suggests Ghab Basin formation commenced around earliest Pliocene.

### *Structure*

The basic structure of the Ghab Basin is a fault-controlled double depocenter. The main depocenter is positioned beneath the southern portion of the surface plain, and slight northward migration of that depocenter with time is clear from the seismic data (Figure 4.4). Also apparent are a mid-basin ridge (on which the Ghab well is drilled) and a second smaller depocenter to the north.

The relatively undeformed nature of much of the basin fill suggests that most subsidence has been accommodated along the major basin-bounding faults. An apparent western bounding fault (marked A on Figure 4.5) when projected to the surface would be close to the foot of the Coastal Ranges. Abrupt sediment thickness changes are very apparent across the eastern bounding fault (marked A in Figure 4.6). Most of the subsidence is clearly asymmetric in the southern depocenter controlled by the more prominent eastern basin-bounding fault (marked F in Figure 4.5). Mesozoic strata encountered by shallow drilling on the western flank (Devyatkin et al., 1997) further support this interpretation. Gravity and

seismic interpretations reveal this southern depocenter to be up to ~3400 m deep (Figure 4.7). Assuming basin formation occurred in the last 4.5 Ma, the approximate subsidence rate in the deepest part of the Ghab Basin is ~0.8 m / 1,000 years. This is comparable with similar strike-slip basins elsewhere (Nilsen and Sylvester, 1995).

In the earlier stages of basin formation, accommodation space was created by movement on cross-basin faults that are now internal to the basin, rather than on the flanking faults. This displacement shifted between the faults, with older displacement on the more interior (western) faults (marked B-E in Figure 4.5), and most recent motion accommodated on the eastern basin-bounding fault (marked F in Figure 4.5).

The geometry of the faults can be appreciated from Figures 4.7 and 4.8a. Two depocenters are illustrated - the larger in the south, and the smaller in the north - both formed against the basin-bounding faults. Cross-basin faults are found particularly in the south of the basin, predominately steeply dipping to the northeast (faults B-E on Figure 4.5). These transverse features are generally northwest – southeast striking, suggest some extension across the basin. The central region is dominated by acutely striking cross-basin faults that bound a horst extending across the basin (faults A-C on Figure 4.6, feature marked R in Figure 4.8a). Confidence in the interpretation of a second depocenter in the northwest of the basin is improved by analysis of gravity data (Figures 4.4 and 4.7). This second basin is somewhat asymmetric toward the western bounding fault and is up to ~1700 m deep.

North-northeast of the Ghab Basin, faults splay out significantly and several depocenters are present. A gravity low east of the Jebel El-Wastani (Figure 4.7) shows another step-over basin, beneath the Balou Trough (Figure 4.2). Whilst no seismic data have imaged this area, our gravity interpretations and previous work (Hricko, 1988) reports 500 - 1000 m of basin

fill in what is apparently another strike-slip basin bounded by left-lateral faults (Ponikarov, 1966). Historical seismicity shows recent activity on some of these fault splays (Ambraseys and Melville, 1995).

East of the south part of the Ghab Basin, (Asharneh Plain, Figure 4.2), there is no significant Bouguer gravity low (Figure 4.6). Seismic interpretations (Figure 4.6) also indicate that there is no significant basin in that area, and this area is not an extension of the Ghab Basin as might be expected from the topographic expression (Figure 4.2). Faults in the Aleppo Plateau area are minor (Figure 4.6), and generally no older than movement on the northern DSFS. Seismic reflection data image deformation associated with the DSFS in this area (labeled A on Figure 4.6). This location corresponds directly with surface faults inferred from topography imagery (Figure 4.7) and Quaternary faults observed in the field. The displacement is distributed among several fault strands that are seen to coalesce at depth. This image is comparable with other examples of continental transform faults (e.g. Ben-Avraham, 1992), and is a typical 'flower structure' such has often been shown to be associated with strike-slip faulting (Harding, 1985).

**Comparison with other basins and basin models**

Despite out interpretations that have used all available data, several issues regarding the evolution of the Ghab Basin remain unresolved. Furthermore, while the fault geometry controlling the Ghab Basin roughly fits the pattern of a 'step-over' basin (Nilsen and Sylvester, 1995), the Ghab Basin shows several departures from this simple transform-parallel extension case. Below we compare the Ghab Basin with other basin studies and basin models (Figure 4.8), thus shedding some light on many of the second-order complexities we have observed.

Asymmetric basins have been documented along the DSFS (especially in the Gulf of Aqaba), the San Andreas Fault, the North Anatolian Fault, and many other major strike-slip faults (Ben-Avraham, 1992; Ben-Avraham and Zoback, 1992). These asymmetric basins are bound on only one side by a major linear strike-slip fault, against which most deposition always occurs. The opposite side of the basin is bound by predominantly normal faults; thus, the overall fault geometry is distinctly different from the classic step-over. The sense of basin asymmetry commonly changes along strike in these fault systems as strike-slip displacement transfers from one en-echelon strike-slip fault to the next. This geometry could be caused by a reorientation of stresses near a weak fault in an otherwise strong crust, so as to minimize shear stress on the fault, resulting in transform-normal extension (Ben-Avraham and Zoback, 1992).

The asymmetry within the Ghab Basin closely follows this pattern of deformation, with the southern depocenter asymmetric to the east. This suggests that, at the latitude of the Ghab Basin most of the lateral movement on the DSFS is accommodated on the eastern bounding fault of the basin. Some displacement steps over to the western bounding fault farther to the north, and the smaller northern depocenter is slightly asymmetric to the west. This geometry agrees with surface observations and indicates a component of extension across the Ghab Basin.

**Figure 4.8:** Comparison of the Ghab Basin structure with physical and mathematical models, and real examples of strike-slip basins. See text for full discussion. Throughout the figure, crosshatched areas indicate major depocenters and bolder lines indicate faults that are more significant. (a) Fault map in the Ghab Basin and immediate surroundings. See Figure 4.2 for location. These faults have been mapped either from surface observations and geomorphology (gray lines) (Ponikarov, 1966), or from seismic reflection and other interpretations (black lines, this study). Letters G, C, T and R correspond to features also observed in (b), see text for discussion. (b) Fault map from sandbox model of step-over basin, after Dooley and McClay (1997). (c) Numerical model of a step-over basin from Rodgers (1999). (d) Simplified structure map of the Cariaco basin, Venezuela, from Schubert (1982). (e) Fault map from Dead Sea Basin, summarized from several sources (Garfunkel and Ben-Avraham, 1996).

a) 20 km  GHAB BASIN  SOUTH

b) 10 cm  SANDBOX MODEL

c) NUMERICAL MODEL  Arbitrary Scale  Areas of normal faulting

d) 40 km  CARIACO BASIN  El Pinar Fault  Moron Fault  NORTH

e) 20 km  DEAD SEA BASIN  NORTH
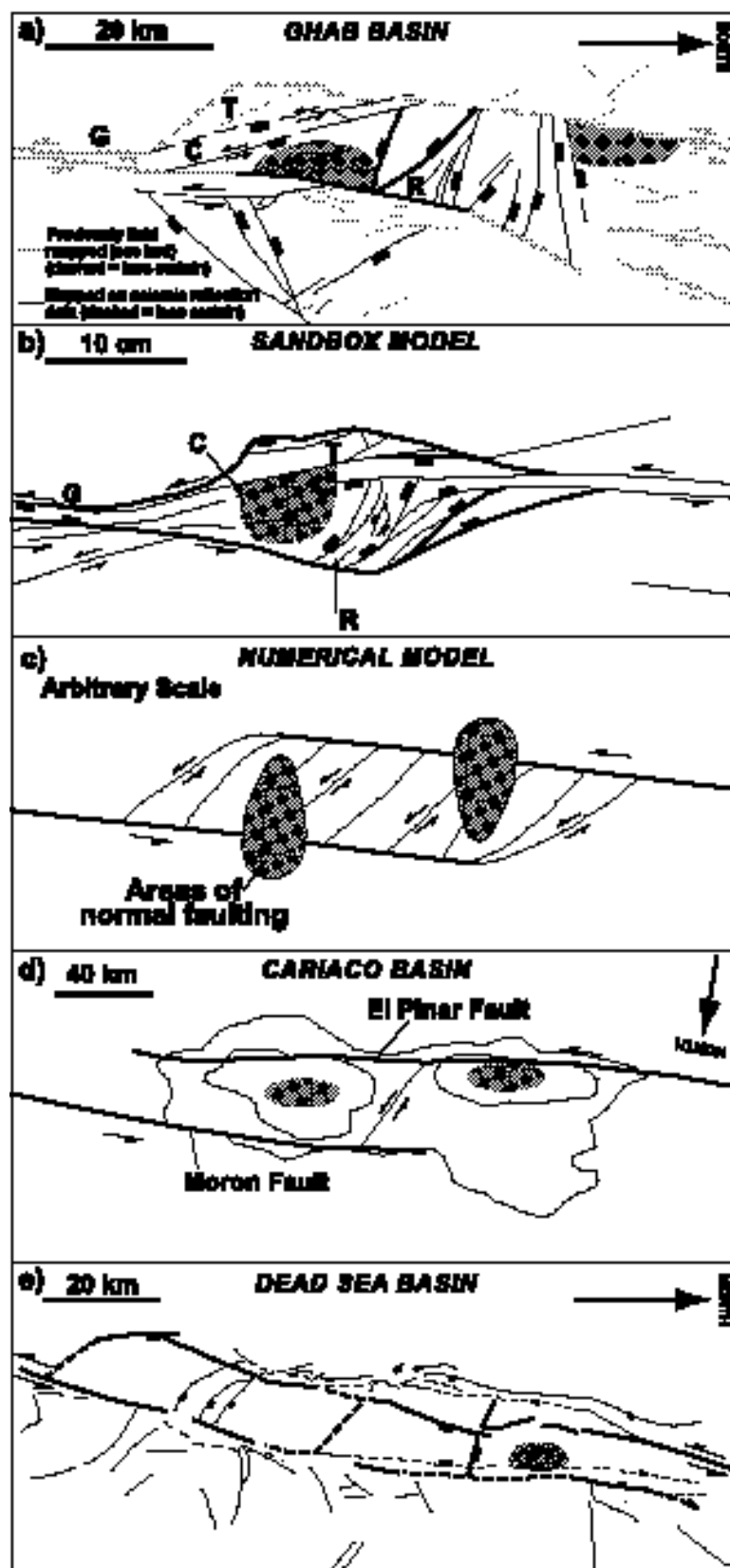
Transverse structures, such as those found in the Ghab Basin, are also commonly observed in other strike-slip basins. The Dead Sea Basin (Figure 4.8e) is bounded by strike-slip faults on which most of the deformation occurs and transverse structures separate smaller sub-basins there (Garfunkel and Ben-Avraham, 1996). Another analog for the Ghab Basin is the Cariaco Basin, Venezuela (Figure 4.8d), where twin depocenters, asymmetric toward the more active strike-slip and separated by a central sill have developed at a dextral fault step-over (Schubert, 1982).

Physical (e.g., sandbox / clay) models of pull-apart basins can provide insight into strike-slip basin evolution by considering simplistic end-member cases that are rare in nature. For Dooley and McClay (1997), their model with resulting deformation most closely resembling the Ghab Basin was a case of an initial 90° releasing sidestep between the two segments of the strike-slip fault (Figure 4.8b). Strong similarities with the Ghab Basin include: Cross-basin faults (C in Figure 4.8), mid-basin ridge (R in Figure 4.8), strongly terraced sidewalls of basin (T in Figure 4.8), and graben along the principal displacement zone at the basin ends (G in Figure 4.8).

Rahe et al. (1998) used unequal motion on the 'crustal' blocks on opposite sides of the strike-slip fault in their physical models. The results show asymmetric basins, with increased subsidence toward the moving boundary. Commonly observed in these models are intrabasin highs, early opening accommodated on oblique-slip transverse faults, and switching basin asymmetry along strike (associated with 'master fault' step-over). Again, all these features are observed in the Ghab Basin.

Mathematical (finite difference) models for the deformation of a basin under strike-slip conditions were made by Rodgers (1980) and Golke et al. (1994), among others. Rodgers (1980) showed that once the total offset across the bounding strike-slip faults is about equal to the separation between the faults, two distinct depocenters begin to form through normal faulting (Figure 4.8c). If considered analogous to the Ghab Basin (Figure 8a), this shows that the northern depocenter in the Ghab developed sometime after the initiation of the southern depocenter owing to increasing displacement on the DSFS. This explains the smaller size of the northern depocenter. Golke et al. (1994) found that two depocenters developed when initial master fault overlap is close to zero - the 90° case of Dooley and McClay (1997). They also saw the formation of asymmetric basins when there is some uneven movement on the master faults. Golke et al. (1994) also observed basin migration, in the same sense as that in the Ghab, because of increasing master fault overlap with time.

### Summary

Seismic reflection interpretations reveal that the Ghab Basin is not a textbook example of a step-over basin. However, through comparison with other basin studies and models we find that many of the second-order structures within the Ghab Basin are common to other strike-slip basins. The basin asymmetry seen in the Ghab is probably related to the amount, and sense, of relative movement across the bounding lateral faults. The results are consistent with the observed surface faults that show a greater amount of relative motion on the eastern basin-bounding strike-slip fault. Observations from the Ghab are echoed in theoretical models that show cross-basin oblique-slip faults accommodating initial basin opening, but most subsidence on the basin bounding faults. A northward shifting depocenter, and the subsequent development of a second depocenter in the Ghab Basin, are due to increasing

fault overlap with time and step-over of the lateral motion from the eastern to the western faults.

## SYRIAN COASTAL RANGES

To properly discuss the evolution of the Ghab Basin and DSFS in Syria we must also mention the adjacent, topographically prominent Syrian Coastal Ranges (Figure 4.2). Although not well studied, this deformation can illuminate the regional tectonic regime under which the basin and DSFS formed.

Based on stratigraphic evidence, uplift in northwest Syria has been episodic since at least the latest Cretaceous. In the Coastal Ranges Ruske (1981) found tilted and eroded Maastrichtian strata unconformably overlain by Paleogene transgressive deposits that reached a high-stand in Middle Eocene time. The geometry of this latest Cretaceous and Paleogene uplift appears to have been similar to the current Coastal Range topography, albeit without the imposition of the Neogene Ghab Basin.

Middle Eocene limestone was deposited in much of the study area, including some of the Coastal Ranges, indicating that the latest Cretaceous and Paleogene uplift had largely subsided by that time. It is unclear whether absence of the Middle Eocene strata in the southern Coastal Ranges was due to continued emergence and non-deposition, or post-Middle Eocene erosion. In any event, uplift of the Middle Eocene strata on parts of the current Coastal Ranges indicates that most of the uplift has occurred since the Middle Eocene.

Structural relationships and outcrop geology indicate that an anticlinorium, sub-parallel to the present Coastal Ranges, formed at some time since the Middle Eocene.  It is this anticlinorium that dominates the current topography.  The crest of the anticlinorium forms the current ridge of the Coastal Ranges.  The doming clearly narrows towards the north, and all evidence of the upwarping is lost near the present Turkish / Syrian border.  The absence of any Late Eocene – Miocene strata on or around the Coastal Ranges  - or beneath the Ghab Basin - strongly suggests that this second stage of uplift started around Late Eocene time, as suggested by Ruske (1981).  Quaternary coastal terraces attest to continued tectonic uplift in this area (Dalongeville et al., 1993).

Clearly the Coastal Range uplift has been very strongly modified by the propagation of the DSFS through northwest Syria, and the related formation of the Ghab Basin. The Plio-Quaternary Ghab Basin formed near what was presumably the crest of the pre-Pliocene Coastal Range uplift.  This created the extremely steep scarp on the eastern face of the Coastal Ranges alongside the Ghab Basin.  Furthermore, the presence of the DSFS has caused asymmetry in the uplift (Figures 4.2 and 4.9).   The Coastal Ranges are topographically and structurally significantly higher directly to the west of the present DSFS. This indicates that some of the post-Middle Eocene uplift has occurred since the DSFS propagated through northwest Syria.

In the remainder of this section we examine two related attributes of the current Coastal Ranges that are presently unexplained.  The first is the strong asymmetry of the current uplift. The second issue is the support of the topography.  The Bouguer gravity anomalies
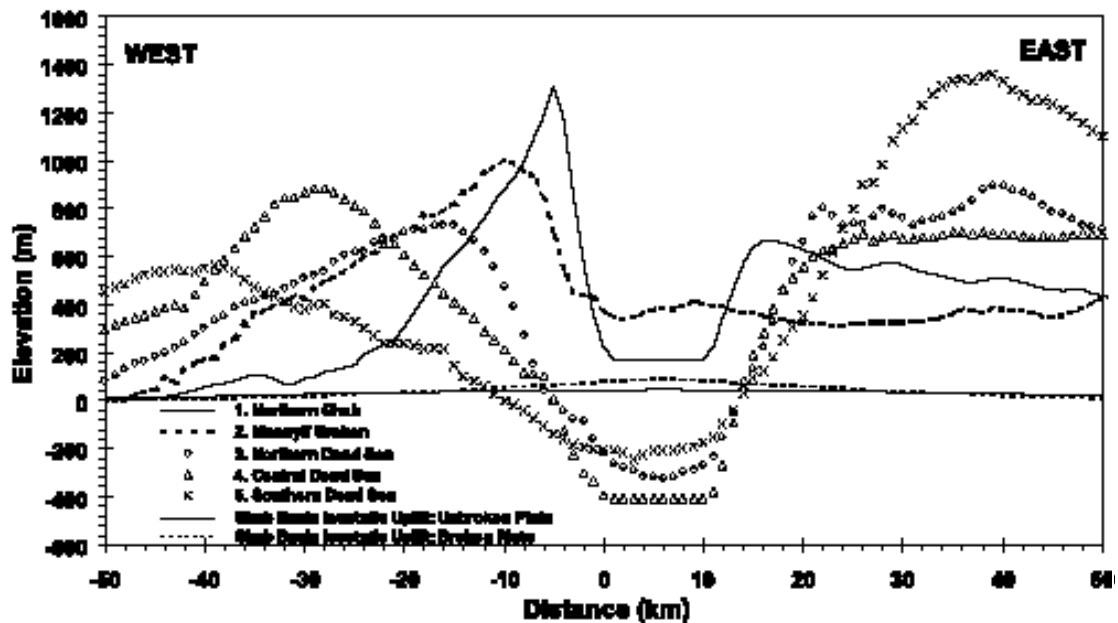
**Figure 4.9:** (a) Graph showing comparison of topographic profiles across the DSFS. These profiles are the average topography across a 20 km wide swath, locations shown on Figure 4.1. The thin black lines are the modeled regional isostatic response of the lithosphere owing to the formation of the Ghab Basin. Each profile has been approximately aligned relative to the fault.

(Figure 4.6) indicate that the current topography is not locally isostatically compensated, thus an explanation of a regional support mechanism is required.

Superficially, the asymmetry of uplift along the southern DSFS is similar to that near the Ghab Basin (Figure 4.2). On closer inspection, however, the half-width of the uplift is much greater in the southern DSFS (~100 - 125 km) than in the Syrian Coastal Ranges in the north (~15 - 25 km) (Figure 4.9). Even so, we may consider the explanations given for the uplift and asymmetry on the southern DSFS when trying to explain that in the north.

Wdowinski and Zilberman (1996; 1997) concluded that the uplift along the southern DSFS is caused by the isostatic lithospheric response to basin formation along the fault. They suggested the asymmetry along the southern DSFS is caused by deeply detached listric normal faults. ten Brink et al. (1990) also invoked flexure with asymmetric loading, elastic parameters, or thermal effects, to explain the asymmetry.

We have shown that a significant proportion of Coastal Range uplift occurred before the propagation of the DSFS through northwest Syria, hence the fault (and related basin formation) cannot be used to explain all the uplift. However, we can consider the additional Pliocene-Quaternary uplift that may have been caused by the faulting. To test this idea we have examined isostatic uplift of the Coastal Ranges due to Ghab Basin formation by assuming an elastic approximation following Turcotte and Schubert (1982). Using their method the uplift of an assumed elastic lithosphere can be modeled as being due to an upward force on a beam. In our case the upward force is the negative loaded created by basin formation. The uplift is then:

$$z_{iU}(x) = \omega_0 \exp \{-x + x_l / \alpha\} \cdot [\sin (x + x_l / \alpha) + \cos (x + x_l / \alpha)] \qquad (1)$$

where:

$$\omega_0 = [L_t \, \alpha^3 / 8 \, D] \tag{2}$$

$$\alpha = [4 \, D / \Delta\rho \, g]^{0.25} \tag{3}$$

$$D = [E \, T_e^3 / 12 \, (1-v^2)] \tag{4}$$

If we consider the case of a broken lithosphere (beam), as could be the case along the DSFS, (1) becomes:

$$z_{iB}(x) = \omega_0 \, \exp \{-x + x_l / \alpha\} \, . \, \cos (x + x_l / \alpha) \tag{5}$$

where:

$$\omega_{0B} = [L_t \, \alpha^3 / 4 \, D] \tag{6}$$

In the above,

$z_{iU,B}(x)$ = flexure of lithosphere as a function of distance for unbroken and broken

lithosphere, respectively

$x$ = distance along profile

$\omega_0$ = maximum amplitude of flexure, unbroken lithosphere

$\omega_{0B}$ = maximum amplitude of flexure, broken lithosphere

$x_l$ = offset distance of point load from center of profile

$\alpha$ = flexure parameter

$L_t$ = 'Negative' Load: force that causes upward flexure

The Ghab Basin is approximated with a 30 km$^2$ cross-sectional area (from seismic data), filled with sediments of density 2200 kg/m$^3$. The surrounding rock density is assumed to be 2600 kg/m$^3$, hence the negative load is $1.2 \times 10^{11}$ N/m.

$D$ = flexural rigidity [$1.8 \times 10^{22}$ N m]

$\Delta\rho$ = density change between air and compensating 'fluid' layer [3300 kg/m$^3$]

$g$ = acceleration due to gravity [9.81 m/s$^2$]

$E$ = Young's Modulus [$6 \times 10^{10}$ Pa]

$T_e$ = elastic thickness of the lithosphere [15,000 m]

$\nu$ = Poisson's ratio [0.25]

The numbers in square brackets given next to the terms above are those used by Wdowinski and Zilberman (1996). We initially use these parameters to model the isostatic response due to the formation of the Ghab Basin. The resulting flexures for the case of the unbroken lithosphere, $z_{iU}(x)$, and the broken lithosphere $z_{iB}(x)$, are shown in Figure 4.9. Clearly, these flexures are of too small amplitude, and of too long a wavelength, to explain more than a small fraction of the present topography of the Syrian Coastal Ranges. The result is little changed if regional isostatic compensation occurs in the lower crust, rather than in the upper mantle (e.g. ten Brink et al., 1993). We conclude that the Pliocene-Quaternary Syrian Coastal Range uplift is not simply a consequence of Ghab Basin formation, and a regional isostatic response to Ghab Basin formation is not supporting the topography.

Thus we consider other mechanism for support of the Coastal Range topography. Recent seismological observations (Sandvol et al., 2000) indicate a zone of strong shear wave attenuation in the uppermost mantle beneath western Arabia, especially along the DSFS. This may indicate elevated mantle temperatures that could be supporting the uplift dynamically. However, a mantle driving force seems unlikely given the small wavelength of the uplift (Figure 4.9), and it also fails to explain the asymmetry of the uplift.

A more likely support mechanism for the Coastal Range uplift could be regional compression. We will see in the following section that regional compression caused the initial Coastal Range uplift. Regional plate kinematics from preliminary GPS data permit small convergence across the DSFS plate boundary (McClusky et al., 2000). The DSFS could be acting to decouple this compression by accommodating strike-slip and reverse slip of the

crust west of the DSFS. In this scenario the Coastal Ranges west of the DSFS are uplifting though reverse faulting along the predominantly strike-slip DSFS, thus providing a support mechanism and explaining the asymmetry.

In summary, the true cause of the Syrian Coastal Range topographic support and asymmetry remains equivocal given the relatively limited data available. However, we favor a scenario in which the Syrian Coastal Ranges uplift began in the latest Cretaceous with regional compression causing folding and uplift. The area experienced similar compression in Late Eocene time onwards. After propagation of the DSFS through northwest Syria in Pliocene time, the Ghab Basin formed thus causing collapse the eastern flank of the Coastal Ranges. Regional compression continued to drive the uplift through reverse movement along the DSFS until present. This compression is largely detached along the DSFS hence explaining the current asymmetric uplift (Figure 4.10).

## EVOLUTION OF NORTHWEST SYRIA

The previous sections have discussed our interpreted evolution of the Ghab Basin and Syrian Coastal Ranges. Now we consider these results in the context of the regional tectonic evolution of northwest Syria. As discussed, the timing of DSFS development in Syria is still controversial. Also, previous tectonic models have largely failed to incorporate findings from northwest Syria. Our results, although somewhat speculative, provide insight of this development for Late Cretaceous to Recent.
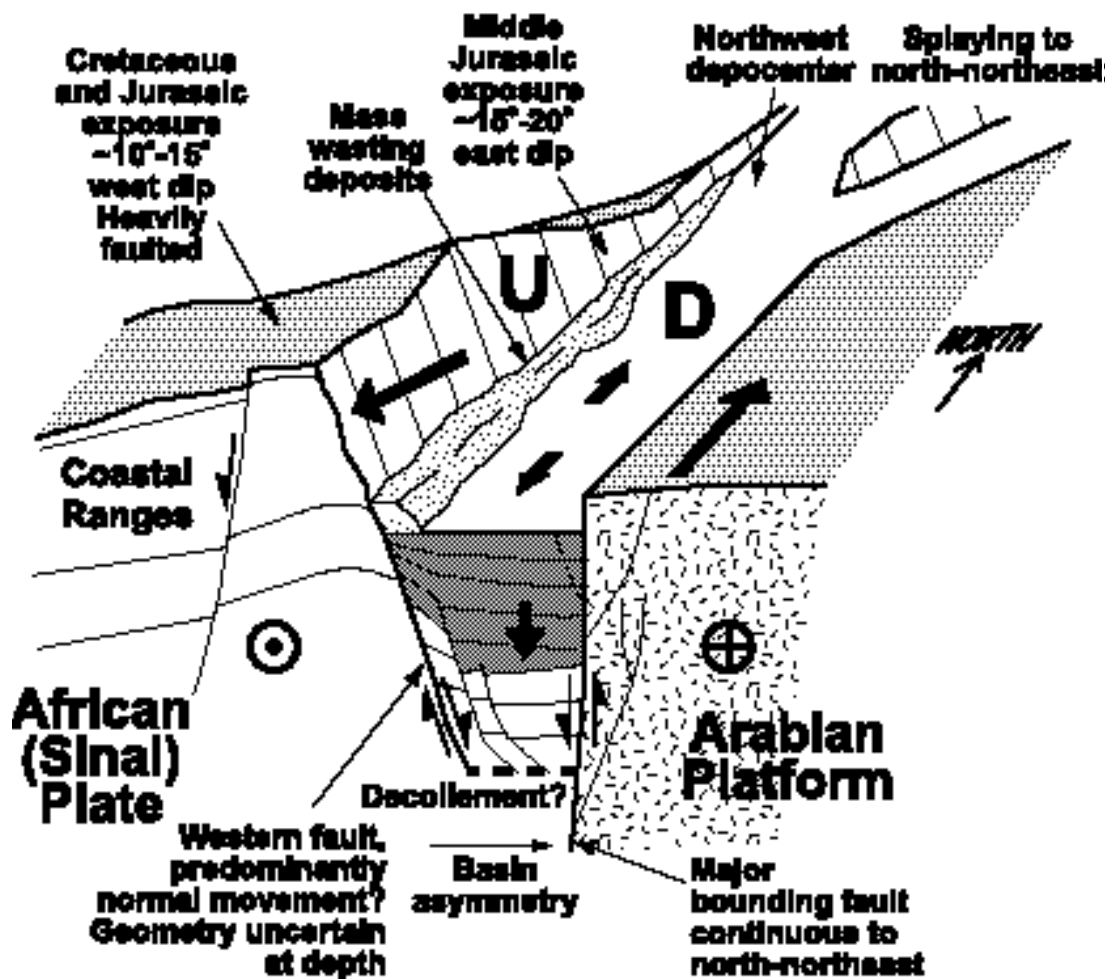
**Figure 4.10:** Highly schematic, vertically exaggerated, three-dimensional representation of Ghab Basin. Large arrows show approximate relative movements; the Coastal Ranges block is depicted uplifting while translating southwards.

**Late Cretaceous**

Deep well data from northwest Syria illustrate some of the Paleozoic and Early Mesozoic history of the area. In general these observations fit previously proposed tectono-stratigraphic models for the region (e.g. Best et al., 1993; Brew et al., 1999). However, the latest Cretaceous period is of most relevance to the current work. The Maastrichtian age initial uplift of the Syrian Coastal Ranges (Figure 4.11a) is coincident with contemporaneous events documented throughout northwestern Arabia (Figure 4.12a). Most notably this time was the first episode in the formation of the 'Syrian Arc'. The Syrian Arc is the swath of folds and structurally inverted faults observed along the Sinai and Levant coasts, sub-parallel to the present shoreline (Figure 4.11a). In the original definition (Krenkel, 1924) the Arc extended northward towards Turkey, although more recent authors have also included Palmyride folds in the definition. The formation of the Syrian Arc is dated as a Maastrichtian phenomenon (Guiraud and Bosworth, 1997), although some subtle precursory compression began earlier in the Late Cretaceous (Bartov et al., 1980; Walley, 1998). Chaimov et al. (1992) considered the initial folding, uplift, and structural inversion in the southwest Palmyride fold and thrust belt to be part of the Syrian Arc and documented this compression as latest Cretaceous. On a more regional scale the cessation of extensional tectonics in eastern Syria is well established as a Maastrichtian phenomenon (Brew et al., 1999).

The Maastrichtian was the time of ophiolite emplacement along the northern Arabian margin, particularly in the Baer-Bassit and Kurd Dagh areas proximal to the present Ghab Basin (Al-Maleh, 1976; Robertson et al., 1991). This emplacement occurred because the north Arabian margin collided with an intra-ocean subduction zone. These

**Figure 4.11:** Map showing schematic structural evolution of the Ghab Basin and immediately surrounding regions, location shown in Figure 4.2. Extents of zones illustrated outside the Ghab are somewhat speculative. Legend shown in (a) applies to all maps.

a) Latest Cretaceous

b) Paleocene - Middle Eocene

c) Middle Eocene - Mid. Miocene

d) Mid. Miocene - Early Pliocene

e) Late Pliocene

f) Quaternary
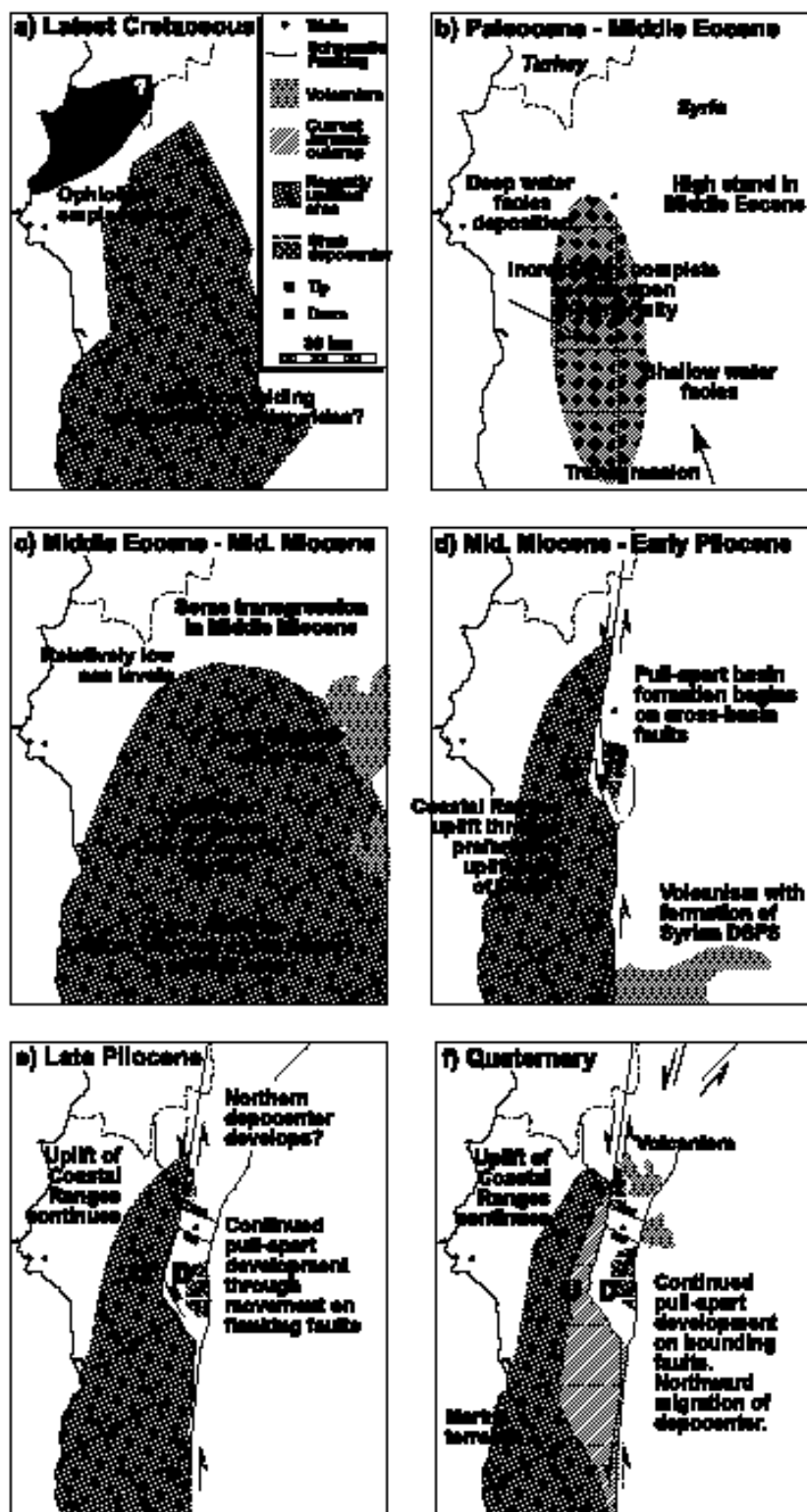
**Figure 4.12:** Map showing schematic structural evolution of the DSFS in a regional setting. Area illustrated is same as Figure 4.1, modern-day geography shown for reference. Bold lines indicate approximate paleo-plate boundaries, and large arrows indicate approximate motion of Arabia relative to Africa. No attempt is made to illustrate all tectonic events on this map; see Figure 4.11 for more detail for the Ghab region in NW Syria. (EAF = East Anatolian Fault).
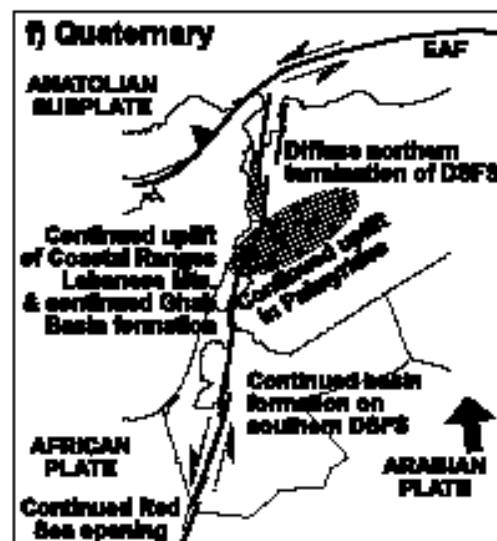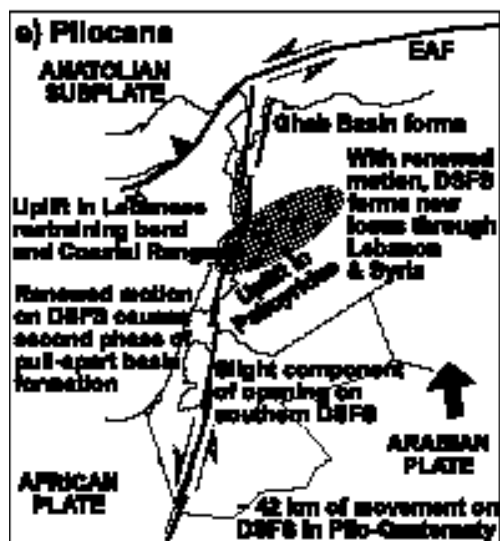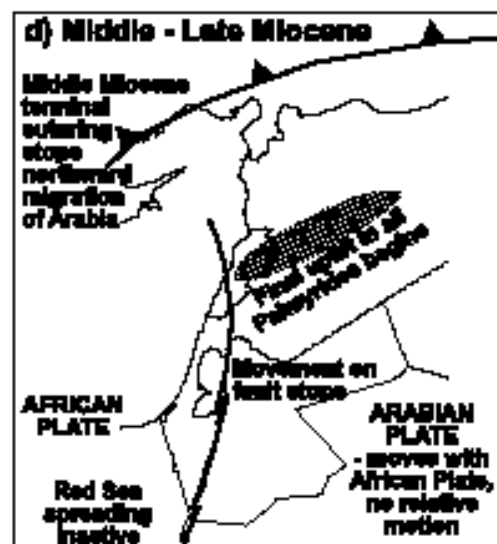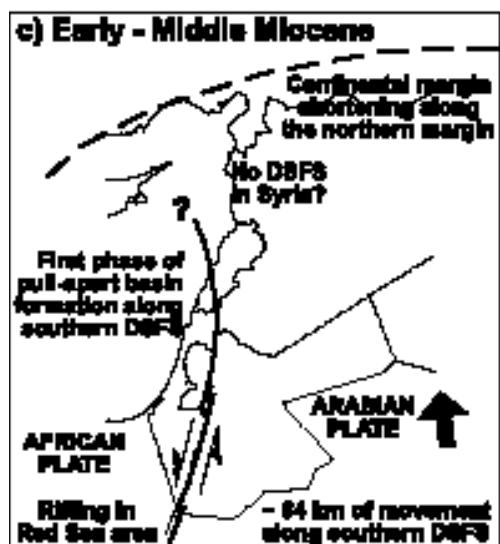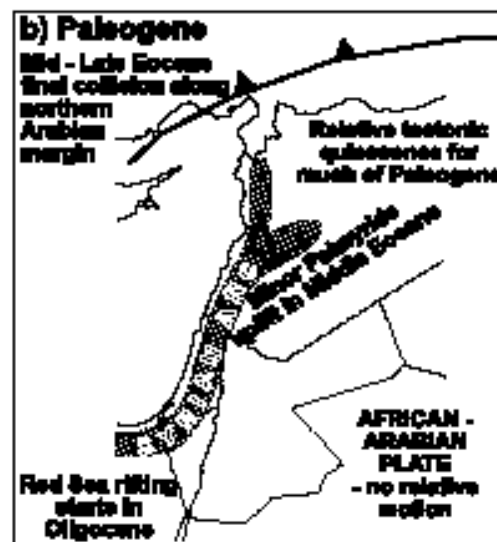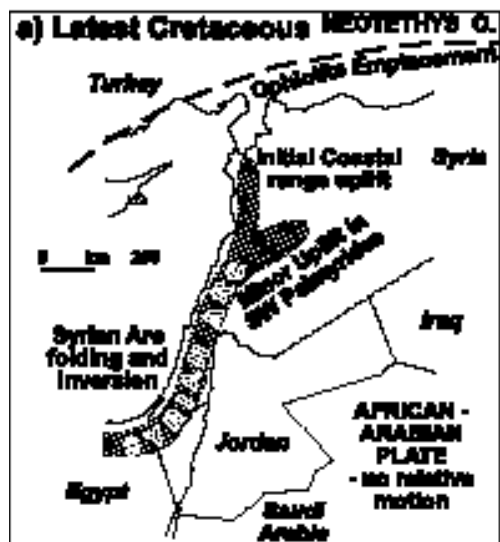
collisions can explain the observations of Maastrichtian age compression throughout the northern

Arabian platform.  Thus, the initial Maastrichtian uplift of the Coastal Ranges fits completely with the previously documented regional plate tectonics.  In this scenario, the Syrian Coastal Ranges are considered part of the Syrian Arc folding, as suggested by Walley  (1998), in accordance with the original definition of the Arc (Krenkel, 1924).

**Paleogene**

The uplift that affected the Coastal Ranges in the latest Cretaceous continued into the Paleogene but was subdued during the Eocene.  Middle Eocene marine deposits were deposited throughout the studied area, with the possible exception of the crest of the Coastal Range uplift that may have remained emerged.  As discussed above, the second episode of Coastal Range uplift was post-Middle Eocene.  This corresponds with the second episode of Syrian Arc development (Guiraud and Bosworth, 1997).  Middle Eocene was also a time of uplift of the Palmyrides (Chaimov et al., 1992) (Figure 4.12b), and some minor structural inversion in northeast Syria (Kent and Hickman, 1997).  Furthermore, through stratigraphic relationships Dubertret (1975) documented how most of the structuration of the Lebanese mountains was emplaced during the Late Eocene and Oligocene, a view supported by the more recent work of Walley (1998).

These periods of renewed compression within the northern Arabian platform are clearly related to the Mid-Late Eocene final collision of Eurasia and Arabia along the northern Arabian margin (Hempton, 1985).  This final obliteration of NeoTethys oceanic crust led to the Bitlis suture that still marks the boundary of these plates (Figure 4.12b).  From Mid-Late

Eocene time until the Middle Miocene, convergence between the Eurasian and Arabian plates was accommodated by continental margin shortening the thickening along this northern margin (Hempton, 1987).  Hence the Syrian Coastal Ranges are shown again to be part of the larger Syrian Arc folding coincident with more regional tectonic development.

**Miocene**

The first phase of rifting in the Red Sea area saw continental stretching there that probably started in the Oligocene (Hempton, 1987).  From Early Miocene time onwards the differential motion between rifting in the Red Sea and the Gulf of Suez began to be accommodated along the newly formed DSFS (Figure 4.12b,c).  Thus ~64 km of sinistral motion occurred on the southern DSFS during this first phase of DSFS movement in Early and Middle Miocene time (Figure 4.12c).  As discussed above, the balance of evidence suggests that the northern DSFS had not formed at this time, and the motion was perhaps transmitted offshore along a fault or faults in northern Israel / Lebanon (Figure 4.11c).

In his model, Hempton (1987) argues that by Middle Miocene time the northern margin of Arabia had reached full crustal thickness after shortening and thickening in the Eurasia / Arabia collision. Hempton (1987) suggests that this was therefore the terminal suturing of Eurasia/ Arabia, after which Arabia was unable to converge any further on Eurasia, and so spreading in the Red Sea halted.  In turn this led to a cessation of movement along the DSFS (Figure 4.12d).  Thus, in the model of Hempton (1987) that we support herein, the first phase of motion on the DSFS came to a close during the Middle Miocene and the DSFS was inactive from around 14.5 Ma until about 4.5 Ma.  Interestingly, this time also approximately corresponds to a period no volcanic activity in Syria (Mouty et al., 1992).

**Pliocene - Recent**

Hempton (1987) goes on to argue that activity on the DSFS commenced again in the Early Pliocene (~4.5 Ma). This was due to commencement of Red Sea seafloor spreading as the northward motion of Arabia was accommodated along the newly formed North and East Anatolian Faults. In accordance with this model, we suggest that with the renewed activity and reoriented stress regime, the DSFS formed its current path though Syria beginning in Early Pliocene time (Figure 4.11e). The balance of our evidence indicates that the Ghab Basin only formed during Pliocene time. This strongly suggests that the northern DSFS only formed since the Miocene, as forwarded by the model of Chaimov et al. (1990) that we support here. Further evidence comes from offsets in Pliocene basalt and Quaternary fans (Trifonov et al., 1991; Fleury et al., 1999), and offsets of ophiolites together with GPS current motion vectors. Preliminary GPS measurements suggest roughly 6 mm/year of relative Africa / Arabia motion in the northern Arabian platform (McClusky et al., 2000), in agreement with field studies (Trifonov et al., 1991). If overall this motion has been constant it indicates ~27 km of movement in the last 4.5 Ma, roughly equivalent to previously suggested totals (Quennell, 1984; Trifonov et al., 1991).

We suggest that after the northern propagation of the DSFS, the Ghab Basin formed owing to the complex splaying left step-over in the sinistral fault system. Cross-basin oblique-slip faults appear to have accommodated the initial extension (Figure 4.11d) that was later transferred onto the basin bounding faults that are still prominent today (Figure 4.10 and 4.11e-f). Despite significant topography to the west, surface and subsurface data show the eastern basin-bounding fault to be the more active, and this fault is continuous north of the basin as readily seen in topography and seismicity data. This suggests an incomplete transfer of lateral motion from the eastern to the western strands of the DSFS across the Ghab Basin.

Thus north of the Ghab Basin the DSFS splays out into a broad zone of deformation with lateral motion distributed amongst several faults.

We suggest that during the Pliocene - Recent the Ghab Basin and northern DSFS were superposed on the pre-Pliocene Syrian Coastal Range topography. This faulting along the crest of the Coastal Ranges has created the very steep western flank of the uplift that we observe today. Continued compression of northwest Arabian since the propagation of the DSFS through the Coastal Ranges has caused further uplift to the west of the DSFS.

**CONCLUSIONS**

Geomorphology, stratigraphic relationships, and seismicity clearly demonstrate the active deformation of the northern, Syrian segment of the DSFS. Sinistral movement at a left-step and splaying of the fault has resulted in the Ghab Basin that, absence evidence to the contrary, we interpret to have formed since earliest Pliocene time. Cross-basin oblique-slip faults accommodated some initial basin opening, but most subsidence has occurred along the more active eastern basin-bounding fault. The basin exhibits two asymmetric depocenters with geometry suggestive of some transform-normal extension. The timing of Ghab Basin formation strongly supports a model in which the current northern strand of the DSFS (in Lebanon and Syria) has only been active since the latest Miocene / earliest Pliocene to Recent.

Uplift of the Syrian Coastal Ranges has been episodic since latest Cretaceous time. The first episode of uplift, in the Maastrichtian, was clearly related to plate-wide compression and folding caused by collision along the northern Arabian margin. Mid-Late Eocene uplift was again contemporaneous with regionally observed folding due to final continent-continent

collision along the northern margin.  This uplift is ongoing, and has been strongly influenced by the formation of the DSFS that has delimited the uplift to the east.

## REFERENCES

Al-Maleh, K., 1976. *Etude stratigraphique, petrographique, sedimentologique et geochimique du Cretace du N.W. Syrien (Kurd Dagh se environs d'Aafrine): Les aspects petroliers de la region*. Universitie Pierre et Marie Curie (Paris VI), Paris. 620 p.

Ambraseys, N.N. and J.A. Jackson 1998. *Faulting associated with historical and recent earthquakes in the Eastern Mediterranean region*. Geophysical Journal International, **133,** 390-406.

Ambraseys, N.N. and C.P. Melville 1995. *Historical evidence of faulting in Eastern Anatolia and Northern Syria*. Annali Di Geofisica, **38,** 337.

Bartov, Y., Z. Lewy, G. Steinitz and I. Zak 1980. *Mesozoic and Tertiary Stratigraphy, Paleogeography and Structural History of the Gebel Areif en Naqa Area, Eastern Sinai*. Israel Journal of Earth Sciences, **29,** 114-139.

BEICIP 1975. *Gravity maps of Syria: Damascus (Syria)*. Bureau d'etudes industrielles et de cooperation de l'institut francais du petrole, Hauts de Seine, 96 p.

Ben-Avraham, Z. 1992. *Development of asymmetric basins along continental transform faults*. Tectonophysics, **215,** 209-220.

Ben-Avraham, Z. and M.D. Zoback 1992. *Transform-normal extension and asymmetric basins: An alternative to pull-apart models*. Geology, **20,** 423-426.

Best, J.A., M. Barazangi, D. Al-Saad, T. Sawaf and A. Gebran 1993. *Continental margin evolution of the northern Arabian platform in Syria*. American Association of Petroleum Geologists Bulletin, **77,** 173-193.

Beydoun, Z.R. 1999. *Evolution and development of the Levant (Dead Sea Rift) Transform System: a historical-chronological review of a structural controversy.* In C. Mac Niocaill and P.D. Ryan (Eds.), Continental Tectonics, Geological Society of London, special publications, **164**, 239-255.

Brew, G., R. Litak, M. Barazangi and T. Sawaf 1999. *Tectonic evolution of Northeast Syria: Regional Implications and Hydrocarbon Prospects.* GeoArabia, **4,** 289-318.

Butler, R.W.H., S. Spencer and H.M. Griffith 1997. *Transcurrent fault activity on the Dead Sea Transform in Lebanon and its implications for plate tectonics and seismic hazard*. Journal of the Geological Society, **154,** 757-760.

Chaimov, T., M. Barazangi, D. Al-Saad, T. Sawaf and A. Gebran 1990. *Crustal shortening in the Palmyride fold belt, Syria, and implications for movement along the Dead Sea fault system*. Tectonics, **9,** 1369-1386.

Chaimov, T., M. Barazangi, D. Al-Saad, T. Sawaf and A. Gebran 1992. *Mesozoic and Cenozoic deformation inferred from seismic stratigraphy in the southwestern intracontinental Palmyride fold-thrust belt, Syria*. Geological Society of America Bulletin, **104,** 704-715.

Dalongeville, R., J. Laborel, P. Pirazzoli, P. Sanlaville, M. Arnold, P. Bernier, J. Evin and L.-F. Montaggioni 1993. *Les variations recentes de la linge de rivage sur le littorial Syrien*. Quaternaire, **4,** 45-53.

Devyatkin, E.V., A.E. Dodonov, E.V. Sharkov, V.S. Zykin, A.N. Simakova, K. Khatib and H. Nseir 1997. *The El-Ghab Rift Depression in Syria: Its Structure, Stratigraphy, and History of Development*. Stratigraphy and Geological Correlation, **5,** 362-374.

Domas, J. 1994. *The Late Cenozoic of the Al Ghab Rift, NW Syria*. Sborn'ik geologick'ych ved Antropozoikum, **21,** 57-73.

Dooley, T. and K. McClay 1997. *Analog modelling of pull-apart basins*. American Association of Petroleum Geologists Bulletin, **81,** 1804-1826.

Dubertret, L. 1932. *Les formes structurales de la Syrie et de la Palestine*. Comptes Rendus l'Academie des Sciences, **195,** 66.

Dubertret, L. 1975. *Introduction a la Carte Geologique a 1:50 000 du Liban*. Notes Memoire Moyen-Orient, **13,** 345-403.

Dzhabur, I. 1985. *Seismological description of Latakia region of Syria according to borehole and surface observations*. Vestnik Moskovskogo Universiteta. Geologiya, **40,** 90-93.

Fleury, J., J. Chorowicz and J. Somma 1999. *Discussion of the active Dead Sea Transform in Lebanon*. Journal of the Geological Society of London, **156,** 1243-1248.

Freund, R., Z. Garfunkel, I. Zak, M. Goldberg, T. Weissbrod and B. Derin 1970. *The shear along the Dead Sea rift*. Philosophical Transactions of the Royal Society of London, **267,** 107-130.

Garfunkel, Z. and Z. Ben-Avraham 1996. *The Structure of the Dead Sea Basin*. Tectonophysics, **266,** 155-176.

Golke, M., S. Cloetingh and K. Fuchs 1994. *Finite-element modelling of pull-apart basin formation*. Tectonophysics, **240,** 45-57.

Guiraud, R. and W. Bosworth 1997. *Senonian basin inversion and rejuvenation of rifting in Africa and Arabia: synthesis and implications to plate-scale tectonics*. Tectonophysics, **282,** 39-82.

Harding, T.P. 1985. *Seismic characteristics and identification of negative flower structures, positive flower structures, and positive structural inversion*. American Association of Petroleum Geologists Bulletin, **69,** 582-600.

Hempton, M. 1985. *Structure and deformation of the Bitlis suture near Lake Hazar, southeastern Turkey*. Geological Society of America Bulletin, **96,** 233-243.

Hempton, M. 1987. *Constraints on Arabian plate motion and extensional history of the Red Sea*. Tectonics, **6,** 687-705.

Hricko, J. 1988. *Geophysical Exploration in Selected Areas of Syrian Arab Republic, Stage Report on Survey in Jisr al Shoghour Area, unpublished internal report*. Strojexport Praha - Geofyzika Brno, Czechoslovakia, Damascus - Brno, 33 p.

Kent, W.N. and R.G. Hickman 1997. *Structural development of Jebel Abd Al Aziz, northeast Syria*. GeoArabia, **2,** 307-330.

Krenkel, E. 1924. *Der Syrische Bogen*. Zentralblatt fuer Mineralogie, Geologie und Palaeontologie, **9,** 274-281.

Lupa, J., 1999. *Structure of the Ghab Basin and surroundings, Northwest Syria, derived from gravity modeling*. Unpublished Thesis, Cornell University, Ithaca, NY, 152 p.

Matar, A. and G. Mascle 1993. *Cinematique de la Faille du Levant au Nord de la Syrie: Analyse Microtectonique du Fosse d'Alghab*. Geodinamica Acta, **6,** 153-160.

McClusky, S., S. Balassanian, et al. 2000. *GPS constraints on plate kinematics and dynamics in the eastern Mediterranean and Caucasus*. Journal of Geophysical Research, **105,** 5695-5719.

Mouty, M. 1997. *Le Jurassique de la Chaine cotiere (Jibal As-Sahilyeh) de Syrie: essai de biozonation par les grands foraminiferes*. Comptes Rondus de l'Academie des Sciences de Paris/Sciences de la terre et des planetes, **325,** 207-213.

Mouty, M., M. Delaloye, D. Fontignie, O. Piskin and J.-J. Wagner 1992. *The volcanic activity in Syria and Lebanon between Jurassic and Actual*. Schweizerische Mineralogische und Petrographische Mitteilungen, **72,** 91-105.

Nilsen, T.H. and A.G. Sylvester 1995. *Strike-slip basins.* In C.J. Busby and R.V. Ingersoll (Eds.), Tectonics of sedimentary basins, Blackwell Science, 425-457.

Ponikarov, V.P. 1966. *The Geology of Syria. Explanatory Notes on the Geological Map of Syria, Scale 1:200 000*. Ministry of Industry, Damascus, Syrian Arab Republic.

Quennell, A.M. 1959. *Tectonics of the Dead Sea Rift*. Proceedings of the 20th International Geological Congress, Mexico, 385-403.

Quennell, A.M. 1984. *The Western Arabia rift system.* In J.E. Dixon and A.H.F. Robertson (Eds.), The Geological Evolution of the Eastern Mediterranean, Geological Society of London, Special Publication, **17**, 775-788.

Rahe, B., D.A. Ferrill and A.P. Morris 1998. *Physical analog modeling of pull-apart basin evolution*. Tectonophysics, **285,** 21-40.

Robertson, A.H.F., P.D. Clift, P.J. Degnan and G. Jones 1991. *Palaeogeographic and palaeotectonic evolution of the Eastern Mediterranean Neotethys*. Palaeogeography, Palaeoclimatology, Palaeoecology, **87,** 289-343.

Rodgers, A.J., W.R. Walter, R.J. Mellors, A.M.S. Al-Amri and Y.-S. Zhang 1999. *Lithospheric structure of the Arabian Shield and Platform from complete regional*

*waveform modelling and surface wave group velocities.* Geophysics Journal International, **138,** 871-878.

Rodgers, D.A. 1980. *Analysis of pull-apart basin development produced by en echelon strike-slip faults.* In P.F. Ballance and H.G. Reading (Eds.), Sedimentation in Oblique-slip Mobile Zones, International Society of Sedimentologists Special Publication, **4**, 27-41.

Ruske, R.v. 1981. *Geologie des syrischen Kustengebirges.* VEG Deutscher Verlag fur Grundstoffindustrie, Leipzig, 91 p.

Sandvol, E., K. Al-Damegh, A. Calvert, D. Seber, M. Barazangi, R. Mohamad, R. Gok, N. Turkelli and C. Gurbuz 2000. *Tomographic imaging of Lg and Sn propagation in the Middle East.* Pure and Applied Geophysics, in press.

Schubert, C. 1982. *Origin of Cariaco Basin, South Caribbean Sea.* Marine Geology, **47,** 345-360.

Seber, D., M. Barazangi, T. Chaimov, D. Al-Saad, T. Sawaf and M. Khaddour 1993. *Upper crustal velocity structure and basement morphology beneath the intracontinental Palmyride fold-thrust belt and north Arabian platform in Syria.* Geophysical Journal International, **113,** 752-766.

ten Brink, U.S., Z. Ben-Avraham, R.E. Bell, M. Hassouneh, D.F. Coleman, G. Andreasen, G. Tibor and B. Coakley 1993. *Structure of the Dead Sea Pull-Apart Basin From Gravity Analyses.* Journal of Geophysical Research, **98,** 21,877-21,894.

ten Brink, U.S., N. Schoenberg, R.L. Kovach and Z. Ben-Avraham 1990. *Uplift and a possible Moho offset across the Dead Sea transform*. Tectonophysics, **180,** 71-85.

Trifonov, V.G., V.M. Trubikhin, Z. Adzhamyan, S. Dzhallad, Y. El' Khair and K. Ayed 1991. *Levant fault zone in northeast Syria*. Geotectonics, **25,** 145-154.

Turcotte, D.L. and G. Schubert 1982. *Geodynamics: The applications of continuum mechanics to geological problems.* John Wiley & Sons, New York, 450 p.

Walley, C. 1998. *Some outstanding issues in the geology of Lebanon and their importance in the tectonic evolution of the Levantine region*. Tectonophysics, **298,** 37-62.

Wdowinski, S. and E. Zilberman 1996. *Kinematic Modelling of large scale structural asymmetry across the Dead Sea Rift*. Tectonophysics, **266,** 187-201.

Wdowinski, S. and E. Zilberman 1997. *Systematic analyses of the large-scale topography and structure across the Dead Sea Rift*. Tectonics, **16,** 409-424.

# CHAPTER FIVE

# Tectonic Evolution of Syria

**ABSTRACT**

For the first time, we document the tectonic evolution of all Syria throughout the Phanerozoic. These interpretations are based on a very extensive database, primarily seismic reflection data, well information, and surface geologic studies.

Syrian tectonic deformation is focused in four major zones that have been repeatedly reactivated in response to activity on nearby plate boundaries currently and throughout the Phanerozoic, especially Mesozoic – Cenozoic time. The most extensive zone is the Palmyrides, that includes the southwest Palmyride fold and thrust belt and the inverted sub-basins that are now the Bilas and Bishri blocks. The Euphrates Fault System and Abd el Aziz / Sinjar grabens in eastern Syria are large extensional features with a more recent history of compression. The final zone includes the Dead Sea transform plate boundary that cuts through western Syria.

Combining the interpreted history of these zones, together with analysis from the remainder of the country, we have constructed a model of tectonic evolution throughout Syria. Integration of lithostratigraphic information into our final model has refined the timing of specific events and provided a paleogeographic framework for the results. The model shows how specific deformation episodes within Syria have been penecontemporaneous with regional scale plate tectonic events. Following a relatively quiescent Early Paleozoic shelf environment, the northeast trending Palmyride / Sinjar trough formed across central

Syria in response to regional Hercynian compression followed by Permo-Triassic opening of the NeoTethys Ocean and the eastern Mediterranean. The trough accumulated thousands of meters of clastic strata, and was the focus of Mesozoic carbonate deposition as subsidence continued. Late Cretaceous tectonics were dominated by extension in the Euphrates Fault System and Abd el Aziz / Sinjar graben in eastern Syria. Repeated collisions and continental margin shortening along the northern Arabian margin from Late Cretaceous to Late Miocene time caused platform-wide compression. This led to the structural inversion and shortening of the Palmyride trough and Abd el Aziz / Sinjar graben. This uplift and compression continues today under the influence of Arabia / Eurasia convergence.

The tectonic evolution of Syria has been critical to the hydrocarbon accumulations in the country. Hydrocarbons, with Miocene to Silurian age sources, are found predominantly in Mesozoic reservoirs with structural traps formed in response to Mesozoic extension and Cenozoic inversion tectonics. Some Paleozoic plays remain to be fully tested.

## INTRODUCTION

The 'Cornell Syria Project', active since the late 1980's, is an ongoing collaboration between Cornell University and the Syrian Petroleum Company (SPC), and recently with Damascus University. Our goal has been to analyze and map the tectonic history of structurally deformed areas of Syria, predominantly through geophysical analysis. Syria is part of the northern Arabian platform that has been proximal to active plate boundaries for most of the Phanerozoic, from Early Paleozoic ProtoTethys Ocean formation until today when plate boundaries still surround the country (Figure 5.1).
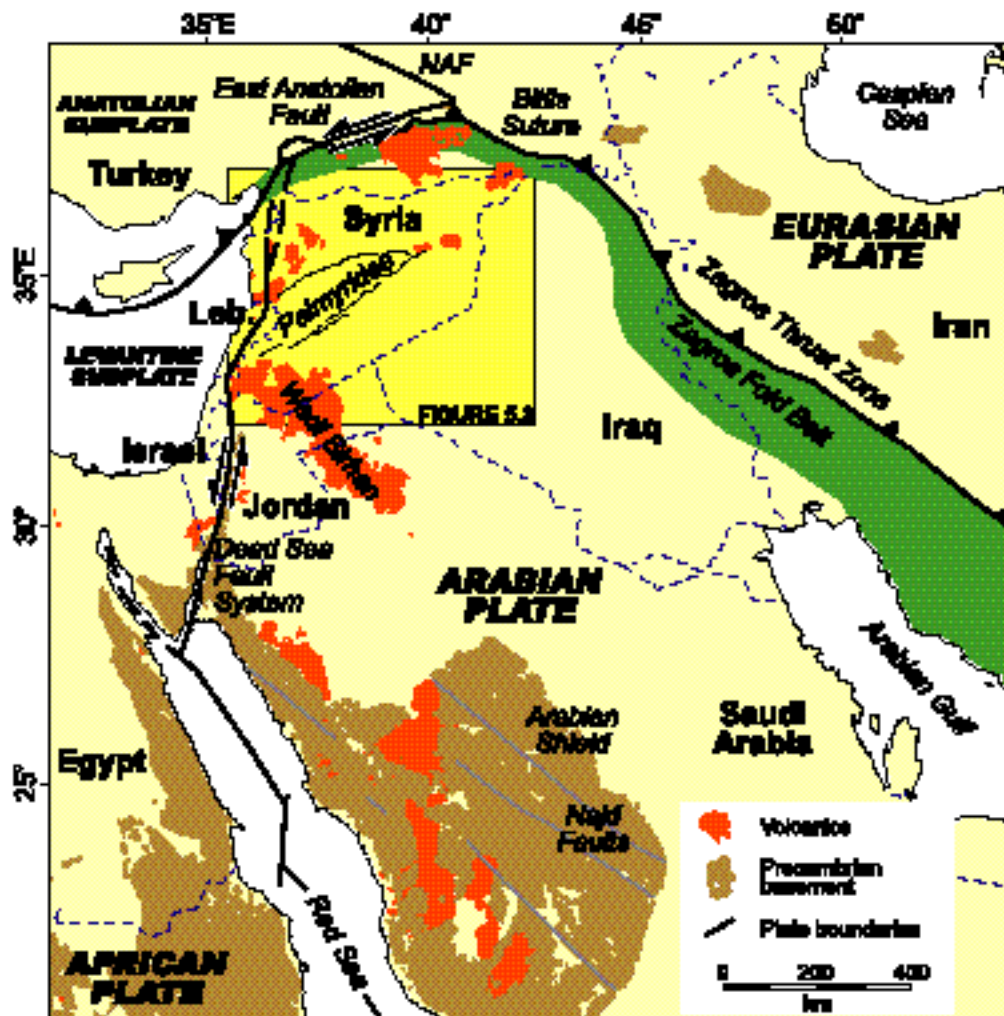
**Figure 5.1:** Regional tectonic map of the northern Arabian Plate and surrounding regions showing the proximity of Syria to many active plate boundaries. Leb. = Lebanon, NAF = North Anatolian Fault.

We show that regional plate tectonics strongly control the continental deformation in Syria (e.g. Brew et al., 1999). This deformation has been long-lived, episodic, and repeatedly focused in previously tectonized areas. Understanding this rich history can yield a fuller appreciation of plate tectonic processes. It can also provide a better understanding of the likely occurrence and distribution of natural resources. While not comparable with the vast reserves of the Arabian Gulf, the hydrocarbon resources of Syria are nonetheless economically important, and the potential for further significant discoveries remains.

Much of our previous work has concentrated on relatively distinct structural provinces within Syria. Our goal in this paper is to document the tectonic evolution of all Syria by integrating our previous interpretations with new regional structural maps and incorporating significant lithostratigraphic knowledge. After outlining the tectonic setting of the studied area, this paper continues with a very brief survey of previous work concerning Syria and a description of the newly expanded database used in the current work. We then describe the structure and interpreted evolution of specific, tectonically deformed zones within Syria. Our regional mapping is then discussed, encompassing a new lithostratigraphic chart, structural maps, and a new tectonic map for Syria. Our ultimate result is a regional evolutionary tectonic model for all Syria, set in a framework of plate tectonic events. We conclude by discussing the implications for hydrocarbon reserves in Syria.

**Tectonic Setting**

Syria is close to the leading edge of a continent / continent collision where the Arabian Plate is converging on Eurasia at $18 \pm 2$ mm/year in a roughly north-northwesterly direction (McClusky et al., 2000). This collision is manifest in the active transform and convergent

plate boundaries that currently surround Syria (Figure 5.1). The events on these boundaries, and their ancestors, have largely controlled Phanerozoic Syrian tectonics.

The most prominent current margin of the collision is the Zagros fold and thrust belt. These mountains, trending roughly northwest through western Iran and eastern Iraq, accommodate the convergence by widespread thrusting and folding with very significant shortening (e.g. Berberian, 1995). Along the northern Arabian margin the Zagros becomes the Eocene - Miocene age Bitlis suture of Eurasian and Arabian Plates (Hempton, 1985). To the northwest of the Arabian Plate the Mio-Pliocene age dextral North Anatolian Fault, and the sinistral East Anatolian Fault accommodate westward movement of the Anatolian subplate escaping under the influence of the convergence (McKenzie, 1970).

Coalescing with the East Anatolian Fault from the south is the Dead Sea Fault System. This system, that extends as far south as the Red Sea, separating Arabia from the African Plate (Levantine subplate). The Dead Sea Fault System is a sinistral transform fault accommodating the differential northward motion between the plates created by the opening of the Red Sea. Restraining bend geometry dominates the Lebanese portion of the sinistral Dead Sea Fault System (Walley, 1988). Total offset south of the bend is well established to be ~105 km (Quennell, 1984). Displacement north of the restraining bend has been documented at less than 25 km (Trifonov et al., 1991), but further work is needed to clarify and document this estimate. Several authors have suggested two phases of strike-slip motion on the fault, one pre-Miocene / Early Miocene and one post-Miocene (Freund et al., 1970; Quennell, 1984). This agrees with a widely accepted model in which Hempton (1987) documented a two-phase opening of the Red Sea. Hempton (1987) went on to correlate these phases of motion with the episodic deformation of many features in the

northern Arabian platform, such as the Dead Sea Fault System. Bitlis suture, and Zagros fold and thrust belt.  The findings of this paper largely support the model of Hempton (1987).


**Previous Geologic Studies by the Cornell Syria Project**

The work of the Syria Project has shown that, to a first-order, Syria can be divided spatially into four major 'tectonic zones' and intervening structural highs (see Figure 5.2 for locations). The first tectonic zone is the Palmyride area.  Work there by Best et al. (1990; 1993), Chaimov et al. (1990; 1992; 1993), McBride et al. (1990), Al-Saad et al. (1991; 1992), Barazangi et al. (1993), Seber et al. (1993), and Alsdorf et al. (1995) documented a Late Paleozoic / Mesozoic depocenter trending northeast across central Syria (namely the 'Palmyride / Sinjar trough').  Compression in the Cenozoic has created the current topography above this trough (the Palmyride fold and thrust belt of the 'southwest Palmyrides' and the Bilas and Bishri blocks of the 'northeast Palmyrides').  This topography defines the areas that in totality we loosely call the 'Palmyrides'.  Late Cretaceous rifting created the second tectonic zone, the 'Euphrates Graben' in the farthest southeast of Syria (Sawaf et al., 1993; Litak et al., 1998), and the associated 'Euphrates Fault System' tectonic zone that extends fully across Syria (Litak et al., 1997).  Brew et al. (1999) mapped the evolution of the third tectonic zone, the Abd el Aziz / Sinjar area in northeast Syria that shows older association with the Palmyride trough, and more recent structural and stratigraphic similarities with the Euphrates Fault System.  Most recent Cornell work has been focused on analyzing the

**Figure 5.2:** Map showing topography of Syria, seismic reflection and well data locations, and locations of other figures in this paper. Wells colors indicate depth of penetration, symbols show best available knowledge regarding hydrocarbon status of the wells as summarized from various literature sources. The map projection listed is used for this and all subsequent maps.
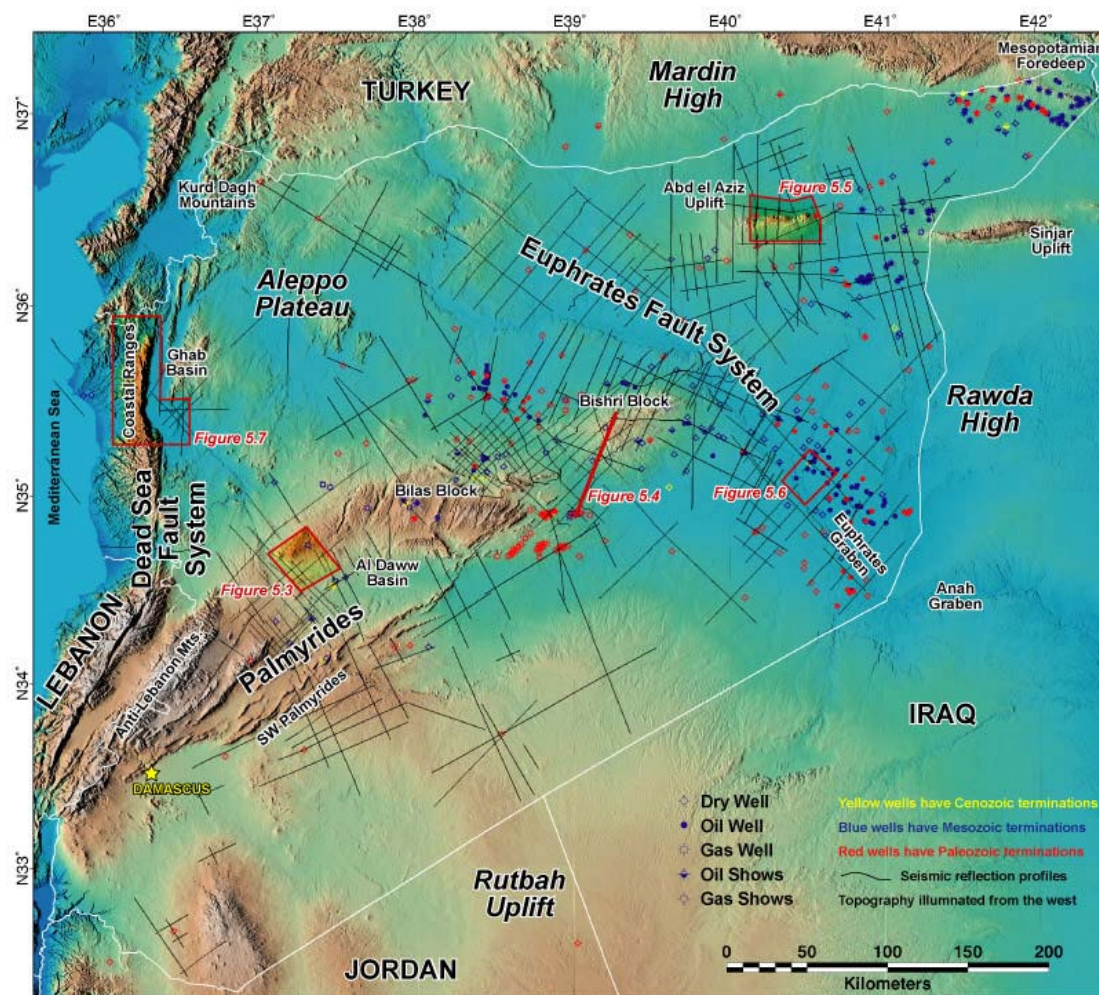
Cenozoic evolution of the final zone, the Dead Sea Fault System in western Syria (Brew et al., 2000; Gomez et al., 2000).

These four tectonic zones have experienced the vast majority of tectonic deformation in Syria, while the stable zones remained structurally high and relatively undeformed. This follows the intuitively simple idea that a pre-existing weakness in the crust will be the focus of future strain accommodation. It has also been shown that the style of reactivation is dependent on the orientation of the tectonic zone to the prevailing stress direction. Detailed interpretations of the tectonics zones, and new ideas regarding their evolution, are further discussed in a later section, before being ultimately tied into our final regional tectonic evolution model for Syria.

Recent contributions to the understanding of Syrian stratigraphy and paleogeographic evolution are relatively numerous (e.g. Ponikarov, 1966; Al-Maleh, 1976, 1982; Al-Maleh and Mouty, 1983, 1988, 1992; Sawaf et al., 1993; Mouty, 1997a, 1997b, 1998). This work has concentrated on the extremely well exposed Mesozoic carbonate section in the Palmyride fold and thrust belt, the Syrian Coastal Ranges, and the Aafrin basin exposed in the Kurd Dagh mountains (Figure 5.2). In contrast, the predominantly clastic Paleozoic section and the Mesozoic of eastern Syria are known only from drilling data, and still present significant challenges to stratigraphic understanding. In addition to detailed mapping of the facies and biostratigraphic variations in the Mesozoic section, researchers have also made important progress in correlating formations regionally (e.g. Mouty, 2000). Currently this correlation, and many new regional maps, are being finalized by Al-Maleh et al. (2001).

**DATABASE**

The database available for this work is extremely extensive by academic research standards (see Figure 5.2 for data locations). It consists of roughly 18,000 km of migrated seismic reflection profiles , drilling records from over 400 different wells, 1,000 km of seismic refraction data, and numerous other datasets such as remote sensing imagery, topography, and geologic maps. We thank the Syrian Petroleum Company (SPC) for providing most of these data.

The seismic reflection data are mostly migrated hardcopies to 4 seconds two-way travel time. They are from a variety of vintages and show large variations in quality. The highest quality data are from the early to mid 1990's collected using Vibroseis sources with a very high fold of coverage. The poorest quality records were shot with dynamic sources and 6-fold coverage in the 1960's. In general the Cenozoic section is fairly unreflective, with the exception of some Miocene evaporite layers. The carbonate Mesozoic section forms very prominent seismic reflectors, and regional unconformities are easily distinguished. The clastic Paleozoic section is poorly reflective with the exception of several abrupt facies changes in Cambrian and Ordovician strata that form regionally observed reflectors. Data quality decreases markedly in areas of complex structure, most notably the deeper areas of the Euphrates Graben and most of the southwest Palmyrides. Recordings are also very poor in areas of Cretaceous limestone outcrop on the Bilas block, and basaltic outcrop in southwest Syria. Metamorphic basement does not form a clear event on reflection records, and so high-quality, multi-fold refraction data have been used to determine basement depth throughout Syria (Seber et al., 1993; Brew et al., 1997).

Formation top data are available for all of the more than 400 wells in the database. Various wire-line logs are available for around a quarter of the wells. These include sonic, density, gamma ray, and other assorted logs. Our stratigraphic data are based on these drilling records and fieldwork by the authors and others. Many of these data have been used in past interpretations of individual tectonic zones within Syria. For the first time, we consider all the data in totality for creating the present structural maps and tectonic model of all Syria.

The locations of our data, and all digitally held data, are stored within a GIS for easy retrieval and analysis. Many data interpretations have been conducted within the GIS, thus harnessing the power of multiple-dataset visualization, manipulation and combination. For more details see Brew et al. (2000).

The limitations of a printed journal do not allow a full appreciation of this digital approach, and space limitations allow only a fraction of our datasets to be shown here. Consequently, we are providing downloadable versions of many of our results and interpretations on the web (http://atlas.geo.cornell.edu/syria/welcome.html). The benefit of the digital distribution includes the facility for any reader to plot their own maps, displaying any of the available coverages, at any scale. The coverages can also be interrogated (for example, 'show only oil producing wells that penetrate deeper than 4000 m').

**STRUCTURAL EVOLUTION OF MAJOR TECTONIC ZONES**

Previous work of the Cornell Syria Project has documented the structure and evolution of individual tectonic zones, based on subsets of the database discussed above. Here we discuss some past results and incorporate new and revised findings from the interpretations

of these tectonic zones. These results will be integrated into our tectonic evolutionary model in a later section.


**Palmyride Area**

The Palmyride area is the most extensive and topographically prominent tectonic zone in Syria (Figure 5.2). Uplift in the Palmyrides is a relative recent phenomenon, however, and during most of the Phanerozoic the zone was a sedimentary depocenter (Palmyride / Sinjar trough), accumulating several kilometers of Paleozoic and Mesozoic strata through episodic rifting and broad subsidence.

Best (1991) was the first to identify Palmyride and describe in detail rift-bounding faults, and presented examples from around the Bishri block in the northeastern Palmyrides, many of which core previously interpreted structures of McBride et al. (1990). Chaimov et al. (1993) documented the southwestern Palmyrides to be controlled by Late Paleozoic and Mesozoic listric normal faults that were structurally inverted in the Neogene. Isolated seismic examples show faults penetrating deep into the Paleozoic section (Chaimov et al., 1992, 1993), and wells from the southwestern fold belt of the Palmyrides encounter repeated sections across reverse faults down to at least Lower Triassic levels. Stratigraphic relationships across these faults indicate movement at least as old as Middle Triassic. Unfortunately, poor seismic reflectivity of the older section and drilling strategy limited to Triassic objectives preclude documenting thickening of Paleozoic horizons that could be used to definitively date initial faulting.

A very significant portion of the Palmyride trough thickening can be related to broad subsidence rather than simple extensional faulting (Chaimov et al., 1992). In particular, the

majority of the Triassic succession shows the typical form of a slow subsiding depocenter – perhaps the thermal subsidence phase above the Permo-Triassic rift. In the Jurassic, however, faulting dominated and many examples of this structural reactivation are found (e.g. Best, 1991; Chaimov et al., 1993; Litak et al., 1997). After gentle subsidence during the Early Cretaceous, in Cenomanian (and especially Maastrichtian) to Eocene time the Palmyride trough experienced accelerated subsidence (e.g. Mouty and Al-Maleh, 1983; Al-Maleh and Mouty, 1988; El-Azabi et al. 1998) with significant Late Cretaceous faulting in the northeast around the Bishri and Bilas blocks (Figure 5.2).

Since the Late Cretaceous the Palmyrides have been subjected to episodic compression leading to folding and the currently observed topography. About 400 km long and 100 km wide this topography can be divided into two distinct parts, the southwest Palmyrides, and the northeast Palmyrides which in turn consists of the Bilas and Bishri blocks. These areas have distinctly different Cenozoic histories as discussed below.

### *Southwest Palmyrides*

The southwest Palmyrides are dominated by a series of short, southeast verging reverse faults that core prominent surface folding. These short wavelength left-stepping anticlines have steeply-dipping (in some case overturned) forelimbs, and more shallowly dipping backlimbs. In general, the forelimbs become progressively steeper toward the southwest of the chain (Chaimov et al., 1993). The crests of the folds are generally 200 – 500 m above the surrounding topography.

Chaimov et al. (1993) argued for fault-propagation folding above inverted normal faults to form the southwest Palmyride folding and shortening. Many of these faults are linked by northwest striking sinistral transfer faults that are reactivated dextral transfers between the

older normal faults. This model is supported by well data and outcrop evidence in the southwest Palmyrides that require significant reverse faulting. For example, at the Abou Zounar anticline ~70 km west-northwest of Damascus in the southwest Palmyrides, Triassic strata are thrust over the Santonian age Rmah formation (Mouty, 1997b). Coward (1996) also suggested that inversion of northwest-facing half graben could explain the Palmyride fault-propagation folds. He indicates decreasing fault dip in the shallow section to explain the tight folds. Chaimov et al. (1993) showed sub-parallel Upper Cretaceous and Lower Paleozoic horizons that argue against regional scale detachment development in the Palmyrides. However, Chaimov et al. (1992) did map a locally well developed Triassic detachment level that precipitated some fault-bend fold formation, especially in the northern area of the southwestern Palmyrides (Figure 5.3). As an extension of the detachment hypothesis, Salal and Seguret (1994) argued for three levels of detachment and very significant thrusting in the southwest Palmyrides.

To the contrary, Searle (1994) suggested there is only very minor reverse faulting in the Palmyrides. He mapped complex folding, often in the form of box folds, above a locally developed Upper Triassic detachment (the predominantly gypsum Hayyan formation). However, in reaching his conclusions Searle (1994) appears to have mapped only the central and northeast parts of the mountains.

Hence we interpret strong along-strike structural variations in the Palmyrides. Fault-propagation folding above reverse faults, occasionally above a locally well developed

**Figure 5.3:** Block model of Abou Rabah anticlinal structure in the northern part of the southwestern Palmyrides. Surface is Thematic Mapper (TM) imagery draped over topography. Seismic lines CH-36 (dip line) and CH-45 are shown. See Figure 5.2 for location. View is looking towards the northeast. See annotation for horizontal and vertical scales.

NORTH

Image is 31 x 32 km with approximately no vertical exaggeration

*Paleogene*

Abou Rabah fault-bend fold (Upper Cretaceous outcrop)

Bilas Block (Upper Cretaceous outcrop)

Jhar Fault, extensive dextral strike-slip feature separating the SW Palmyrides from the Bilas block

*Neogene*

*Paleozoic*

Onlapping and thinning Middle Eocene strata shows Cenozoic structural uplift

Velocity 'pull-up' of imaged horizons

*Jurassic and Triassic repeated section*

Upper Cretaceous strata onlapping anticline indicating minor Late Cretaceous tectonics

*Cretaceous*

Triassic evaporite detachment surface, only locally developed

Two-way time (sec)

0
1
2
3
4

Upper Triassic detachment, appears to be the predominant shortening mode in the far southwestern Palmyrides. Folding, probably above the same detachment but with no appreciable thrusting, is predominant farther northeast. This would agree with the cross-sections of Chaimov et al. (1990) that show total shortening decreasing from ~20 km in the southwest Palmyrides to almost no shortening in the farthest northeast.

West of the tightly folded Palmyride anticlines, the Anti-Lebanon Mountains (Figure 5.2), form the highest topography in Syria. These mountains expose Jurassic and Triassic strata and most of the Cretaceous section has been eroded (Mouty, 1998). Walley (1998) suggests that the majority of Anti-Lebanon uplift was likely during the second-stage of "Syrian Arc" deformation in the Late Paleogene. Lebanese structures were later modified as part of the restraining bend architecture of the Dead Sea Fault System during the Neogene (Chaimov et al., 1990).

Northeast of the tightly folded Palmyrides the extensive, low-relief Al-Daww basin (90 x 25 km, Figure 5.2) lies between the southwest Palmyrides and the Bilas block. Seismic stratigraphic relationships in the Al-Daww basin date its formation to Miocene time onwards. This intermontane basin contains more than 2 km of Cenozoic strata.

### *Northeast Palmyrides*

To the north of the Al-Daww basin, the Jhar fault separates the southwest from the northeast Palmyrides (Plate 1). The Jhar fault has been traced nearly 200 km striking east-northeast and shows an average of 1 km of up-to-the north movement, and significant, but undetermined amounts of dextral strike-slip (Al-Saad et al., 1992). Surface mapping indicates Quaternary movement (Ponikarov, 1966). Well data indicate this was an active extensional fault at least as early as Jurassic time. Additional interpretations suggest this fault

may be the surface manifestation of a Proterozoic suture zone, as discussed further in a later section. The structural inversion along the Jhar fault is controlling the southern edge of the Bilas block (Figure 5.2) in a style of thick-skinned deformation typical of the northeastern Palmyrides. Uplift within the Bilas block is dominated by strike-slip duplexing where relatively undeformed, large anticlines are bounded by steep faults that show very little shortening (Chaimov et al., 1990).

To the north and east of the Bilas block, the Bishri fault is a prominent right-lateral fault separating the Bilas from the Bishri block. Similar to the Jhar fault, the Bishri fault accommodates uplift of the Bilas block relative to the Bishri block. Folding directly adjacent to the fault again suggests a transpressional feature. Focal mechanisms also show these dextral and reverse components of slip (see later Tectonic Map, Plate 1, and Chaimov et al., 1990). Northeast striking Mesozoic normal faulting was more active in the Bishri block than in any other part of the Palmyrides. Total throw is often distributed amongst several closely-spaced, steep, deeply-penetrating faults (Figure 5.4, and see Best, 1991). Jurassic was a time of significant fault movement, a Jurassic thickness of up to ~900 m is reached in the Bishri block. The area is also the only part of the Palmyrides to show significant normal faulting in the Late Cretaceous (thickness up to ~1600 m, Figure 5.4). Cenozoic structural inversion of these faults is controlling the present northeast-plunging anticlinal morphology of the block, flanked by much smaller folds (McBride et al., 1990; Best, 1991).

**Figure 5.4:** Interpretation of migrated seismic profile from the southwestern edge of the Bishri block in the northeastern Palmyrides (seismic profile ALAN-90-10). Surface is Thematic Mapper (TM) imagery draped over topography. See Figure 5.2 for location. See annotation for horizontal and vertical scales, depths are below sea level.

Approximate vertical scale (km)

NORTHEAST

Bishri Well

Bishri block: structurally inverted basin with thickened Triassic to Upper Cretaceous strata

Lithology change from marls to more resistant sandstones and limestones

Erosional depression

Al Hyr Well

Surface faulting mapped here

Fault propagation folds on normal faults reactivated in a reverse sense

Najeeb Well

SOUTHWEST

Topography (m)

Two-way time (sec)

Uppermost Cretaceous

Upper Cretaceous

Lower Cretaceous

Jurassic

Upper Triassic

M & L Triassic

Paleozoic

Neogene

Paleogene

Bishri block southern bounding faults: normal faulting in Mesozoic, reverse in Cenozoic

No detachment surface here in contrast to northern SW Palmyrides

Dashed interpretation speculative because of poorer data

Close to southern limit of Palmyride deformation

**Abd el Aziz / Sinjar Area**

In northeast Syria (and extending eastward into Iraq) there exist two prominent topographic highs, the Abd el Aziz and the Sinjar Uplifts (Figure 5.2) that suggest recent deformation. However, the origin of these features goes far back in geologic history.

From Late Paleozoic to Late Cretaceous time the Sinjar area and surroundings was the northeastern portion of the Palmyride / Sinjar trough. Strata are correlative throughout this trough, with some thinning of all formations above the Derro High (Plate 1). Accommodation space for sedimentation in northeast Syria was created largely through broad subsidence, although some Late Paleozoic and Mesozoic northeast striking faults have been identified (Brew et al., 1999). As in the Palmyrides, many thousands of meters of Late Paleozoic clastic strata and Mesozoic carbonates were deposited in this trough.

During Senonian time the formative Euphrates Fault System affected the southwestern portion of the Abd el Aziz / Sinjar area, forming faults that were to bound the western extent of the later deformation. But no significant extension occurred around the Abd el Aziz and Sinjar structures until the formation of a network of east - west striking faults in the latest Cretaceous that accommodated moderate extension. These normal faults (the largest of which were predominantly south-facing), and the resulting half graben, formed in the latest Campanian and Maastrichtian and accommodated up to 1600 m of syn-rift calcareous marly sedimentation (Figure 5.5). The Abd el Aziz and Sinjar graben were the most prominent of these features. Many of the extensional structures were linked by strike-slip faults that were also structurally reactivated Early

**Figure 5.5:** Block model of the Abd el Aziz uplift in northeast Syria. Surface is Thematic Mapper (TM) imagery draped over topography. Seismic lines UN-350 (dip line) and SY-48N are shown. See Figure 5.2 for location. View looking towards the southwest. See annotation for horizontal and vertical scales, depths are below sea level.

Two-way time (sec)

Average elevation north of Jebel Abd el Aziz is ~300 m

Surface Faulting

Cretaceous outcrop

Jebel Abd el Aziz peak elevation (932 m)

5 km

Strike-slip faulting

Limits of Middle Miocene outcrop

Middle and Lower Triassic

Lower Paleozoic

NORTH

Mid-Cambrian and older

Maghlouja Well

Lower Cretaceous & Upper Triassic

Neogene

Paleogene

Shiranish (syn-rift) formation

Upper Cretaceous

Approximate depth (km)

Image is 29 x 41 km, topographic exaggeration ~5, subsurface vertical exaggeration ~2
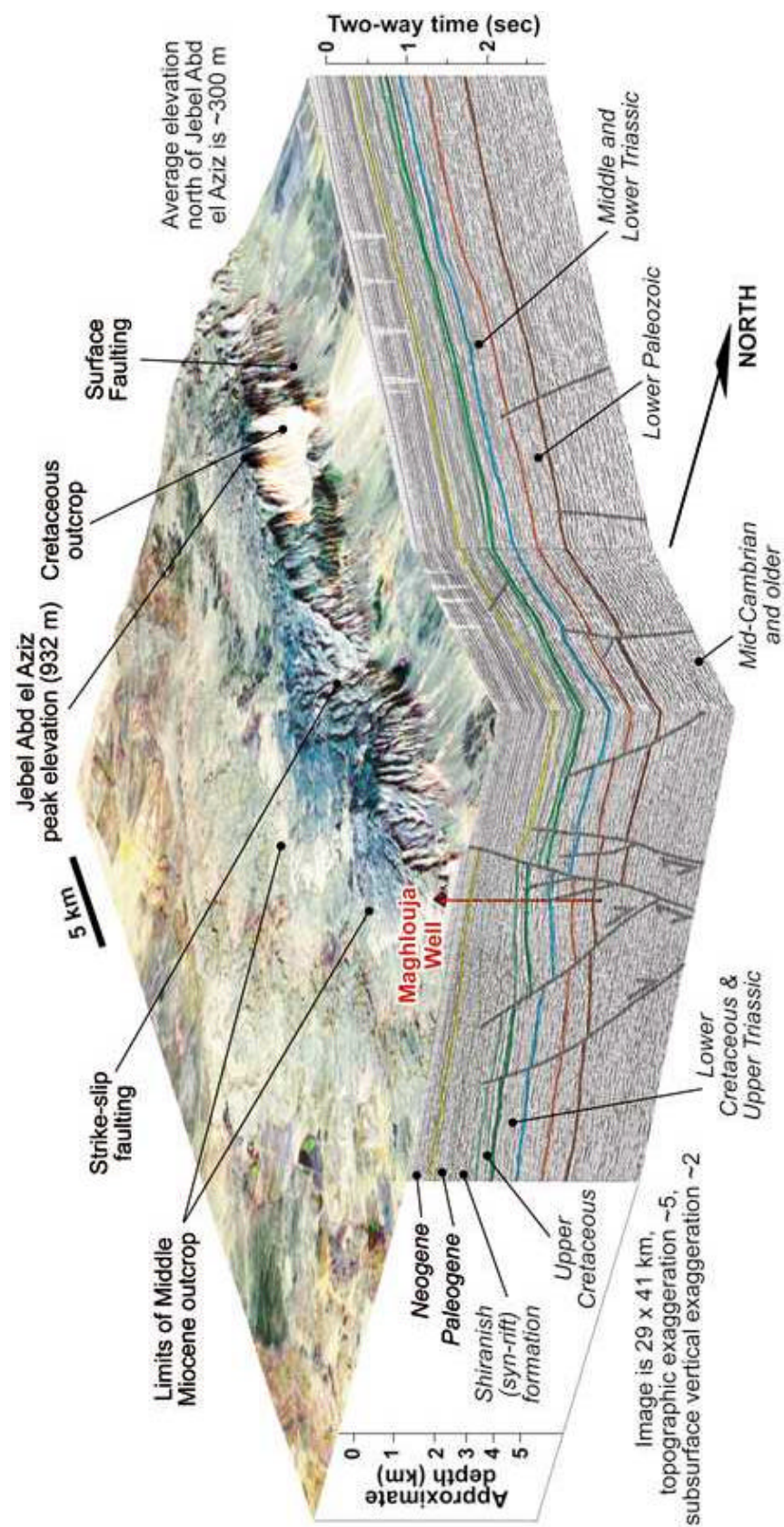
Mesozoic northeast striking normal faults. The extensional event was contemporaneous with further extension in the Euphrates Graben. However, the cessation of the extension, indicated by termination of faulting, came abruptly at the end of the Cretaceous, a little later than the cessation observed in the Euphrates Graben.

The currently observed topographic highs (the Abd el Aziz and Sinjar Uplifts) are the result of structural inversion that has been ongoing throughout the Cenozoic, most particularly in the Late Pliocene – Recent (Kent and Hickman, 1997; Brew et al., 1999). Specifically, stress caused by collision along the northern Arabian margin is reactivating, in a reverse sense, the Late Cretaceous east - west striking normal faults causing fault-propagation folds above their tip lines (Figure 5.5). Some of the northeast striking faults were also reactivated, in a strike-slip and reverse sense, during Cenozoic compression. One such fault is bounding the present structural inversion of the Abd el Aziz Uplift. The three major systems of fault in the Abd el Aziz / Sinjar area (Late Paleozoic / Early Mesozoic northeast-southwest striking; Senonian northwest – southeast striking; and Maastrichtian east – west striking) are clearly illustrated in the structure maps we present below.

Based on limited data, similar deformation appears to have contemporaneously affected the Mesopotamian foredeep in the farthest corner of northeast Syria. There, reactivated Late Cretaceous faults are observed beneath tight, Late Cenozoic fault-propagation folds (Figure 5.2).

**Euphrates Fault System**

The Euphrates Graben is a fault-bounded rift studied extensively by Litak et al. (1998) and de Ruiter et al. (1994). Litak et al. (1997) further showed that the Euphrates Fault System,

a related but less deformed zone of extension, extends from the Iraqi border in the southeast to the Turkish border in the northwest, including the Euphrates Graben.  The Euphrates Fault System is relatively unexpressed topographically (Figure 5.2) because, unlike the other tectonic zones of Syria, it has experienced very little tectonic reactivation in the Cenozoic.

A Turonian age unconformity - probably marking pre-rift uplift - is extensively developed in the Euphrates Graben, and the underlying limestone are eroded and dolomitized.  Extension then followed causing widespread redbed deposition  (Litak et al., 1998) that graded into progressively deeper water carbonate facies.  Senonian rifting, that resulted in around 6 km of extension and an undetermined amount of strike-slip movement, was accommodated on a distributed system of steep normal faults.  This is unlike some more 'simple' grabens that are bounded by more clearly defined major faults (Litak et al., 1997).   Transtensional deformation was increasingly dominant with time.   The syn-rift carbonate deposition culminating in the Campanian – Early Maastrichtian with the deposition of up to 2300 m of deep water marly limestone within the graben (Figure 5.6).  Extension stopped during the Maastrichtian.

Paleogene time was marked by widespread thermal subsidence above the aborted rift.  This sag has been shown to fit theoretical models of thermal equilibrium after rifting  (Litak et al., 1998) suggesting that likely the whole lithosphere was involved in rifting

**Figure 5.6:** Block model for Euphrates Graben, location shown in Figure 5.2. Surface is Thematic Mapper (TM) imagery draped over topography. Seismic profiles are PS-11 (dip line) and PS-11. View looking towards the southwest. See annotation for horizontal and vertical scales, depths are below sea level.
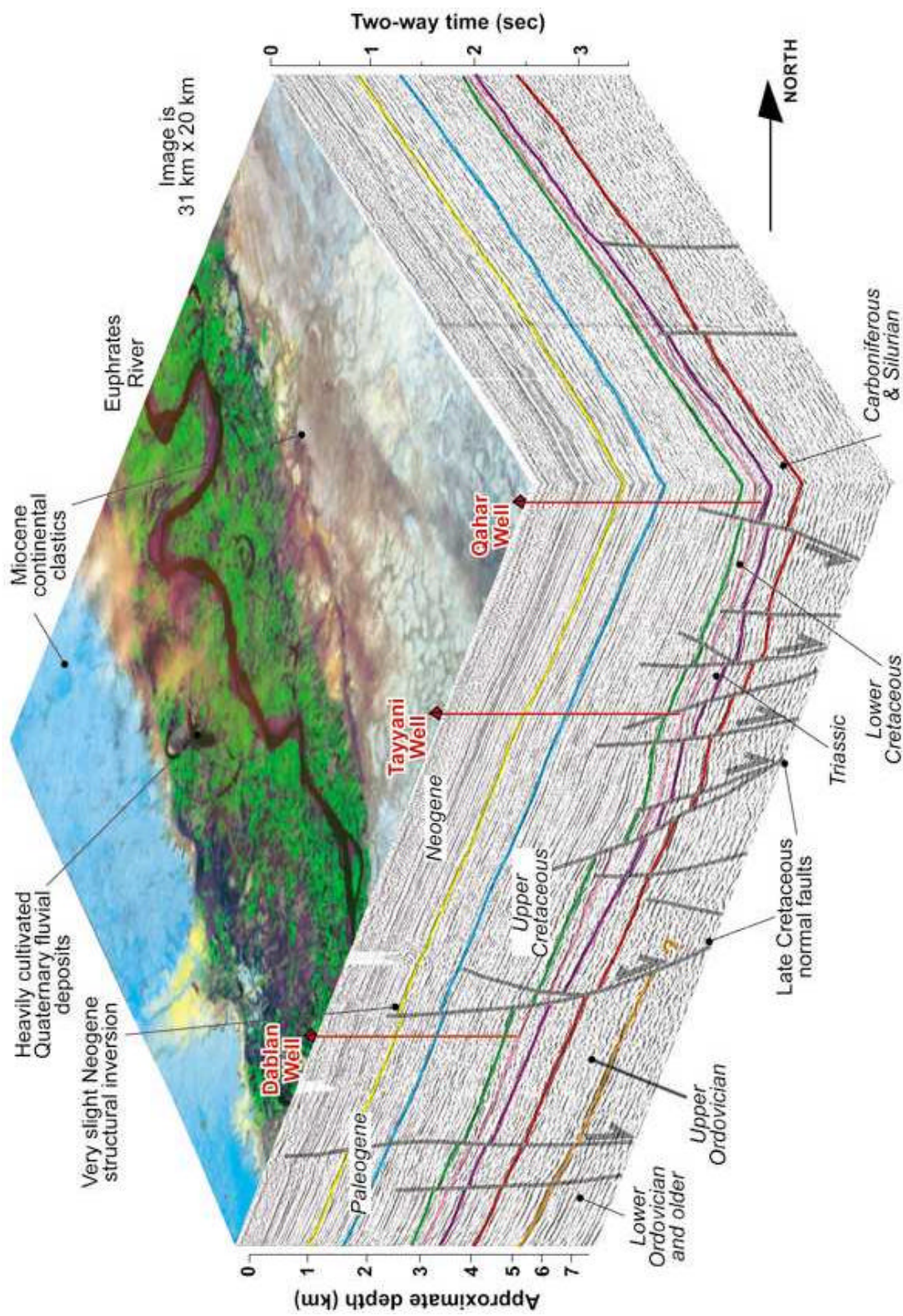
event.  This is in contrast to the Abd el Aziz / Sinjar Graben that shows no clear port-rift subsidence.  The relatively quiescent Paleogene tectonic regime is in contrast to the minor transpression and reactivation experienced by the Euphrates Fault System in the Neogene. Compressional features are very mild everywhere within the Fault System.  They are most developed in the northwest where reverse and strike-slip movement, with some associated minor fault-propagation folding, is observed on reactivated Late Cretaceous normal faults.

## Dead Sea Fault System

The Dead Sea Fault System is a major transform plate boundary separating Africa (Levantine subplate) from Arabia, and accommodating the differential movement between them.  Several authors have suggested two phases of strike-slip motion on the Dead Sea Fault System, a pre-Miocene / Early Miocene slip of 60 – 65 km, and post-Miocene slip of 40 – 45 km (Freund et al., 1970; Quennell, 1984).  Along the northern segment of the fault the age and rates of faulting are unclear due to a lack of piercing points, although total post-Miocene offset has been reported as less than 25 km (Trifonov et al., 1991).   These observations and work in the Palmyrides have been combined into a model in which the northern Dead Sea Fault has been active only during the second (post-Miocene) phase of Dead Sea Fault System motion.  In this model 20 - 25 km of post-Miocene sinistral motion has been accommodated along the northern fault segment, and another 20 km in the shortening of the adjacent Palmyride fold and thrust belt (Chaimov et al., 1990).  Ongoing work aims to clarify this issue.

The northern segment of the Dead Sea Fault System strikes parallel to the coast through western Syria. The fault is clearly defined topographically and structurally near the Lebanese border in western Syria (Walley, 1988), but becomes diffuse and distributed as it

approaches and crosses the Turkish border (Figure 5.2). Along the fault in western Syria is the Ghab Basin (Figure 5.7), a deep Pliocene – Recent pull-apart structure (Brew et al., 2000). The Ghab Basin opened in response to a left-step in the fault, although sinistral motion fails to be fully transferred across the basin, resulting in the 'horse-tailing' of the fault system observed to the north. Extension in the basin is accommodated by a series of northwest striking normal faults and significant subsidence on the Dead Sea Fault that bounds the basin to the east. Late Quaternary volcanism is found at the north of the basin that indicates opening of the basin there has occurred since 2 Ma.

The Syrian Coastal Ranges, in places more than 1500 m high, occupy most of the Syrian onshore area west of the Dead Sea Fault and Ghab Basin. They extend from the Mediterranean coast to the Dead Sea Fault System and from Lebanon to Turkey. This extensive monocline exposes the Mesozoic section from Upper Triassic to Upper Cretaceous (e.g. Mouty, 1997). The area is characterized by extensive karst terrain, a gently dipping (~10°) western limb, and a chaotic, uplifted eastern limb where the oldest strata are exposed (Figure 5.7). Stratigraphic relationships indicate that the uplift of the Coastal Ranges has occurred since the Middle Eocene. They could be part of the extensive Syrian Arc deformation that has been documented in Lebanon and Israel (Walley, 2000). However, the Ranges are clearly bound to the east by the active Dead Sea Fault System (Figure 5.2) that, in our model, has only been active since the latest Miocene in its current position. This suggests that most of the uplift is post-Miocene. While some component of compression across the Dead Sea Fault may be causing uplift of the Coastal Ranges, isostatic and dynamic uplift are most probably the main driving force (Brew et al., 2000).

**Figure 5.7:** Block model for Coastal Ranges / Ghab Basin along the Dead Sea Fault System in western Syria. Along-basin profile is GA-6 and cross-basin profile is GA-3. Surface is Thematic Mapper (TM) imagery draped over topography. See Figure 5.2 for location. View looking towards the southwest. See annotation for horizontal and vertical scales.

Heavily karstified
Jurassic and
Cretaceous limestone
(~10° west dip)

Surface trace
of Dead Sea
Fault System

5 km

Coastal Ranges;
max. elevation (1562 m)

Pull-apart
Ghab Basin;
elevation 170 m

Pliocene / Quaternary
basin fill

Ghab
Well

NORTH

Paleogene and
Upper Cretaceous

Middle and
Lower Triassic

Lower Cretaceous,
Jurassic and
Upper Triassic

TD of well
3085 mbsl

Deepest basin
fill ~ 3400 m

Dead Sea
Fault

Ordovician
and Upper
Cambrian

Mid-Cambrian
and older

Note strong lateral
velocity variation;
vertical scale varies
along profile

Image is 90 x 41 km,
topographic
exaggeration ~4

Two-way
time (sec)

0
1
2
3
4

**REGIONAL MAPPING**

We now consider the structure and stratigraphy of Syria as a whole, rather than the physiographically distinct areas just discussed. The lithostratigraphic and structural mapping presented below is based on all available data from Syria, as well as work from previous Cornell researchers. In the section to follow 'Regional Tectonic Evolution', we will integrate these regional maps into our final model.

**Lithostratigraphic Evolution**

We have used extensive drilling records from Syria, together with surface observations, and preexisting studies (e.g. Ponikarov, 1966; Al-Maleh, 1976; Mouty and Al-Maleh, 1983; Al-Maleh and Mouty, 1988, 1992; Sawaf et al., 1993; Mouty, 1997a, 1997b; 1998) to construct the most accurate summary of Syrian lithostratigraphy. Figures 5.8, 5.9 and 5.10 compare and contrast lithostratigraphic evolution of all Syria. More detailed discussion of tectono-stratigraphy of individual tectonic zones is given chronologically in our final regional tectonic evolution model.

Figure 5.8 is a generalized lithostratigraphic chart showing the variations of Syrian strata in time and space. Note that we have used the time-scale of Harland et al. (1990) throughout this work. Most clearly illustrated is the shift from predominantly clastic Paleozoic deposition to Mesozoic and Cenozoic carbonates. Furthermore, numerous widespread unconformities, showing long-lived hiati and erosion, are observed throughout the section, most especially around Devonian and Late Jurassic times. The long-lived Rutbah / Rawda and Aleppo uplifts (Figure 5.2) show the least complete sections. Also of some note is the very prominent Palmyride / Bishri / Sinjar

**Figure 5.8:** Generalized lithostratigraphic chart for all Syria based on extensive surface observations and drilling records. Time intervals are not drawn to scale. Red dots and numbers correspond to time points on Plate 2. Note the alternative formation names for the Lower Mesozoic section in the Euphrates Graben System (Mulussa A, B, C etc.). See text for full discussion.
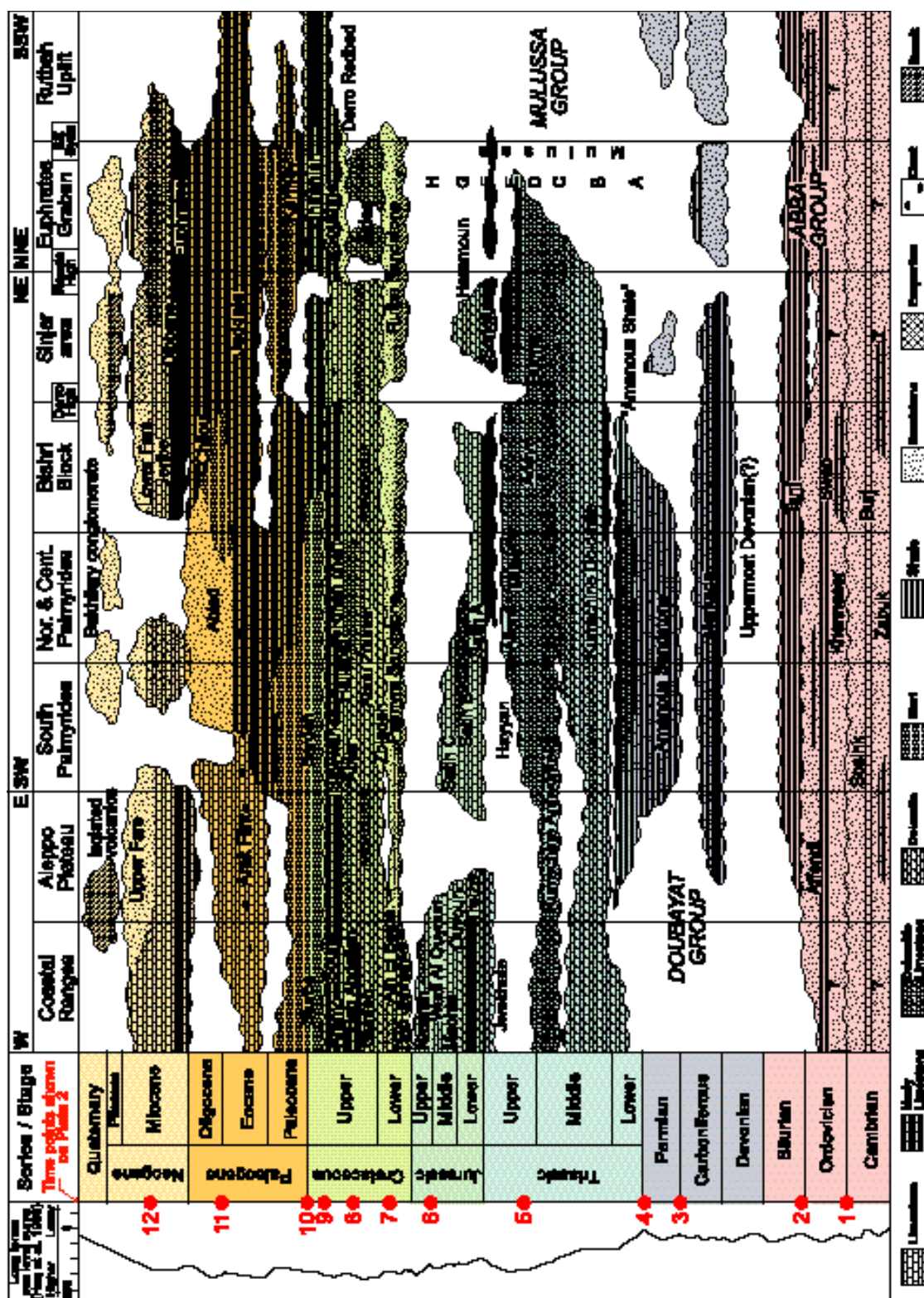
**Figure 5.9**: Isopach maps of Syria showing the present thickness of the four major Mesozoic and Cenozoic sedimentary packages, as derived from well and seismic data. Contour interval is 250 m in each frame. See text for discussion.

a) Cenozoic

b) Upper Cretaceous

c) Lower Cretaceous and Jurassic

d) Triassic

Thickness (m)

0
250
500
750
1000
1250
1500
1750
2000
2250
2500
2750
3000+

Faults and Folds

0 40 80 120 160
km
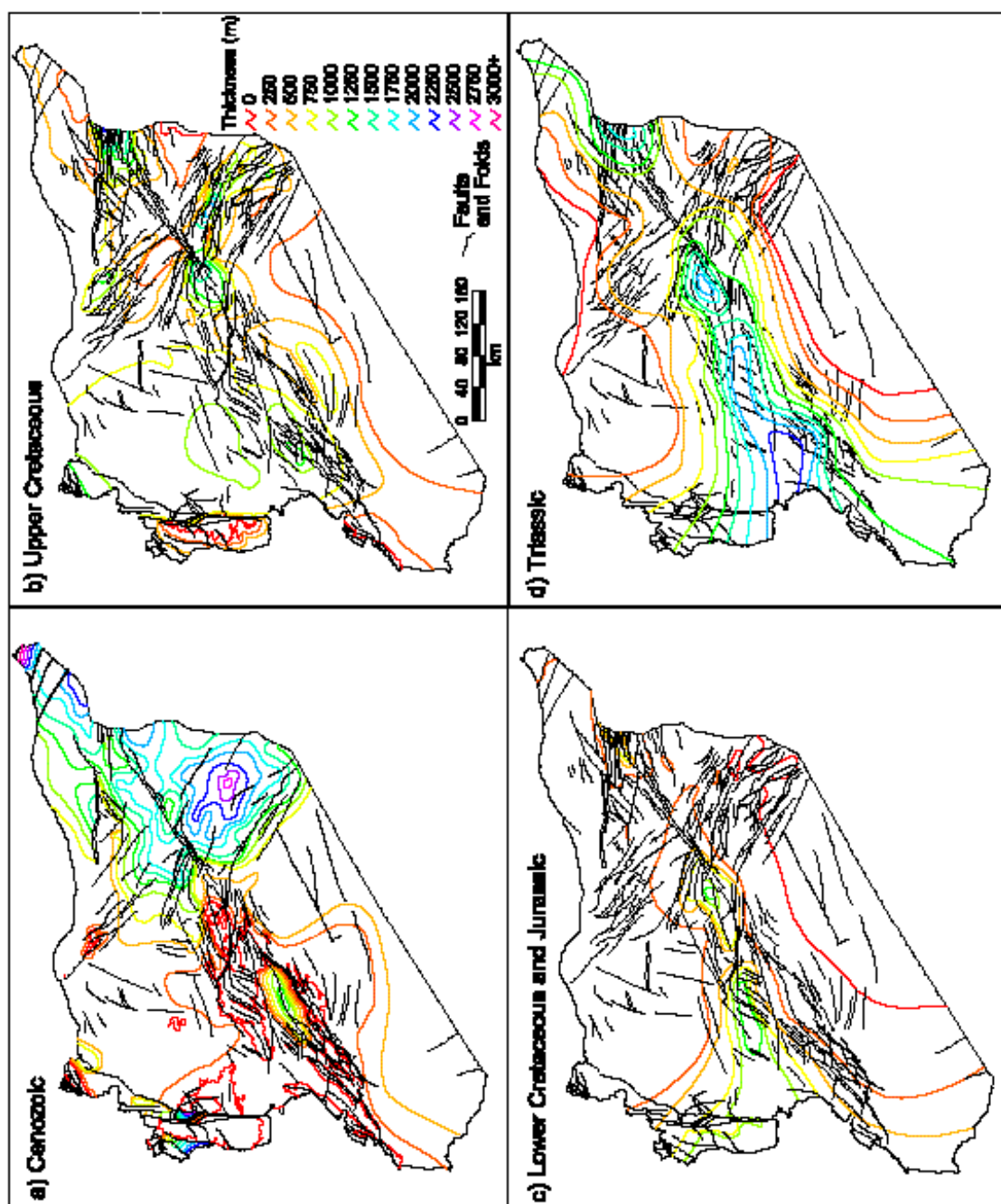
**Figure 5.10:** 3-D fence diagram generalizing the current sedimentary thickness variations in Syria. The view is from the northwest with illumination from the north. The name of the well used in the correlation and its total depth are shown at the top of each data point. Vertical and horizontal scales change with perspective.

Legend:
- Neogene
- Paleogene
- Cretaceous
- Jurassic
- Triassic
- Upper Paleozoic
- Lower Paleozoic
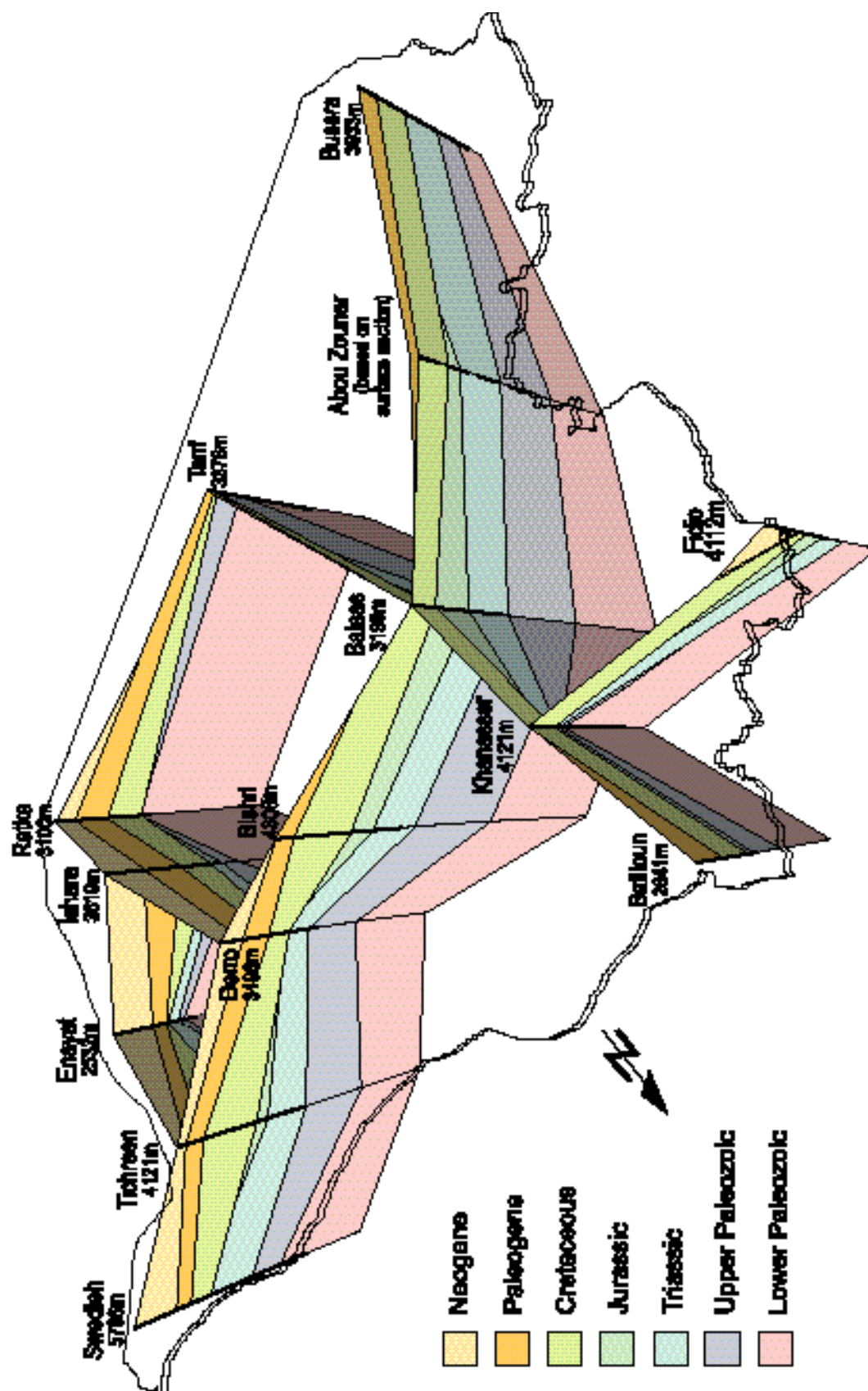
depocenter.  For much of early Mesozoic time the Palmyride deposition was linked to the Sinjar area, whereas for the Upper Cretaceous Sinjar strata show much closer affinity to similar age rocks in the Euphrates Graben.  This reflects the shift in tectonics from the Palmyride / Sinjar trough to the Late Cretaceous fault-bounded extension in eastern Syria. Figure 5.9 shows details of the shifting deposition throughout Syria.  Note the limited Jurassic / Lower Cretaceous section caused by widespread erosion and non-deposition related to regional Late Jurassic / Early Cretaceous uplift.  Preserved Cenozoic patterns are dominated by subsidence along the Euphrates Fault System.

The various formation names used in Syria are often site-specific (Figure 5.8), leading to a clutter and confusing nomenclature.  Furthermore, different nomenclatures have historically been used by surface and subsurface geologists, compounding the already difficult task of correlating subsurface and surface formations.  Paleozoic formations in particular are notoriously difficult to distinguish from scattered drilling penetrations, and are often poorly differentiated in drilling logs, rendering detailed chronology impossible  (e.g. Ravn et al., 1994).  Regarding Mesozoic nomenclature, several long-standing problems have hindered regional correlation.  A well-known confusion involves the Kurrachine to Serjelu formations that, for many years, were regarded as Liassic in Iraq (as shown in Beydoun, 1991).  More recent dating has established ages comparable with the similarly named formations in Syria (Middle – Upper Triassic) (Beydoun and Habib, 1995).  In our discussion of Triassic and Jurassic strata we have used traditional formation names (as maintained by SPC) and their modern (Mulussa Group) equivalents because the older names are widespread in the literature.  Al-Maleh et al. (2001) provide a more detailed description and discussion of Syrian Mesozoic stratigraphy and attempt a definitive regional correlation.

Figure 5.10 shows general thickness variations for all the major sediment packages. The main trends include a southward and eastward thickening of Early Paleozoic strata (Ratka well) caused by the Gondwana passive margin off the east of Syria at that time. In the Late Paleozoic and Mesozoic deposition shifted to the west (Abou Zounar section) as the Levantine passive margin developed (Best et al., 1993). From Late Paleozoic time onward the influence of the long-lived structural highs of the Rutbah / Rawda Uplift (Tanf well) and Aleppo Plateau (Khanasser well) are easily observed. Upper Paleozoic and Mesozoic strata are concentrated in the Palmyride / Sinjar trough, with significant along strike variation apparent (Bishri well and Derro well). Rapid thickness changes in eastern Syria are associated with Late Cretaceous basin formation (Ishara well in the Euphrates Graben and Tichreen well in the Sinjar graben), and the influence of Neogene Mesopotamian foredeep formation (Swedieh well). Finally, uplift and erosion of the Cenozoic section is observed in the Palmyrides (Balaas well and Abou Zounar section) and Sinjar Uplift (Tichreen well).

**Subsurface Structural Maps**

We present new subsurface structural maps of four horizons throughout Syria (Figure 5.11a-d). Each map shows the present depth to top of the subject horizon, along with current structure, and the sub-cropping formation on the top of each horizon. A fuller appreciation of how the depths of these horizons vary in respect to one another can be gained from a perspective view of the four surfaces, plus topography, shown together (Figure 5.12).

**Figure 5.11:** Maps of Syria showing depth, structure, and stratigraphy of various subsurface geologic horizons derived from seismic and well data. Colors in each map represent best estimates of depths to chosen horizon, black contours indicate extents of uppermost subcropping formation of the chosen horizon, and faults and folds are marked in red. Surface geology modified from Ponikarov (1966). Surfaces shown are (a) top Cretaceous, (b) top Lower Cretaceous, (c) top Triassic, (d) top Paleozoic. In (a) only two different formations subcrop, except in exposed areas. Therefore, a stippled pattern is used to show where the Soukhne formation subcrops, and the Shiranish formation subcrops in all other areas. There is only one Lower Cretaceous formation, therefore in (b) the stippled pattern indicates an absence of the Lower Cretaceous. The Lower Cretaceous is present in all other areas.

a)

Top Cretaceous

229

**Figure 5.11 (continued):**



Figure 5.11 (continued)c

b)

**Figure 5.11 (continued):**



Figure 5.11 (continued): c)
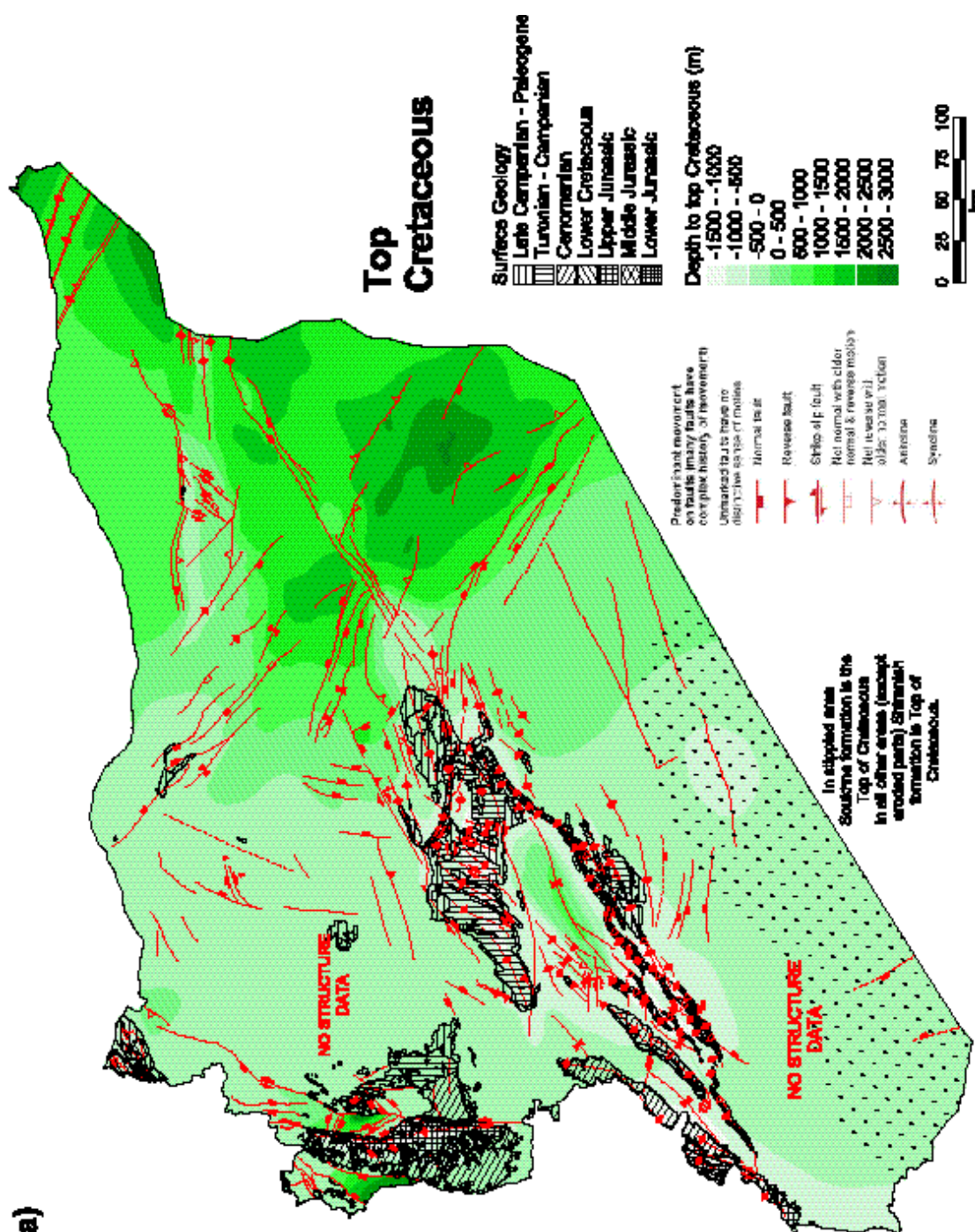
**Figure 5.11 (continued):**
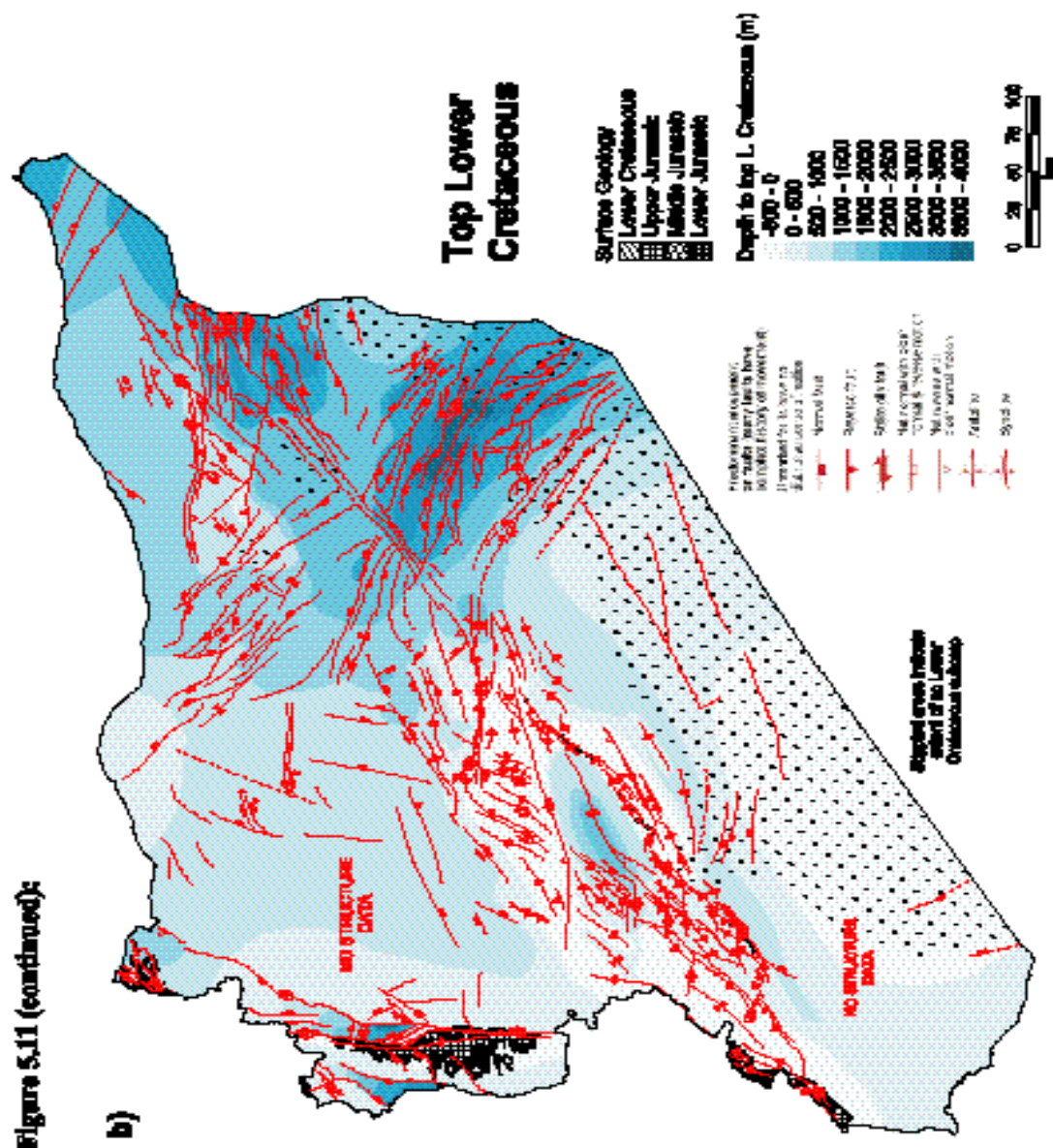


Figure 5.11 (continued):

d)
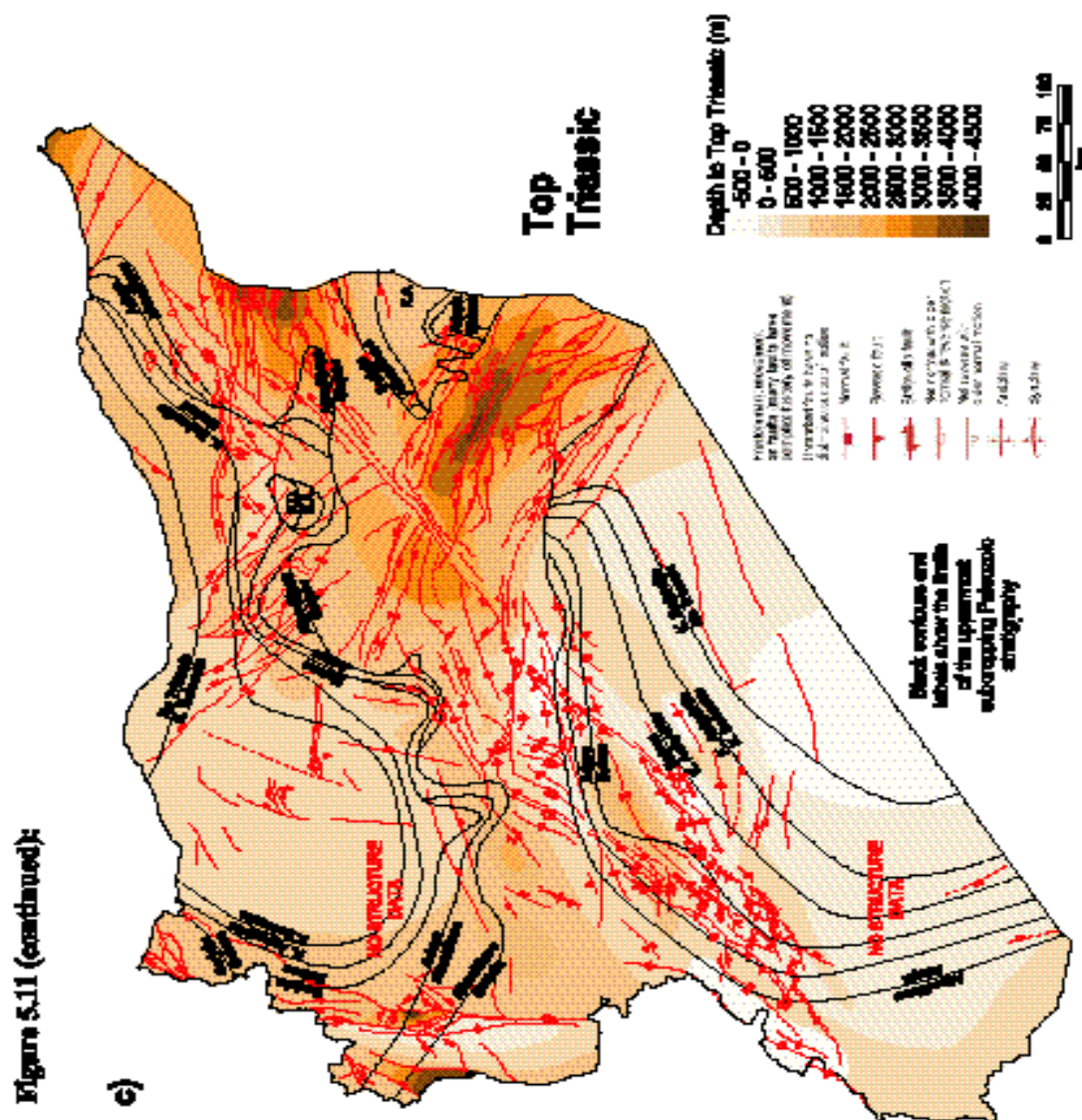
**Figure 5.12:** Perspective views of the four structural surfaces shown in Figure 5.11. (a) View from the southeast with ten times vertical exaggeration to illustrate some of the through-going structural relationships. (b) View from the north.

Topography

Top Cretaceous

Top Lower Cretaceous

Top Triassic

Top Paleozoic

Abd el Aziz Uplift

Bilas Block

Sinjar Trough

Euphrates Graben

Topography (km)

Top Cretaceous (km)

Top Lower Cretaceous (km)

Top Triassic (km)

Top Paleozoic (km)
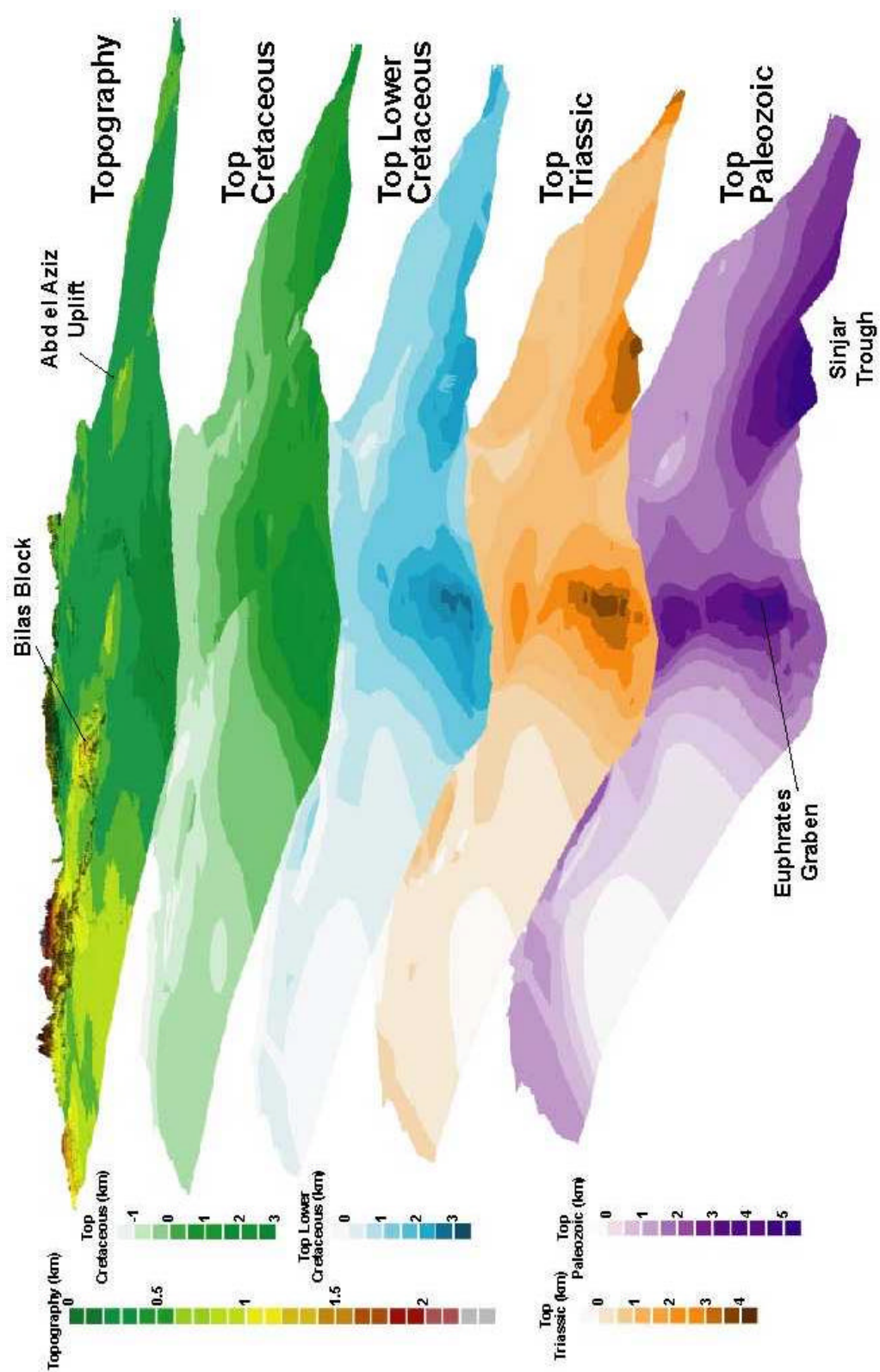
**Figure 5.12 (continued):**
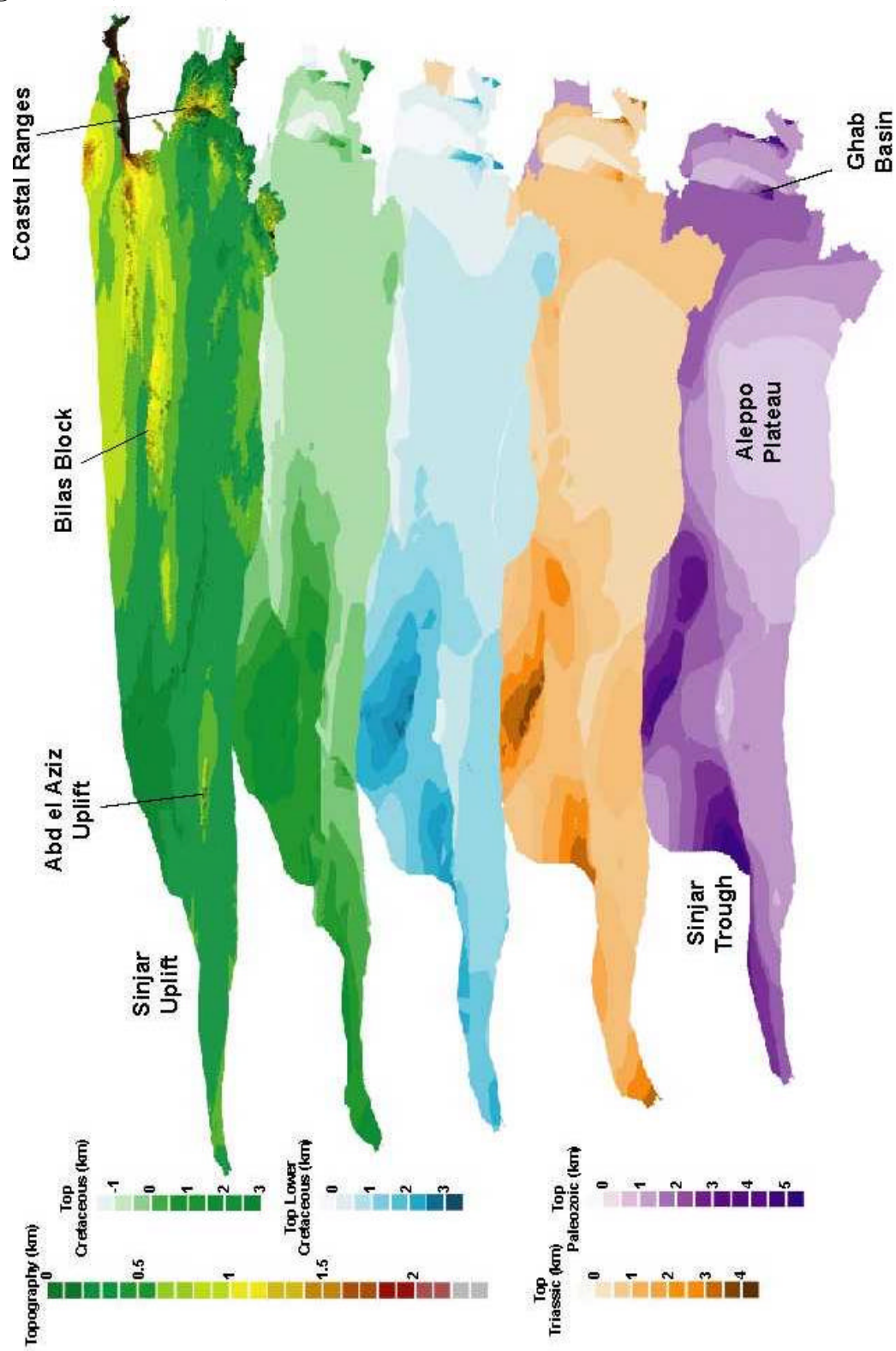
The non-uniform distribution in quality and quantity of geophysical data in Syria gives somewhat uneven coverage to any resulting map. Areas of highest data density are those of most hydrocarbon production. Hence, these structural maps are most accurate for the Euphrates Fault System, portions of the Palmyrides, and northeast Syria, and are least accurate for the Aleppo and Rutbah Highs. Furthermore, as data quality and density decreases with depth so does the accuracy of these maps. For example, 460 wells penetrate the top of Cretaceous horizon while only 190 reach as deep as the Paleozoic (Figure 5.2). The Lower Mesozoic and Paleozoic of the Palmyride region, where seismic data are generally not interpretable and deeper well penetrations few, has the least reliability of all the mapping for these strata.

The maps are presented at a small scale. In many cases, particularly in the east, the mapping was conducted at a much larger scale, typically 1:500,000. There are countless small structures beyond the mapping resolution, and in areas of very low data density some faults are undoubtedly not mapped even at the smaller scale. The chosen scale of presentation represents a compromise between these situations.

The maps are not structurally restored. They show present deformation rather than the structure and depths at the time of deposition of the target horizon. This is why, for example, the top Triassic horizon demonstrates reverse faulting in the southwest Palmyrides although at the time of deposition these were normal faults. The symbols on the faults are designed to show the approximate past history of fault movement. Also, present-day depths are shown, not those during deposition. For example, the top of Paleozoic in the Palmyrides is shown as predominantly uplifted (Figure 5.11d), whereas during deposition this area was a topographic trough. Full-scale restoration is a future planned project.

*Top Cretaceous*

The top of Cretaceous horizon (Figure 5.11a) indicates the effects of Syrian Cenozoic compressional tectonics. Note the strongly inverted Palmyride trough, especially the Bilas block, and Abd el Aziz / Sinjar Uplifts. The large sag above the Euphrates Graben is a result of the Paleogene thermal subsidence. Recent basin formation in western Syria is also illustrated. In general, faulting in eastern Syria halted before the end of the Cretaceous. Hence, unless there has been Cenozoic reactivation and fault-propagation of these features, the faulting is not observed at the top Cretaceous level. The well-developed Al-Daww basin in the central Palmyrides is present at all stratigraphic levels.

*Top Lower Cretaceous*

The Lower Cretaceous sandstone, a good seismic reflector, forms many hydrocarbon reservoirs in the Syria, hence this horizon (Figure 5.11b) is of particular economic interest. As shown by the subcrop distribution, this sandstone was deposited across most of Syria except on the Rubah / Rawda Uplift that was exposed and from which these sands were largely derived.

This map shows the full extent of the Euphrates Fault System and Abd el Aziz / Sinjar deformation. Note the distributed nature of normal faulting in the Euphrates Graben with no major rift bounding faults. In northeast Syria the superposition of the three prominent fault directions is illustrated. This map, and the ones on horizons beneath it (Figure 5.11c,d), show generally very similar structures. This is because much of the structure in Syria is on deeply penetrating, high angle faults. The net sense of offset of any particular horizon changes down section; this is observed on many of the faults mapped here. However, the location of the faults remain essentially fixed at this scale of presentation. Although some

faults only cut the lower portion of the sedimentary column, they are often either too small or too poorly imaged to be mapped.  The biggest difference between these maps is the depth to top of the chosen horizon.  Obviously, this is a function of the thickness of the strata above it.  As we have seen (Figure 5.10), this can change considerable throughout Syria.

### *Top Triassic*

The Triassic subcrop distribution shows the extensive Mulussa F (Uppermost Triassic, Serjelu formation) deposition that covered much of the country.  This formation marks the beginning of regional transgression that continued through the Early Jurassic.  Note that some of the formation was removed by Late Jurassic / Early Cretaceous erosion; the original deposition was even more extensive.  The underlying Mulussa group shows progressively limited extent up-section, showing the increasingly limited deposition as water depths decreased following rifting.

### *Top Paleozoic*

This map (Figure 5.11d) has the poorest accuracy of the four maps presented here due to severe decrease in the quality of seismic reflection data from Paleozoic depths, and lower density of well penetrations.  As with the overlying horizons, the greatest depths are found in the Sinjar trough and the Euphrates Graben, and in isolated basins of western Syria.  Note the broader downwarping at this level in the Sinjar area indicating the broad extent of the Triassic Sinjar trough.

The subcrop pattern is dominated by the Permian Amanous formation that was broadly deposited.  This map also shows the continuation of the Permian Palmyride trough into the Sinjar area. Note that in the inverted areas of the Palmyrides and Sinjar uplifts, reverse faults are still shown at this level based on well and seismic data showing uplift across these

structures. However, associated fold-propagation folds are greatly subdued or absent at this depth (Chaimov et al., 1993). Furthermore, in the southwest of the Palmyride fold and thrust belt, the top of Paleozoic is below the local Triassic age detachment, and therefore not significantly faulted or folded. However, in the Bilas and Bishri blocks, the thick-skinned deformation has affected all structural levels. Again, the quality of the mapping is relatively poor for these structures.

## Integrated Tectonic Map

The new tectonic map of Syria (Plate 1) shows general tectonic elements, outcrop distribution, shaded relief imagery, and seismicity. The faults and folds shown in black were mapped on the surface by Ponikarov (1966) and Dubertret (1955), or from our surface observations and limited remote sensing imagery interpretation. The subsurface structure, in red, is modified from the top Lower Cretaceous structure map (Figure 5.11b). This level was chosen to represent the subsurface as most faulting cuts this horizon, yet it is still relatively close to the surface. As shown in Figure 5.11, the sense of motion on these faults may change according to the structural level considered.

This map, although relatively complete for this scale of presentation (1:1,000,000) is undoubtedly incomplete for some areas. The sense of motion on many of the mapped structures is also ambiguous. In particular, we have mapped many of the reverse faults that core the anticlines of the southwest Palmyrides as being reactivated normal faults. Although this is true for many of the faults, some may be thrust faults detached in the Triassic, not reactivated normal faults. Strike-slip activity is also extremely difficult to map accurately. On this map it is only noted where it is known with some certainty. Assuredly, many more faults have strike-slip components that are not identified by this map. The map shows again

how most deformation in Syria is focused within the four major structural zones: the Palmyrides, the Abd el Aziz / Sinjar area (northeast Syria), the Euphrates Fault System, and the Dead Sea Fault System.

Earthquake locations are from the International Seismological Center (ISC) database (1964-1994), and locations from the local Syrian seismograph network (1995-1996). Some of the apparent clustering of locations is probably a consequence of the station distribution. For example, the apparent lack of events along the northern Dead Sea Fault system relative to the southern Dead Sea Fault system is a consequence of station distribution. Regardless, there is an obvious concentration of events along the Dead Sea Fault System, some events within the other Syrian tectonic zones, and very few events in the stable areas of Syria. The Harvard CMT focal mechanism (1977-1996), supplemented by work at Cornell, are only loosely constrained because of the relatively small size of the events involved.

**Deeper Crustal Structure**

Metamorphic basement in Syria is generally deep (> 6 km) and has not been penetrated by drilling. Furthermore, the basement does not form a good seismic reflector. Hence, we have mapped the basement using seismic refraction data (results shown in Figure 5.13, Seber et al., 1993; Brew et al., 1997). In addition, Moho depth beneath Syria has been estimated from receiver function analysis (E. Sandvol, personal communication, 2000). The limits of Moho depths shown on Figure 5.13 are calculated using a range of average crustal velocities (6.2 – 6.8 km/s).

The Bouguer gravity anomaly field for Syria (BEICIP, 1975) shows a clear difference between northern and southern Syria with the boundary roughly within the Palmyrides

(Figure 5.13). Using the inputs for basement and Moho depths, we developed new gravity models along two profiles across the Palmyrides (see Figure 5.13 for locations).

The first profile (Figure 5.14a) crosses the Aleppo Plateau, southwest Palmyrides, and the Rutbah Uplift. The dichotomous 'observed' gravity anomaly (green circles) on either side of the Palmyrides is clear. External controls on Moho and basement depths, some projected tens of kilometers along strike into the section, are shown as white annotations in Figure 5.14. Using these constraints, we modified the density model until the 'observed' and 'calculated' anomalies were acceptably close (difference less than ~3 mGal). In the first instance, we investigated crustal-scale effects without concern for the second-order anomalies in the Palmyride area. The result (black line) shows that a large difference in crustal thickness and crustal density on either side of the Palmyrides is required to satisfy the gravity data. This change in crustal properties can be modeled to occur along the present position of the Jhar fault. Furthermore, a small 'crustal root', of the order 2 – 3 km, is required beneath the southwestern Palmyrides to satisfy the receiver function Moho depth. This is significantly different from Best et al. (1990) who, lacking information to the contrary, modeled the gravity response of Syria using a flat Moho.

**Figure 5.13:** Map of Bouguer gravity field of Syria (BEICIP, 1975) shaded with topography imagery. Black numbers indicate depth to top of metamorphic basement determined from seismic refraction profile (black lines) interpretations. White numbers indicate approximate depth to Moho near seismograph stations (white triangles). Red lines are gravity profiles shown in Figure 5.14. All depths are in kilometers below sea level. Note the abrupt along strike variation in gravity anomalies in the Palmyrides coincident with topographic change. Note also the contrast between Bouguer anomalies north and south of the Palmyrides. See text for full discussion.

Seismic Refraction Profiles

**6.0** Depth to metamorphic basement from refraction interpretation

**>3.1** Minimum depths to basement from well data

Gravity Profiles (Figure 5.14)

Seismograph Stations

**28 - 31** Probable Moho depth range using reasonable crustal velocities (see text) using receiver function analysis from seismological data

0    km    100

Rmah intrusives trend

mGal

50
25
0
-25
-50
-75
-100

**Figure 5.14:** Gravity models through central Syria, see Figure 5.13 for profile locations. Densities in g/cm$^3$ are given parenthetically. Constraints on the model - other than through gravity modeling - are shown in white. (a) Profile across Aleppo Plateau, southwest Palmyrides, and Rutbah uplift. The modeled anomaly is shown both with and without two otherwise unconstrained intrusive bodies in the Palmyrides that can be used to map the second-order gravity anomalies. (b) Profile sub-parallel to profile (a), but across the Bilas block, a significant crustal root is not indicated by gravity modeling.
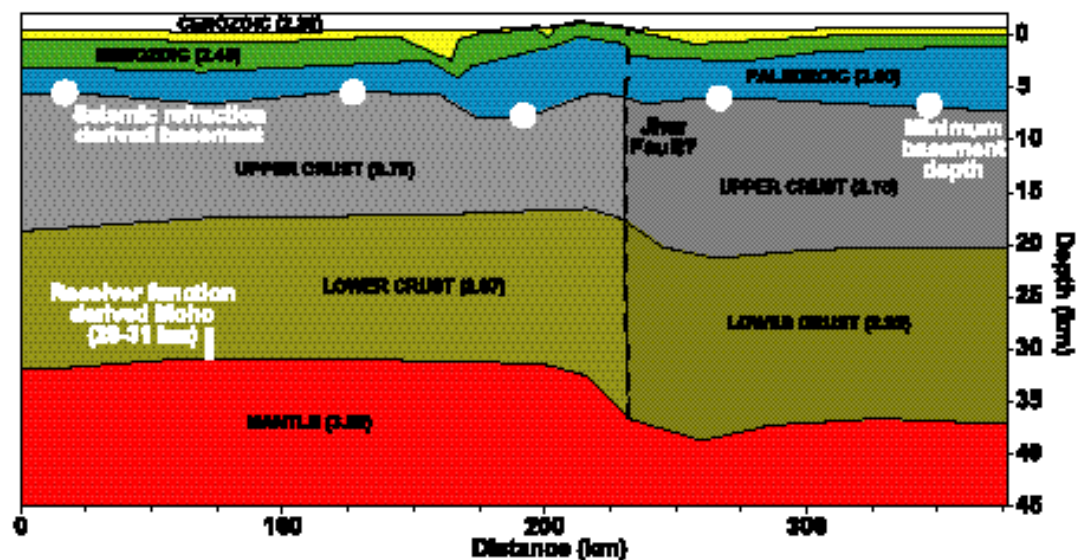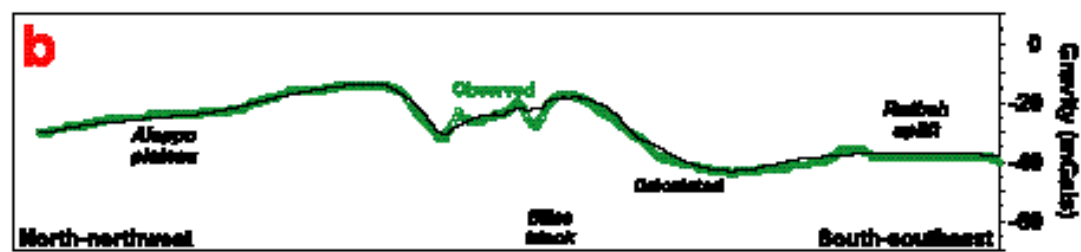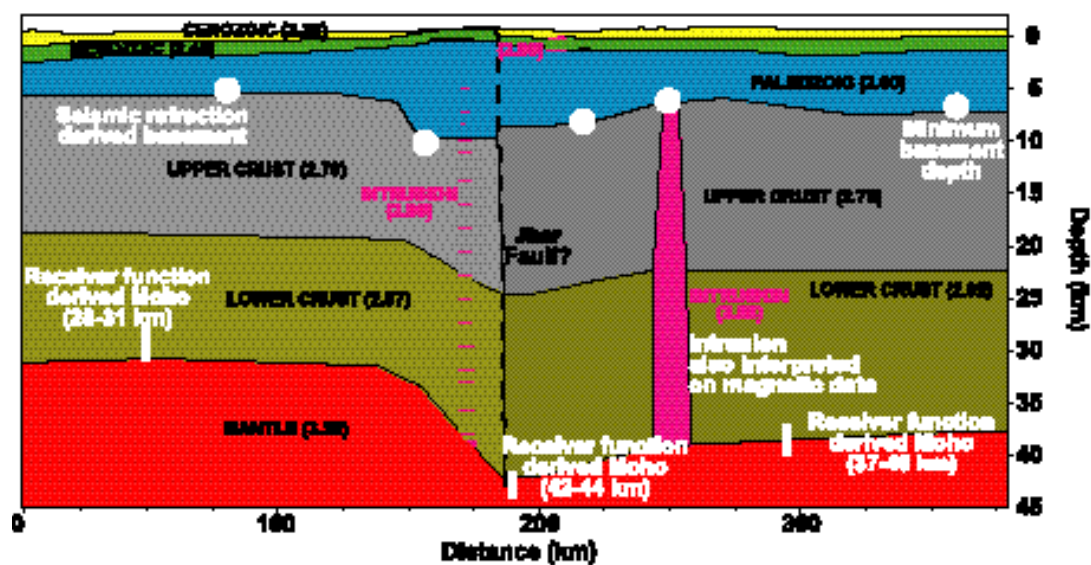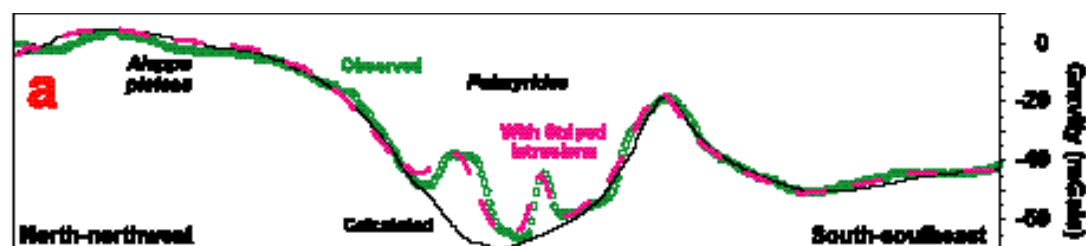
Modeling the second-order anomalies along this transect (dashed pink model and anomaly in Figure 5.14a) shows that arbitrary, high-density intrusions beneath the Palmyrides can be used to match the observed anomalies very closely. These could perhaps be an extension of the Rmah trend of intrusions that is clearly imaged by the gravity data (Figure 5.13), and described by Best et al. (1990). However, lacking additional information, this second-order modeling should be considered *ad hoc*.

The second gravity profile also crosses the Aleppo and Rutbah highs, but traverses the Bilas block area of the Palmyrides (Figure 5.14b). Large density and thickness differences on either side of an interface at or near the Jhar fault are again required. There is no requirement for a well-developed crustal root, but a small flexing of the southern block on the southern margin of the Palmyrides improves the fit of the model.

When these results are taken in a regional context, they support the hypothesis that Syria, like the rest of the Arabian Plate formed through a Proterozoic amalgamation of microplates and island arcs, i.e., the Pan African system (Stoesser and Camp, 1985). This left a series of suture / shear zones underlying the continent that have acted as zones of weakness throughout the Phanerozoic. The difference in basement depth, and crustal thickness and density on either side of the Palmyrides could be indicating that northern and southern Syria are different crustal blocks, sutured along the Palmyride trend. Furthermore, the Jhar fault, one of the major structural features of the Palmyride area, could be marking the position of the suture (as first suggested by Best et al., 1990). Assuming this scenario, crust of 'Rutbah / Rawda Uplift' affinity would underlay the predominantly thin-skinned deformation of the southwest Palmyrides, while 'Aleppo Plateau' crust underlies the Bilas and Bishri blocks that exhibit predominantly thick-skinned tectonics. This might be demonstrating that the

Proterozoic architecture of the Arabian Plate is controlling the style, as well as the location, of Phanerozoic deformation.

Walley (1998) went further to argue that the suture zone could be traced westwards through Lebanon. He correlated the deformation style of the north and south Lebanese Mountains with the northeast and southwest Palmyrides. However, Walley (1998) maps many tens of kilometers of north – south separation between the present locations of his 'Lebanese' and 'Syrian' sutures. Thus his model appears to require much more than the currently accepted ~25 km of translation on the northern Dead Sea Fault System

The presence of a crustal root appears to follow the leading edge of the southern block. The root observed in Figure 5.14a and the flexure observed in Figure 5.14b can both be considered as bending at the leading edge of the southern block. This could be a loading effect created by the Palmyrides themselves preferentially affecting the Rutbah block, suggesting it may be the 'weaker' block. Alternatively, this could be explained by the proximity of profile 'a' to the Anti-Lebanon, a very significant load much larger than the Palmyrides. This is could be causing a crustal root beneath the southwestern Palmyrides, whereas in the northeast the loading is supported by the strength of the lithosphere.

## REGIONAL TECTONIC EVOLUTION

Our regional tectonic evolutionary model (Plate 2) shows two different views of regional tectonics at twelve time-points throughout the Phanerozoic. On the left (parts 'a') are paleo-plate reconstructions around Arabia; on the right (parts 'b'), are shown schematic tectonic activity and the sedimentary environment within Syria at each time-point. Timelines of

regional and local tectonic events are shown in the middle of Plate 2. The time-points on Plate 2 are also indicated on the stratigraphic record (Figure 5.8).

There are many paleo-plate reconstructions for the Tethys Ocean and the eastern Mediterranean evolution (e.g. Robertson and Dixon, 1984; Dercourt et al., 1986; Ricou, 1995; Stampfli et al., 2000). Shown here (Plate 2, parts 'a') are reconstructions mostly adapted from Stampfli et al. (2000) developed with other members of IGCP 369. They are shown necessarily approximate and generalized for this presentation. These reconstructions are still the focus of some debate, especially concerning the position of many microplates, and the exact timing of oceanization of the eastern Mediterranean. We show them as an aid to discussion, rather than an endorsement of validity. Nevertheless, the model of Stampfli et al. (2000) is broadly in agreement with our findings.

Some of the regional tectonic events depicted by timelines in Plate 2 are only approximately dated. The dashed bars illustrate some of this uncertainty and the approximate build-up and decay of the tectonism. Such details need not overly concern us since we are interested in the general scheme of plate divergence and collision; the reader is referred to the original sources for detailed discussions.

Note that in the discussions below we refer to present-day polarities. For example, what we refer to as an Early Paleozoic east-facing passive margin, was predominantly north-facing at that time (Plate 2, frame 1a), but was subsequently rotated approximately ninety degrees. All the frames in Plate 2 are oriented with north roughly toward the top of the page.

**Proterozoic (>570 Ma) – End Cambrian (510 Ma)**

It has long been accepted that the southern Arabian Plate formed through Late Precambrian accretion of island arcs and microplates against northeast Africa, most probably between ~950 Ma and ~640 Ma (Beydoun, 1991) as part of the Pan African orogenic system. Suture zones relic from this accretion, and the Nadj faults that formed when these sutures reactivated, are well-exposed in the Arabian shield (Stoesser and Camp, 1985). Based on geophysical evidence (see discussion above and Best et al., 1990; Seber et al., 1993; Brew et al., 1997) we suggest that the northern Arabian Plate is a result of a similar concatenation. Specifically, we find that the current Palmyride fold and thrust belt may lie approximately above the location of a Proterozoic suture / shear zone. Reactivation of this crustal weakness appears to have profoundly affected the tectonics of Syria throughout the Phanerozoic with the formation of the Palmyride / Sinjar trough, and later the Palmyride fold and thrust belt.

From ~620 Ma to ~550 Ma continental failure and intracontinental extension followed the accretion. This included strike-slip movement on the Nadj fault system, and the deposition of thick Infracambrian and Early Cambrian syn-rift deposits (Husseini, 1989). Owing to their great depth, no direct dating of the oldest sediments in Syria is available. However, from refraction interpretation we infer Infra - Lower Cambrian strata between 1 and 2.5 km thickness across Syria (Seber et al., 1993; Brew et al., 1997). Significant thickness of Infracambrian age sandstone and conglomerates are also observed in southeast Turkey (the Derik and Camlipinar formations), and in Jordan (the Saramuj formation). Husseini (1989) suggested that these syn- and post-rift strata resulted from the 'Jordan Valley Rift' that formed between Sinai and Turkey during the Infracambrian.

The penetrated Cambrian section in Syria is composed of arkose sandstone with some siltstone and shale probably eroded from granitic basement in the south (Plate 2, frame 1a). The exception to the clastic Cambrian section is the Early - Middle Cambrian Burj limestone formation that is observed across all of Syria (Figure 5.8); contemporaneous carbonates are found in most parts of Arabia (Beydoun, 1991). The regional extent of this monotonous formation (both sides of the 'Palmyrides suture') is more evidence for the cessation of cratonization and regional intra-continental extension of northern Arabia before the Middle Cambrian (~525 Ma) as discussed above (Best et al., 1993).

An erosional unconformity at the top of the Cambrian sequence (Figure 5.8), is just one of many unconformities that punctuate the Paleozoic section. This was a time of relatively shallow water over much of Arabia, relatively minor eustatic variations easily caused hiati and erosion.

## Ordovician (510 Ma) – Early Silurian (424 Ma)

Ordovician strata are extensive across all Arabia, especially along the northern and eastern margins, deposited on the wide epicontinental shelf. The Syrian Ordovician section increases from 1.6 km beneath the Aleppo Plateau, to more than 3.5 km in the southeast beneath the Rutbah / Rawda Uplift (Figure 5.10). Wells in the west of Syria penetrate an almost wholly sandy Ordovician section, whereas those in the southeast encounter significant components of siltstone and shale (Figure 5.8 and Plate 2, frame 1b). These facies and thickness trends in Syrian Ordovician strata are indicative of the open marine conditions to the east. The source areas for the Ordovician, and other Paleozoic clastics, were the extensive Arabian and Indian shield areas exposed to the south (Plate 2, frame 1a), and an ever-increasing proportion of reworked sediments.

The top Ordovician unconformity is most probably related to falling sea levels during Late Ordovician Arabian glaciation following a drift to higher latitudes. Although not definitively identified in Syria, extensive glacial deposits are found farther south (Husseini, 1990). The far eastern areas of Syria, the Rawda High and western Iraq (Plate 2, frame 2b), were exposed during this Late Ordovician to Early Silurian regression. The Upper Ordovician Affendi formation is missing in the farthest southeast of Syria, and thinned dramatically above the Rawda High. Beydoun (1991) showed this exposed / structurally high area extending from Turkey to Saudi Arabia during the Late Ordovician and Early Silurian, and likely has some tectonic component of uplift.

Deglaciation in the Early Silurian, as Gondwana drifted towards the tropics, caused sea levels to rise sharply flooding much of Arabia and depositing what is now an extremely important regional hydrocarbon source rock (Husseini, 1991). In Syria, these Lower Silurian grapholitic shales (the Tanf formation, Figure 5.8), although now thickest beneath the Palmyride / Sinjar trough (Best et al., 1993), were probably deposited to ~500 to ~1000 m thickness across the entire region during this transgression (Plate 2, frame 2b).

**Late Silurian (425 Ma) – Devonian (363 Ma)**

The Syrian Lower Silurian section is directly overlain by Carboniferous clastics, marking an unconformity of major temporal and spatial extent. This hiatus, strong tectonism and volcanism are observed contemporaneously in many localities around northern Gondwana. Some authors cite two events, loosely referred to as 'Caledonian' and 'Hercynian', the first is of Late Silurian age and the other is of Middle to Late Devonian / Early Carboniferous age, (Husseini, 1992). The absence of preserved strata in Syria prevents such a distinction

there. Suggestions of the cause of this tectonism include a regional compressive phase caused by the obduction of the ProtoTethys on what is now Iran (Husseini, 1992); uplift on the flanks of the PaleoTethys rifting (Stampfli et al., 2000); or a more localized thermal uplifting event (Kohn et al., 1992) (Plate 2, frame 2a).

In any event, Upper Silurian and Devonian strata are almost universally absent from Arabia and underlying Lower Silurian shales are substantially eroded. The current subcrop pattern of Silurian strata in Syria shows an elongate depocenter roughly along the trend of the current Palmyrides (Best et al., 1993), and thinned to absent Silurian to the north and south. This could be interpreted as evidence for an Early Silurian age initiation of the major Palmyride / Sinjar trough. However, based on slight angular unconformity observed at the top of Silurian (Best et al., 1993), we suggest that this subcrop pattern is a result of Late Silurian and Devonian preferential erosion on the Rutbah / Rawda and Aleppo structural highs southeast and northwest of the Palmyrides, respectively.

During both the Late Ordovician and Late Silurian / Devonian manifestations of the Rutbah and Rawda Uplifts the most prominent exposure appears to the east of the current structural and topographic high (compare Figure 5.2 with Plate 2, frame 2b), around the current location of the Euphrates Graben. Previous publications (e.g. Litak et al., 1997) have examined the possibility that the Euphrates Fault System may have formed above a Proterozoic suture / shear zone similar to that advocated beneath the Palmyrides. However, given little evidence of subsidence or faulting along the Euphrates trend before Late Cretaceous time, this is now discounted. The Rutbah and Rawda highs (Figure 5.2) were evidently connected through most of geologic time until Late Cretaceous dissection by the Euphrates Fault System. Other than a few episodes of minor subsidence, after emergence in the Devonian the basement-cored 'Rutbah / Rawda Uplift' remained structurally high for the

rest of the Phanerozoic, strongly affecting Syrian tectono-stratigraphy. The difference in basement depth across the Euphrates Fault System (Brew et al., 1997) (Figure 5.13) could be explained by a continuation of the 'Palmyrides suture' to the east, combined with the deep-seated Euphrates faulting.

A very few wells in central and eastern Syria encounter what are thought to be latest Devonian age rocks (Ravn et al., 1994). No major hiatus between the Devonian and Carboniferous is observed (Ravn et al., 1994), and a possible Upper Devonian section is also found in western Iraq (Aqrawi, 1998). This could suggest that incipient subsidence along the Palmyride / Sinjar trough had begun in eastern Syria by latest Devonian time. However, several deep wells in the Palmyrides encounter Lower Silurian strata directly below the Carboniferous, indicating that the Palmyride / Sinjar trough was not undergoing large-scale subsidence before the Carboniferous.

## Carboniferous (363 Ma - 290 Ma)

In Carboniferous time the Palmyride / Sinjar depositional trough formed fully across central Syria, in strong contrast to the relatively uniform and parallel-bedded Early Paleozoic deposition. In various forms, this trough was the main depocenter in Syria from Carboniferous to Late Cretaceous time, continuously flanked to the northwest by the Aleppo Plateau and to the southeast by the Rutbah / Rawda Uplift. On many seismic lines the Carboniferous can be seen onlapping the Silurian (Brew et al., 1999) and over 1700 meters of Carboniferous sand, sandy shale, and some minor carbonates, were deposited in the Palmyride / Sinjar trough (Plate 2, frame 3b). We interpret this Carboniferous trough to be a broad crustal downwarping between anticlinoria identified to the north and south of Syria (Plate 2, frame 3b) (Gvirtzman and Weissbrod, 1984). This Devonian / Early Carboniferous

age folding could also be responsible for the major Devonian hiatus observed in Arabia, as discussed above (Husseini, 1992). The cause of this folding could be the same as the Devonian / Carboniferous uplift, namely regional 'Hercynian' compression.

Alternatively, Stampfli et al. (2000) suggests that the Early Carboniferous was a time of continental rifting along the north African margin (and consequently in the Palmyride trough), possibly a precursor to the NeoTethys Ocean formation. The cause could be regional stress reorganization after the collision of the Hun superterrane and Laurussia (Plate 2, frame 3a). However, many previous models (e.g. Robertson and Dixon, 1984) envisage no such Carboniferous rifting along northern Gondwana. Hence, while poor seismic data beneath the Palmyrides prevent definitive detection of possible Paleozoic faults, we favor Carboniferous folding rather than initial rifting.

Interestingly, the Carboniferous (and Permian) trough are found along a trend parallel to, but a few tens of kilometers south of, the Mesozoic depocenter and present Palmyrides. This suggests that the locus of deposition shifted during the formation of the Palmyride trough, probably in response to differential uplift and subsidence of the bounding Aleppo Plateau and Rutbah / Rawda Uplift. Furthermore, the limit of the Paleozoic and Mesozoic Palmyride trough is fairly sharply defined to the northwest, while the trough shows a more gradual flank to the southeast showing a greater interaction of the Rutbah / Rawda Uplift with the Palmyride deformation (McBride et al., 1990).

Husseini (1992) identifies the Mid-Late Carboniferous and Early Permian as a time of regional glaciation in southern Arabia. Although glacial deposits have not been definitively observed in Syria, the thick siliciclastic Carboniferous strata are typical of northern

Gondwana deposition of the time. The glaciation also contributed to the wide-spread Late Carboniferous / Early Permian hiatus observed throughout Syria (Figure 5.8).

**Permian (290 Ma - 245 Ma)**

Opening of the NeoTethys Ocean in the Permo-Triassic (Plate 2, frames 3a and 4a) instigated profound changes in regional tectonics that persisted until the final consumption of the NeoTethys in the Miocene. On the northern and eastern margin of Gondwana, oceanic spreading separated the Cimmerian superterrane (including present-day Iran) that proceeded to drift northeastwards (Stampfli et al., 2000). Along the northern African margin Permian and Early Mesozoic rifting is documented by Stampfli et al. (2000) as being the second phase of the extension that began in the Early Carboniferous. Other authors cite this event as the initiation of faulting (Robertson and Dixon, 1984).

Debate still surrounds the precise timing of tectonics in the eastern Mediterranean region. While consensus has generally been reached concerning the oceanic nature of the eastern Mediterranean crust (see Robertson et al., 1996), the exact initiation of spreading remains uncertain. Robertson et al. (1996) examined various NeoTethys models. They concluded the most promising reconstruction is similar to that of Robertson and Dixon (1984), who advocated Permo-Triassic rifting, under conditions of northward PaleoTethys subduction, leading to Triassic sea-floor spreading in the eastern Mediterranean.

The reconstructions that we show (Stampfli et al., 2000) are mostly similar to the model of Robertson and Dixon (1984). One of the main differences is the presence in the Stampfli model of oceanic, rather than continental, crust along north Gondwana at the end of the Permian. In any event, this set of models differs markedly from those advocating Early

Cretaceous oceanization of the eastern Mediterranean (e.g. Dercourt et al., 1986). The models of Robertson and Dixon (1984), Stampfli et al. (2000) and others see the Early Cretaceous as a time of renewed activity in the eastern Mediterranean, rather than sea-floor spreading initiation.

Hence, we interpret the Late Permian development of the Palmyride trough to be a consequence of extension along the north African margin that lead to east Mediterranean sea-floor spreading. In this scenario, the Palmyride rift could be an aulacogen (e.g. Ponikarov, 1966; Best et al., 1993), and we note that in most respects the Palmyride rift fits the definition of an aulacogen as used by Sengor (1995). The plate reconstructions of Stampfli et al. (2000) favor this interpretation (Plate 2, frame 4a).

An enticing variation to this is the reconstruction of Walley (2000). He argues for two different Permo-Triassic extensional phases, one in the Late Permian – Early Triassic that opened the Palmyride rift, and another in the Mid-Late Triassic that led to the opening of the eastern Mediterranean in a slightly different direction. Thus, this model allows for Late Permian rifting of the Palmyrides while not requiring Permian sea-floor spreading of the eastern Mediterranean. Furthermore, in this scenario the Palmyride / Sinjar trough is not required to be an aulacogen. Additional work concerning the exact timing of faulting will help test this model further.

Syn-rift Permo-Triassic siliciclastic deposits are only preserved in the Palmyride / Sinjar trough where they reach more than 1000 m thickness. Our hypothesis of the Palmyride / Sinjar trough as a Late Permian aulacogen suggests that faulting may be responsible for most of the thickening in the trough. Rapid thickness changes observed in well data show that rift-bounding faults controlled at least some of the Permian deposition in the Palmyride trough,

and deeply penetrating faults were imaged by Chaimov et al. (1992). Furthermore, stratigraphic relationships indicate that the Aleppo Plateau and Rutbah Uplift were emerged throughout the Permian, possibly uplifted flanks of the rift (Stampfli et al., 2000). Cohen et al. (1990) find Permian age normal faults in southwest Israel sub-parallel to the Palmyrides trend and increasing sediment thickness westward, consistent with the hypothesis of an aulacogen extending from the central Syria to the eastern Mediterranean. Beydoun (1981), based on limited data, also speculated on the occurrence of a Late Paleozoic / Mesozoic aulacogen extending through Lebanese territory. Unfortunately, poor seismic data limit our ability to better image structure at depth and hence obtain a complete picture of the style of deformation. We conclude that rifting – as opposed to downwarping and subsidence – controlled a significant proportion, if not the majority, of Permo-Triassic deposition.

The exception to the pattern of NE-SW rifting in Syria is the Derro high of central Syria (Figure 5.2). This area was a structural high in the Early Triassic and possibly the Carboniferous, and represents the 'Beida Arch' of Kent and Hickman (1997) that connects the adjacent Rawda and Mardin highs (Figure 5.2). The work of Brew et al. (1997) suggests that the Derro high is a basement uplift, partially bounded by faults.

**Triassic (245 Ma - 208 Ma)**

Syn-rift deposition in the Palmyride trough appears to have continued into Early Triassic time. The 'Amanous Shale' formation (actually part of the Doubayat group according to Beydoun (1995), or the Mulussa group member A of most petroleum explorationists, Figure 5.8), is the uppermost syn-rift sequence consisting of sandstone and shale, with increasing dolomite and dolomitic limestone upwards in central Syria. The continuity from Amanous Sandstone (Permian) to Amanous Shale (Lower Triassic) sedimentation results in the lack of

distinction between these two formations in many central Syrian wells, a common problem in northern Arabia (Gvirtzman and Weissbrod, 1984). See Al-Maleh et al. (2001) for a complete discussion of Syrian Mesozoic strata and depositional environments.

By the end of the Early Triassic, rifting in the Palmyrides had ceased, whereas spreading in the Eastern Mediterranean was still active. This is demonstrated by the 'Amanous Shale' formation that thickens westwards in Syria reaching more than 250 meters near the Levantine margin. Furthermore, stratigraphic thickening in Israel suggests that rifting may have been longer-lived there than in the Palmyrides (Flexer et al., 2000). The cessation of Palmyride rifting could be a consequence of the eastern Mediterranean spreading ridge moving away along a Levantine transform fault (Stampfli et al., 2000). With the removal of the spreading, rifting in the Palmyrides stopped. Alternatively, the hypothesis of Walley (2000) considers the extension in the Palmyrides and eastern Mediterranean as being two separate events that can be explained by a change in regional stress direction.

Timing of Palmyride rifting cessation is indicated by an extensive Early Triassic unconformity found in most parts of Syria (Figure 5.8) – most likely a post-rift unconformity, compounded by extremely low sea-levels (Haq et al., 1988). The only conformable Permian through Middle Triassic sequence is in central Syria were shaly dolomites of the 'Amanous Shale' formation (Mulussa A) grade into the overlaying Kurrachine Dolomite (Mulussa B). This area, with the deepest depocenter, remained submerged as all other areas were exposed and eroded.

While the syn-rift Permian and earliest Triassic clastics are confined to the Palmyride / Sinjar trough, the first post-rift formation, the Middle Triassic Kurrachine Dolomite (Mulussa B) is spatially extensive, covering most of Syria (Figure 5.11c). This formation shows facies

variations between dolomite and limestone, with greater carbonate content in paleogeographically deeper waters. Thus, Middle Triassic formations overlay Permian, Carboniferous, and sometimes even Silurian strata (Figure 5.11d). This extensive Early / Middle Triassic strata across almost all Syria indicates that the Paleozoic stratigraphic arrangements we observe today are not a consequence of Late Mesozoic or Cenozoic erosion. These post-rift strata are predominantly restricted-water carbonates and evaporites, as opposed to the overwhelmingly clastic syn-rift fill (Figure 5.8). This is a consequence of a drift to lower latitudes (Plate 2, frame 5a), lack of sediment source areas after plate reorganization, and shallower, more restricted waters of the post-rift environment. The evaporitic content generally increases up-section in the Triassic, indicating progressive shallowing.

The extents of the various Triassic formations are progressively more limited to the internal Palmyride / Sinjar trough through time (Figures 5.8 and 5.11c). However, some transgression of younger formations beyond the limits of older formations (especially on the Aleppo Plateau, Figure 5.11c) suggests the influence of minor sea-level variations on a relatively flat platform (Sawaf et al., 2000). This pattern is partially influenced by extensive Late Jurassic and Early Cretaceous non-deposition and erosion on the Aleppo and Rutbah / Rawda highs that removed much of the Lower Mesozoic section from those areas. Furthermore, this erosion led to anomalously thick preserved Triassic formations in the Palmrides that were previously interpreted as evidence of Palmyride Triassic rifting (McBride et al., 1990).

The exception to progressively restricted Triassic formations is in southeast Syria where Triassic onlap developed along what is now roughly the axis of the Euphrates Fault System. The members of the Mulussa group progressively onlap the Rutbah / Rawda Uplift to the

southeast, with a full Triassic sequence present near the Bishri block, but only the Mulussa F found in the southeast (Guyot and Zeinab, 2000). The Triassic onlaps Carboniferous and, in the extreme southeast, Silurian strata (Figure 5.11d) on the persistent Rutbah / Rawda high.

Subsidence curves from within the Palmyride trough shows a decreasing subsidence rate typical of post-rift subsidence (Sawaf et al., 2000; Stampfli et al., 2000) and indicate that this thermal relaxation probably continued until Early Cretaceous time. Well and seismic data show no widespread Triassic faulting around the Palmyrides, although some faults are locally observed (Best, 1991). Broad subsidence was the dominant control of the Triassic depocenter.

Triassic sedimentation halted before the deposition of the youngest Triassic Mulussa F formation (Serjelu). This interruption is marked by emergence and erosion, especially of the Aleppo and Rutbah / Rawda highs (Figure 5.8 and 11c). The subsequent Mulussa F deposition shows a distinct facies change, being largely clay and siltstone, as opposed to the underlying carbonates and evaporites. These clastics were sourced from the Rutbah Uplift in the south and southwest that remained exposed during the Late Triassic, with increasing calcareous content northward. The Mulussa F formation marks the beginning of regional transgression that continued through the Early Jurassic as described by Mouty (2000).

From a regional perspective Syria changed during the Permo-Triassic from being an east-facing to a westward-facing passive margin (Best et al., 1993). This occurred as the Levantine passive margin formed in western Syria to a backdrop of the continued formation of the eastern Mediterranean. This margin development, linked to the continued post-rift subsidence in the Palmyrides, is shown by preservation of more than 1.6 km of Triassic-Jurassic sedimentation along the present coastline. Triassic strata in Lebanon are very similar

to those in Syria. In fact, a Triassic evaporite layer is found off-shore Lebanon coring compressional features (Beydoun and Habib, 1995) in a very similar way to the salt in Syria (Chaimov et al., 1990; Searle, 1994). In northeast Syria thickening of the Triassic eastwards indicates that the Sinjar region was linked to another major basin that was developing along the northern passive margin of Gondwana (Lovelock, 1984), as well as being influenced by subsidence along the Palmyride / Sinjar trough (Brew et al., 1999).

### *The Rutbah Uplift verses the Hamad Uplift*

There is some overlap and confusion in the literature concerning the nomenclature of the Rutbah Uplift compared to the 'Hamad Uplift'. The term Hamad Uplift was first introduced by Mouty and Al-Maleh (1983). They used it to describe the northeast – southwest trending topographic high they documented in the paleogeographic environment of the Mesozoic Palmyrides. This usage distinguished the Hamad from the 'Rutbah Uplift' that is often used to describe uplift in western Iraq. Later authors largely failed to follow the nomenclature of Mouty and Al-Maleh (1983). Some oil company workers (e.g. de Ruiter et al., 1994) referred to the 'South Syrian Platform', thus distinguishing this from the Rutbah Uplift, but it is unclear if the Hamad and the South Syrian Platform are anything more than superficially synonymous.

The past work of the Cornell Syria Project has defined the Rutbah Uplift as a large, basement cored uplift dating since at least the Paleozoic. It covers western Iraq, parts of Jordan, and southern Syria (Figure 5.2). In this paper we acknowledge that the Hamad Uplift is a second-order feature on the north edge of the Rutbah Uplift that influenced Mesozoic paleogeography of the Palmyrides. However, we will maintain consistency with past work by not using the name 'Hamad Uplift', but rather using 'Rutbah Uplift' to include all elevated areas in southern Syria.

**Jurassic (208 - 145 Ma)**

The transgression begun in the latest Triassic continued through the Early Jurassic. Characterized by limestone, dolomite, and occasional marl (Mouty, 2000), it progressively replaced the Triassic lagoonal evaporitic deposition with characteristically deeper water facies (Figure 5.8). The transgression covered all Syria except the Rutbah / Rawda (including the present Euphrates Graben area) and Aleppo / Mardin highs that remained emerged throughout the Jurassic (Mouty and Al-Maleh, 1983; Mouty, 2000). During the Jurassic, the Palmyride / Sinjar trough extended through southwest Syria (up to 2100 m of Jurassic section) and Lebanon (up to 2250 m) toward the still developing eastern Mediterranean (Walley, 2000).

Liassic tholeiitic basalts found in the Anti-Lebanon (Mouty, 1998, 2000) and Israel (Wilson et al., 1998), illustrate the continued rifting activity along the eastern Mediterranean margin. As a possible consequence, the Liassic was a time of renewed regional faulting activity in the northern Arabian platform (Wilson et al., 1998). Seismic profiles and wells throughout the Palmyrides, especially around the Bishri and Bilas blocks (Figure 5.4), demonstrate Jurassic age faults (Best, 1991; Chaimov et al., 1992; Chaimov et al., 1993; Litak et al., 1997), possibly a reactivation of Permian rift-bounding faults. Paleozoic faults reactivated in the Jurassic have been identified in Israel (Flexer et al., 2000).

Minor Lower Jurassic thickness changes (few tens of meters) within southwestern Palmyride anticlines (Mouty, 1997) are only a hint of the larger architecture of the time. Stratigraphic relationships preclude these thickness changes being due to later erosion. Two Jurassic depocenters are evident along strike in the Palmyrides, one centered around the current Bilas

block, and one around the Bishri block (Sawaf et al., 2000).  Widespread Jurassic faulting clearly focused deposition in these areas, with less significant accumulation in the southwest Palmyrides and Sinjar area.  This further indicates that the Jhar and Bishri faults are old structural features.

Regression, beginning at the base of Bathonian (Plate 2, frame 6b), is evidenced by thinning of the Middle Jurassic formations eastward, the full sequence of Middle Jurassic formations showing this is not an erosional artifact (Mouty, 2000).  However, a more pronounced regression, that was accompanied by widespread erosion, is recorded beginning in Kimmeridgian strata, and most of Syria was uplifted by the end of the Kimmeridgian (Mouty, 2000).  Consequently, Jurassic strata are only preserved in the deepest areas of the Palmyride / Sinjar trough.  The Upper Jurassic and Lower Cretaceous was a time of major sedimentary hiatus.  Tithonian through Barremian strata are almost entirely absent from Syria (Figure 5.8), and much of the rest of northern Arabia (see summary in Guiraud, 1998), in concert with globally low sea levels.  Heavily karstified surfaces further attest to long-lived exposure of the Jurassic limestone, except in the eastern Mediterranean basin where subsidence continued.  Oxfordian – Kimmeridgian alkaline volcanics, with continuing volcanism through to Aptian time, were identified in the Anti-Lebanon, the Syrian Coastal Ranges, the Palmyrides, and other parts of the eastern Mediterranean (Mouty et al., 1992).  Laws and Wilson (1997) combined observations of volcanism, regional titling and uplift to suggest mantle plume activity centered around Syria in the Late Jurassic and Early Cretaceous (also see Wilson et al., 1998).  Garfunkel (1992) goes on to suggest that the Darfur volcanism in North Africa is the present expression of this still-existent hot spot.

**Early Cretaceous (145 Ma) – Coniacian (84 Ma)**

The Late Jurassic non-depositional hiatus and erosion continued well into the Cretaceous. This extensive unconformity together with widespread Early Cretaceous volcanics (as far afield as the Euphrates and Sinjar areas) has led to suggestions of continued mantle plume activity (Laws and Wilson, 1997; Wilson et al., 1998). The somewhat accelerated deposition and fault reactivation found in the Sinjar area (Brew et al., 1999) and the Palmyrides (Chaimov et al., 1992) at this time could also be a result of this regional volcanic event. In a possibly connected event, accelerated spreading in the eastern Mediterranean may have also contributed to the pronounced Late Jurassic / Early Cretaceous faulting (Robertson and Dixon, 1984).

The regional Early Cretaceous transgression that followed uplift covered most areas of the northern Arabian platform with hundreds of meters of fluvial-deltaic to shallow marine sands (maximum >550 m in Bishri block). This Cenomanian and Early Cretaceous Rutbah sandstone in eastern Syria has largely equivalent Aptian and pre-Aptian members in the Palmyrides (Palmyra sandstone, Mouty and Al-Maleh, 1983), Lebanon (Gres de Base, Dubertret, 1955; Tixier, 1972) and Aafrin Basin (Al-Maleh, 1976). The only region of Syria not covered by the Rutbah sandstone or equivalent was the Rutbah / Rawda Uplift (Figure 5.11b and Plate 2, frame 7b). These areas were still elevated, as they had been for most of the Phanerozoic, and eroding Carboniferous and Permian sandstone as the source for the sandstone (Figure 5.11c,d) (Guyot and Zeinab, 2000).

Several interesting facies variations within the Lower Cretaceous sandstones reveal ambient paleogeographic conditions. Palmyra sandstone mapped in the Coastal Ranges is generally much more marly than in the Palmyrides, indicating deeper water to the west. The Gres de

Base sand shows significant thickening toward Lebanon, with observations of limited chalk showing occasional shallowing (Tixier, 1972).  This fits within a scenario of a continually subsiding eastern Mediterranean passive margin.  The Rutbah and Palmyra sandstones become progressively more shaly and carbonaceous to the north, reflecting increasing distance from sediment source (the Rutbah Uplift).

In central and western Syria slow subsidence continued after the sandstone deposition.  In general this broad Albian – End Cenomanian carbonate platform deposition (sometime referred to as the 'Middle Cretaceous', Mouty and Al-Maleh, 1983) is distinctly different from the underlying sandstones and overlying Senonian transgressive strata.  The Zbeideh and Abou Zounar formations (Figure 5.8) mark two cycles of a shallowing depositional environment superposed on a general trend of decreasing water depth, suggesting a decreasing rate of subsidence.  As with the majority of the Cretaceous and Jurassic strata, these formations show clear trends indicating deeper water depth, less restricted circulation, and a smaller proportion of clastics in the west and southwest.  For example, in the Euphrates Graben in eastern Syria, the Cenomanian – Turonian Judea limestone (Figure 5.8) suggests marginal to shallow water depths and calm conditions.  The equivalent Palmyride strata (Abou Zounar and Abtar formations) show medium depth to shallow marine conditions.  The Cenomanian in the Coastal Ranges and Anti-Lebanon  shows increasing marl with occasional planktonic foraminifera and pelagic, open marine facies (Slenfeh and Bab Abdallah formations).  The northwestern Kurd Dagh region records hemipelagic strata.  Maximum 'Middle Cretaceous' transgression is recorded around the Early Cenomanian to Early Turonian, coincident with all-time global maximum sea levels (Haq et al. 1988).

*Formation of the Euphrates Fault System*

The first hint of Euphrates rifting activity comes in Turonian / Coniacian time. The initiation is marked by a widespread unconformity and associated volcanics and anhydrite. The underlying Judea formation is eroded and dolomitized. This could mark the pre-rift unconformity created by initial heating and uplift of the lithosphere under conditions of incipient rifting. Subsequent redbed deposition that was restricted to eastern Syria (Derro redbeds, Figure 5.8) marks the next stage in this evolution.

The exact cause of the Euphrates rifting is still unclear. Alsdorf et al. (1995) suggested that Latest Cretaceous continental collision along the northern margin of the Arabian Plate caused tensional forces orthogonal to the collision, thus creating the Euphrates Fault System and Abd el Aziz / Sinjar faulting. However, the much earlier initiation of faulting in the Euphrates Graben and the increasing tectonism away from the collision tend to invalidate this suggestion. Lovelock (1984) was the first to suggest trench-pull as a possible passive rifting mechanism. By Senonian time subduction in the NeoTethys was approaching the Arabian margin, and continued to approach until latest Cretaceous collision (Plate 2, frames 8-10a). This could explain the increasing extension with time, and the cessation of rifting with the collision of the trench and the northern Arabian margin during the Maastrichtian. However, the stresses created by such a distant trench may not be sufficient to cause the observed extension. Furthermore, the presence of pre-rift unconformity and volcanics might favor an active rifting scenario. This could be associated with the Early Cretaceous phase of plume activity observed in western Syria. Geochemical findings of deep mantle material in limited Late Cretaceous volcanism, if made, might suggest the plume over the trench-pull hypothesis.

**Santonian (84 Ma) – Campanian (74 Ma)**

*Palmyride Area*

The Senonian was a time of global high sea levels, and also a time of subsidence throughout the northern Arabian platform. In the Palmyrides facies suggest a clear increase in water depth after Turonian time. The Soukhne group (Rmah and Sawwaneh formations) exhibit increased marl and decreasing calcareous content. The top of the Soukhne group (Upper Campanian) is marked by a locally phosphatic limestone bed (Al-Maleh and Mouty, 1988). Studies of the Soukhne group (Mouty and Al-Maleh, 1983) show differentiation between pelagic and hemipelagic strata recorded in the Bilas area, and shallower conditions on the southern margin of the Palmyrides that was not completely submerged until the Late Senonian. This caused the preferential development of phosphatic deposits along the southern margin (Al-Maleh and Mouty, 1992).

Significant Late Cretaceous faulting in the Palmyrides is only observed in the Bishri area. Even so, central Syria at this time was undergoing accelerated regional subsidence that covered all areas. This was possibly due to the influence of northeast - southwest directed stress that we have invoked as the cause of formation of the Euphrates Fault System formation as discussed above.

On a regional scale Bartov et al. (1980) reported significant Santonian structural inversion in northern Sinai. However, Guiraud and Bosworth (1997) note that this was an isolated case, and was generally minor compared to later events. They claim no widespread compression of the "Syrian Arc" (inverted structures sub-parallel to the eastern Mediterranean coast from Sinai to Syria, see Walley, 2000) is observed before Maastrichtian time.

*Abd el Aziz / Sinjar Area*

Although the Senonian was the time of significant rifting in the Euphrates Fault System (discussed below), similar large scale faulting is not observed in the Abd el Aziz / Sinjar area until Maastrichtian time. Deposition in the northeast of Syria was limited during the Late Cretaceous (excluding Maastrichtian), often not more than a few hundred meters of strata are encountered. The depositional environment was calm, with massive limestone prograding from Turkey in the north and mudstone deposition farther south (Kent and Hickman, 1997). Towards the southwest of this area, the northwest striking faults of the Euphrates Fault System controlled deposition (Brew et al., 1999).

*Euphrates Fault System*

The Euphrates Fault System rifted across oblique-normal faults from Santonian time onwards, although was most active during the Campanian and Early Maastrichtian. The first graben-fill were the Rmah chert in the west (directly equivalent to the Palmyride Rmah chert), and the Derro redbeds in the east (Figure 5.8) deposited during southeastward transgression. Progressively deeper water carbonate facies of the syn-rift sequence then filled the graben. This culminated in the accumulation of up to 2300 m of pelagic marly limestone of the Shiranish formation. At this time the Euphrates Fault System and Bishri depocenters were linked by a fault-controlled topographic low (Figure 5.9).

We suggest, as originally proposed by Lovelock (Lovelock, 1984), that Euphrates rifting was driven by trench pull of the approaching subduction zone in the NeoTethys (Plate 2, frames 9a,b). The Wadi Sirhan graben in Jordan (Figure 5.1) shows a very similar orientation, and timing of evolution, to the Euphrates Fault system (Litak et al., 1997). This suggests that the tensional forces responsible for transtension in the Euphrates were transmitted across the Arabian Plate and were causing similarly oriented extension in Jordan.

*Aafrin Basin and Coastal Ranges Area*

During the Late Cretaceous the Aafrin Basin formed around the northwestern corner of the Arabian platform, roughly along the line of the current Syrian / Turkish border.  The basin has subsequently been inverted in the Kurd Dagh mountains (Figure 5.2).  As in other areas of Syria, subsidence and deposition in the Aafrin basin was increased throughout the Senonian.  The basin fill contains progressively deeper water facies from this period (Al-Maleh, 1976; 1982).  Hemipelagic open marine strata of Santonian age lay beneath pelagic Campanian strata.  The beginnings of recognizable Aafrin Basin geometry developed in the Campanian.  Again, this may be related to the increased stress within the platform  as  a consequence of subduction approaching from north and northeast.  It may also be related to the loading of ophiolites that were being progressively obducted onto the northern Arabian margin a short distance north of the basin.  Surface mapping shows a typical preserved Santonian – Campanian section of more than 200 m  (Al-Maleh, 1976).  During this time, pelagic open marine strata were deposited in the Coastal Range area.  However, this area was not a significant depocenter in comparison to the Aafrin Basin.

**Maastrichtian (74 - 65 Ma)**

*Palmyride Area*

The Early Maastrichtian was marked by accelerated deposition throughout the Palmyrides. This was the initiation of a major phase of Palmyride trough development recorded by the deposition of the carbonate pelagic Maastrichtian to Lower Eocene age Bardeh formation (Mouty and Al-Maleh, 1983).  The Bardeh formation (its lower part equivalent to the Shiranish of Euphrates and northeast Syria, Figure 5.8) has been studied extensively in outcrop (e.g. Al-Maleh and Mouty, 1988; El-Azabi et al., 1998).  It shows great contrast to

the depositional environment of the majority of Senonian Palmyride strata. The Bardeh formation was monotonously deposited marl contained very few quartz grains, with some planktonic and occasional benthic foraminifera, indicating great water depths in a low-energy open marine setting (El-Azabi et al., 1998). Thickness changes within the Bardeh formation emphasize the continuous development of the Palmyrides with the thickest strata recorded in the central areas.

Minor compression and uplift are well documented in the Palmyrides and the foothills of Turkey (Chaimov et al., 1992) in the latest Cretaceous. A coincident minor sedimentary hiatus at the Cretaceous / Tertiary boundary is observed in the Bardeh formation (El-Azabi et al., 1998). This is also regarded as one of two prominent phases in the development of the Syrian Arc that caused inversion of Permo-Triassic normal faults along the Levant margin (Guiraud and Bosworth, 1997). This transition from an extensional to a compressional regime was due to collision of the Arabian platform with the intra-oceanic subduction trench in the north and east (Plate 2, frame 10b), as first suggested by Lovelock (1984). This event was related to widespread Maastrichtian southward obduction of ophiolites along the northern and northeastern margin of Arabia (Hempton, 1985). This was not the final Eurasian - Arabia collision, however, and the NeoTethys Ocean, with associated subduction, persisted to the north and east (Plate 2, frame 10a).

### Abd el Aziz / Sinjar Area

The significant period of Late Cretaceous deformation in northeast Syria began in the latest Campanian or earliest Maastrichtian (Brew et al., 1999). The boundary between the Soukhne (Massive Limestone) formation, and the syn-extensional Shiranish is unconformable, (Kent and Hickman, 1997) suggesting this is the major pre-extensional unconformity. The Shiranish is predominantly a marly limestone with occasional sands

eroded from exposed areas to the north (Kent and Hickman, 1997). It correlates with the Shiranish in the Euphrates Fault System. Extension took place on east-west striking faults that are limited to the west by the Euphrates faulting, and coalesce with Zagros deformation to the east in Iraq (Figure 5.11b). This extension created the Abd el Aziz and Sinjar half grabens (Figure 5.5). This faulting and half graben formation ultimately led to the deposition of up to 1600 m of Shiranish strata (Figure 5.9).

We suggest that these east - west oriented faults formed as a consequence of tension created by subduction located to the north and northeast margins of the Arabian peninsula (Plate 2, frame 10a). Perhaps the strain was accommodated in the Abd el Aziz / Sinjar area because it represented a structurally weak zone of thick sedimentation on the northern edge of the Palmyride / Sinjar trough. A gradual shift in the orientation in this subduction zone might explain the transition from general northwest - southeast extensions in the early Senonian (manifest by the Euphrates and Wadi Sirhan grabens) to more north - south extension in the Maastrichtian (Adb el Aziz and Sinjar half grabens). This was also the time of maximum extension in the east-west trending Anah graben (Plate 2, frame 9b) (Ibrahim, 1979). The relative southerly advance of ophiolitic nappes that were to obduct onto the northern margin could have contributed to normal faulting in northeast Syria through loading effects (Yilmaz, 1993).

Facies changes from marly limestone to lime grainstone (Kent and Hickman, 1997), and the abrupt termination of faulting at the top of Cretaceous level, together with a post-extension unconformity, signal the end of Late Cretaceous extension in northeast Syria. This was caused when Arabia collided with a NeoTethys subduction zone, as discussed above.

*Euphrates Fault System*

While a vast thickness of the Shiranish formation continued to be deposited in the Euphrates Fault System during the Maastrichtian, subtle indications suggest a reorienting stress direction, and a slowing of extension before final abortion of the rifting.  Litak et al. (1997) reported that strike-slip features that are more common amongst the northwest - southeast striking faults of the Euphrates deformation, than amongst the west-northwest - east-southeast striking features.  Furthermore, faults within the Shiranish formation were less active during the Maastrichtian, faulting ceased before the end of the Cretaceous (Guyot and Zeinab, 2000), and an unconformity is observed within the Shiranish formation (Litak et al., 1998).  These observations could be explained by reorientation of extension from southwest - northeast to north - south) in agreement with that suggested for the Abd el Aziz / Sinjar area above, related to reorienting NeoTethys subduction (Plate 2, frame 10a).

*Aafrin Basin and Coastal Ranges Area*

Early Maastrichtian time saw continued subsidence and pelagic deposition in the northeast – southwest trending depocenter of the Aafrin basin.  More than 600 m of Maastrichtian strata are found in measured sections exposed by Cenozoic basin inversion  (Al-Maleh, 1976).  However, during Maastrichtian time ophiolitic nappes encroached on the northwest margin of the basin, hence these areas experienced considerable shallowing.  To the southeast and especially the southwest, the basin remained and Maastrichtian turbidities deposited there contain considerable ophiolitic ditrital content (Al-Maleh, 1976).  Stratigraphically above the ophiolite, clastic lenses within the Uppermost Cretaceous strata indicate transgression after ophiolite emplacement.

In the Early Maastrichtian, the Coastal Ranges show a continuation of Campanian depositional trends with marly strata and only limited subsidence.  The Late Maastrichtian is

marked by the initial uplift of the Coastal Ranges (Brew et al., 2000). This is recorded stratigraphically by an angular unconformity between Paleocene and Maastrichtian strata (Ponikarov, 1966). This uplift occurred as part of the development of the 'Syrian Arc', resulting from collision along the northern Arabian margin as discussed above.

## Paleocene (65 Ma) – Eocene (35 Ma)

The Paleogene was largely a time of quiescence in the northern Arabian platform. All areas remained under marine conditions with extensive pelagic deposition. In the Euphrates and Wadi Sirhan Graben areas, widespread thermal subsidence following Late Cretaceous rifting (Plate 2, frame 11b). The Paleocene Kermev formation in the Euphrates Graben contains more chert than underlying Shiranish, and indicates shallowing water. This progressive shallowing is indicated throughout the Paleogene section here, and in the Abd el Aziz / Sinjar area.

During the Paleogene the Palmyrides area continued the prominent subsidence begun in the Maastrichtian, and deposition of the Bardeh formation continued. The Paleocene portion of this again shows monotonous pelagic marly limestone deposition with high levels of nanoplankton. The Lower Eocene Arak Flint marks the relatively shallower conditions that interrupted this period. Upper Eocene and Oligocene strata (the Abiad group) show continued subsidence. Facies are sandy limestones of shallow water origin related to the oncoming regression in the Palmyrides, Anti-Lebanon and Aafrin basin.

Chaimov et al. (1992) documented minor tectonism in the southwest Palmyride fold and thrust belt in Middle Eocene time, Late Eocene is clearly documented as the main stage of Syrian Arc deformation (Guiraud and Bosworth, 1997). This included uplift of the Syrian

Coastal Ranges (Brew et al., 2000) that is recorded by a stratigraphic gap during the Late Eocene and Oligocene in the Coastal Range area. This 'Syrian Arc' development also included formation of the major topographic elements in Lebanon (Walley, 1998). Minor shortening in southern Turkey (Hempton, 1985), very minor transpression in the Euphrates Fault System (Guyot and Zeinab, 2000), and minor compression in the Abd el Aziz uplift (Kent and Hickman, 1997) are all reported for this time.

Hempton (1985) documented the Middle to Late Eocene as the initial period of final collision on the northern Arabian margin. This final obliteration of oceanic lithosphere thus formed the Bitlis suture in the western part of the northern Arabian margin (Plate 2, frame 11a). The plate-wide compression caused by this suturing can explain the numerous instances of Mid-Late Eocene compressional tectonics mentioned above.

## Miocene (35 Ma) – Recent

Miocene time witnessed the final transition to continental conditions in Syria. One exception to this was the Lataqia / Aafrin basin along the northwestern margin of Arabia that includes Miocene marine strata. Marine incursions of the eastern Mediterranean Sea into western Syria continued well into the Pliocene (Ponikarov, 1966).

After the Middle to Late Eocene suturing of Africa / Arabia to Eurasia convergence between the plates was partially accommodated by the shortening and thickening of the Arabian continental margin (Hempton, 1985). The stress created by this ongoing convergence continued the formation of the compressional features that began forming in the Mid-Late Eocene, but at a slower rate. This stress regime was changed again by the Late Oligocene / Early Miocene initiation of continental stretching and rifting in the Red Sea. Rifting in the Red

Sea lead to first phase of motion along the southern Dead Sea Fault System (Hempton, 1987). This, in turn, precipitated accelerated and still ongoing uplift of the Palmyrides (Chaimov et al., 1992).

By the Mid-Late Miocene the colliding edge of the northern Arabian continental margin had reached full thickness. This occurrence is thus regarded as the terminal suturing of Arabia to Eurasia. In the model of Hempton (1987) this collision can be correlated in time with the cessation of the first phase of Red Sea rifting and Dead Sea Fault System movement.

Hempton (1987) suggests that around the end of the Miocene the North and East Anatolian Faults formed to accommodate the continued convergence of Arabia and Eurasia. This coincided with a resumption of extension in the Red Sea, leading to full-scale sea-floor spreading. This also lead to the second phase of motion along the Dead Sea Fault System. This episode of movement caused a shift in the path of the fault north of Israel, and hence formed the Syrian portion of the Dead Sea Fault System (Chaimov et al., 1990).

Late Miocene onwards is marked as a time of increased compression in Syria, presumably caused by the cessation of shortening along the northern margin. Evidence for increased compression includes accelerated basin inversion of the Palmyride fold and thrust belt (Chaimov et al., 1992), minor shortening in the northwest portion of the Euphrates fault system, the Turkish foot hills, and the Zagros (Litak et al., 1997), and minor shortening in the Abd el Aziz uplift (Kent and Hickman, 1997). Furthermore, Feraud et al. (1985), using dykes and volcanic alignments as paleostress indicators, documented a shift in maximum stress direction from roughly northwest – southeast to north – south around the end of the Miocene.

Full-scale inversion of the Abd el Aziz and Sinjar uplifts did not take place until the Late Pliocene (Brew et al., 1999). Fault-propagation folds forming above reactivated Late Cretaceous east – west striking normal faults have created the current east – west trending topography. While small outcrops of Senonian strata are found on the Abd el Aziz structure, Cretaceous levels are more extensively exposed on the Sinjar Uplift in Iraq owing to increasing fault inversion to the east. Inversion in the Euphrates Fault System, however, is very minor and transpression is largely limited to the northwest segment of the system. This could be a consequence of the Abd el Aziz / Sinjar structures accommodating most of the Late Cenozoic strain. Also the oblique angle that the Euphrates Fault System forms in relation to the Alpine collision favors strike-slip reactivation (which is harder to detect in subsurface data). Seismicity, Quaternary volcanism (Plate 1) and very minor Quaternary faulting suggests the aborted graben in eastern Syria are still actively inverting (Ponikarov, 1966).

To the northeast of the Sinjar area, sediment thickness increases rapidly into the Mesopotamian Foredeep (Figure 5.11a). This depression formed due to the loading of the Zagros Mountains located to the northeast. In Syria some small Zagros-related folding is observed, with deeper structure reminiscent of the Sinjar graben. Well data indicate more than 1.3 km of Neogene clastic fill (Figure 5.9), shed from the uplifting Zagros since the Mid-Late Miocene terminal continental collision along this margin.

A series of eruptive volcanics from 24 – 16 Ma is found throughout western Syria, with the exception of the Coastal Ranges. As noted by Mouty et al. (1992), this period roughly coincides with the final stages of Arabian – Eurasian convergence. Interestingly, a gap in volcanism between about 16 and 8 Ma roughly corresponds to the episode of inactive Red Sea spreading, and no movement on the Dead Sea Fault (Hempton, 1987).

Penecontemporaneous with renewed movement on the transform, the volcanism shifted from the Aleppo Plateau to locations along the Dead Sea Fault in Syria. In particular, formation of the northern Ghab Basin appears to have focused the most recent volcanism there from 1 – 2 Ma (Devyatkin et al., 1997). Holocene volcanic centers south of Damascus show strong alignments trending about north-northwest (Plate 1). This could be reflecting a modern stress direction trending north - south (Feraud et al., 1985), or evidence for reactivation of the underlying Wadi Sirhan structures that strike in a very similar direction (Figure 5.1).

Currently the Palmyride region is deforming by dextral transpression (Chaimov et al., 1990; Searle, 1994), under the influence of compression from the north and northwest (Plate 2, frame 12b). Evidence for active deformation on the Jhar fault includes small Quaternary offsets (Ponikarov, 1966) and seismicity. Additional, possible dextral strike-slip faults on the Aleppo Plateau (Plate 1) have also been identified (McBride et al., 1990). Our analysis suggests that the northeast trending faults mapped from the Bishri block towards the Abd el Aziz (Alsdorf et al., 1995) (Figures 5.2 and 5.11b) could be acting to translate right lateral shear away from the Palmyride region. The exact interaction between the Palmyrides, Euphrates, and Sinjar tectonic zones is still unclear. Forthcoming GPS surveys should help to resolve many of these uncertainties in the current tectonics of Syria.

**IMPLICATIONS FOR HYDROCARBONS**

Estimated recoverables from Syria are about 2.5 Bbbl of oil and 8.5 TCF of gas (Oil & Gas Journal, December 1999). The vast majority of hydrocarbon discoveries have been made in three of the four major Syrian tectonic zones (Figure 5.2) and hence understanding the tectonic evolution of these structures is critical to hydrocarbon exploration. The Dead Sea

Fault System is host to some hydrocarbons in Israel, but none have been found so far in this zone in Syria. The three hydrocarbon-bearing zones are all abandoned rifts, with varying degrees of subsequent structural inversion. As a gross generalization, the source and reservoir rocks of Syria were deposited under the extensional conditions in the Late Paleozoic and Mesozoic, and traps were formed by Mesozoic extension and Late Cenozoic compression (Figure 5.15).

The discoveries in the Palmyrides are generally gas because of the greater paleo-burial depths of source rocks relative to elsewhere in Syria (Figure 5.11c). Most of the gas is found in the Triassic carbonate section, especially the Middle Triassic Kurrachine Dolomite formation; fracturing largely controls porosity as primary porosity is poor (3 to 10%; Al-Otri and Ayed, 1999). This reservoir is sealed by the Kurrachine Anhydrite formation, and was charged by Permo-Triassic and Carboniferous shale (0.8% - 5% TOC; Al-Otri and Ayed, 1999). Traps have been created in Late Paleozoic / Mesozoic fault blocks and the folds created during structural inversion and shortening (Figure 5.15).

A combination of oil and gas are produced from the Bishri block (Figure 5.2) in the transition between the Euphrates and Palmyride petroleum systems. Lower Cretaceous sandstone is the most common reservoir and fault blocks the usual trap. Potential Upper Cretaceous source rocks have not been sufficiently buried to reach full maturity in the Bishri block, and are positioned structurally higher than the reservoirs (Figures 5.11a and b). Hence, charging of the Bishri system may have resulted from westward migration of Upper Cretaceous oil originating in the adjacent Euphrates Graben (Illiffe et al., 1998).

As clearly demonstrated in Figure 5.2, the hydrocarbon discovery wells in the Abd el Aziz / Sinjar area are most directly correlated with current topography. The main trapping

mechanism in the northeast is Late Pliocene fault-propagation folding, therefore indicating very recent oil migration (Figure 5.15). The degree of structural

**Figure 5.15:** Chronological chart showing development of most significant stratigraphic and structural elements in selected hydrocarbon provinces. Proven elements are shown as solid colored lines, uncertain elements as dashed lines. A generalized distribution of the relevant stratigraphy is also shown. Tectonic events generalized from Plate 2. Formations names vary in Turkey. Patterns indicate lithologies, same legend as Figure 5.8. Red dots refer to time-points detailed in Plate 2.

inversion is critical to successful trapping. In Turkey, greater shortening has breached many of the fault-propagation fold reservoirs. Some deeper traps are fault blocks. Source rocks in northeast Syria are commonly Cretaceous and Triassic (Ala and Moss, 1979). Reservoirs are predominately Mesozoic and Cenozoic fractured carbonates and many fields have multiple objectives in the Miocene, Cretaceous and Triassic (Figure 5.15). Sealing is accomplished by shale and evaporites that are distributed throughout the Mesozoic and Cenozoic sections.

The Mesopotamian foredeep, in far northeastern Syria is the longest established production in the country, within many different fields (see well distribution in Figure 5.2). Trapping is in the simply folded strata of Late Cretaceous and Cenozoic strata, charged by Late Cretaceous and Triassic sources. Late Cretaceous fault blocks may also be trapping deeper reserves.

Although mostly unknown before the 1980's, the Euphrates Graben harbors the most important hydrocarbon plays in Syria. More than 400,000 barrels of light, sweet crude are estimated to be produced daily from the graben, out of a national average of 540,000 barrels (Oil & Gas Journal, December, 1999). The bulk is from the Lower Cretaceous Rutbah sandstone (Figure 5.8), a high porosity (up to 20%) fluvio-deltaic sandstone with well maintained permeability, that was deposited during the Neocomian transgression in eastern Syria (Plate 2, frame 7b). Minor production comes from other levels (Figure 5.15) and trapping is most commonly in fault blocks (Figure 5.6), similar in many respects to the North Sea. Alternating carbonates and evaporites of the transgressing Triassic (Figure 5.8) have created a series of potential reservoir / seal pairs, and the widespread Serjelu (Mulussa F) could be a reservoir quality sandstone. The Thayyem field is typical of the southern Euphrates Graben, it was the first discovery in the Euphrates Graben in 1984, and is still the

most productive.  Rutbah sandstone forms the reservoir that is both charged and sealed by Upper Cretaceous marly limestone of the Shiranish formation.  The Shiranish, deposited under widespread extension in eastern Syria (Plate 2, frame 9b), has been juxtaposed against the Rutbah by the Latest Cretaceous normal faulting that created the rotated fault block trap (Litak et al., 1998).  While appreciable structural inversion in the northwest of the system may have breached some reservoirs, further southeast trapping has been enhanced by the very mild folding resulting from the Cenozoic compression.

In all of Syria, declining yields have pushed the search for hydrocarbons deeper, and exploration now focuses on Paleozoic plays.  Grapholitic shale source rocks of the Silurian Tanf formation and Lower Ordovician Swab formation (Figure 5.15), as well as Late Paleozoic shales, are found through most of the Middle East (Husseini, 1990).  Tests show 2 - 5 % TOC in the Tanf formation increasing southwards with perhaps up to 16 % TOC in Iraq (Aqrawi, 1998).  Drilling from the Rutbah uplift, however, shows an over-mature Tanf formation, reinforcing that a viable source is the most elusive component part of a Paleozoic play.

Paleozoic reservoir rocks in Syria could include Permo-Carboniferous and Ordovician sandstones (both up to 25 % porosity) that are present at various depths over most of the region (Figure 5.11d).  The Akkas oil shows (oil from a Lower Silurian sandstone and gas from the Upper Ordovician, sourced and sealed by Lower Silurian shales) in Iraq (Aqrawi, 1998), and Paleozoic discoveries in Euphrates Graben confirm viable Paleozoic plays in southeast Syria.  The presence of suitably-aged structural traps could be the main control on this play (Aqrawi, 1998).  The Maghlouja well on the Abd el Aziz structure had shows of gas in the Silurian section, and limited shows of relatively light oil (39 API gravity) in the Upper Ordovician Affendi formation  (Kent and Hickman, 1997).  Perhaps this oil was

sourced in the Silurian and migrated after fault inversion juxtaposed that unit with the Ordovician in the Neogene, thus providing insufficient time for economically adequate charge.

## SUMMARY

Integration of a vast amount of detailed geophysical and geological data, together with experience based on many previous investigations, has allowed us to compose a new regional tectonic evolutionary model for Syria. We find that tectonic deformation within specific Syrian tectonic zones was often contemporaneous with deformation in other adjacent zones. Moreover, in almost all cases these episodes of tectonism can be related to activity on nearby Arabian Plate margins. In particular, the opening and closing of the various elements of the Tethys Ocean throughout the Phanerozoic profoundly affected Syrian tectonic evolution.

After Proterozoic cratonic accretion, for the vast majority of the Phanerozoic time Syria was part of the northern passive margin of Gondwana bordering the Tethys Ocean. Gentle Early Paleozoic subsidence of this east-facing margin led to the regional accumulation of thick clastic deposits eroded from nearby shield areas. For most of this time Arabia experienced either glacial-fluvial or marginal marine conditions, that changed to a shelf environment during frequent transgressions. Towards the end of the Paleozoic Hercynian compression, followed by extension related to opening of the NeoTethys Ocean led to the formation of the Palmyride / Sinjar trough that accumulated over two thousand meters of clastic Carboniferous and Permo-Triassic strata.

After drifting to lower latitudes in the Mesozoic, huge carbonate platforms developed on the exceptionally wide northern Arabian epicontinental shelf. Thermal subsidence above the Permo-Triassic Palmyride rift created a thick Triassic and Jurassic section in the Palmyrides, enhanced by periods of reactivated faulting. Development of the east Mediterranean, west-facing, passive margin also concentrated deposition in that area and was another dominant control on Mesozoic sedimentation. Observations of extensive Late Jurassic / Early Cretaceous uplift, widespread volcanism and renewed fault activity have led to suggestions of contemporaneous mantle plume activity.

Barremian - Aptian transgression deposited thick fluvio-deltaic sands across much of Syria. In the Late Cretaceous a northeast – southwest directed regional extension dominated. This led to the formation of the Euphrates Fault System, and accelerated subsidence elsewhere. Shifting to a more north - south extension direction in the Maastrichtian caused the opening of the Abd el Aziz, Sinjar and Anah grabens. Collision along the northern margin in the latest Cretaceous with associate ophiolite emplacement terminated extension and caused slight uplift in the Syrian Arc, including the southwest Palmyrides.

The thick carbonate sequences continued to form in the Paleogene, with some uplift and compression in Mid-Late Eocene time related to initiation of final collision along the northern Arabian margin. Neogene clastics indicate the shift to the continental conditions that prevail today. This occurred in tandem with renewed compressional tectonics related to terminal suturing on the northern margin causing the majority of the Palmyride uplift and inversion of the Abd el Aziz / Sinjar structures. Pliocene development of the northern Dead Sea Fault System led to the creation of the Ghab Basin, and added to the compressional tectonics within the platform.

The combined effect of this complex tectonic evolution has been to form conditions highly suitable for the preservation of hydrocarbon resources. Reservoirs are formed in the extensive clastic and carbonate deposits, most particularly in the Mesozoic, with shaly sources throughout the section. The traps are most often structural in fault blocks or fault-propagation folds.
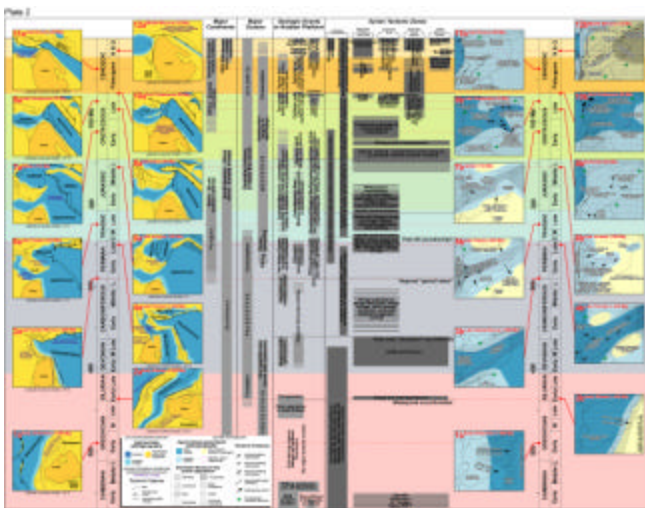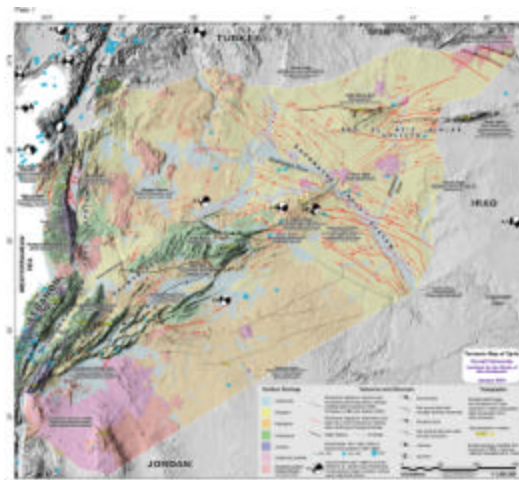
**REFERENCES**

Ala, M.A. and B.J. Moss 1979. *Comparative petroleum geology of southeast Turkey and northeast Syria*. Journal of Petroleum Geology, **1,** 3-27.

Al-Maleh, K., 1976. *Etude stratigraphique, petrographique, sedimentologique et geochimique du Cretace du N.W. Syrien (Kurd Dagh se environs d'Aafrine): Les aspects petroliers de la region*. Universitie Pierre et Marie Curie (Paris 6). 620 p.

Al-Maleh, K., 1982. *Evolution de la sedimentation Carbonatee dans le Nord - ouest de la Syrie pendant le cretace*. Memoire Geologique, **4**, University of Dijon, p. 437-479.

Al-Maleh, K. and M. Mouty, 1988. *The sedimentation and paleogeographic evolution of the Palmyridean region during the Jurassic and Cretaceous (Central part of Syria)*. Third Jordanian Geology Conference, Amman, p 213-244.

Al-Maleh, K. and M. Mouty, 1992. *The Senonian in the Palmyridian Chaine, Final Report AECG-G/FRSR63*. Atomic Energy Commission, Damascus, Syria. 43 p.

Al-Maleh, K. and M. Mouty, 1992. *Lithostratigraphic characteristics of phosphorite deposits and the regional sedimentational and paleogeographic framework of their formation in the Palmyrides mountain chain, Middle Syria*. 29th International Geological Congress abstracts, Kyoto, Japan, 97.

Al-Maleh, K., M. Mouty, G. Brew, M. Barazangi and I. Bach-Imam 2001. *Mesozoic stratigraphy and geologic development of Syria*. for submission to GeoArabia.

Al-Otri, M. and H. Ayed 1999. *Evaluation of hydrocarbon potentials of the sedimentary basins in Syria*. Evaluation of hydrocarbon potential in Arab sedimentary basins, Ruiel - Malmaison, France, July 1999.

Al-Saad, D., T. Sawaf, A. Gebran, M. Barazangi, J. Best and T. Chaimov 1992. *Crustal structure of central Syria: The intracontinental Palmyride mountain belt*. Tectonophysics, **207,** 345-358.

Al-Saad, D., T. Sawaf, A. Gebran, M. Barazangi, J. Best and T. Chaimov 1991. *Northern Arabian platform transect across the Palmyride mountain belt, Syrian Arab Republic*. Global Geoscience Transect 1, The Inter-Union Commission on the Lithosphere and the American Geophysical Union, Washington, D. C.

Alsdorf, D., M. Barazangi, R. Litak, D. Seber, T. Sawaf and D. Al-Saad 1995. *The intraplate Euphrates depression-Palmyrides mountain belt junction and relationship to Arabian plate boundary tectonics*. Annali Di Geofisica, **38,** 385-397.

Aqrawi, A.A.M. 1998. *Paleozoic stratigraphy and petroleum systems of the western and southwestern deserts of Iraq*. GeoArabia, **3,** 229-248.

Barazangi, M., D. Seber, T. Chaimov, J. Best, R. Litak, D. Al-Saad and T. Sawaf 1993. *Tectonic evolution of the northern Arabian plate in western Syria.* In E. Boschi, E. Mantovani and A. Morelli (Eds.), Recent Evolution and Seismicity of the Mediterranean Region, Kluwer Academic Publishers, 117-140.

Bartov, Y., Z. Lewy, G. Steinitz and I. Zak 1980. *Mesozoic and Tertiary Stratigraphy, Paleogeography and Structural History of the Gebel Areif en Naqa Area, Eastern Sinai*. Israel Journal of Earth Sciences, **29,** 114-139.

BEICIP 1975. *Gravity maps of Syria: Damascus (Syria)*. Bureau d'etudes industrielles et de cooperation de l'institut francais du petrole, Hauts de Seine, 96 p.

Berberian, M. 1995. *Master "blind" thrust faults hidden under the Zagros folds: active basement tectonics and surface morphotectonics*. Tectonophysics, **241,** 193-224.

Best, J.A., 1991. *Crustal evolution of the northern Arabian platform beneath the Syrian Arab Republic*. Ph.D. Thesis, Cornell University, Ithaca, New York. 152 p.

Best, J.A., M. Barazangi, D. Al-Saad, T. Sawaf and A. Gebran 1990. *Bouguer gravity trends and crustal structure of the Palmyride Mountain belt and surrounding northern Arabian platform in Syria*. Geology, **18,** 1235-1239.

Best, J.A., M. Barazangi, D. Al-Saad, T. Sawaf and A. Gebran 1993. *Continental margin evolution of the northern Arabian platform in Syria*. American Association of Petroleum Geologists Bulletin, **77,** 173-193.

Beydoun, Z. 1981. *Some open questions relating to the petroleum prospects of Lebanon*. Journal of Petroleum Geology, **3,** 303-314.

Beydoun, Z.R. 1991. *Arabian plate hydrocarbon geology and potential – a plate tectonic approach*. Studies in Geology, 33, American Association of Petroleum Geologists, Tulsa, Oklahoma, USA, 77 p.

Beydoun, Z.R. and J.G. Habib 1995. *Lebanon Revisited: New Insights into Triassic Hydrocarbon Prospects.* Journal of Petroleum Geology, **18,** 75-90.

Brew, G., M. Barazangi, T. Sawaf and K. Al-Maleh 2000. *Tectonic map and geologic evolution of Syria: The role of GIS*. The Leading Edge, **19,** 176-182.

Brew, G., R. Litak, M. Barazangi and T. Sawaf 1999. *Tectonic evolution of Northeast Syria: Regional Implications and Hydrocarbon Prospects.* GeoArabia, **4,** 289-318.

Brew, G., J. Lupa, M. Barazangi, T. Sawaf, A. Al-Imam and T. Zaza 2000. *Structure and tectonic development of the Dead Sea Fault System and Ghab Basin in Syria*. Submitted to Journal of the Geological Society, London.

Brew, G.E., R.K. Litak, D. Seber, M. Barazangi, A. Al-Imam and T. Sawaf 1997. *Basement depth and sedimentary velocity structure in the northern Arabian platform, eastern Syria*. Geophysical Journal International, **128,** 617-631.

Chaimov, T., M. Barazangi, D. Al-Saad and T. Sawaf 1993. *Seismic fabric and 3-D upper crustal structure of the southwestern intracontinental Palmyride fold belt, Syria.* American Association of Petroleum Geologists Bulletin, **77,** 2032-2047.

Chaimov, T., M. Barazangi, D. Al-Saad, T. Sawaf and A. Gebran 1990. *Crustal shortening in the Palmyride fold belt, Syria, and implications for movement along the Dead Sea fault system*. Tectonics, **9,** 1369-1386.

Chaimov, T., M. Barazangi, D. Al-Saad, T. Sawaf and A. Gebran 1992. *Mesozoic and Cenozoic deformation inferred from seismic stratigraphy in the southwestern intracontinental Palmyride fold-thrust belt, Syria*. Geological Society of America Bulletin, **104,** 704-715.

Cohen, Z., V. Kaptsan and A. Flexer 1990. *The Tectonic Mosaic of the Southern Levant: Implications for Hydrocarbon Prospects.* Journal of Petroleum Geology, **13,** 437-462.

Coward, M.P. 1996. *Balancing Sections Through Inverted Basins.* In P.G.N. Buchanan, D.A. (Eds.), Modern Developments in Structural Interpretation, Validation and Modelling, Geological Society Special Publication, **99**, 51-77.

de Ruiter, R.S.C., P.E.R. Lovelock and N. Nabulsi 1994. *The Euphrates Graben, Eastern Syria: A New Petroleum Province in the Northern Middle East.* In M. Al-Husseini (Eds.), Geo 94, Middle East Petroleum Geosciences, Gulf PetroLink, **1**, 357-368.

Dercourt, J., L.P. Zonenshain, L.-E. Ricou, V.G. Kazmin, X. LePichon, A.L. Knipper, C. Grandjacquet, I.M. Sbortshikov, J. Geyssant, C. Lepvrier, D.H. Pechersky, J. Boulin, J.-C. Sibuet, L.A. Savostin, O. Sorokhtin, M. Westphal, M.L. Bazhenov, J.P. Lauer and B. Biju-Duval 1986. *Geological evolution of the Tethys belt from the Atlantic to the Pamirs since the Lias*. Tectonophysics, **123,** 241-315.

Devyatkin, E.V., A.E. Dodonov, E.V. Sharkov, V.S. Zykin, A.N. Simakova, K. Khatib and H. Nseir 1997. *The El-Ghab Rift Depression in Syria: Its Structure, Stratigraphy, and History of Development*. Stratigraphy and Geological Correlation, **5,** 362-374.

Dubertret, L., 1955. *Carte Geologique du Liban*. Ministere des Travaux Publics, Beyrouth.

El-Azabi, M.H., A.K. Al-Maleh and M.K. Yzbek 1998. *Facies characteristics and depositional environments of the Maastrichtian-Paleocene succession in Jabal El-Bardeh and Jabal Anter, Kasr Al Heir-Turfa area, Southern Palmyridian region, Syria*. M.E.R.C. Ain Shams University, Earth Sciences, **12,** 1-20.

Feraud, G., G. Giannerini and R. Campredon 1985. *Dyke Swarms as Paleostress Indicators in Areas Adjacent to Continental Collision Zones: Examples from the European and Northwest Arabian Plates*. Mafic Dyke Swarms, Erindale College, University of Toronto, Ontario, Canada, International Lithosphere Program, 273-278.

Flexer, A., M. Gardosh, I. Bruner and A.Y. Dror 2000. *The tale of an inverted basin: Eastern Mediterranean - offshore Israel (abstract).* American Association of Petroleum Geologists Bulletin, **84,** 1426.

Freund, R., Z. Garfunkel, I. Zak, M. Goldberg, T. Weissbrod and B. Derin 1970. *The shear along the Dead Sea rift*. Philosophical Transactions of the Royal Society of London, **267,** 107-130.

Garfunkel, Z. 1992. *Darfur-Levant array of volcanics - a 140 Ma-long record of a hot spot beneath the African-Arabian continent, and its bearing on Africa's absolute motion*. Journal of Israeli Earth Sciences, **40,** 135-150.

Gomez, F., M. Meghraoui, A.N. Darkal, C. Tabet, M. Khawlie, K. Khair, R. Sbeinati, R. Darawcheh, K. Khair and M. Barazangi 2000. *Coseismic displacements along the Serghaya fault: An active branch of the Dead Sea fault system in Syria and Lebanon*. Journal of the Geological Society, London, in review.

Guiraud, R. 1998. *Mesozoic rifting and basin inversion along the northern African Tethyan margin: an overview.* In D.S. Macgregor, R.T.J. Moody and D.D. Clark-Lowes (Eds.), Petroleum Geology of North Africa, Geological Society of London, Special Publication, **132**, 217-229.

Guiraud, R. and W. Bosworth 1997. *Senonian basin inversion and rejuvenation of rifting in Africa and Arabia: synthesis and implications to plate-scale tectonics*. Tectonophysics, **282,** 39-82.

Guyot, C. and H. Zeinab 2000. *Euphrates graben - East Syria - basin evolution and petroleum habitat*. GeoArabia, **5,** 100-101.

Gvirtzman, G. and T. Weissbrod 1984. *The Hercynian Geanticline of Helez and the Late Palaeozoic history of the Levant.* In J.E. Dixon and A.H.F. Robertson (Eds), Geological Society of London, Special Publication, **17**, 177-186.

Haq, B.U., J. Hardenbol and P.R. Vail 1988. *Mesozoic and Cenozoic chronostratigraphy and cycles of sea-level change.* In C.K. Wilgus, B.S. Hastings, C.A. Rosset al (Eds.), Sea-level changes; an integrated approach, Special Publication - Society of Economic Paleontologists and Mineralogists, **42**, 72-108.

Harland, W.B., R.L. Armstrong, A.V. Cox, L.E. Craig, A.G. Smith and D.G. Smith  1990. *A geologic time scale, 1989*. Cambridge University Press, Cambridge, United Kingdom, 263 p.

Hempton, M. 1985. *Structure and deformation of the Bitlis suture near Lake Hazar, southeastern Turkey*. Geological Society of America Bulletin, **96,** 233-243.

Hempton, M. 1987. *Constraints on Arabian plate motion and extensional history of the Red Sea*. Tectonics, **6,** 687-705.

Husseini, M.I. 1989. *Tectonic and deposition model of late Precambrian-Cambrian Arabian and adjoining plates*. American Association of Petroleum Geologists Bulletin, **73,** 1117-1131.

Husseini, M.I. 1990. *The Cambro-Ordovician Arabian and ajoining plates:  A glacio-eustatic model*. Journal of Petroleum Geology, **13,** 267-288.

Husseini, M.I. 1991. *Tectonic and depositional model of the Arabian and adjoining plates during the Silurian-Devonian*. American Association of Petroleum Geologists Bulletin, **75,** 108-120.

Husseini, M.I. 1992. *Upper Palaeozoic tectono-sedimentary evolution of the Arabian and adjoining plates*. Journal of the Geological Society of London, **149,** 419-429.

Ibrahim, M.W. 1979. *Shifting Depositional Axes of Iraq: An outline of geosynclinal history*. Journal of Petroleum Geology, **2,** 181-197.

Illiffe, J., C. Blackstock and I. Bulley 1998. *The hydrocarbon charge to the Bishri block, Palmyrides, Syria: An integrated multi-disciplinary study (Abstract)*. GeoArabia, **3.**

Kent, W.N. and R.G. Hickman 1997. *Structural development of Jebel Abd Al Aziz, northeast Syria*. GeoArabia, **2,** 307-330.

Kohn, B., M. Eyal and S. Feinstein 1992. *A Major Late Devonian-Early Carboniferous (Hercynian) Thermotectonic Event at the NW Margin of the Arabian-Nubian Shield: Evidence from Zircon Fission Track Dating*. Tectonics, **11,** 1018-1027.

Laws, E.D. and M. Wilson 1997. *Tectonics and magmatism associated with the Mesozoic passive continental margin development in the Middle East*. Journal of the Geological Society, London, **154,** 459-464.

Litak, R.K., M. Barazangi, W. Beauchamp, D. Seber, G. Brew, T. Sawaf and W. Al-Youssef 1997. *Mesozoic-Cenozoic evolution of the intraplate Euphrates fault system, Syria: implications for regional tectonics*. Journal of the Geological Society, **154,** 653-666.

Litak, R.K., M. Barazangi, G. Brew, T. Sawaf, A. Al-Imam and W. Al-Youssef 1998. *Structure and Evolution of the Petroliferous Euphrates Graben System, Southeast Syria*. American Association of Petroleum Geologists Bulletin, **82,** 1173-1190.

Lovelock, P.E.R. 1984. *A review of the tectonics of the northern Middle East region*. Geological Magazine, **121,** 577-587.

McBride, J.H., M. Barazangi, J. Best, D. Al-Saad, T. Sawaf, M. Al-Otri and A. Gebran 1990. *Seismic reflection structure of intracratonic Palmyride fold-thrust belt and surrounding Arabian platform, Syria*. American Association of Petroleum Geologists Bulletin, **74,** 238-259.

McClusky, S., S. Balassanian, et al. 2000. *GPS constraints on plate kinematics and dynamics in the eastern Mediterranean and Caucasus*. Journal of Geophysical Research, **105,** 5695-5719.

McKenzie, D.P. 1970. *Plate Tectonics of the Mediterranean Region*. Nature, **226,** 239-243.

Mouty, M. 1997a. *Le Jurassique de la Chaine cotiere (Jibal As-Sahilyeh) de Syrie: essai de biozonation par les grands foraminiferes*. Comptes Rondus de l'Academie des Sciences de Paris/Sciences de la terre et des planetes, **325,** 207-213.

Mouty, M. 1997b. *Le Jurassique de la chaine des Palmyrides (Syrie centrale)*. Bulletin Societe Geologie France, **168,** 181-186.

Mouty, M. 1998. *Le Jurassique du Mont Hermon (Anti-Liban). Decouverte de Trias et de Lias*. Archives des Sciences et Compte Rendu, Geneve, **51,** 295-304.

Mouty, M. 2000. *The Jurassic in Syria: an overview. Lithostratigraphic and biostratigraphic correlations with adjacent areas.* In S. Crasquin-Soleau and E. Barrier (Eds.), New data on Peri-Tethyan sedimentary basins, Peri-Tethys Memoir #5, Museum National d'Historie Naturelle, Paris, 159-168.

Mouty, M. and Al-Maleh, K., 1983. *The geological study of the Palmyridian chain using ideal geological sections for exploration purposes and geological survey.* General Establishment of Geology and Mineral Resources, Ministry of Petroleum and Mineral Resources, Damascus, Syria, 4 volumes, 950 p.

Mouty, M., M. Delaloye, D. Fontignie, O. Piskin and J.-J. Wagner 1992. *The volcanic activity in Syria and Lebanon between Jurassic and Actual*. Schweizerische Mineralogische und Petrographische Mitteilungen, **72,** 91-105.

Ponikarov, V.P. 1966. *The Geology of Syria. Explanatory Notes on the Geological Map of Syria, Scale 1:200 000*. Ministry of Industry, Damascus, Syrian Arab Republic.

Quennell, A.M. 1984. *The Western Arabia rift system.* In J.E. Dixon and A.H.F. Robertson (Eds.), The Geological Evolution of the Eastern Mediterranean, Geological Society of London, Special Publication, **17,** 775-788.

Ravn, R.L., B. McPhilemy, M. Rutherford, S. Talli and G. Bahra 1994. *Late Devonian and Early Carboniferous palynostratigraphy and its applications in northeastern Syria.* In

M.D. Simmons (Ed.), Micropalaeonology and Hydrocarbon Exploration in the Middle East, Chapman & Hall, 5-21.

Ricou, L.E. 1995. *The Plate Tectonic History of the Past Tethys Ocean.* In A.E.M. Nairn, L.-E. Ricou, B. Vrielynck and J. Dercourt (Eds.), The Ocean Basins and Margins: The Tethys Ocean, Plenum Press, **8**, 3-70.

Robertson, A.H.F. and J.E. Dixon 1984. *Aspects of the geological evolution of the Eastern Mediterranean.* In J.E. Dixon and A.H.F. Robertson (Eds.), The Geologic Evolution of the Eastern Mediterranean, Geological Society of London, Special Publication, **17**, 1-74.

Robertson, A.H.F., J.E. Dixon, S. Brown, A. Collins, A. Morris, E. Pickett, I. Sharp and T. Ustaomer 1996. *Alternative tectonic models for the Late Paleozoic-Early Tertiary development of the Tethys in the Eastern Mediterranean region.* In A. Morris and D.H. Tarling (Eds.), Paleomagnetism and tectonics of the Mediterranean region, Geological Society of London, Special Publication, **105**, 239-263.

Salel, J.F. and M. Seguret 1994. *Late Cretaceous to Palaeogene thin-skinned tectonics of the Palmyrides belt (Syria).* Tectonophysics, **234,** 265-290.

Sawaf, T., D. Al-Saad, A. Gebran, M. Barazangi, J.A. Best and T. Chaimov 1993. *Structure and stratigraphy of eastern Syria across the Euphrates depression.* Tectonophysics, **220,** 267-281.

Sawaf, T., G.E. Brew, R.K. Litak and M. Barazangi 2000. *Geologic evolution of the intraplate Palmyride Basin and Euphrates fault system, Syria.* In W. Cavazza, A. Robertson and P. Ziegler (Eds.), Peritethyan rift/wrench basins and margins, PeriTethys Memoir #6, in press, Museum National d'Historie Naturelle, Paris.

Searle, M.P. 1994. *Structure of the intraplate eastern Palmyride Fold Belt, Syria.* Geological Society of America Bulletin, **106,** 1332-1350.

Seber, D., M. Barazangi, T. Chaimov, D. Al-Saad, T. Sawaf and M. Khaddour 1993. *Upper crustal velocity structure and basement morphology beneath the intracontinental Palmyride fold-thrust belt and north Arabian platform in Syria.* Geophysical Journal International, **113,** 752-766.

Sengor, A.M.C. 1995. *Sedimentation and tectonics of fossil rifts.* In C.J. Busby and R.V. Ingersoll (Eds.), Tectonics of Sedimentary Basins, Blackwell Science, 53-117.

Stampfli, G.M., J. Mosar, P. Favre, A. Pillevuit and J.-C. Vannay 2000. *Permo-Triassic evolution of the western Tethyan realm: The NeoTethys / east Mediterranean basin connection.* In W. Cavazza, A.H.F. Robertson and P. Ziegler (Eds.), Peritethyan rift/wrench basins and margins, PeriTethys Memoir #6, in press, Museum National d'Historie Naturelle, Paris.

Stoesser, D.B. and V.E. Camp 1985. *Pan-African microplate accretion of the Arabian shield.* Geological Society of America Bulletin, **96,** 817-826.

Tixier, B., 1972. *Le 'Gres de Base' Cretace du Liban: Etude stratigraphique et sedimentologique.* Notes et Memoires sur le Moyen-Orient, **12**, 187-215.

Trifonov, V.G., V.M. Trubikhin, Z. Adzhamyan, S. Dzhallad, Y. El' Khair and K. Ayed 1991. *Levant fault zone in northeast Syria*. Geotectonics, **25,** 145-154.

Walley, C. 1988. *A braided strike-slip model for the northern continuation of the Dead Sea Fault and its implications for Levantine tectonics*. Tectonophysics, **145,** 63-72.

Walley, C. 1998. *Some outstanding issues in the geology of Lebanon and their importance in the tectonic evolution of the Levantine region*. Tectonophysics, **298,** 37-62.

Walley, C. 2000. *The Lebanon passive margin and the evolution of the Levantine Neotethys (in press).* In W. Cavazza, A.H.F. Robertson and P. Ziegler (Eds.), Peritethyan rift/wrench basins and margins, PeriTethys Memoir #6, Museum National d'Historie Naturelle, Paris.

Wilson, M., R. Guiraud, C. Moureau and Y. Bellion 1998. *Late Permian to Recent magmatic activity on the African-Arabian margin of Tethys.* In D. MacGregor, R. Moody and D. Clark-Lowes (Eds.), Petroleum Geology of North Africa, Geological Society of London, Special Publication, **132**, 231-263.

Yilmaz, Y. 1993. *New evidence and model on the evolution of the southeast Anatolian orogen*. Geological Society of America Bulletin, **105,** 251-271.